A STUDY OF THE ELECTRON SPIN RESONANCE SPECTRA OF RADICALS GENERATED FROM PHENOLS AND FROM RELATED COMPOUNDS

A thesis presented for the degree of
Doctor of Philosophy in the Faculty
of Science of the University of London

by

Pat Moi Kok

October, 1977

Bedford College, London

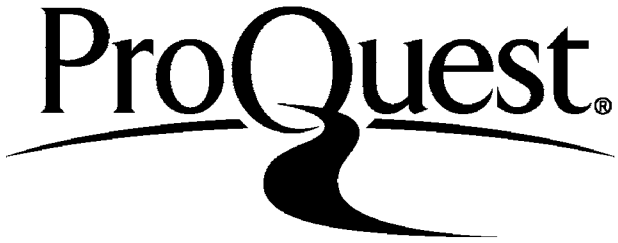

To My Mother and Family

Acknowledgements

The author wishes to express her sincere gratitude to her joint supervisors, the late Dr. W.T. Dixon and Dr. D. Murphy for their guidance, discussions and encouragement. Her sincere thanks are also due to Professor G.H. Williams, for his advice and assistance, and also for providing the facilities which made the work possible. The assistance provided by the staff of the Bedford College Computer Centre is also gratefully acknowledged.

Thanks are also accorded to the Bedford College Council for the award of the Beilby Research Scholarship, and to the British Council for an award.

Finally, the author wishes to express her sincere appreciation to her husband, Dr.K.H. Lee, for his constant encouragement and advice, to her mother for financial and moral support throughout her education, and to other members of her family, especially her sister Jenny, for constant interest in her research.

Publications

The work presented in this thesis has been published:-

(i) The Electron Spin Resonance Spectra of Radicals formed in the Autoxidation of Phenols, Tetrahedron Letters, 1976, 623-626.

(ii) Calculations of Substituent Effects on the Spin Distribution in Radicals formed by Electron Loss from Phenols and from Alkyl Aryl Ethers, J. Chem. Soc., Faraday II, 1977, 73, 709-713.

Abstract

The work reported in this thesis started as an investigation of the autoxidation of naphthols, phenols and dihydroaromatics in hexamethylphosphoramide (HMPA). Attention was then focussed particularly on the calculation of ring proton coupling constants and those of the substituents using McLachlan's method and including the structures of the substituents in the theory. A theoretical interpretation of the g-factors of radicals examined has also been made.

The autoxidation is base-catalysed and HMPA was chosen as a solvent because the bases used such as sodium methoxide were of low solubility so that the basic strength of the medium could be kept at a minimum. Also secondary radical formation was minimised. The radical intermediates of the autoxidation were identified from their electron spin resonance spectra.

Primary radicals were observed from the 1,2-; 1,4-; 1,5-; 1,7-; and 2,6-naphthalenediols, the latter three radicals being of transient existence only. The electron spin resonance spectrum from 1,7-naphthalenediol shows a large hyperfine splitting of 0.930 mT which is the largest ever observed for an aromatic proton in a static system. At later stages of the autoxidation, β-naphthols gave 1,2-naphthosemiquinones as intermediates, while in the case of α-naphthols, though 1,2-naphthosemiquinones were generally observed first, these soon decayed leaving weaker spectra of 1,4-naphthosemiquinones. The structures of the secondary radicals were deduced from sets of identical spectra obtained from different starting materials. The possible mechanism for the formation of secondary radicals was suggested.

Where no primary radicals were observed, there was an induction period of an hour or even more. A characteristic of such cases was that the sudden rise of radical concentration was accompanied by a fluorescence; the colour of which was characteristic of the starting materials. The complex (I), between the naphthoxide ion and oxygen was suggested as the species responsible for the fluorescence phenomenon.

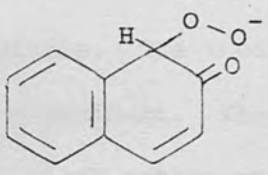

(I)

Phenol, monosubstituted phenols, resorcinols and dihydroaromatics were also found to be successfully autoxidised in this system, giving rise to 1,2- and 1,4-semiquinones.

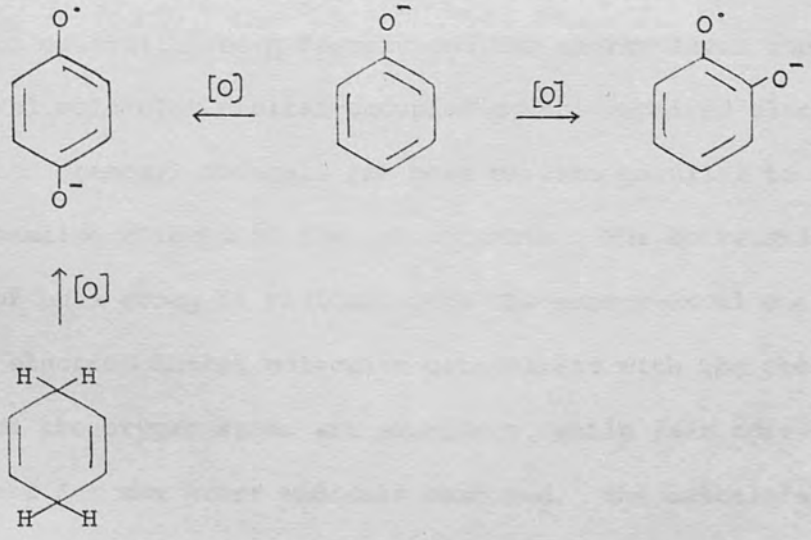

To have theoretical interpretation of the esr spectra, the McLachlan method was used to calculate the spin densities in some phenoxyl radicals, phenol radical cations and some alkyl aryl ether radical cations using a full set of basis π atomic orbitals for

the substituents concerned. The methyl- and methoxy-substituents were treated in terms of the hyperconjugation model so that the aliphatic hydrogen coupling constants can be calculated directly. An unusual parameter was chosen for the methyl group in order that the odd electron in the toluene anion might go to the antisymmetrical orbital with respect to the plane passing through the substituent and the aromatic ring. In the calculations of spin density distributions of carbonyl-substituted radicals, the carbonyl- group was described in terms of two basis π atomic orbitals. The theoretical values were in excellent agreement with experiment. The methylene proton splittings in the 1,3-benzodioxole radical cation and its derivatives were well accounted for by the hyperconjugation theory.

The larger values of g-factors of phenoxyl radicals compared with those of hydrocarbon radical anions and cations arise from the larger spin-orbit coupling constant of the oxygen atom and the smaller excitation energy from the non-bonding orbital of the oxygen to the odd electron orbital. The g-factors and the energy level coefficients of the Hückel molecular orbitals occupied by the unpaired electron in m-substituted phenoxyl radicals are more or less parallel to the electron donating effects of the substituents. The correlation of g-factors of this group of radicals with the energy-level coefficients of the odd electron Hückel molecular orbitals and with the total spin densities on the oxygen atoms are excellent, while fair correlations were obtained for the ether radicals examined. The calculated g-factors using Stone's semiempirical equation agreed well with experimental results.

CONTENTS

CHAPTER 1

INTRODUCTION TO BASIC THEORY OF ELECTRON SPIN RESONANCE AND THEORIES OF π-ELECTRON SPIN DENSITIES

1.1 Introduction

Electron spin resonance (esr) spectroscopy is a technique that permits the study of those species with one or more unpaired electrons without altering or destroying the species. The first esr spectrum was obtained by Zavöiskii in 1944.[1] Following its discovery, the subject grew rapidly. Initially it was almost exclusively in the province of physicists who studied the behaviour of spins in single crystals or metals, in semiconductors or dielectrics and sometimes in gases. It was after the first esr spectrum of organic radical of cyclopentadienyl being reported by Salikov[2] that chemists began to study a wide range of organic free radicals, whether stable and long-lived, or unstable and transient, in the solid and in the liquid state, and more recently in the gas phase.[3]

Unlike many physical techniques, esr spectroscopy is of high sensitivity and can be used to detect radicals in concentration as low as 10^{-8}M, under favourable circumstances. Esr spectra provide a wealth of information about the radicals concerned: the hyperfine splitting constants and g-factors contain information about the basic structure and conformation of the radicals and the line-widths can provide kinetic data about physical or chemical changes associated with the radical. The experimental spin densities provide a sensitive test for approximate molecular orbital calculations.

1.2 Basic theory of esr

A. The resonance condition[4,5,6]

The electron is a charged particle. It possesses an intrinsic spin angular momentum, S, with an associated magnetic moment, μ_e. This

spin angular momentum has no strict analogue in classical mechanics. The squared spin S^2 is the square of the magnitude of the total spin angular momentum of a particle and is given by

$$S^2 = S_x^2 + S_y^2 + S_z^2 \qquad (1.1)$$

where S_x, S_y, S_z are the x, y, and z components of the particle's spin angular momentum respectively.

The magnitude of S_z is represented by $m_s\hbar$ where m_s is known as the spin quantum number, $\hbar$ is the Planck's constant h divided by 2π. The possible values of m_s are

$$m_s = -S, -S+1, -S+2, \ldots, S-1, S \qquad (1.2)$$

where S can have integral or half integral values 0, ½, 1, 3/2, etc. The magnitude of S^2 has the value $S(S+1)\hbar$, where S in this case is the total spin.

The magnetic moment of the electron is related to the angular momentum by the following expression:

$$\mu_e = -\underline{g}\beta S \qquad (1.3)$$

$\underline{g}$ - $\underline{g}$-factor. For a free electron, it is equal to 2.0023.

β - Bohr magneton = $e\hbar/2m_e$ = 9.3 m^2 A, e and m_e are the charge and mass of the electron respectively.

The negative sign shows that the magnetic moment vector of the electron is opposite in direction to the angular momentum vector S, due to its negative charge.

In addition to its spin, an electron can have an orbital angular momentum, because it moves not only around its own axis, but also in an orbit. This orbital angular momentum (L) has an associated magnetic moment (μ_o). The relationship between the orbital magnetic moment and the angular momentum is given by the following expression:

$$\mu_o = -\beta L \qquad (1.4)$$

The direction of the orbital magnetic moment is parallel to the orbital angular momentum. The possible values of L^2 are

$$\ell(\ell + 1) \tag{1.5}$$

The z-component of the orbital angular momentum is restricted to the values $m_L\hbar$ where

$$m_L = \ell, \ \ell - 1, \ \ldots, \ -\ell \tag{1.6}$$

m_L is called the orbital quantum number.

When an electron is placed in a magnetic field, there is an interaction between the magnetic field and the magnetic moments of the electron. (For simplicity the orbital angular momentum will not be considered as it is 'quenched' in solution.) The interaction energy between the intrinsic spin magnetic moment of the electron and the magnetic field applied in the z-direction with field strength B, when expressed in quantum mechanical version, is given by the spin Hamiltonian:

$$\mathcal{H} = -\mu_e B = g\beta B\hat{S}_z \tag{1.7}$$

(The operators for S, I (page 10) and L (page 23) are designated with a circumflex throughout the thesis.)

The eigen values of S_z for eigen functions α and β are $m_s = +\frac{1}{2}$ and $m_s = -\frac{1}{2}$ in units of $\hbar$ respectively.

i.e.
$$\begin{aligned} \hat{S}_z|\alpha\rangle &= +\tfrac{1}{2}|\alpha\rangle \\ \hat{S}_z|\beta\rangle &= -\tfrac{1}{2}|\beta\rangle \end{aligned} \tag{1.8}$$

Therefore
$$\begin{aligned} \mathcal{H}|\alpha\rangle &= g\beta B\hat{S}_z|\alpha\rangle = \tfrac{1}{2}g\beta B|\alpha\rangle \\ \mathcal{H}|\beta\rangle &= g\beta B\hat{S}_z|\beta\rangle = -\tfrac{1}{2}g\beta B|\beta\rangle \end{aligned} \tag{1.9}$$

The zeroth order energy is given by

$$E = \frac{\langle\alpha|\mathcal{H}|\alpha\rangle}{\langle\alpha|\alpha\rangle} \tag{1.10}$$

For normalised wave functions $\langle\alpha|\alpha\rangle = 1$

Therefore

$$E_\alpha = \langle \alpha | \mathcal{H} | \alpha \rangle = \tfrac{1}{2} g \beta B \quad (1.11)$$

$$E_\beta = \langle \beta | \mathcal{H} | \beta \rangle = -\tfrac{1}{2} g \beta B \quad (1.12)$$

E_α and E_β are the Zeeman energies.

Thus it can be seen that in the presence of a magnetic field, the degeneracy of the electronic energy states is lifted and the difference between the two energy states is given by

$$\Delta E = g \beta B \quad (1.13)$$

If an oscillating field of frequency ν is applied perpendicularly to the magnetic field, transitions between the two states will be induced provided that the resonance condition (equation 1.14) is satisfied.

$$h\nu = g \beta B \quad (1.14)$$

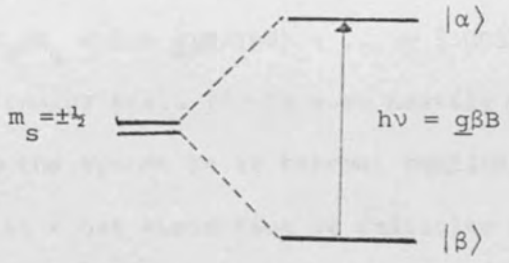

Fig. 1. Electron spin levels in a fixed magnetic field

Transitions of the electron in both directions are equally probable. Transitions from the lower to the upper energy level result in the absorption of radiation, and transitions from the upper to the lower energy level result in the emission of radiation.

The method customarily adopted for detecting the absorption is to apply a single precisely controlled frequency while the magnetic

field is varied. For most laboratory work, one of two frequency bands is usually chosen, namely the radar X-band (wave length 3.2 cm) with a magnetic field of about 300 mT, and the Q-band (wave length 0.8 cm) with a magnetic field of about 1,300 mT. In the work reported here, an X-band spectrometer was used.

B. Thermal equilibrium and spin relaxation[4,6]

For a spin system in thermal equilibrium, the distribution of spins (α and β) between the the two energy states is given by the Boltzmann distribution law. If N_α and N_β are the number of spins in the upper and lower levels, T is the absolute temperature and k is the Boltzmann distribution constant, the ratio of the population in the two levels is given by

$$N_\beta/N_\alpha = \exp(\underline{g}\beta B/(kT)) \qquad (1.15)$$

and since at normal temperature $kT >> \underline{g}\beta B$,

$$N_\beta/N_\alpha = 1 + \underline{g}\beta B/(kT) + \ldots \approx 1.0014 \qquad (1.16)$$

Thus the lower energy state $|\beta\rangle$ is more heavily populated than the upper $|\alpha\rangle$ state, when the system is at thermal equilibrium. Hence the overall result is a net absorption of radiation energy at resonance and this is the esr signal observed.

If these transitions processes were to be continued and the unpaired spins were in an isolated system, the two levels would rapidly become equally populated and then there would be no absorption of energy and no esr signal would be observed. This phenomenon is known as saturation.

This situation can be examined in simple mathematical terms, viz:- A particle of spin ½ is considered. Let n denote the population difference and N the total population.

$$n = N_\beta - N_\alpha \tag{1.17}$$

$$N = N_\beta + N_\alpha \tag{1.18}$$

Let $P_{\beta\alpha}$, $P_{\alpha\beta}$ be the probabilities of stimulated transitions: $\beta \to \alpha$, $\alpha \to \beta$ respectively. (The transitions caused by an oscillating field are called stimulated transitions.)

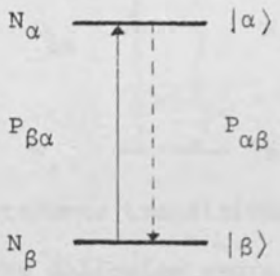

Fig. 2. Stimulated transitions for a spin ½

Then the rate of change of population of the $|\beta\rangle$ state is given by

$$dN_\beta/dt = N_\alpha P_{\alpha\beta} - N_\beta P_{\beta\alpha} \tag{1.19}$$

For stimulated transitions, the probabilities of transitions in each direction are equal, i.e. $P_{\alpha\beta} = P_{\beta\alpha} = P$

$$dN_\beta/dt = (N_\alpha - N_\beta)P = -nP \tag{1.20}$$

and

$$dn/dt = d(N_\beta - N_\alpha)/dt = -2nP \tag{1.21}$$

The solution of this differential equation for the rate of change of the population difference is

$$n = n_o e^{-2Pt} \tag{1.22}$$

where n_o is the difference at time t=0. From the above equation, it is obvious that the population difference decays exponentially as a result of the application of a magnetic field and eventually the system becomes saturated. However, there is a mechanism known as the spin-lattice relaxation process by which energy absorbed and stored in the spin system is transferred to the surroundings known as the lattice. These non-radiative transitions between the two states enable the system to achieve thermal equilibrium.

Let $W_{\alpha\beta}$ and $W_{\beta\alpha}$ be the probabilities of non-radiative transitions from upper and lower states respectively. The two probabilities of transitions are not equal, i.e. $W_{\beta\alpha} \neq W_{\alpha\beta}$

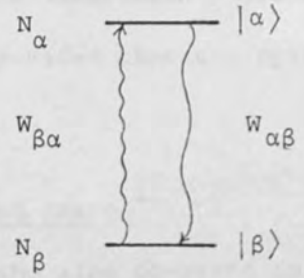

Fig. 3. Spontaneous transitions for a spin ½

Similarly, the following expression can be derived.

$$dN_\beta/dt = N_\alpha W_{\alpha\beta} - N_\beta W_{\beta\alpha} \tag{1.23}$$

At thermal equilibrium, $dN_\beta/dt = 0$,

therefore
$$N_\beta^o/N_\alpha^o = W_{\alpha\beta}/W_{\beta\alpha} \tag{1.24}$$

where N_α^o and N_β^o are the populations at equilibrium. Expressing N_α and N_β in terms of N and n as before, the following expression is obtained.

$$dn/dt = N(W_{\alpha\beta} - W_{\beta\alpha}) - n(W_{\alpha\beta} + W_{\beta\alpha}) \tag{1.25}$$

Since the population difference at thermal equilibrium is given by

$$n_o = N[(W_{\alpha\beta} - W_{\beta\alpha})/(W_{\alpha\beta} + W_{\beta\alpha})] \tag{1.26}$$

Thus equation (1.25) could be written as

$$dn/dt = -(n - n_o)/T_1 \tag{1.27}$$

where

$$T_1 = 1/(W_{\alpha\beta} + W_{\beta\alpha}) \tag{1.28}$$

and T_1 is called the spin-lattice relaxation time. It is a measure of the time taken for the energy to be transferred to other degrees of freedom, that is for the spin system to approach thermal equilibrium; large value of T_1 indicates very slow relaxation.

Combination of equations (1.21) and (1.27) gives the description

of the spin system under the influence of spin-lattice relaxation and induced excitations. Under steady conditions, $dn/dt = 0$

$$n = n_o/(1 + 2PT_1) \qquad (1.29)$$

Thus we can see that saturation could best be avoided by employing low microwave power, provided that the spin-lattice relaxation time is sufficiently short.

C. Line-widths and shapes[12]

The shape of the line observed for organic free radicals in solution where anisotropic interactions between molecules are averaged to zero is the first derivative of the Lorentzian line shape.

In crystalline solids where anisotropic interactions are non-zero, the resonance line is the first derivative of the Gaussian absorption curve.

For the Lorentzian line shapes, the line-width = $1/T_2$, where T_2 is called the line-width parameter and has the dimension of time. It governs the distribution of nuclear magnetisation in the plane perpendicular to the magnetic field. It is affected by spin energy level fluctuations.

If the resonance occurs at a precise frequency, the observed esr signal will have a line-width of about a few milligauss. In practice, several factors cause the broadening of the line-widths. The life-time of the spin states could be reduced by the spin-lattice relaxation, spin-orbit and spin-spin interactions. The decrease in life-time of the radical broadens the lines. This can be estimated from the uncertainty principle,

$$\Delta\nu.\Delta t \geqslant 1/(2\pi)$$

Certain rate processes can have extremely specific effects on the

shape of the esr spectrum. These include inter- and intra-molecular electron transfer, rotational isomerisation, inter- and intra-molecular atom transfer and interconversion between conformers. When the time spent by the electron on one molecule in the electron transfer reaction $N_1 + N_2^- \rightleftharpoons N_1^- + N_2$ becomes comparable with the inverse frequency separation between the hyperfine components, the hyperfine lines are broadened; as the rate of electron transfer increases still further, all the hyperfine structure is lost until finally a simple 'electron exchanged narrowed' line is obtained. When the rate of rotational isomerisation is slow compared with the hyperfine splittings, the esr spectra show hyperfine splittings of both isomers. When the rate is comparable with the hyperfine splittings, alternation of line-width is observed.

D. Hyperfine interactions[4,5,6]

When the electron is near an atomic nucleus which has a magnetic moment, the magnetic moment of the electron interacts with that of the nucleus. This interaction is called hyperfine interaction. There are two distinct physical mechanisms of hyperfine interactions, namely the anisotropic dipolar interaction and the isotropic Fermi-contact interaction.

(i) Fermi-contact interaction

The Fermi-contact interaction requires a finite spin density at the nucleus. Therefore the unpaired electron has to be in an orbital which has a finite electron density at the nucleus, i.e. in an orbital with some s-character. The Fermi-contact interaction of a hydrogen-like atom in the absence of a magnetic field is given by the expression

$$\mathcal{H} = a\hat{S}.\hat{I} \qquad (1.31)$$

The coupling constant, a, is proportional to the squared amplitude of

the electron wave function at the nucleus, and has the dimensions of energy. It denotes the interaction between the nucleus and the electron.

$$a = \frac{8\pi}{3} \underline{g}\beta \underline{g}_N \beta_N |\psi(0)|^2 \qquad (1.32)$$

where $|\psi(0)|^2$ is the probability of finding the electron at the nucleus. The general form of the wave function for the 1s orbital is

$$\psi_{1s} = \{1/(\pi r_o^3)\}^{1/3} e^{-r/r_o} \qquad (1.33)$$

r_o - Bohr orbit radius = 0.0529 nm = 0.529 A^o.

Substitution of the above function into Equation (1.32) gives the formula:

$$a = 50.8 \text{ mT} \qquad (1.34)$$

(ii) Anisotropic dipolar interaction

The anisotropic dipolar interaction arises from the interaction of two dipoles of μ_e and μ_N; where μ_e and μ_N are the magnetic dipoles of electron and nucleus respectively. μ_e is as defined before (page 2) while

$$\mu_N = \gamma_N \hbar I = \underline{g}_N \beta_N I \qquad (1.35)$$

γ_N - magnetogyric ratio of the nucleus and is measured in radians sec^{-1} $gauss^{-1}$.

I - nuclear spin angular momentum. The resolved component in any direction is represented by m_I, the m_I have the values I, I-1, ..., -I+1, I.

$\underline{g}_N$ - nuclear $\underline{g}$-factor.

β_N - nuclear magneton = $e\hbar/2m_p$, where m_p is the mass of the proton.

The corresponding term in the Hamiltonian is

$$\mathcal{H} = -\underline{g}_N \beta_N \underline{g} \beta \{\hat{I}.\hat{S}/r^3 - 3(\hat{I}.\underline{r})(\hat{S}.\underline{r})/r^5\} \qquad (1.36)$$

where $\underline{r}$ is the radius vector from μ_e to μ_N and r is the distance between the two moments.

From the above expression we can see that the anisotropic interaction is orientation dependent, i.e. it depends on the radius vector, r, between the two magnetic dipole moments. This type of interaction is therefore only significant for radicals in the solid state or in viscous media because the orientations of the nuclei are more or less fixed. For organic free radicals in solution, this interaction averages to zero by the rapid tumbling (Brownian motion) of the radicals.

E. Isotropic hyperfine splittings[4]

The spin Hamiltonian for the hydrogen atom in the presence of an applied magnetic field in the z-direction is

$$\mathcal{H} = g\beta B\hat{S}_z - g_N\beta_N B\hat{I}_z + a\hat{S}.\hat{I} \qquad (1.37)$$

$$= g\beta B\hat{S}_z - g_N\beta_N\hat{I}_z B + a(\hat{S}_x\hat{I}_x + \hat{S}_y\hat{I}_y + \hat{S}_z\hat{I}_z)$$

The first and the second term is the energy of interaction between the electron and nuclear magnetic moments with the magnetic field respectively. The third term is the energy of hyperfine interaction between the electron and the nucleus.

The hyperfine splittings observed in the esr spectrum can be explained in terms of perturbation theory. The spin Hamiltonian can be split into two distinct parts, i.e.

$$\mathcal{H} = \mathcal{H}_o + \mathcal{H}_1 \qquad (1.38)$$

$$\mathcal{H}_o = g\beta B\hat{S}_z - g_N\beta_N\hat{I}_z \qquad (1.39)$$

$$\mathcal{H}_1 = a\hat{S}.\hat{I} = a\hat{S}_z\hat{I}_z \qquad (1.40)$$

(The net effect of the term $a(\hat{S}_x\hat{I}_x + \hat{S}_y\hat{I}_y)$ is to produce second order change in the energies and therefore it is not considered.)

Consider the hydrogen atom ($S=\frac{1}{2}$, $I=\frac{1}{2}$), with electron spin eigen functions $|\alpha_e\rangle$ and $|\beta_e\rangle$ with eigen values $m_s=+\frac{1}{2}$ and $m_s=-\frac{1}{2}$ respectively, and with nuclear spin eigen functions $|\alpha_N\rangle$ and $|\beta_N\rangle$ with eigen values

$m_I=+\frac{1}{2}$ and $m_I=-\frac{1}{2}$ respectively, i.e.

$$S_z|\alpha_e\rangle = +\tfrac{1}{2}|\alpha_e\rangle$$
$$S_z|\beta_e\rangle = -\tfrac{1}{2}|\beta_e\rangle \qquad (1.41)$$
$$I_z|\alpha_N\rangle = +\tfrac{1}{2}|\alpha_N\rangle$$
$$I_z|\beta_N\rangle = -\tfrac{1}{2}|\beta_N\rangle \qquad (1.42)$$

For the two electron spin orientations and the two nuclear spin orientations there are four possible combinations

$$|\alpha_e\alpha_N\rangle \quad |\alpha_e\beta_N\rangle$$
$$|\beta_e\alpha_N\rangle \quad |\beta_e\beta_N\rangle$$

Let $\phi_1 = |\alpha_e\alpha_N\rangle$, $\phi_2 = |\alpha_e\beta_N\rangle$, $\phi_3 = |\beta_e\alpha_N\rangle$, $\phi_4 = |\beta_e\beta_N\rangle$ (1.43)

The above are all zeroth order functions and are eigen functions of $\mathcal{H}_o$. In the absence of a magnetic field, the four energy states corresponding to the four wave functions exist in two degenerate states. However, in the presence of an applied magnetic field, the degeneracy is removed. The four zeroth order energies are as follows:

$$E_1^o = \tfrac{1}{2}\underline{g}\beta B - \tfrac{1}{2}\underline{g}_N\beta_N B \text{ for } |\alpha_e\alpha_N\rangle$$
$$E_2^o = \tfrac{1}{2}\underline{g}\beta B + \tfrac{1}{2}\underline{g}_N\beta_N B \quad |\alpha_e\beta_N\rangle$$
$$E_3^o = -\tfrac{1}{2}\underline{g}\beta B - \tfrac{1}{2}\underline{g}_N\beta_N B \quad |\beta_e\alpha_N\rangle \qquad (1.44)$$
$$E_4^o = -\tfrac{1}{2}\underline{g}\beta B + \tfrac{1}{2}\underline{g}_N\beta_N B \quad |\beta_e\beta_N\rangle$$

By perturbation theory, the first order energy is given by the general expression

$$\langle n|\mathcal{H}_1|n\rangle \qquad (1.45)$$

where n is the zeroth order wave function (normalised), therefore the first order perturbation energies are as follows:

$$E_1^1 = \langle \alpha_e \alpha_N | \mathcal{H}_1 | \alpha_e \alpha_N \rangle$$

$$= \langle \alpha_e \alpha_N | a\hat{S}.\hat{I} | \alpha_e \alpha_N \rangle$$

$$= \tfrac{1}{4}a$$

$$E_2^1 = \langle \alpha_e \beta_N | \mathcal{H}_1 | \alpha_e \beta_N \rangle$$

$$= -\tfrac{1}{4}a \qquad (1.46)$$

$$E_3^1 = \langle \beta_e \alpha_N | \mathcal{H}_1 | \beta_e \alpha_N \rangle$$

$$= -\tfrac{1}{4}a$$

$$E_4^1 = \langle \beta_e \beta_N | \mathcal{H}_1 | \beta_e \beta_N \rangle$$

$$= \tfrac{1}{4}a$$

Hence the energies of the four states become

$$E_1 = E_1^o + E_1^1$$

$$= \tfrac{1}{2}\underline{g}\beta B - \tfrac{1}{2}\underline{g}_N\beta_N B + \tfrac{1}{4}a$$

$$E_2 = E_2^o + E_2^1 \qquad (1.47)$$

$$= \tfrac{1}{2}\underline{g}\beta B + \tfrac{1}{2}\underline{g}_N\beta_N B - \tfrac{1}{4}a$$

$$E_3 = -\tfrac{1}{2}\underline{g}\beta B - \tfrac{1}{2}\underline{g}_N\beta_N B - \tfrac{1}{4}a$$

$$E_4 = -\tfrac{1}{2}\underline{g}\beta B + \tfrac{1}{2}\underline{g}_N\beta_N B + \tfrac{1}{4}a$$

The above results are summarised in the form of energy level diagram in Fig. 4a (see page 15).

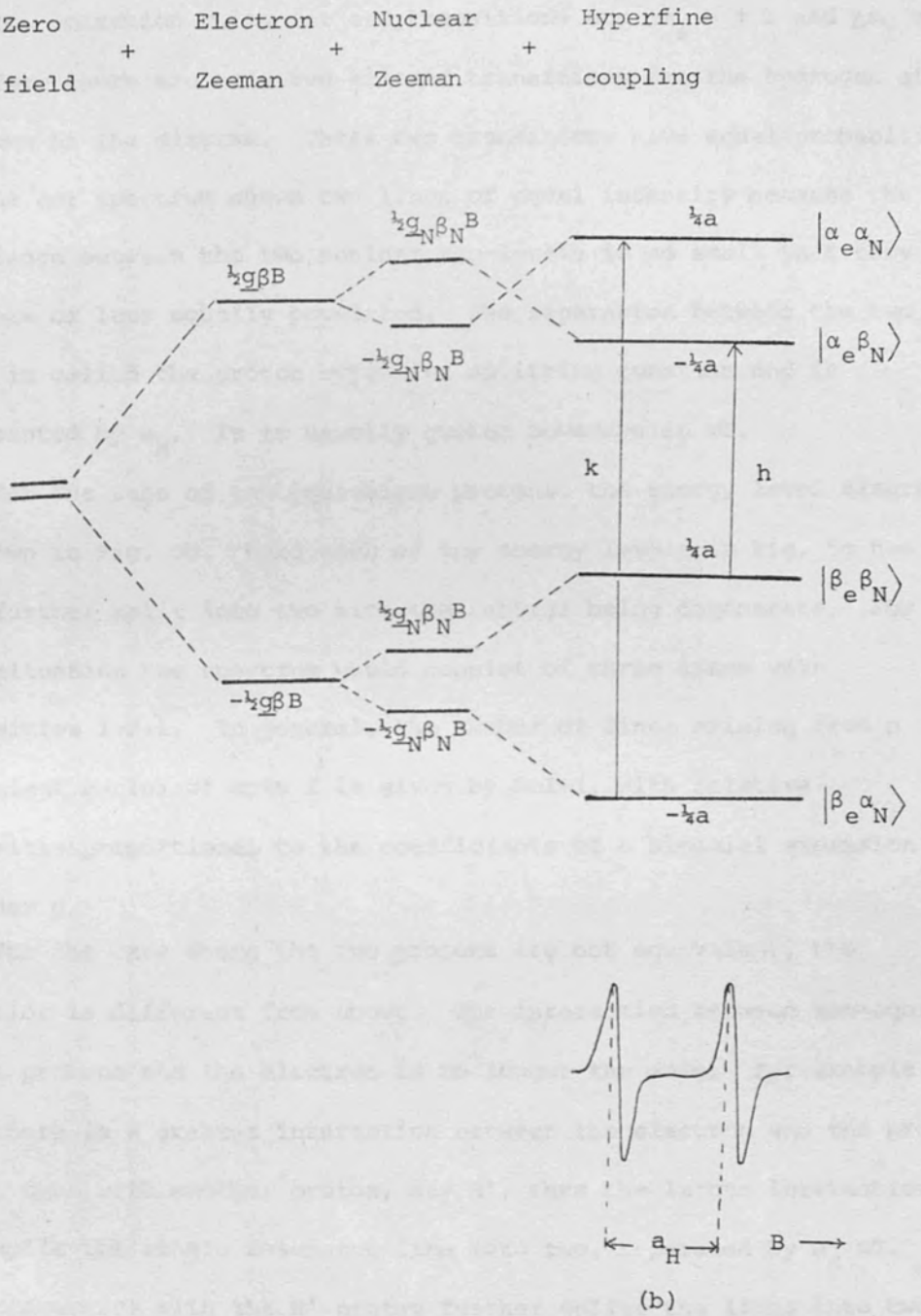

Fig. 4(a). The energy levels and allowed transitions (k and h) for the hydrogen atom.

(b). Spectrum at constant frequency.

The selection rules for esr transitions are $\Delta m_s = \pm 1$ and $\Delta m_I = 0$. Therefore there are only two allowed transitions for the hydrogen atom, as shown in the diagram. These two transitions have equal probabilities and the esr spectrum shows two lines of equal intensity because the difference between the two nuclear sub-levels is so small that they are more or less equally populated. The separation between the two lines is called the proton hyperfine splitting constant and is represented by a_H. It is usually quoted nowadays in mT.

For the case of two equivalent protons, the energy level diagram is shown in Fig. 5b. Here each of the energy levels in Fig. 5a has been further split into two with the central being degenerate. For this situation the spectrum would consist of three lines with intensities 1:2:1. In general, the number of lines arising from n equivalent nuclei of spin I is given by 2nI+1, with relative intensitiesproportional to the coefficients of a binomial expansion of order n.

For the case where the two protons are not equivalent, the situation is different from above. The interaction between non-equivalent protons and the electron is no longer the same. For example, when there is a greater interaction between the electron and the proton, say H, than with another proton, say H', then the larger interaction will split the single resonance line into two, separated by a_H mT. The interaction with the H' proton further splits the lines into two, the separation is $a_{H'}$ mT. Therefore four lines of equal intensity are observed. This is shown diagramatically in Fig. 6.

In general, for a radical containing n equivalent protons of one type and m equivalent protons of another, an esr spectrum consisting of (n+1)(m+1) lines will be observed, if fortuitous overlapping of

lines is excluded.

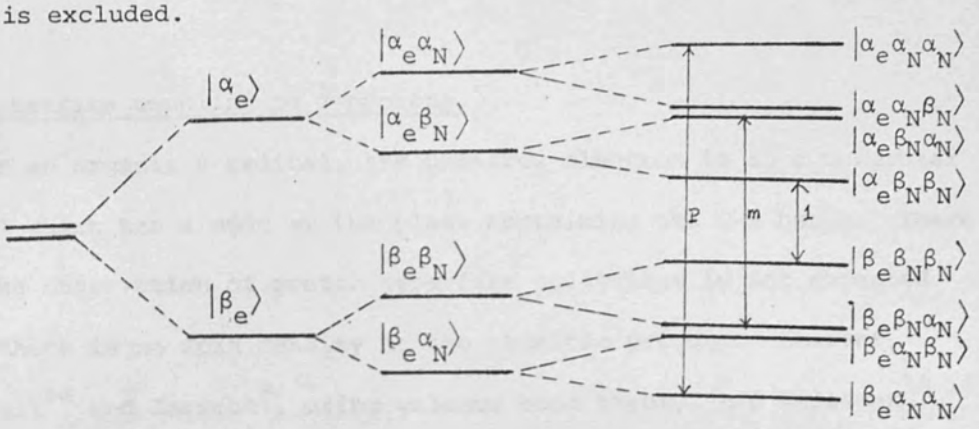

Fig. 5 (a). Fig. 5 (b).

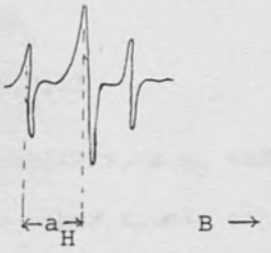

Fig. 5 (c).

Fig. 5 (a). Energy levels at constant field for one proton.

(b). Energy levels at constant field for two equivalent protons; p,m,l are the allowed transitions and m will be twice as intense as p and l.

(c). Spectrum at constant frequency.

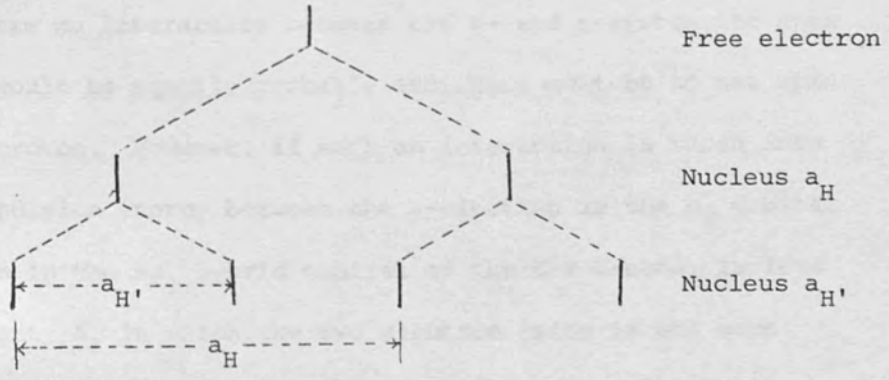

Fig.6. Hyperfine splittings produced by two non-equivalent protons

F. Hyperfine coupling to α-protons

In an organic π radical, the unpaired electron is in a molecular orbital which has a node at the plane containing the C-H bonds. Therefore the observation of proton hyperfine splittings is not expected since there is no spin density at the aromatic protons. However, McConnell[8a] and Jarrett[9], using valence bond theory, and Weissman[10], using molecular orbital theory, have been able to account for these hyperfine splittings observed for organic π radicals. The most complete investigations are those of McConnell and Chesnut[8b].

(i) Qualitative description of spin polarisation[8,9,11]

Consider a $\dot{C}$-H fragment with three atomic orbitals, a p_π atomic orbital in which the odd electron resides, and two other atomic orbitals which make a C-H σ-bond.

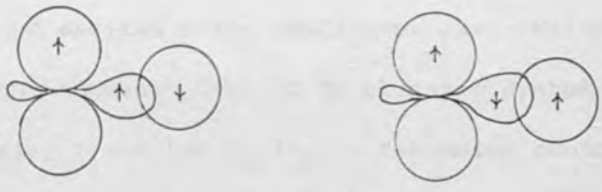

(A) (B)

Fig. 7. Spin arrangement in a $\dot{C}$-H fragment

If there were no interaction between the σ- and π-systems the spin states A and B would be equally probable and there would be no net spin density at the proton. However, if such an interaction is taken into account, the repulsion energy between the α-electron in the p_π orbital and the electron in the sp_2 hybrid orbital of the C-H σ-bond, is less in the arrangement A, in which the two electron spins in the same carbon atom are parallel, than in the arrangement B. As a result, there will be a net negative spin density (i.e. excess of β-spin over α-spin)

at the proton and a positive spin density at the carbon nucleus. The presence of the electron spin density at the hydrogen nucleus leads to the interaction between the electron spin and the proton magnetic moment and thus gives rise to the isotropic hyperfine structure observed in the esr spectrum.

McConnell[8] proposed a simple relationship between the ring proton coupling constant, a_H, and the spin density ρ_π, at the attached carbon. This is represented by

$$a_H = Q_{CH}\rho_\pi \qquad (1.48)$$

where Q is an empirical constant with values ranging from -2.0 to -3.0 mT.

(ii) Molecular orbital theory approach[10,11]

In this approach, electron spin density is introduced into the hydrogen atom by configuration interaction which involves the mixing of ground state and excited state configurations. Weissman[10] considered the three electron fragment $\dot{C}$-H, of an aromatic system with three normalised orbitals, π and two σ_B (σ_B - σ-bonding orbital) orbitals.

The ground state wave function with $S=\frac{1}{2}$, $m_s=+\frac{1}{2}$ and with the electron configuration $(\sigma_B)^2\pi^1$ is represented by a Slater determinant in an abbreviated form as follows:

$$\Phi_1 = \frac{1}{\sqrt{6}}\left|\left|\sigma_B(\alpha)\sigma_B(\beta)\pi(\alpha)\right|\right| \qquad (1.49)$$

There are three possible determinantal wave functions for the singly excited molecular state, i.e. in which an electron has been promoted into the C-H σ-antibonding orbital (σ_A). They are written as follows:

$$D_1 = \frac{1}{\sqrt{6}}||\sigma_B(\alpha)\sigma_A(\alpha)\pi(\beta)||$$

$$D_2 = \frac{1}{\sqrt{6}}||\sigma_B(\alpha)\sigma_A(\beta)\pi(\alpha)|| \qquad (1.50)$$

$$D_3 = \frac{1}{\sqrt{6}}||\sigma_B(\beta)\sigma_A(\alpha)\pi(\alpha)||$$

There are two excited configurations with spin $S=\frac{1}{2}$ and $m_s=+\frac{1}{2}$ which are constructed by the linear combination of the several determinants with different spin arrangements. They are

$$\Psi_1 = \frac{1}{\sqrt{2!}}(D_2 - D_3)$$
$$\Psi_2 = \frac{1}{\sqrt{3!}}(2D_1 - D_2 - D_3) \qquad (1.51)$$

Since there is no unpaired spin in the σ-orbitals for Ψ_1 while there is some in Ψ_2, only Ψ_2 is considered. The mixing of the ground state wave function Φ_1 and the excited state wave function Ψ_2 leads to a resultant χ described as follows:

$$\chi = \Phi_1 + \lambda\Psi_2 \qquad (1.52)$$

where λ is the admixture coefficient and would be obtained by first order perturbation theory. It was found that

$$(a_H)_i = \frac{32\pi}{3\sqrt{6}}\lambda\mu_N\mu_e\sigma_B(\underline{r}_N)\sigma_A(\underline{r}_N) \qquad (1.53)$$

where $(a_H)_i$ is the proton coupling constant at carbon atom i. Thus a negative proton hyperfine splitting constant was found.

G. Hyperfine coupling to β-protons[7,14]

The hyperfine coupling of the β-proton with the odd electron proceeds via two distinct processes: one is spin polarisation. In this mechanism, the odd electron at α-carbon induces a negative spin density at C_β which in turn polarises the C-H bond so as to induce a small positive spin density at the β-proton. The other process is hyperconjugation. It can be formulated in terms of molecular orbital theory as follows: The three atomic orbitals of the three hydrogen

atoms, ϕ_1, ϕ_2, ϕ_3 of the methyl group can be combined to form three orthonormal molecular orbitals:

$$\Phi_1 = \frac{1}{\sqrt{3}}(\phi_1 + \phi_2 + \phi_3)$$
$$\Phi_2 = \frac{1}{\sqrt{2}}(\phi_2 - \phi_3) \qquad (1.54)$$
$$\Phi_3 = \frac{1}{\sqrt{3}}(2\phi_1 - \phi_2 - \phi_3)$$

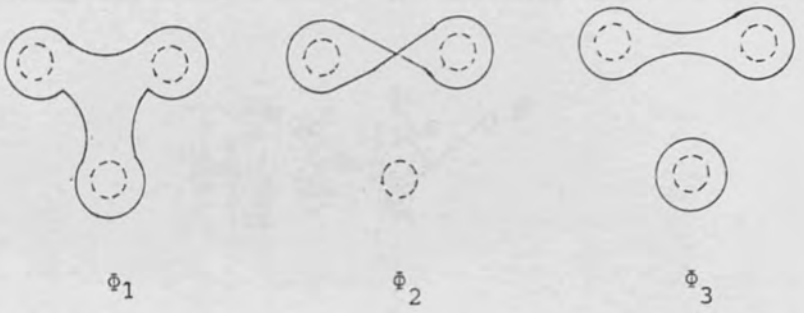

Fig. 8 Group orbitals in the methyl group.

Φ_1 is roughly spherical and has no node therefore it overlaps with the p_x orbital of the β-carbon to form the C-H σ-bond. The other two molecular orbitals Φ_2 and Φ_3 are of π symmetry; Φ_2 has its nodal plane on the xz-plane and can overlap with the p_y orbital; Φ_3, which has a nodal plane comparable to the nodal plane of the p_z orbital of the β-carbon, can therefore overlap with this orbital. The p_z orbital of the β-carbon can overlap with the p_z orbital of the α-carbon. Consequently the odd electron is delocalised directly into the H_3 group orbital, Φ_3. As a result, the odd electron can directly couple with the hydrogen nucleus resulting in a larger β-proton hyperfine coupling constant than that of α-proton. The β-proton hyperfine coupling constant is positive because the odd electron (α-spin) penetrates directly to the hydrogen nucleus.

When the methyl group is freely rotated, the esr spectrum shows the presence of three equivalent proton hyperfine splittings. It is found experimentally that the β-proton coupling constant is given by

$$a_H = (B_o + B_1\cos^2\theta)\rho_\alpha \qquad (1.55)$$

where ρ_α is the spin density at the α-carbon, and θ is the dihedral angle between the singly occupied p_z orbital and the plane containing the β-proton and the C-H bond. The dihedral angle is defined in Fig. 9.

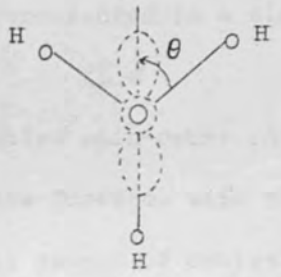

Fig. 9. Defination of the dihedral angle, θ, defining the orientation of a β-proton relative to a π system.

The constant B_o is attributed to spin-polarization effects and is conformational-independent and B_1 is a measure of hyperconjugative effect which is dependent on the $\cos^2\theta$. For unit spin density in a p-orbital, B_o = 0 - 0.3 mT, B_1 = 4.5 - 5.0 mT. If the methyl group rotates rapidly, then an average $B_o + B_1\langle\cos^2\theta\rangle_{av} = B_o + \frac{1}{2}B_1$ is observed for each proton.

The large methylene proton hyperfine splittings in organic π radicals can also be attributed to the coupling of the methylene protons with the odd electron via hyperconjugation.

H. g-Factors[12,78]

An electron in a free radical may possess in addition to the spin angular momentum, an orbital angular momentum, but for most organic π radicals in the ground state, the orbital angular momentum is equal to zero. Therefore the g-factors of the free radicals should have precisely the free spin value of 2.0023. However, deviations from the free spin value are observed. This is accounted by the fact that the odd electron acquires some orbital angular momentum through the effects of spin-orbit coupling, which can be represented in a simplified form by the expression

$$\zeta \hat{L}.\hat{S} \tag{1.56}$$

where ζ is a constant called spin-orbit coupling constant. This operator mixes the ground state wave function with the excited states. The interaction introduces a small amount of orbital angular momentum into the ground state. However, the spin-orbit operator for an electron in a molecule no longer has the simpler form $\zeta\hat{L}.\hat{S}$ because the electrons moves over several atoms with different values of ζ. It can be shown that the electronic Hamiltonian contains a term $\xi(r)\hat{L}.\hat{S}$.

$$\xi(r) = \frac{e\hbar^2}{2m^2c^2}\left(\frac{1}{r}\frac{\partial V}{\partial r}\right) \tag{1.57}$$

The simpler term $\zeta\hat{L}.\hat{S}$ derived for an electron in a particular atomic orbital $\phi_k(r)$ on atom k by averaging over the radial probability distribution is:

$$\zeta_k = \int \phi_k^* \xi_k(r_k) \phi_k dv \tag{1.58}$$

where $\xi_k(r_k)$ refers to the atom on which the orbital is centered and decreases rapidly to zero at small distances from the nucleus.

The time-averaged g-tensor can in principle be calculated by using

second order perturbation theory.[12] It was shown to have the following expression:

$$\underline{g}_{zz} = 2.0023 + 2\sum_{n}\sum_{k,j}\frac{\langle\psi_o|\zeta_k\hat{L}_{zk}|\psi_n\rangle\langle\psi_n|\hat{L}_{zj}|\psi_o\rangle}{E_n - E_o} \qquad (1.59)$$

where $\underline{g}_{zz}$ denotes the z-component of the $\underline{g}$-tensor;

$\hat{L}_{zk}$ - the orbital angular momentum about the k^{th} nucleus;

E_o - the energy of the singly occupied molecular orbital;

E_n - the energy of the n^{th} molecular orbital.

The sign of $(E_n - E_o)$ changes as the ψ_n changes from an occupied to an unoccupied so that the filled and empty gives opposite contributions to the $\underline{g}$-tensor.

The theory when applied to organic π radicals with some approximations and simplifications of the equation leads to the following expression for the $\underline{g}$-shift[78].

$$\Delta\underline{g} = \underline{g}_x - \underline{g}_e = b + c\lambda \qquad (1.60)$$

where λ is the energy level coefficient of the singly occupied Hückel molecular orbital; b and c are semi-empirical constants.

The difference in $\underline{g}$-factor for a free radical and that for a free electron is analogous to the chemical shift. As $\underline{g} = \frac{h\upsilon}{\beta B}$, spectra of different radicals will have their centres at different field strength (see fig. 10).

Fig. 10. Esr spectra of 1,4-benzosemiquinone and Fremy's salt, centres $\underline{g}_1$ and $\underline{g}_2$ respectively.

1.3 Theories of π-electron spin densities

The usual procedure in explaining the esr spectra of aromatic radicals is to calculate the π-electron spin density by Hückel molecular orbital theory. Then with the use of the McConnell relationship, (ref. page 19)the theoretical coupling constants are obtained. The electron spin distributions in a large number of radical ions have been explained successfully by Hückel molecular orbital theory. However, there are discrepancies where the total width of the esr spectrum is greater than the value of Q. The resolution of this difficulty lies in the considerations of possible negative spin densities associated with some carbon atoms. The Hückel molecular orbital theory, in which all interactions between the electrons themselves are neglected, and which manifestly predicts positive spin densities, cannot account for the negative spin densities. McLachlan's method of considering all the π electrons and taking π electron correlation effects into account in an approximate way, can estimate negative spin densities. As a general rule, negative spin densities occur whenever the simple Hückel molecular orbital theory predicts zero spin density on a position close to one of high spin density. McLachlan's method is now well established as a convenient and reasonably reliable way of determining spin densities of radical ions. It often provides a good description of electron spin distributions in a large number of conjugated molecules. This is why the McLachlan method is used in this work. The Hückel molecular orbital theory and the McLachlan method are described below.

A. Hückel molecular orbital method (HMO)

In the linear combination of atomic orbitals (LCAO) approximation, the molecular orbitals are taken to be the linear combinations of atomic orbitals.

i.e. $$\psi_j = \sum c_{jr}\phi_r \qquad (1.61)$$

where the molecular orbitals ψ are orthonormal, ψ_j is the j^{th} molecular orbital, ϕ_r is the atomic orbital of r^{th} atom and c_{jr} is the coefficient of the r^{th} atomic orbital in the j^{th} molecular orbital.

The best values for the coefficients and energy of the molecular orbitals are obtained by the variation method.

$$\varepsilon = \frac{\int \psi \hat{\mathcal{H}} \psi d\tau}{\int \psi^2 d\tau} \geqslant E_o \qquad (1.62)$$

where E_o is the actual ground state energy of the molecule. Substitution of (1.61) into (1.62) and then differentiating with respect to the coefficients to obtain the lowest energy, secular equations (1.63) is obtained.

$$\sum_r c_r (H_{rt} - ES_{rt}) = 0 \qquad (1.63)$$

where $$H_{rt} = \int \phi_r \hat{\mathcal{H}} \phi_t d\tau$$

$$S_{rt} = \int \phi_r \phi_t d\tau$$

In order for the sets of secular equations to have non-trivial solutions the secular determinant must be equal to zero. i. e.

$$\begin{vmatrix} H_{11} - ES_{11} & H_{12} - ES_{12} & H_{13} - ES_{13} & \cdots & H_{1n} - ES_{1n} \\ H_{21} - ES_{21} & H_{22} - ES_{22} & H_{23} - ES_{23} & \cdots & H_{2n} - ES_{2n} \\ \vdots & \vdots & \vdots & \vdots & \vdots \\ H_{n1} - ES_{n1} & H_{n2} - ES_{n2} & H_{n3} - ES_{n3} & \cdots & H_{nn} - ES_{nn} \end{vmatrix} = 0$$

The following approximations are applied in the above LCAO method and this constitutes the Hückel molecular orbital method (HMO).

(i) All the H_{rr} are equal for all 'identical' orbitals regardless of their positions. i.e. $H_{11} = H_{22} = H_{33} \ldots = H_{rr}$. H_{rr} is called the coulomb integral and is represented by α_{rr}.

(ii) For bonded atoms, H_{rs} is written as β_{rs} and is assumed a constant having the same value for similar bonds. β_{rs} is called the resonance integral.

(iii) H_{rs} is equal to zero, when r and s are not adjacent atoms.

(iv) All the overlap integrals, S_{ij}, for $i \neq j$ are neglected; for $i = j$, $S = 1$.

Therefore the secular determinant for the system that consists of carbon atoms only, becomes

$$\begin{vmatrix} \alpha - E & \beta_{12} & \beta_{13} & \ldots & \ldots & \beta_{1n} \\ \beta_{21} & \alpha - E & \beta_{23} & \ldots & \ldots & \beta_{2n} \\ \vdots & \vdots & \vdots & \vdots & \vdots & \vdots \\ \beta_{n1} & \beta_{n2} & \beta_{n3} & \ldots & \ldots & \alpha - E \end{vmatrix} = 0$$

Solutions of the above secular determinant gives a set of energies having the form $E_i = \alpha + m_i\beta$ where the m_i are the eigen values. Corresponding to each such eigen value is a set of eigen vectors which are the coefficients, c_{ir}, of a molecular orbital. The squares of the coefficients of the atomic orbitals of the odd electron molecular orbital give the spin densities and all the spin densities are positive.

B. McLachlan SCF method[15]

When the interactions between all the bonding π electrons and the odd electron are taken into account, the total wave functions for the system of 2n+1 electrons can be written in the form of Slater determinants with different orbitals for different spins, as suggested by Pople and Nesbet[16].

$$\psi = ||\psi_1\bar{\psi}_1\psi_2\bar{\psi}_2 \cdots \psi_n\bar{\psi}_n\psi_o|| \tag{1.64}$$

where the space molecular orbital ψ_k is not, in general, equal to the space molecular orbital $\bar{\psi}_k$. ψ_o is the space orbital occupied by the odd electron of α-spin. The bar over an orbital indicates that the electron in that space orbital is in a β-spin state; no bar indicates an α-spin state.

For two electrons of the same spin, the repulsion between them is decreased by an amount equal to the exchange energy γ_{mo} (i.e. relative to the repulsion between electron of opposite spin).

$$\gamma_{mo} = \iint \psi_m(i)\psi_o(i)\frac{e^2}{r_{ij}}\psi_m(j)\psi_o(j)d\tau_i d\tau_j \tag{1.65}$$

The exchange 'stabilisation' of the odd electron and spin α can be taken into account by changing the effective values of the coulomb integral α' and the resonance integral β for bonding π electrons of α-spin. Thus the coulomb integral for the α-spin at atom r is no longer taken equal to α'_r but becomes instead

$$\alpha_r = \alpha'_r - c^2_{or}\gamma_{rr} \tag{1.66}$$

where c^2_{or} is the Hückel spin density at atom r of the odd electron molecular orbital.

McLachlan then assumed

$$\tfrac{1}{2}\gamma_{rr} = -\lambda\beta \tag{1.67}$$

where λ is an adjustable parameter with a value approximately equal to 1.2. Therefore Equation (1.66) becomes

$$\alpha_r = \alpha'_r + 2\lambda c_{or}^2 \beta \tag{1.68}$$

The resonance integral of the bond r-s is modified to

$$\beta_{rs} = \beta'_{rs} - c_{or}c_{os}\gamma_{rs} \tag{1.69}$$

Since $c_{or} \times c_{os} = 0$ for all alternant hydrocarbon radicals (for which the theory was at first derived), the resonance integral remains unchanged.

With the approximations that all γ_{ii} are equal, he arrived at the following expression ρ_r for the spin density at atom r:

$$\rho_r = |c_{or}|^2 + \sum_{j=1} |c_{jr}|^2 - |c'_{jr}|^2 \tag{1.70}$$

where c_{jr} are calculated by leaving β' unchanged and using the coulomb integral $\alpha = \alpha' + 2\lambda c_{or}^2 \beta$; c'_{jr} are the calculated coefficients of the Hückel molecular orbital; c_{or} is the coefficient of the odd electron molecular orbital.

An alternative procedure for the calculation of spin density was also suggested. This involves the explicit calculation of the mutual polarisability (π_{rs}) of the atoms r and s. This is given by the following expression :

$$\rho_r = c_{or}^2 + \lambda \sum_{s=1}^{n} \pi_{rs} c_{os}^2 \tag{1.71}$$

$$\pi_{rs} = -4\beta \sum_{j}^{occ} \sum_{k}^{unocc} \frac{c_{jr}c_{ks}c_{js}c_{kr}}{E_k - E_j} \tag{1.72}$$

E_k and E_j are the Hückel energies of the unoccupied k^{th} levels and the occupied j^{th} levels respectively.

In the work reported in this thesis, the former method is adopted.

To illustrate the calculation of spin densities of organic π-radicals by the McLachlan method, the simple molecule , the allyl radical is taken as an example.

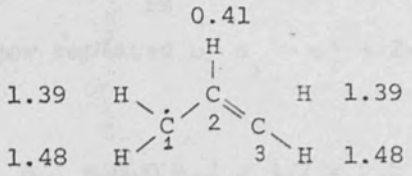

The following matrix (A) for the allyl radical is set up

Matrix (A)

$$\begin{bmatrix} 0.0 & 1.0 & 0.0 \\ 1.0 & 0.0 & 1.0 \\ 0.0 & 1.0 & 0.0 \end{bmatrix}$$

Hückel molecular orbitals were found by diagonalising the above matrix. The molecular orbitals are

$$\psi_1 = \tfrac{1}{2}(\psi_1 + \sqrt{2}\psi_2 + \psi_3)$$

$$\psi_2 = \tfrac{1}{\sqrt{2}}(\psi_1 - \psi_3)$$

$$\psi_3 = \tfrac{1}{2}(\psi_1 - \sqrt{2}\psi_2 + \psi_3)$$

and the energies are

$$E_1 = \alpha + 1.414\beta$$

$$E_2 = \alpha$$

$$E_3 = \alpha - 1.414\beta$$

The unpaired electron occupied ψ_2, hence the Hückel spin densities are

$$\rho_1 = \rho_3 = 0.5$$

$$\rho_2 = 0.0$$

The calculated coupling constant using McConnell's relationship with $Q = |3.0|$mT are given below:

$$a_1 = a_3 = 1.5 \text{ mT}$$

$$a_2 = 0.0$$

The McLachlan spin densities (α-) are then calculated by using the

matrix (A) in which the β_{rs} are the same as for the β-spin densities, but the α_r are now replaced by $\alpha_r = \alpha_r' + 2\times\lambda c_{or}^2$ with the value of $\lambda = 1.2$. Thus

$$\alpha_{11} = 0.0 + 2 \times 1.2 \times 0.5 = 1.2$$

$$\alpha_{22} = 0.0 + 2 \times 1.2 \times 0.0 = 0.0$$

$$\alpha_{33} = 0.0 + 2 \times 1.2 \times 0.5 = 1.2$$

Therefore a new matrix is set up.

Matrix B

$$\begin{bmatrix} 1.2 & 1.0 & 0.0 \\ 1.0 & 0.0 & 1.0 \\ 0.0 & 1.0 & 1.2 \end{bmatrix}$$

This matrix is solved as before. The McLachlan spin densities calculated from equation (1.70) are listed below:

$$\rho_1 = \rho_3 = 0.50 + 0.3476 - 0.25 = 0.5976$$

$$\rho_2 = 0.0 + 0.3047 - 0.50 = -0.1953$$

Hence it can be seen that the McLachlan method predicts the spin density at carbon atom 2 to be negative which is consistent with experimental observations.

The calculated coupling constants with $Q = |3.0|$ mT are

$$a_1 = a_3 = 1.79 \text{ mT}$$

$$a_2 = -0.59 \text{ mT}$$

In summary, the computer programme written for the McLachlan method in the present work* followed the following procedure: Hückel molecular orbitals are found by using coulomb integral α_r' which give the β-spin coefficients. α_r are then found using Equation (1.68) with a value of $\lambda = 1.2$. The calculation is then repeated with the new α_r but leaving the resonance integral unchanged. This gives the α-spin coefficients and the McLachlan spin densities are then calculated using Equation (1.70).

* See appendix.

CHAPTER 2

HISTORICAL SURVEY OF PHENOXYL RADICALS AND ALKYL ARYL ETHER RADICAL CATIONS

2.1 General

The chemistry of phenols has been studied extensively because of their participation in many important processes in nature and in industry. For example, sterically hindered phenols, and a mixture of unhindered and hindered phenols are effective antioxidants in the inhibition of the autoxidation process of organic substances such as fats and edible oils.[18] They are also widely employed as antioxidants in industry in the stabilisation of hydrocarbons.[18] Considerable interest has been shown too, in the chemistry of phenols from the standpoint of biosynthesis of various natural products[18,24,26] such as alkaloids, lignins, aphid pigments and antibiotics, i.e. processes in which phenoxyl radicals are thought to be intermediates.[18,24,26]

A. Formation of phenoxyl radicals

Phenoxyl radicals may be generated by one electron transfer from phenol or its anion to a suitable oxidant[26a] such as ceric sulphate, lead dioxide, potassium ferricyanide, ferric chloride, manganese dioxide, silver dioxide, or potassium permanganate.

$$ArO^- \xrightarrow{-e} ArO\cdot \qquad (2.1)$$

$$ArOH \xrightarrow{-e} Ar\overset{+}{O}H \xrightarrow{-H^+} ArO\cdot \qquad (2.2)$$

Phenoxyl radicals can also be formed by homolytic cleavage of the O-H bond by a free radical (Equation 2.3) or by electrochemical methods.[20]

$$ArOH + R\cdot \longrightarrow ArO\cdot + RH \qquad (2.3)$$

Recently, new methods of generating phenoxyl radicals have been developed. These include the *in situ* radiolysis of phenols in alkaline solution[32] and flash photolysis of phenols in aqueous solutions.[21,22]

The following mesomeric structures can be drawn for the phenoxyl radicals and these account for the fact that although the life-times of phenoxyl radicals are relatively short, their reactivity is reduced

by resonance stabilisation.

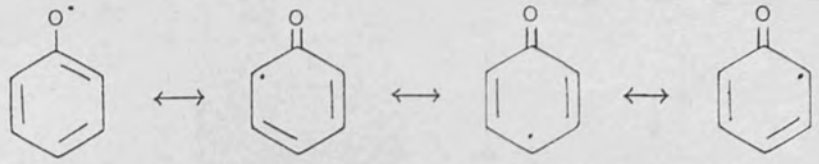

B. Dimerization

The radicals may be destroyed by dimerization[23] via C-C or C-O linkages but not via O-O coupling, in which an unstable peroxide would result. In the C-C and C-O coupling, coupling takes place at the o- and the p-positions. There are two other routes[24] leading to the formation of dimeric products. One involves the phenoxyl radical attack on another phenol molecule forming the cyclohexadienyl radical which is further oxidised to give the coupled products (Reaction 2.5). The other involves the addition of phenoxonium ion, which is formed by further oxidation of phenoxyl radical by strong oxidants such as cerium(IV) or hexachloroiridate(IV), on a second phenol molecule. (Equation 2.6).

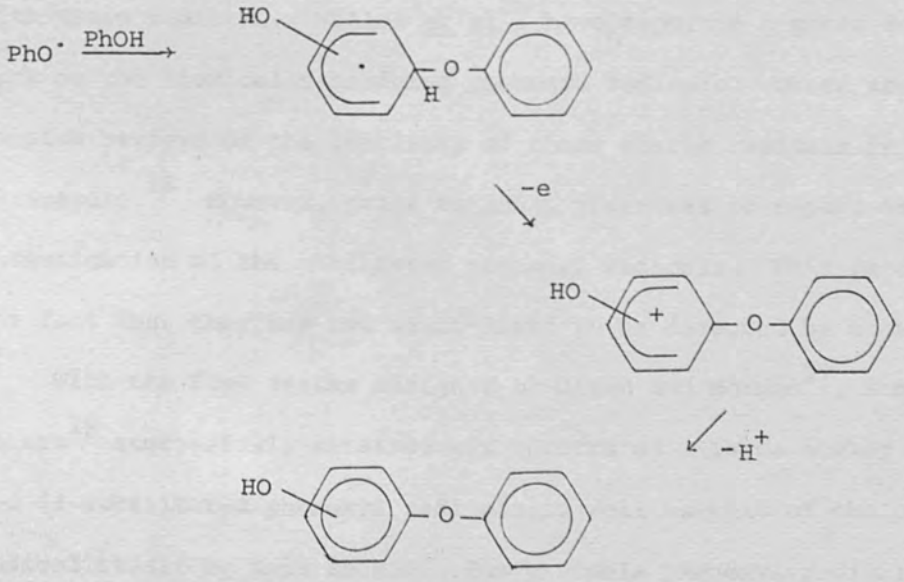

(2.5)

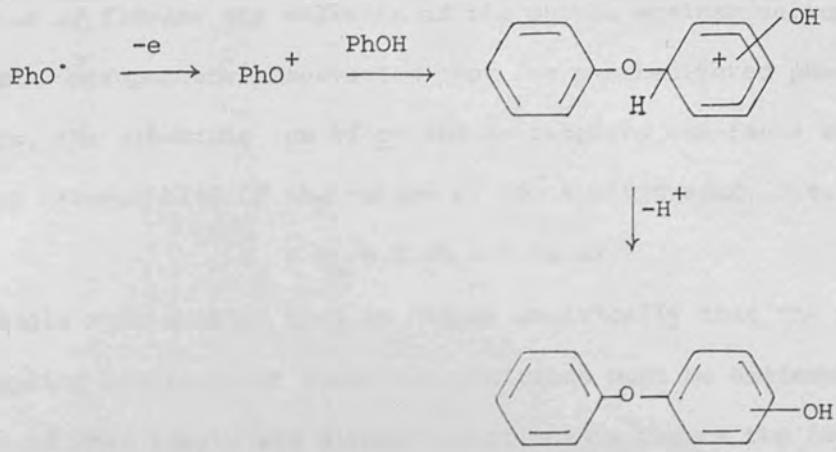

(2.6)

However, dimerization of phenoxyl radicals can be prevented by blocking the available coupling positions (i.e. carbon-2 and carbon-4) with bulky groups, when the radicals may persist for a long time, even in solution.

2.2 Previous esr studies of phenoxyl radicals

A. Monohydric phenols

Since 2,4,6-trisubstituted phenoxyl radicals are stable enough to be detected by static methods,[25] the early esr studies were concerned with these radicals. Müller et al[25] have reported a great deal of work on the sterically hindered phenoxyl radicals. There are comprehensive reviews on the chemistry of these stable radicals in the literature.[26] However, prior to 1964, there was no report on the esr investigation of the unhindered phenoxyl radicals. This is due to the fact that they are too short-lived to be detected by static-methods.[26]

With the flow system designed by Dixon and Norman[27], Stone and Waters[19] successfully obtained esr spectra of a large number of mono- and di-substituted phenoxyl radicals as well as that of the phenoxyl radical itself by this method. The unstable phenoxyl radicals were

generated by flowing the solution of the phenol against cerium(IV) sulphate. They made the important observation that for p-substituted phenoxyl radicals, the algebraic sum of o- and m- coupling constants was almost constant irrespective of the nature of the substituents, i.e.

$$a_o + a_m = 0.45 \pm 0.02 \text{ mT} \qquad (2.7)$$

This simple rule enabled them to deduce empirically that the sign of the coupling constants at these two positions must be different. They also found that alkyl- and alkoxy- substituents reduce the coupling constants of the o- and the p-positions whereas the electron attracting groups, e.g. carboxyl-, , carbonyl- and nitro- enhanced them.

Dixon and Norman[28] have also successfully detected the phenoxyl radical by using the titanium(III) chloride-hydrogen peroxide system. The phenoxyl radical was thought to be formed by hydrogen abstraction from the phenol by the hydroxyl radical:

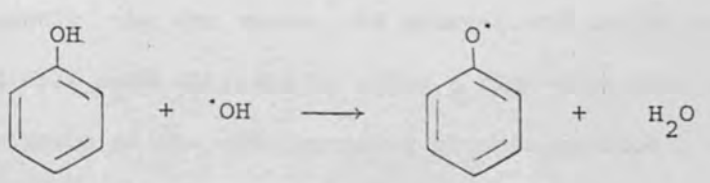

(2.8)

But in a later investigation[31] of the phenol in this system at varying pH, this was found not to be the case. In this study, it was found that at pH ∿ 1, phenoxyl radical was observed, then as the pH was raised, first the adduct (I), formed by the addition of hydroxyl radical on the phenol molecule, and then the o- and p-benzosemiquinones were observed. The observation of the adduct (I) suggested that the formation of phenoxyl radical was via the adduct (I) followed by the acid-catalysed elimination of water (Equation 2.9) as suggested by Adams.[30] The formation of semiquinones was found to be a base-catalysed reaction in

which hydrogen peroxide acts as a two electron oxidising agent (Equation 2.10).

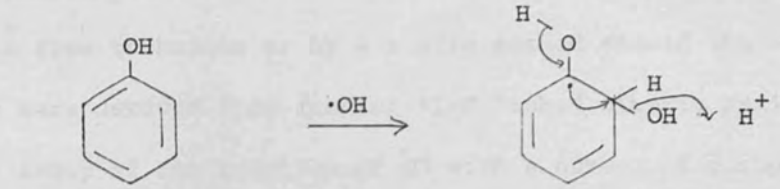

(I)

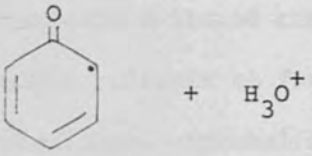

(2.9)

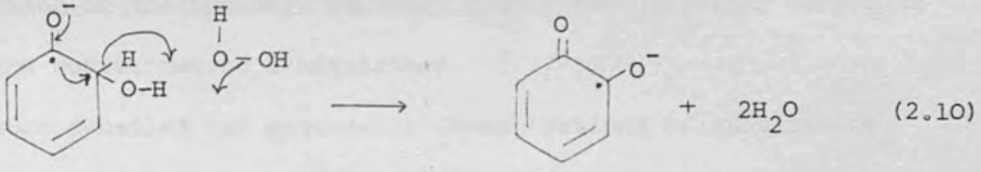

(2.10)

Subsequently, the esr spectra of short-lived alkyl- and alkoxy-phenoxyl radicals were obtained by using a flow technique by flowing a benzene solution of the corresponding phenols through a bed of silver oxide or lead dioxide placed within the cavity of an esr spectrometer.[73] By comparing the results obtained with those of Stone and Waters,[19] the authors found that the coupling constants of p-substituted phenols are significantly solvent dependent, regardless of the nature of the substituents at the o-positions. Thus, changing the solvent from water to benzene, both decreases the coupling constants of p-alkyl and p-alkoxy groups, and increases the coupling constants for the o- and the m-positions. However, this effect is not observed for those 2,6-di-substituted phenoxyl radicals which have a free p-position.[73a] By stopping the flow, secondary radicals formed by the coupling of the phenoxyl

radicals were detected and this led them to a further identification and characterisation of these radicals. The esr spectra obtained by a stopped flow technique or by a static method showed that the dimeric radicals were derived from (carbon-4)-O linked dimeric radicals.[73b]

The study of the reaction of $\dot{O}H$ with a number of carboxyl- and amino-substituted phenols, by the *in situ* radiolysis esr technique, has been made by Neta and Fessenden.[33] The radicals produced from the phenols were phenoxyl radicals, and the corresponding *o*- and *p*- benzosemiquinones. The formation of phenoxyl radicals followed the same pathway as suggested by Adams.[30] The phenoxyl radicals so formed undergo disproportionation reactions producing hydroquinone, catechol and phenol. The reaction of the hydroxyl radicals with these dihydroxy compounds yields the corresponding semiquinones.

A more detailed and systematic investigations of substituent effects on phenoxyl radical has recently been made by Dixon, Moghimi and Murphy.[34] They found that not only the *p*-substituted phenoxyl radicals investigated in their work followed the same simple rule that was deduced by Stone and Waters[19] (Equation 2.7), but that simple relationships were obtained for the *o*- and *m*-isomers as well. The coupling constants of *o*- and *m*-substituted phenoxyl radicals were assigned with the use of such a rule in conjunction with graphical procedures. The assignments for di- and tri-hydroxybenzenes were made in an analogous manner. It was also noted that for *o*- and *m*- and *p*-substituted phenoxyl radicals, the effects of substituents on the spin distribution of these radicals can be arranged in the following regular series, depending on the electron donating power of the substituents;

$$-NO_2,\ -CO_2H,\ -H,\ -CH_3,\ -Cl,\ -F,\ -OMe,\ -NH_2,\ -O^-$$

They also made an initial attempt to explain the hyperfine splittings of the phenoxyl radicals investigated by calculating the coupling constants using the McLachlan method[15] and the INDO (intermediate neglect of differential overlap) method.[127] Using the McLachlan method, the substituents were treated in terms of a heteroatom model and an inductive model.[34] They have successfully found sets of parameters for the $-O^-$, $-CH_3$, and the -OMe groups, but could find no satisfactory parameters for electron withdrawing groups such as $-CO_2H$, -CHO, and $-NO_2$. However, they were able to confirm the assignments made by graphical procedures for CO_2H-substituted phenoxyl radicals using an inductive model[34] for the CO_2H group. INDO calculations fail to account satisfactorily for the hyperfine splittings in phenoxyl radicals.[34]

It has been found that many oxygen heterocyclic radicals such as kojic acid, maltol, flavones[126a], and coumarins[126b] gave radicals analogous to phenoxyl radicals on oxidation with Ce(IV). Since the McLachlan method has been found to be successful in accounting for the spin distribution of phenoxyl radicals in their previous studies,[34] this method was applied on these radicals[126] using the same sets of parameters to account for the hyperfine splittings observed. The nature of a novel heterocyclic radical has been characterised by this method of calculation.[126a]

More recently, it was shown that phenoxyl radicals exist in equilibrium with their protonated forms in acid solutions[76b] (containing 0 to 75 % of sulphuric acid). (Equation 2.11)

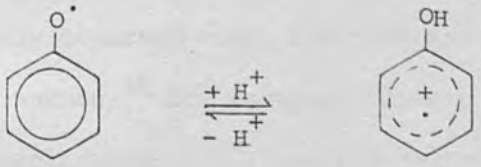

(2.11)

As the phenoxyl radicals are progressively protonated over the range, the g-factors change from about 2.0045 to 2.0035 and the change can be followed by means of titration-type curves. From these curves, pK_a's of various phenoxyl radicals were determined.[76b] The effects of substituents on the spin distributions of phenol radical cations can be arranged in the same order as that for phenoxyl radicals.[76b] There is also a loose correlation between the substituent effects and the change in g-factors in going from a radical cation to the corresponding phenoxyl radical.[76b]

B. Naphthols

Although the esr spectra of α- and β-naphthoxyl radicals should indicate features about the electronic structures of these species which are simple extension of the phenoxyl radicals, they have received relatively little attention. Stone and Waters[19] obtained poorly resolved esr spectra of α- and β-naphthoxyl radicals. They were not able to analyse them. In 1974, Dixon, Foster and Murphy[35] obtained well resolved esr spectra of a large number of α- and β-naphthoxyl radicals using the flow technique.[27] The coupling constants of these naphthoxyl radicals were tentatively assigned by comparison with simple Hückel theory for the corresponding benzyl-type radical and by comparison with the π electron radical formed by eliminating carbon 1 or 2 as appropriate. The carbonyl and sulphonate substituents were found to have little effect on the coupling constants of such radicals.

C. Dihydric phenols, naphthalenediols and quinones

Many naturally occuring compounds that are of biological importance are quinonoid in nature;[29] for example, Vitamin E is a highly substituted p-benzoquinone , Vitamin K and co-enzyme Q[36,37] are

derivatives of quinones. It is believed that semiquinones are intermediates in the metabolism of certain cellular constituents.[38a] Quinones have also been used in the studies of enzyme reactions.[38b] Thus it is not surprising that the chemistry of quinones have received a great deal of attention.

(i) Characterisation of semiquinones and the elucidation of mechanism of autoxidation

It has been well established that the autoxidation of hydroquinone in alkaline media proceeds through the stable semiquinone (II) intermediates. This was first postulated by Michaelis[39] from the results of potentiometric measurements and magnetic susceptibility determinations. p-Benzosemiquinone was first detected directly using esr by Fraenkel and Venkataraman[40] in 1955. Since then many esr studies of semiquinones have been reported.[41-46]

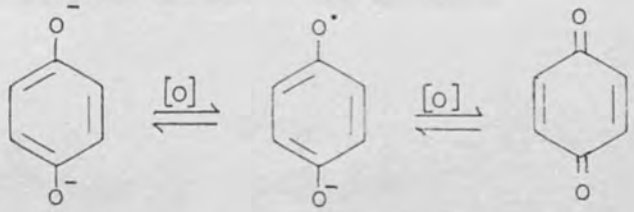

(2.12)

(II)

The formation of p-benzosemiquinone is only the first step in the autoxidation of dihydric phenols in aqueous solution because the esr spectrum showed lines in addition to the expected five-lined spectrum.[40] It was suggested that these lines were due to secondary radicals forming at the later stage of the autoxidation.[40]

Anderson and his co-workers[57] found that complex reactions took place during the autoxidation of halogenated hydroquinones. It was suggested that the halogen had been replaced, and that the esr spectra observed were due to dimeric species, e.g. (III), (IV), and (V).

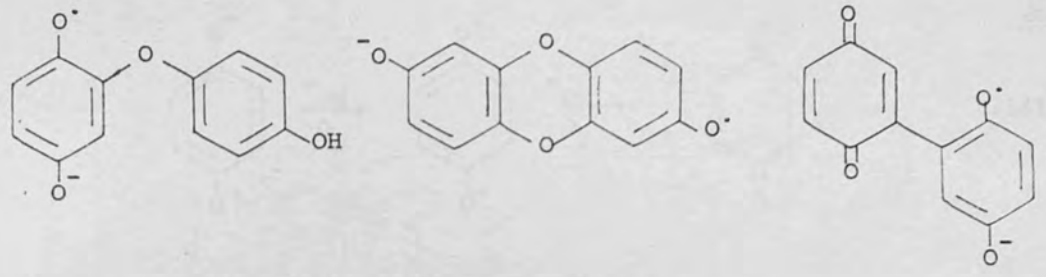

(III) (IV) (V)

However, it was later demonstrated that the spectra observed by Anderson et al[57] were due to the radical (VI), formed by alkoxide ion attack on the quinone or the hydroquinone.[58] The nucleophilic addition of alkoxide ions on the quinone or hydroquinone has also been observed in strongly alkaline alcoholic media.[59a] Atherton and Blackhurst[59b] also obtained esr spectra of alkoxy-substituted semiquinones arising from the alkoxide ion attack on the quinones.

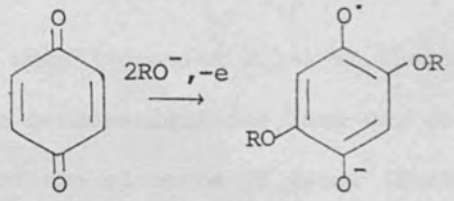

R = Me, Ethyl (2.13)

(VI)

The mechanism of the autoxidation reaction of hydroquinone and of quinone was clarified by Ashworth and Dixon[61a] who made a systematic study using solutions of varying alkalinity. Primary radicals were observed from hydroquinones and quinones in dilute alkali, but in strong alkali, secondary radicals (semiquinones of trihydroxybenzene (VII)) were observed. The following reaction scheme was suggested[61a] to account for the observations.

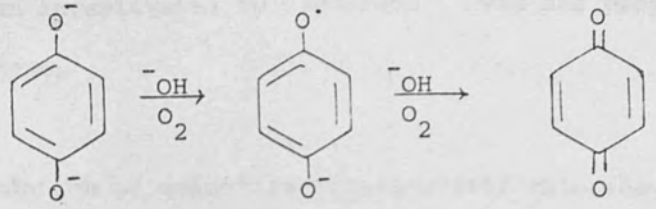

(2.14)

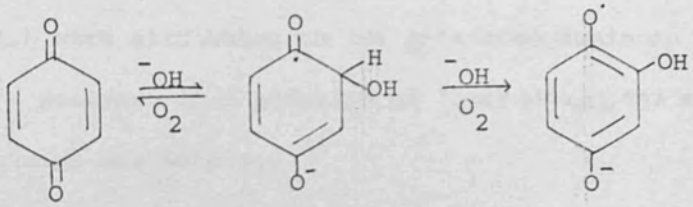

(2.15)

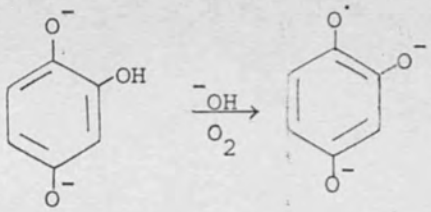

(2.16)

(VII)

The first step (Equation 2.14) in the autoxidation of hydroquinone led to the benzosemiquinone, and was followed by a base-catalysed addition of the elements of water (Equation 2.15). A further attack by oxygen gave the semiquinone of trihydroxybenzene (Equation 2.16)

Dimeric species formed in the autoxidation of hydroquinone or quinone in very strong alkali[61a] were later identified as radicals (VIII) and (IX).[62]

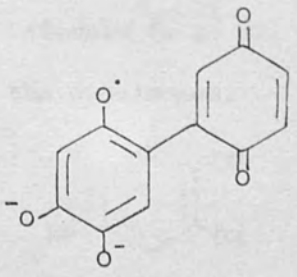

(VIII)

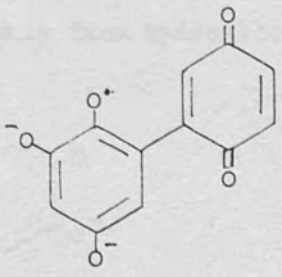

(IX)

The autoxidation of hydroquinones and quinones in aqueous solution has also been investigated by Pedderson[61b] who has proposed a different reaction scheme.

The oxidation of quinol in titanium(III) chloride-hydrogen peroxide at pH∿5 was found to give a spectrum consisting of a mixture of radicals, which were attributed to the p-benzosemiquinone and the adduct (X).[31] However, in a solution of lower pH only the monoprotonated p-benzosemiquinone was detected.[31]

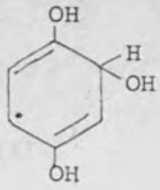

(X)

Irradiation of deoxygenated solutions of quinols in water at pH∿8 results in the formation of benzosemiquinone intermediates.[33]

Although the electronic structure of o-benzosemiquinone has been established since the 1950's, those of the substituted o-semiquinones were only established about ten years later.[54] It was found that when substituted catechols were oxidised in aqueous solution, both primary and secondary radicals could be observed by the conventional static method. However, clear spectra due to primary radicals could only be observed in water if the flow technique was used. The formation of secondary radicals (e.g. XI) arose apparently from hydroxide ion attack on the o-quinones.

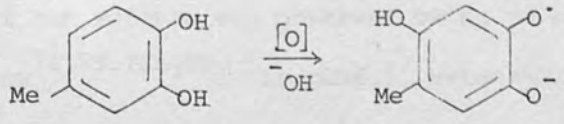

(XI)

The position of attack depends on the nature of the substituents.[54] For p-alkyl-substituted o-quinones, all the ring positions seem liable to be attacked by hydroxyl group while with p-carbonyl substituents, position 3 is more susceptible to nucleophilic attack, owing to the electron withdrawing effect of the carbonyl group.[54] However, for catechol itself, the signal due to the primary radical was later replaced by another signal which was not due to the hydroxylated benzosemiquinone but was apparently due to the dimeric species (XII).[60]

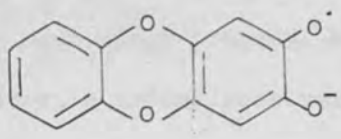

(XII)

m-Benzosemiquinone, the life-time of which is too short-lived to be detected by the static method, has only been observed[53] by means of the rapid mixing technique. The esr parameters for the m-benzosemiquinone[53] showed that about 82% of the spin density was associated with carbon-4 and carbon-6. This value is quite different from those in the o- and p-benzosemiquinones which have about 60 and 65% respectively of the spin density associated with the two oxygen atoms. The esr spectra obtained from resorcinols in acid solution were not as well resolved as in alkaline media, and these have been attributed to the monoprotonated m-benzosemiquinones.[53]

The esr spectra of radicals from various trihydroxybenzenes[34,55,49] have also been observed.

When dihydric phenols were oxidised in solution at varying pH, a variation of esr spectra was observed owing to the protonation of the anionic forms[74,75,76a,79]. At pH∿8.3, benzosemiquinone radical anions

were observed; at pH ∿ 2.2, monoprotonated semiquinones were detected. As the acidity was increased further to pH ∿ 0, esr spectra corresponding to the diprotonated semiquinones were observed. At pH values intermediate between the above mentioned values, alternation of line-widths were observed.[74,75,76a] The diprotonated p-benzosemiquinone has also been observed in aluminium chloride-nitromethane system.[127]

The esr spectrum of 1,4-naphthosemiquinone has been reported several times.[41-46] Wertz and Vivo[63] interpreted the spectrum of 1,4-naphthosemiquinone in terms of two equivalent sets of ring protons: one set consists of two equivalent protons, the other consist of four equivalent protons. Later, a better resolved spectrum which showed the non-equivalence of protons at positions 5,6,7, and 8 was reported by Fraenkel and Vincow.[49] The existence of intramolecular hydrogen bonding in the 1,4-dihydroxy-5,8-naphthosemiquinone was demonstrated by analysis of the esr spectra obtained from the oxidation of this compound in basic media.[64]

The autoxidation of co-enzyme Q10 and Vitamin K in alkaline ethanol solution produced the corresponding semiquinones.[16,37] Freed and co-workers[64] made an even more detailed analysis of the structure of Vitamin E and Q using the electron nuclear double resonance (ENDOR). Their analysis provided satisfactory agreement with molecular orbital calculations and confirmed earlier findings[36,37] that the introduction of a long conjugated chain in semiquinone has little effect on the spin distribution . The structures of some naturally occuring pigments of sea urchins which are naphthoquinone derivatives have been characterised by analysis of the esr spectra of the semiquinones.[65,66] Methoxy proton splittings were observed from a number of alkoxy substituted naphthosemiquinones in which the methoxy group is sterically unhindered.[66b]

The information gained from the study of the autoxidation of hydroquinones and quinones in alcoholic-alkaline media, led Ashworth and Dixon[67] to investigate the autoxidation of hydroxylated naphthalenes under the analogous conditions. It was found that primary radicals were only observed in the autoxidation of 1,2- and 1,4-naphthalenediols, while the dihydroxynaphthalenes with two oxygen atoms in conjugation with each other (except the 2,3-naphthalenediol) gave rise to secondary radicals or complex esr spectra. Other isomers apparently did not undergo autoxidation reactions.[67] However, when the autoxidation was carried out in the presence of hydrogen peroxide, oxidation was found[67] to take place exclusively at the 2-position giving rise to the 1,2-naphthosemiquinones detected by esr. The following reaction scheme was suggested to account for the observation of 1,2-naphthosemiquinones, in which hydrogen peroxide reacts with naphthols in its anionic form.

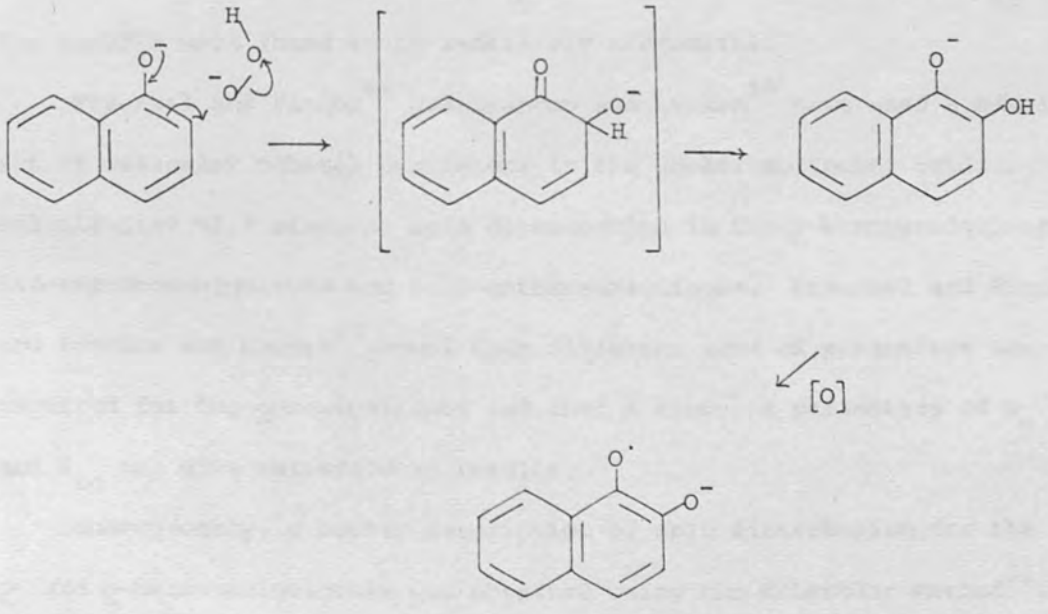

(ii) Theoretical studies of semiquinones

Theoretical interpretations of the esr spectra of semiquinones have been made by using π electron molecular orbital theory and the McConnell relationship.[8] The molecular orbital calculations of semiquinones involve the choice of appropriate parameters for the coulomb integral α_o (ref. page 112) and the resonance integral β_{co}, (ref. page 112) for the oxygen atom and the carbon-oxygen bond respectively.

Bersohn[48] explained the methyl proton hyperfine splittings of toluosemiquinone in terms of the molecular orbital theory of hyperconjugation. He used the parameters $\alpha_o = \alpha + 1.0\beta$, $\beta_{co} = 1.0\beta$ and two values of β_1 (the resonance integral for the bond between the methyl carbon and the ring carbon) as well as Coulson and Crawford's parameters. Bersohn[48] found that the results of $\beta_1 = 0.9\beta$ were better than those of $\beta_1 = 0.7\beta$. Later, Vincow and Fraenkel[49] also performed the Hückel molecular orbital calculations on this radical using various values for the coulomb integral, α_o, and the resonance integral β_{co} The results were found to be moderately successful.

Fraenkel and Vincow[49] and Brandon and Lucken[50] have used a single set of molecular orbital parameters in the Hückel molecular orbital calculations of π electron spin distribution in the p-benzosemiquinone, 1,4-naphthosemiquinone and 9,10-anthrasemiquinone. Fraenkel and Vincow[49] and Brandon and Lucken[50] found that different sets of parameters are required for the o-semiquinones and that a range of parameters of α_o and β_{co} can give satisfactory results.

Subsequently, a better description of spin distribution for the p- and o-benzosemiquinones was obtained using the McLachlan method[52]. The spin density of the carbon atom 3 of the 1,2-benzosemiquinone was predicted to be negative. In addition, good agreement was obtained with experiment for the pyrogallol semiquinone radical anion, where

only poor results could be obtained using Hückel molecular orbital theory. This was because this radical is an odd alternant[124] and therefore negative spin density occurs.[15]

Hückel molecular orbital calculations were performed[51] on a series of chloro- and alkyl-substituted semiquinones previously studied[47] by considering the inductive effects of the substituents. For the methyl-substituted semiquinones, the assignment made by this calculation was found to be in agreement with the additive rule (i.e. the variation of the ring proton splittings and the methyl proton splittings show an additive relationship) suggested by Vincow, Segal and Fraenkel.[47] Their calculations indicated that the inductive effect of the tert-butyl group was greater than that of the methyl group.

Trapp et al[55] have performed HMO calculations on a number of tert-butyl benzosemiquinone using an inductive model for the tert-butyl group. Their results also agreed with earlier findings that the tert-butyl group has a greater inductive effect than methyl.

McLachlan SCF calculations on 1,2,4-trihydroxybenzene and its derivatives were made by Lott et al[56] using the inductive model for the methyl group. Their results were in good agreement with experiment. It was also observed that various pairs of parameters (for α_o and β_{co}) could give satisfactory results for this radical.

The spin density distributions of derivatives of o- and p-benzosemiquinones, 1,2,4- and 1,2,3-trihydroxybenzenes[34] were found to be successfully accounted for by the McLachlan method using the oxygen parameters chosen for the phenoxyl radical (i.e. $\alpha_o = \alpha + 1.6\beta$ and $\beta_{co} = 1.3\beta$).

(iii) Solvent effects on semiquinones

It was reported by Stone and Maki[68] that there is a variation in the ring proton hyperfine splittings of semiquinones in the range of 1 - 45% as the solvent changed from aqueous to aprotic, and that the variation was most marked for the smallest coupling constants. Gendel, Freed and Fraenkel[69] examined solvent effects on the esr spectra of benzosemiquinones using a theoretical approach. It was suggested that the carbonyl group of semiquinone readily interacted with polar solvent molecules by forming radical-solvent complexes, often through hydrogen bonding. This effected a redistribution of spin density in the radical in such a way that the position of the smallest spin density would have a large fractional change, and the spin density on the oxygen atom and the contiguous bonded carbon atom, are subjected to drastic changes. Thus the electronegativity of the oxygen is very sensitive to the polarity of the solvent. As the solvent changes from non-polar to polar, it was noted that the electronegativity of the oxygen atoms in the semiquinone is enhanced, probably due to the formation of radical-solvent complexes. This explanation has been suggested by molecular orbital calculations in which a larger coulomb integral for the oxygen atom is needed to fit the experimental values of semiquinones obtained in polar solvents.[69] Simple esr spectra provided no information about the spin distribution in the carbonyl group. However, more direct information about these spin densities change can be obtained from the measurement of oxygen-17 or carbon-13 interactions. These measurements have been made for the p-benzosemiquinones in a variety of solvents[70-72].

(iv) g-Factors

The g-factors of semiquinones have been reported in a number of articles[40-45] but the theoretical interpretations have only appeared in a few reports.[78,80] Stone has obtained a good correlation between

the g-factors and the energy-level coefficients of the unpaired Hückel molecular orbitals of o- and p- benzosemiquinones. The g-factors of semiquinones in different solvent system have been calculated[80] by using Stone's semi-empirical equation[78] and the results calculated were found to be in satisfactory agreement with experiment.

2.3 Previous esr studies of alkyl aryl ether radical cations

Radical cations of alkoxybenzenes can be produced by flash photolysis, by ultraviolet irradiation[81], by radiolysis[82] of the parent compounds, and also by chemical or electrochemical methods[87].

When simple anisole derivatives are treated in 96% sulphuric acid, protonation is found to occur but no formation of radical cations was observed.[83,84] However, anisole in 98% sulphuric acid containing an oxidising agent gave an esr spectrum identical to that of hydroquinone cation radical.[85] The oxidation of anisole by lead tetraacetate in boron trifluoride gave 4,4'-dimethoxy-biphenyl[86].

In 1964, the esr spectra of the methoxybenzene cation radicals[87] were observed by means of controlled potential electrolysis in the microwave cavity of the esr spectrometer and also by the oxidation of the methoxybenzene in concentrated sulphuric acid. A good correlation between the oxidation potentials and the energy levels of the singly occupied molecular orbitals were obtained. The HMO calculations of these radicals showed that they have almost the same value for the ratios of the methoxy proton splittings to the spin density on the oxygen atom.[87]

Subsequently, Forbes and Sullivan[88] investigated the oxidation of 1,4-dimethoxybenzene in concentrated sulphuric acid by esr, nuclear

magnetic resonance spectroscopy and ultra-violet spectroscopy. They suggested that the observed data were consistent with the reaction scheme as shown below:

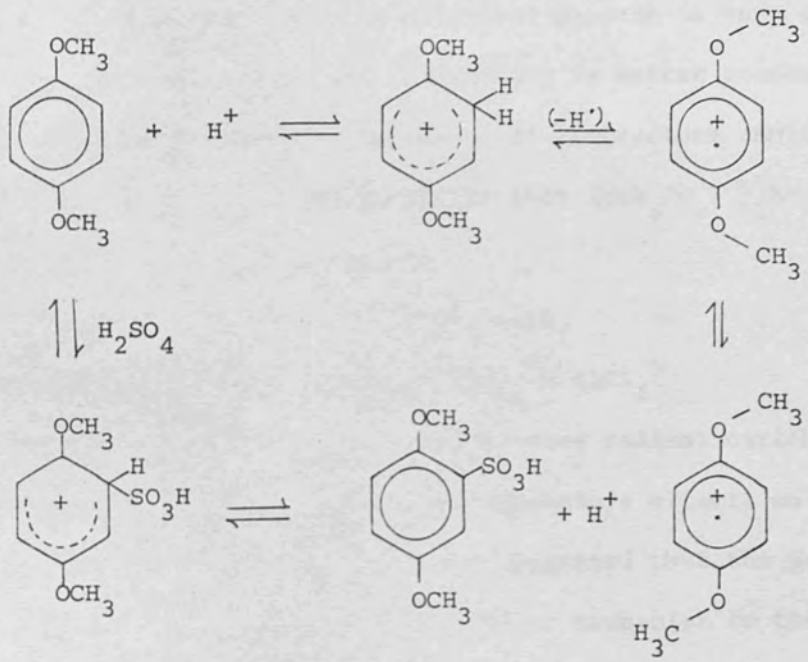

The esr spectra obtained were interpreted in terms of cis - trans isomerism:

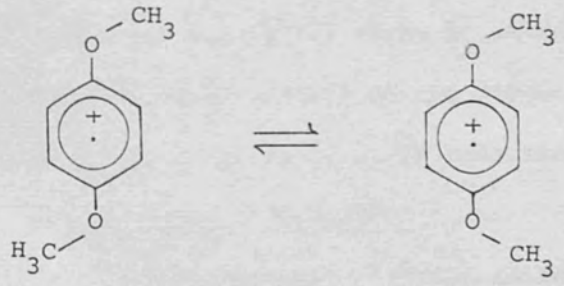

trans cis

The coupling constants of cis- and trans- p-dimethoxybenzene radical cations were assigned by molecular orbital calculations in which α-effects (page 156) were considered, and methoxy groups were treated as two heteroatoms.[88]

Later, Forbes and Sullivan [89] found that the nitro-methane-aluminium chloride system was superior to sulphuric acid for the generation of radical cations because (1) the concentration of radicals generated in this system is higher, (2) the oxidation process is very clean, (3) the esr spectrum obtained at low temperature is better resolved, (4) the study of oxidation over a wide range of temperature could be achieved.

Nishinaga *et al* [90,91] have suggested that $[(CH_3NO_2)]_2AlCl_2^+$ was the oxidising species in this system.

$$CH_3NO_2 + AlCl_3 \longrightarrow CH_3NO_2.AlCl_3 \qquad (2.17)$$

$$2\ CH_3NO_2AlCl_3 \longrightarrow (CH_3NO_2)_2AlCl_2^+ + AlCl_4^- \qquad (2.18)$$

Most of the esr studies of methoxybenzene radical cations were centered on the investigations of the temperature effects on the methoxy proton splittings.[92-97] It was suggested that the methoxy proton splittings arose via hyperconjugation mechanism to the unpaired spin on the oxygen, which is at a maximum when the methoxy group is in the plane of the ring. The coupling constant is given by [88,94,98]

$$a_{OMe} = Q_{OMe}\rho_o \qquad (2.19)$$

where Q_{OMe} = 2.0 mT, ρ_o is the spin density on the oxygen atom. When the methoxy group is twisted out of the plane by an angle θ, the above equation is modified as the spin density on the oxygen changes with θ and this change is supposed to follow a $\cos^2\theta$ relationship [88] i.e. Eq.(2.2).

$$a_{OMe} = Q_{OMe} \times \rho_o \cos^2\theta \qquad (2.20)$$

It was found that the p-dimethoxybenzene radical cation showed *cis-trans* isomerism at room temperature and the methoxy proton splittings were independent of temperature.[92-97] These observations suggested[92-97] that the C-OMe bond has double bond character and therefore rotation of the methoxy group is restricted. In addition it tends to be coplanar with the benzene ring. Thus the methoxy proton coupling constants were calculated using Equation (2.19).

However, the alkoxy proton hyperfine splittings of diethoxynaphthalene, dimethoxyanthracene, diethoxybenzene and higher dialkoxybenzene were temperature dependent[95] indicating the torsional motion of the alkoxy group as the temperature changes, and the alkoxy proton splittings are given by Equation (2.20).

In the molecular orbital calculations of alkoxybenzene radical cations, the methoxy group was treated as two heteroatoms[88] or using the hyperconjugation model[94,98] with the inclusion of α-effect[88,94,98] to simulate the asymmetric ring proton splittings and also to improve the results obtained by the usual method of calculations.

The esr spectra of sulphur analogues of p-dimethoxybenzene and p-diethoxybenzene were interpreted in terms of cis-trans isomerism.[98] It was found that the sulphur atom has a greater spin density than the oxygen. The former was found to have a larger g-factor and a correlation of g-factors of these radicals with spin density on the oxygen and sulphur was obtained.[98]

Recently, the reactions of anisole, dimethoxybenzene, and trimethoxybenzene with Tl^{2+}, Ag^{2+}, $SO_4^{\cdot-}$ and $\dot{O}H$ respectively were investigated[101] in aqueous solution using optical and conductometric pulse radiolysis and in situ radiolysis using esr for detection. It was deduced that 1,2-dimethoxybenzene (XIII), 1,3-dimethoxybenzene (XVI) and the 1,2,3-trimethoxybenzene (XV) exist in only one isomeric form.

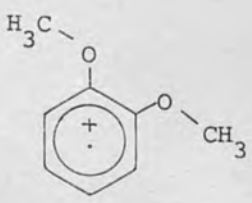

(XIII)

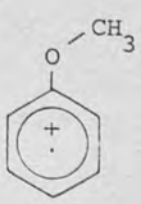

(XIV)

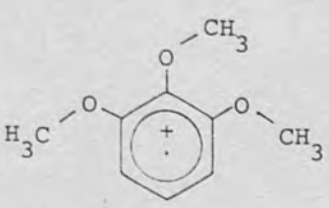

(XV)

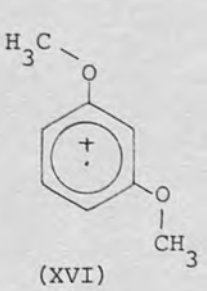

(XVI)

The esr spectrum of the anisole radical cation also showed non-equivalence of ring proton splittings, indicating the restricted rotation of the methoxy group about the C-OMe bond.

More recently, a novel method for the generation of alkyl aryl ether radical cations has been reported.[102] The radical cations were generated by Ce(IV) in sulphuric acid solution (H_2SO_4, $4H_2O$) in a flow system. The spin density distributions and g-factors of methoxybenzene radical cations are similar to those in the corresponding phenol radical cations. The 1,3-benzodioxole radical cations show large methylene proton hyperfine splittings[102] which can be explained in terms of hyperconjugation theory. The assignment of the large coupling constants were made by comparison with those in the corresponding phenoxyl radicals or semiquinones while the small splittings were assigned by graphical methods.

2.4 Object of research

Although the autoxidation of sterically hindered phenols and dihydric phenols has received a great deal of attention, the corresponding reaction of sterically unhindered phenols has not so far been made. It was our hope therefore to investigate the autoxidation of phenols in hexamethylphosphoramide (HMPA) in which many autoxidation reactions have been studied.

Since the autoxidation of naphthols in ethanolic media was found to be complex, we resorted to the use of an aprotic solvent, HMPA, hoping to obtain a clean reaction.

The previous calculations of spin distributions of phenoxyl radicals by the McLachlan method was extended to include calculations of aliphatic proton splittings in methyl- and methoxy-substituted phenoxyl radicals. The failure to find an appropriate parameters for the heteroatom model for the aldehyde group gave us the challenge of finding a different model.

The esr spectra of alkyl aryl ether radical cations have not been explained theoretically, so it is of great interest to perform molecular orbital calculations for these radicals and compare the theoretical results with experiment. Since the McLachlan method has been found to be successful in the calculations of phenoxyl radicals, this gave us confidence in using this method again in these calculations.

The theoretical interpretations of g-factors remain as a virgin field. It is our fervent hope to explore the possibility of obtaining quantitative values of g-factors for the phenoxyl radicals, phenol radical cations and alkyl aryl ether radical cations, and to obtain correlation of g-factors with the energy level coefficients of the Hückel molecular orbital containing the unpaired electron and with the spin densities on the oxygen atoms.

CHAPTER 3

THE ELECTRON SPIN RESONANCE SPECTRA OF RADICALS FORMED IN THE AUTOXIDATION OF PHENOLS

3.1 Introduction

The work reported in this chapter arose from the hope of gaining more information about factors controlling autoxidation of phenolic compounds and dihydroaromatics in hexamethylphosphoramide $[(CH_3)_2N]_3PO$ (HMPA).[103] The situation of solute molecules would be very different from that in water, for HMPA is a highly polar aprotic solvent and is also stable towards base and oxygen. It has been used successfully as a medium for the study of autoxidation reaction.[103,104]

3.2 Experimental

All of the compounds studied were commercially available and were purified by the usual methods. The author is indebted to Dr. D.Murphy for providing pure specimens of many of the compounds studied.

Commercial HMPA was purified by distillation from a solution containing sodium metal (2.0 g/3500 cm^3) when it was collected as a colourless liquid, b.p. 65^o (0.4 mm Hg) (lit.[103] $68-70^o$ (1 mm Hg)). The distilled HMPA was finally stored over Linde 13X molecular sieve.

Esr spectra were recorded using a Varian E4 spectrometer with a magnetic field strength of about 395 mT, 100 KHz field modulation and a microwave frequency of about 9.5 GHz.

Esr spectra were obtained by dissolving 20 mg of the starting material in about 10 cm^3 of the solvent. Then about 50 mg of powdered sodium methoxide or potassium tert-butoxide were added with stirring. This mixture was transferred to an aqueous cell and placed in the cavity of the esr spectrometer. The esr spectrum was then scanned at appropriate intervals.

3.3 Results and analysis of esr spectra

The proton hyperfine splitting constants of semiquinones produced by the autoxidation of naphthols, phenols and dihydroaromatics in HMPA containing sodium methoxide or potassium tert-butoxide are given in Tables I and II respectively (pages 60 and 61-62). Table III, (pages 63-64), contains coupling constants of alkyl-substituted semiquinones produced by the autoxidation of alkyl-substituted phenols and resorcinols. Table IV (page 65) shows the coupling constants of radicals formed by the autoxidation of alicyclic compounds.

The assignments of the coupling constants of semiquinones were made by comparing with values in aqueous media, allowing for solvent effects.

A. Autoxidation of naphthols

(i) Autoxidation of α- and β-naphthol

When the solution of HMPA containing α- or β-naphthol was treated with sodium methoxide and the solution was shaken in air, no change in colour was observed in the solution and no esr signal was detected at first . However, after an induction period of about an hour, both naphthols gave rise to identical esr spectra (as can be seen from Fig. 1(a) and 1(b)), accompanied by a blue fluorescence around the sodium methoxide particles. In the case of α-naphthol, this radical decayed after a few minutes and was replaced by a weaker but well defined spectrum (Fig. 1(c)) consisting of three groups of lines with relative intensities (1:2:1) separated at 0.330 mT. Within each group there were nine lines with intensity ratios approximately (1:2:1:2:4:2:1:2:1) corresponding to coupling constants a_H = 0.025 mT (two equivalent protons) and 0.065 mT (two equivalent protons).

Table I

Esr parameters (a/mT) of radicals from autoxidation of naphthols in HMPA in the presence of NaOMe or $KOBu^t$.

Positions of oxygens (i) in radical	(ii) in precursor	a_1	a_2	a_3	a_4	a_5	a_6	a_7	a_8	a_H
1,2-	1-,2-, 1,2-			0.038	0.405	0.075	0.152	0.038	0.115	
1,2,4-	1,3-, 1,2,4-			0.035		0.060	0.245	0.060	0.155	
1,2,3,4-	1,3-					0.095	0.122	0.122	0.095	
1,2,6- †	1,6-, 2,6-			0.035	0.525	0.110		0.010	0.190	
1,2,7- †	1,7-, 2,7-			0.048	0.460	0.0	0.268		0.085	
1,4-	1-, 1,4-		0.330	0.330		0.025	0.065	0.065	0.025	
1,4,5-	1,5-, 1,4,5-		0.245	0.420			0.085	0.065	0.100	0.035
1,4,6-	1,6-, 1,7-		0.330	0.220		0.048		0.096	0.048	
2,6-	2,6-	0.425		0.130	0.070	0.425		0.130	0.070	
1,7-	1,7-		0.020	0.345	0.135	0.0	0.120		0.930	
1,5-	1,5-		0.380	0.055	0.525		0.380	0.055	0.525	

* Where a precursor is autoxidised to a mixture of 1,2- and 1,4-naphthosemiquinones the signal from the 1,4-semiquinone is seen after the decay of the spectrum of the 1,2-semiquione.

† Obtained using $KOBu^t$/HMPA only; use of NaOMe gives sodium splittings, a_{Na} = 0.040 mT

Table II

Esr parameters (a/mT) of semiquinones produced by autoxidation in HMPA in the presence of NaOMe or $KOBu^t$

Radical	Starting materials	a_1	a_2	a_3	a_4	a_5	a_6	a_7	a_8
1,2-benzo-semiquinone	phenol, catechol, 1,2-benzoquinone			0.110	0.350	0.350	0.110		
1,4-benzo-semiquinone	phenol, hydroquinone, 1,4-benzoquinone, and 1,4-dihydrobenzene		0.240	0.240		0.240	0.240		
2-hydroxy-1,4-benzosemiquinone	resorcinol, 1,2,4-trihydroxybenzene			0.055		0.490	0.140		
1,2-naphtho-semiquinone	1,2-dihydro-naphthalene			0.038	0.405	0.075	0.152	0.038	0.115
9,10-anthra-semiquinone	9,10-anthraquinone, 9,10-dihydroxy-anthracene, anthrone	0.024	0.100	0.100	0.024	0.024	0.100	0.100	0.024

Table II contd.

Radical	Starting material	Coupling constants (a/mT)
pyrene-4,5-semiquinone	4,5-dihydropyrene	0.015 (×2), 0.085 (x2), 0.185 (x2), 0.330 (x2)

Table III

Esr parameters (a/mT) of semiquinones produced by autoxidation of alkyl substituted phenols and resorcinols in HMPA in the presence of NaOMe or $KOBu^t$.

Radical	Starting material	a_2	a_3	a_4	a_5	a_6
4-methyl-1,2-benzosemiquinone	4-methylphenol, 4-methylcatechol		0.075	a_{Me} = 0.410	0.360	0.155
2-methyl-1,4 benzosemiquinone	2-methylphenol, 2-methylhydroquinone, 2-methylquinone	a_{Me} = 0.183	0.200		0.270	0.245
2-hydroxy-5-methyl-1,4-benzosemiquinone	4-methylresorcinol		0.050		a_{Me} = 0.50	0.085
2-hydroxy-6-methyl-1,4-benzosemiquinone	5-methylresorcinol		0.050		0.430	a_{Me} = 0.090

Table III contd.

Radical	Starting material	a_2	a_3	a_4	a_5	a_6
3-methyl-1,2-benzosemiquinone	3-methylcatechol		a_{Me} = 0.105	0.360	0.290	0.110
2-tert-butyl-1,4-benzosemiquinone	2-tert-butylphenol, 2-tert- butyl-1,4-benzoquinone, 2-tert-butylhydroquinone		0.180		0.210	0.290

Table IV

Esr parameters of radicals produced by autoxidation of alicyclic compounds in HMPA in the presence of NaOMe or $KOBu^t$.

Radical	Starting material	Coupling constants (a/mT)
cyclopentane-1,2-semidione	cyclopentanone	0.663 (×2), 0.963 (×2)
3-methyl-cyclopentane-1,2-semidione	3-methyl-cyclopentanone	0.563 (×3), 0.275 (×2), 0.675 (×2)
cyclohexane-1,2-semidione	1,2-cyclohexanone, 2-hydroxy-cyclohexanone	0.996 (×4), a_{Na} = 0.040
cycloheptane-1,2-semidione	cycloheptanone	0.200 (×2), 0.700 (×2)
Indane-1,2-semidione	1-indanone, 2-indanone	0.295, 0.290, 0.050, 0.075, a_{CH_2} = 0.275

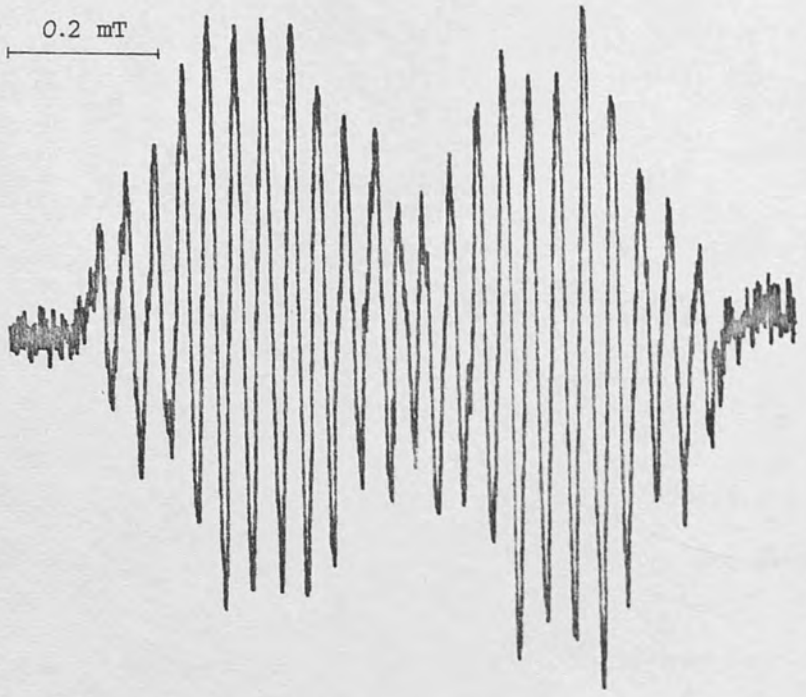

Fig. 1(a). 1,2-Naphthosemiquinone from α-naphthol.

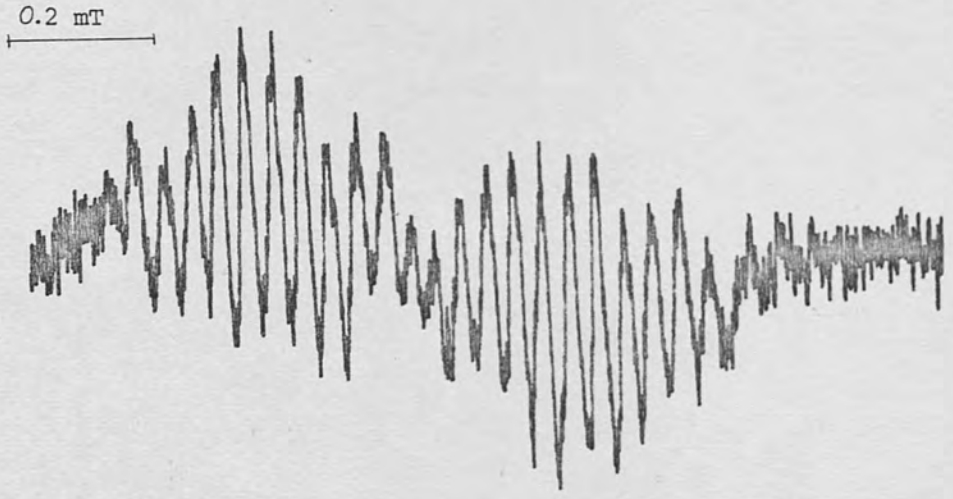

Fig. 1(b). 1,2-Naphthosemiquinone from β-naphthol

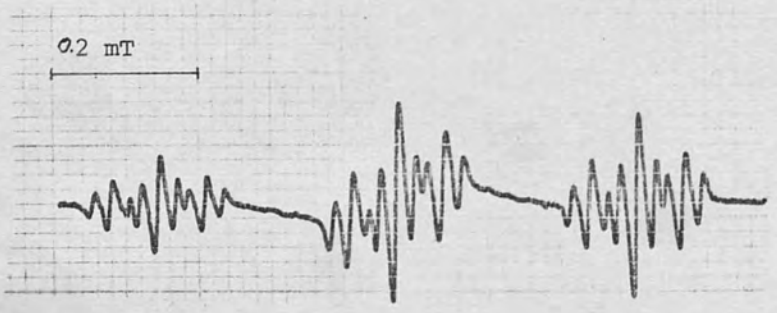

Fig. 1(c). 1,4-Naphthosemiquinone from α-naphthol

The fact that both α- and β-naphthols gave identical esr spectra suggested that they had gone through the same intermediate during the reaction. A careful analysis of the spectrum (Fig. 1(a)) showed that the odd electron coupled with four non-equivalent protons (a_H = 0.075 mT, 0.405 mT, 0.152 mT, 0.115 mT) and two equivalent protons (a_H = 0.038 mT) instead of seven protons which are present in the starting materials. This suggested that some reaction had been taken place, either oxidation (replacement of hydrogen by oxygen), or some other reactions involving the displacement of hydrogen by some species present in the reaction medium.

In order to deduce the structure of the first radical observed, 1,2-dihydroxynaphthalene and 1,2-naphthoquinone which on autoxidation gave the primary radical 1,2-naphthosemiquinone in aqueous media,[67] were treated under the same conditions. It was found that they both gave the spectrum shown in Fig. 2(a) which was identical to that obtained from α- and from β-naphthol. Therefore the esr spectrum obtained from β-naphthol and the first spectrum from α-naphthol was that of 1,2-naphthosemiquinone.

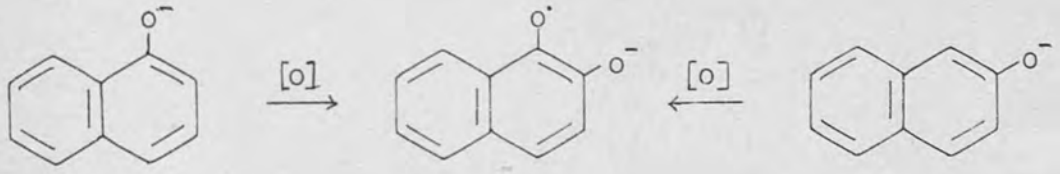

The assigned coupling constants (a/mT) are:

a_3	a_4	a_5	a_6	a_7	a_8
0.038	0.405	0.075	0.152	0.038	0.115

Comparing with those in aqueous media[67]:

a_3	a_4	a_5	a_6	a_7	a_8
0.042	0.446	0.028	0.142	0.014	0.130

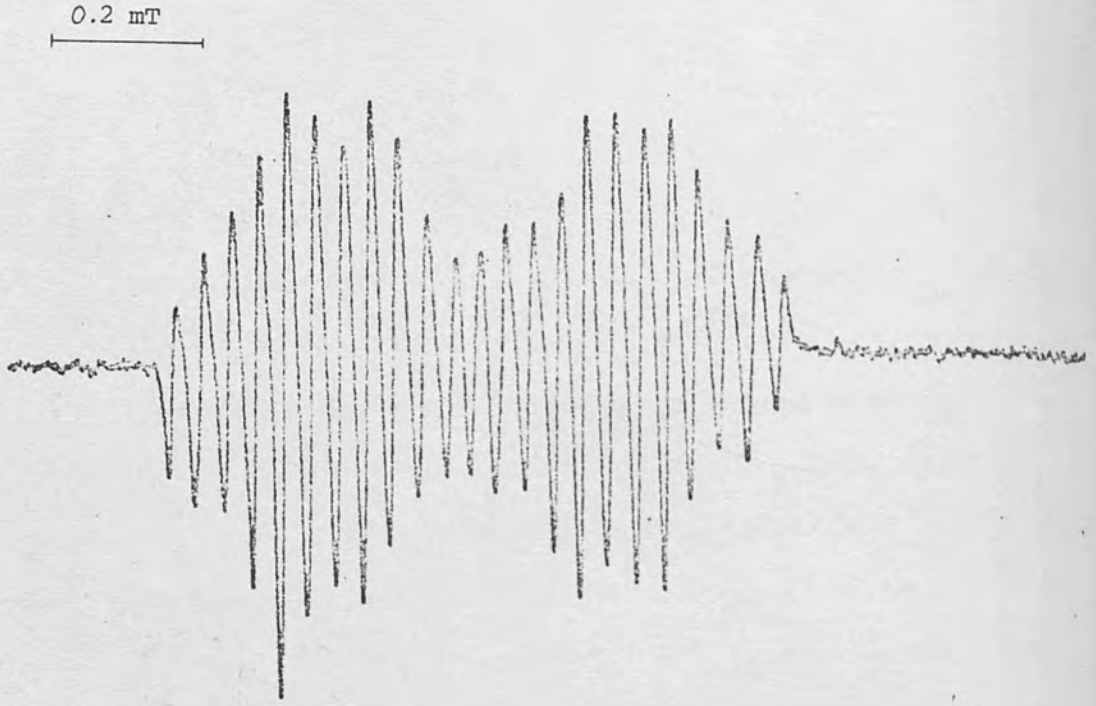

Fig. 2(a). 1,2-Naphthosemiquinone from 1,2-dihydroxynaphthalene

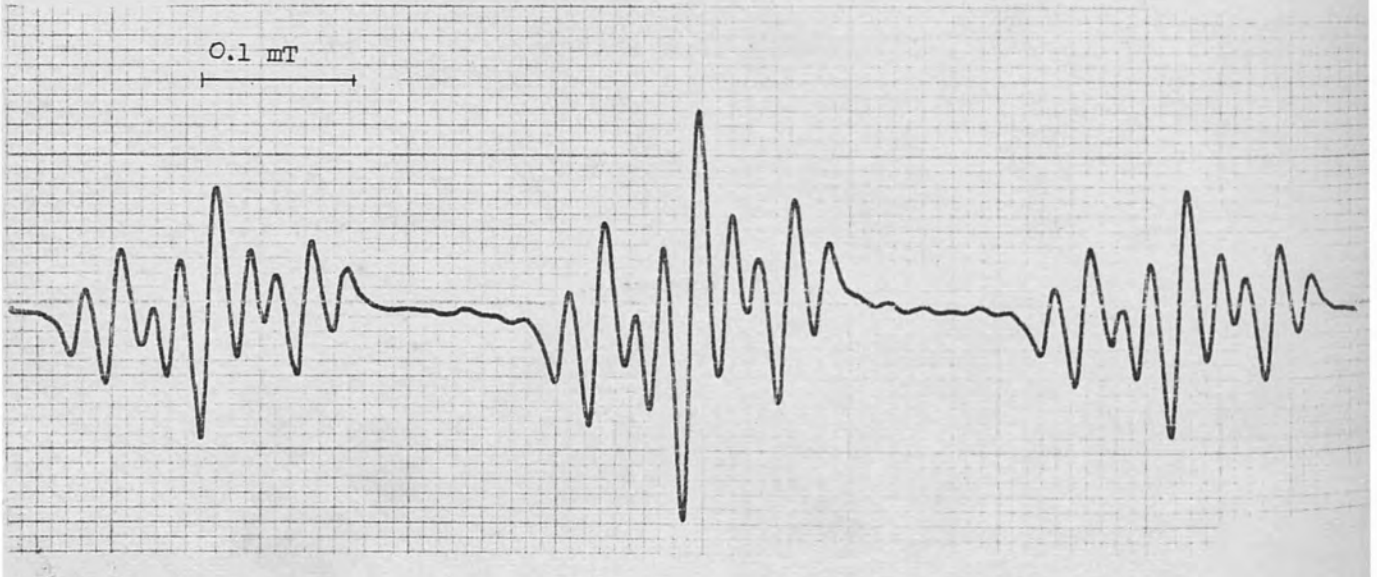

Fig. 2(b). 1,4-Naphthosemiquinone from 1,4-dihydroxynaphthalene.

it can be seen that the coupling constants are quite different in the two solvent systems.

To identify the structure of the second radical observed from α-naphthol, 1,4-dihydroxynaphthalene or 1,4-naphthoquinone were treated under the same conditions. They both gave esr spectra (Fig. 2(b)] identical to the second spectrum obtained from α-naphthol (i.e. Fig.1(c)]. Consequently the radical observed was 1,4-naphthosemiquinone.

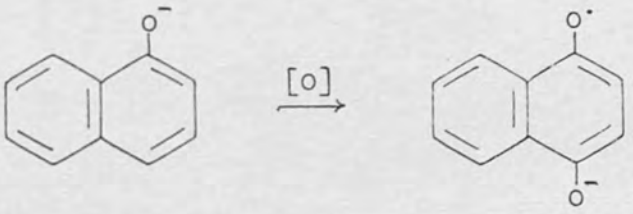

The coupling constants assigned by comparison with those in aqueous media[67], allowing for solvent effects are listed below:

a_2	a_3	a_5	a_6	a_7	a_8
0.330	0.330	0.025	0.065	0.065	0.025

The coupling constants in aqueous solution are listed below for comparison.

a_2	a_3	a_5	a_6	a_7	a_8
0.324	0.324	0.065	0.058	0.058	0.065

The formation of 1,2- and 1,4-naphthosemiquinones from different starting materials are summarised diagramatically as follows:

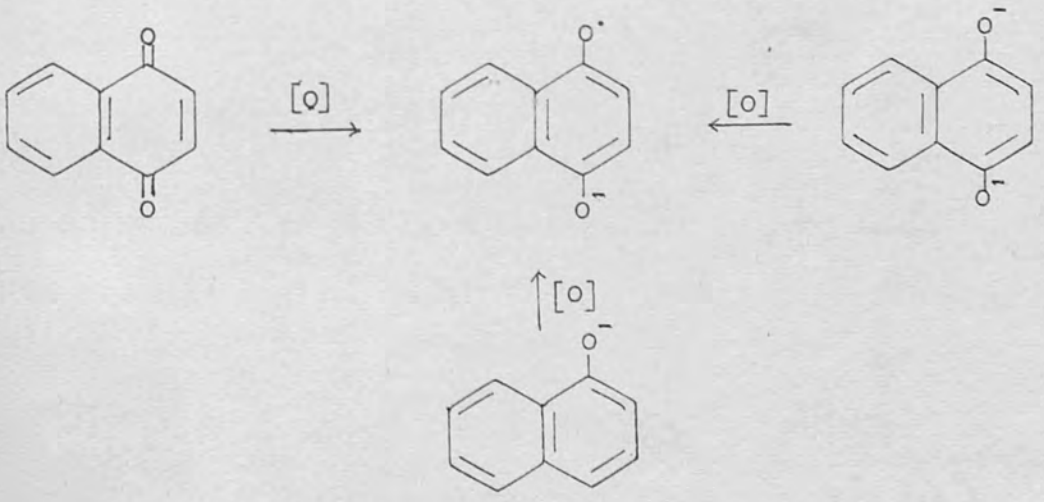

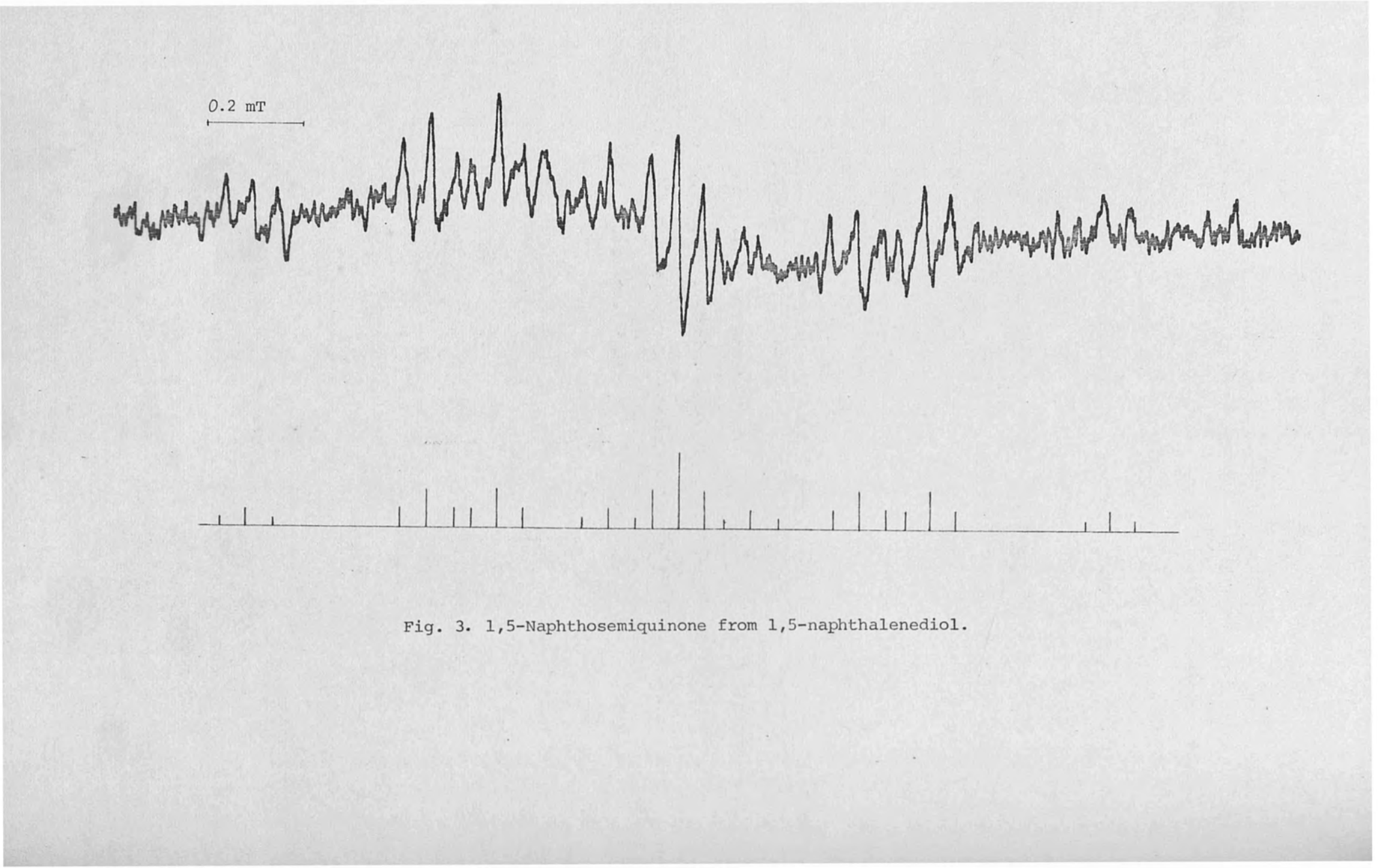

Fig. 3. 1,5-Naphthosemiquinone from 1,5-naphthalenediol.

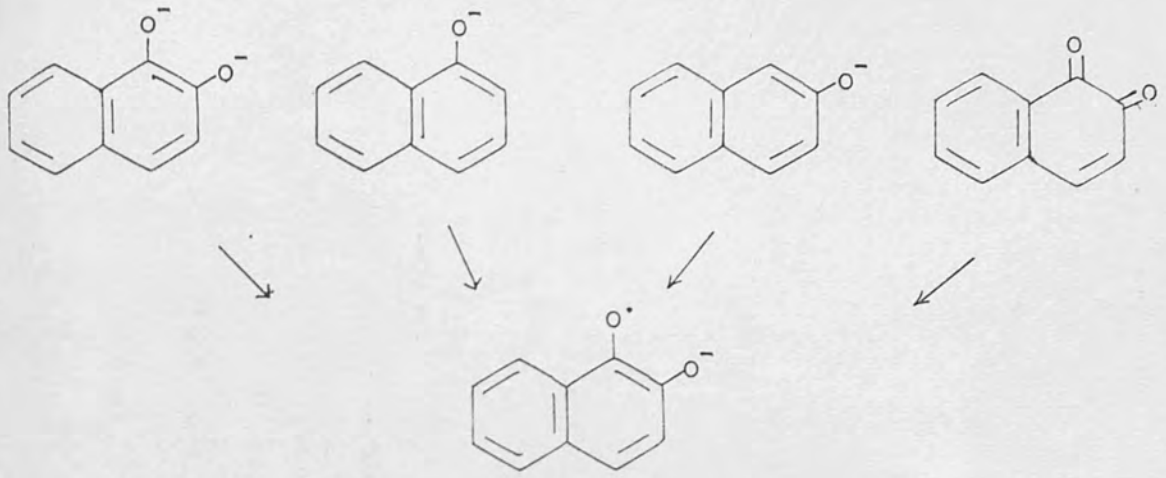

1,2-Naphthosemiquinone

(ii) Autoxidation of naphthalenediols

1,5-naphthalenediol

When the 1,5-naphthalenediol was oxidised in HMPA containing potassium tert-butoxide, the esr spectrum shown in Fig. 3 was observed instantaneously and decayed after about two minutes. The spectrum consists of three sets of triplets indicating the spin being coupled with three pairs of equivalent protons. This is attributed to the primary radical 1,5-naphthosemiquinone

with assigned coupling constants

a_2	a_3	a_4	a_6	a_7	a_8
0.380	0.055	0.525	0.380	0.055	0.525

Immediately after the decay of this transient primary radical, another esr spectrum (Fig. 4(a)) was detected and a violet fluorescence was observed. This spectrum was identical to that obtained from juglone (A) (see Fig. 4(b)) when it was oxidised in HMPA containing sodium

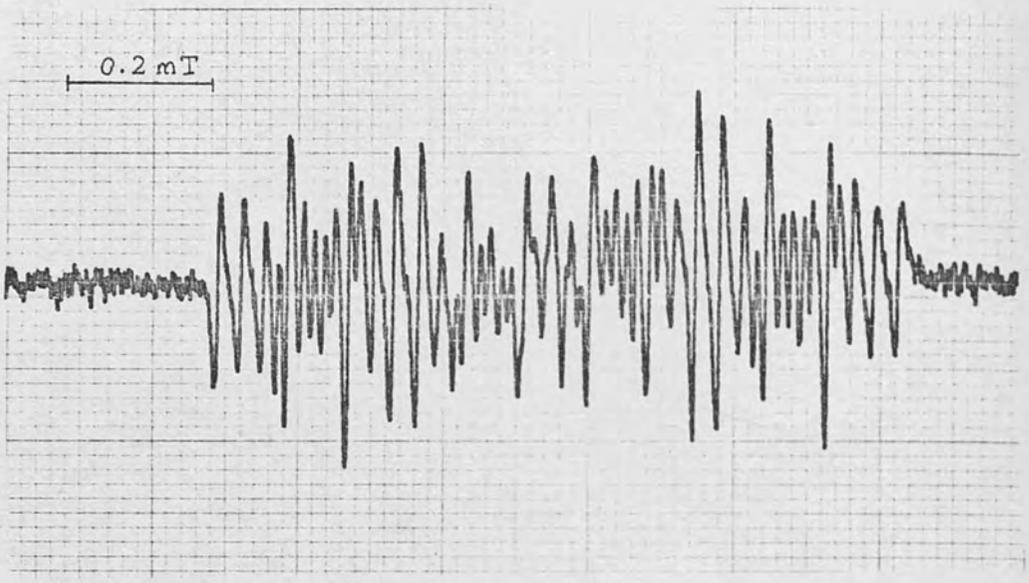

Fig. 4(a). 5-Hydroxy-1,4-naphthosemiquinone from 1,5-naphthalenediol.

Fig. 4(b). 5-Hydroxy-1,4-naphthosemiquinone from juglone.

methoxide. This suggested that oxidation had taken place at the 4-position and not at the 2-position as is usually the case.[110] The fact that only the 1,4-naphthosemiquinone was detected could possibly be due to the extra stability which is provided by the peri-hydrogen[113] or due to the stability of the 1,4-naphthosemiquinone.

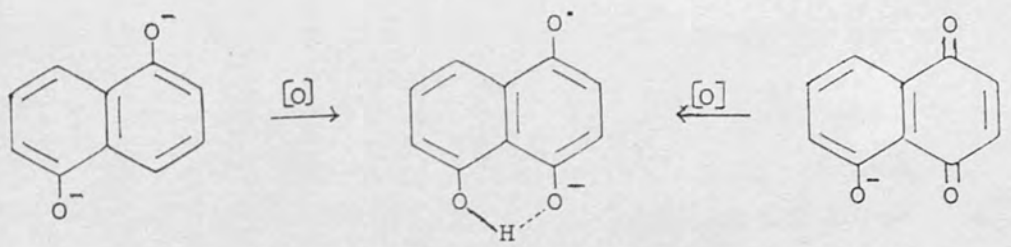

(A)

The ring proton hyperfine splittings are:

a_2	a_3	a_6	a_7	a_8
0.245	0.420	0.085	0.065	0.100

and with a small peri-hydrogen splitting of 0.035 mT. In aqueous solution, the peri-hydrogen splitting was 0.080 mT[67] and the ring proton coupling constants[67] listed below are also differed from those in HMPA.

a_2	a_3	a_6	a_7	a_8
0.390	0.270	0.080	0.030	0.112

Thus:

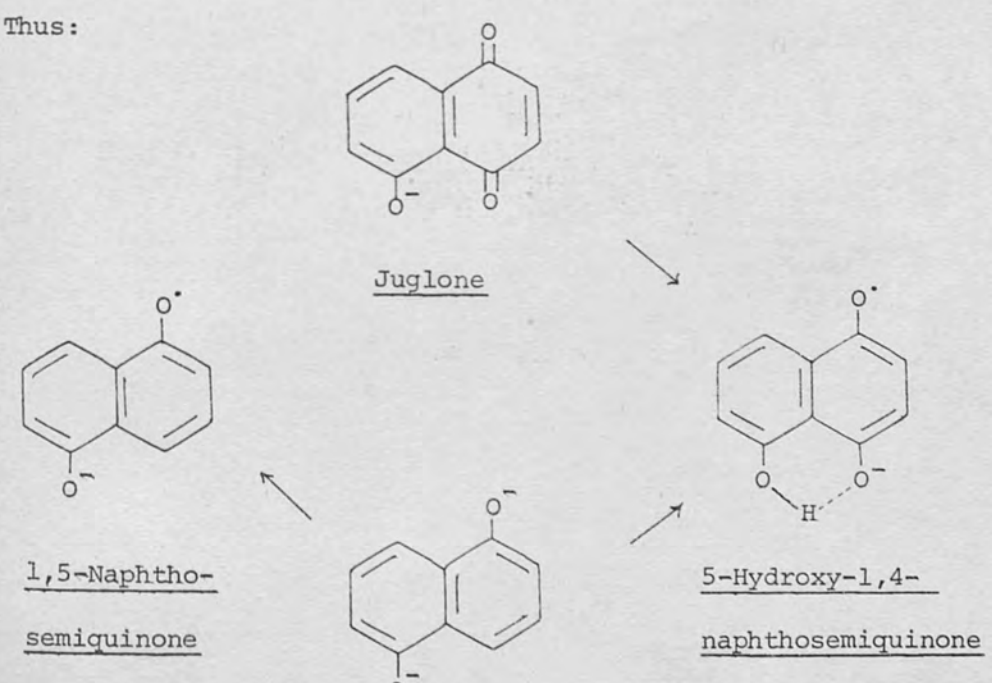

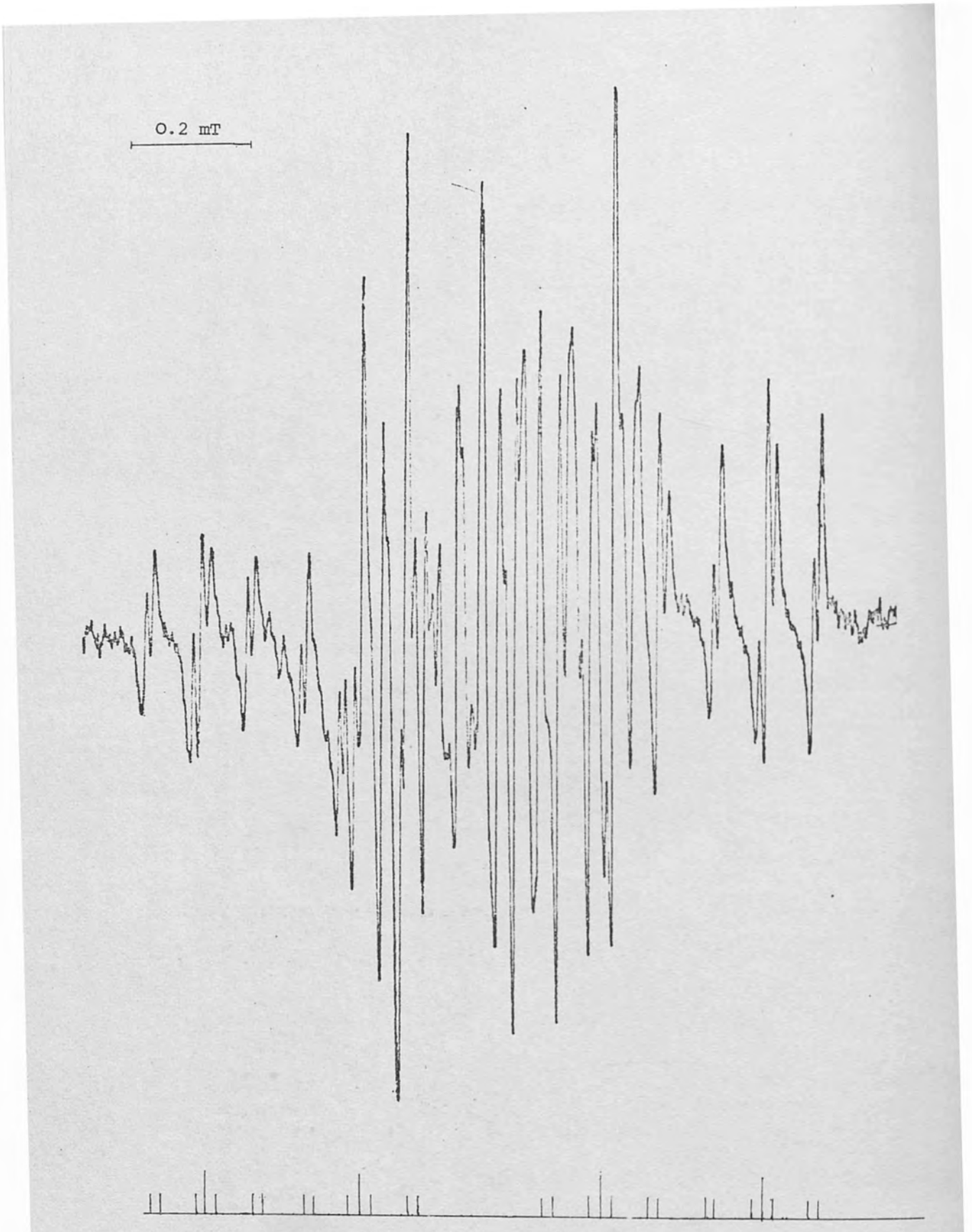

Fig. 5. 1,7-Naphthosemiquinone from 1,7-naphthalenediol.

1,7-Naphthalenediol gave a mixture of signals instantaneously but 28 lines could be picked out and assigned to the primary radical 1,7-naphthosemiquinone. The spectrum is shown in Fig. 5.

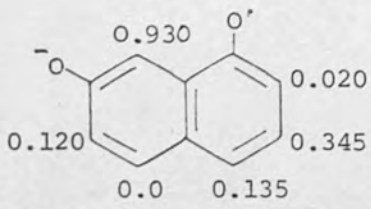

The signal due to the primary radical decayed after a few minutes and was replaced by a complex spectrum due to the presence of sodium metal splittings when sodium methoxide was used as a base. However, the spectrum was not so complicated in this way when potassium tert-butoxide was used, and was ascribed to the secondary radical 7-hydroxy-1,2-naphthosemiquinone (see Fig. 6).

Solvent	a_3	a_4	a_5	a_6	a_8
HMPA	0.048	0.460	0.0	0.268	0.085
Water[61a]	0.048	0.447	0.048	0.243	0.102

This radical decayed after a few minutes and was replaced by another spectrum which was attributed to the radical 7-hydroxy-1,4-naphthosemiquinone.

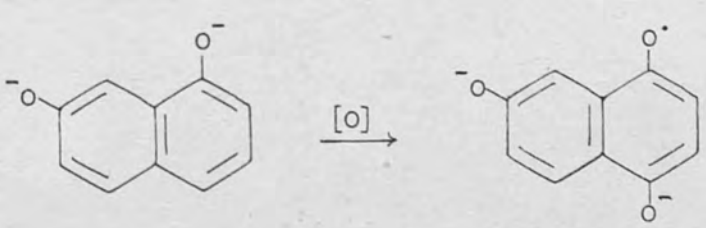

Solvent	a_2	a_3	a_5	a_6	a_8
HMPA	0.330	0.220	0.048	0.096	0.048
Water[61a]	0.442	0.278	0.0	0.164	0.600

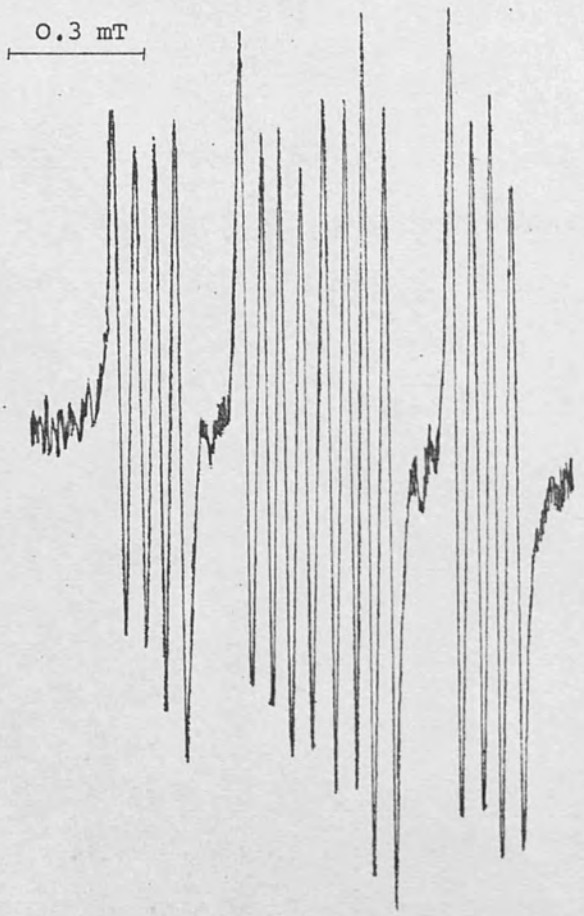

Fig. 6. 7-Hydroxy-1,2-naphthosemiquinone from 1,7-naphthalenediol

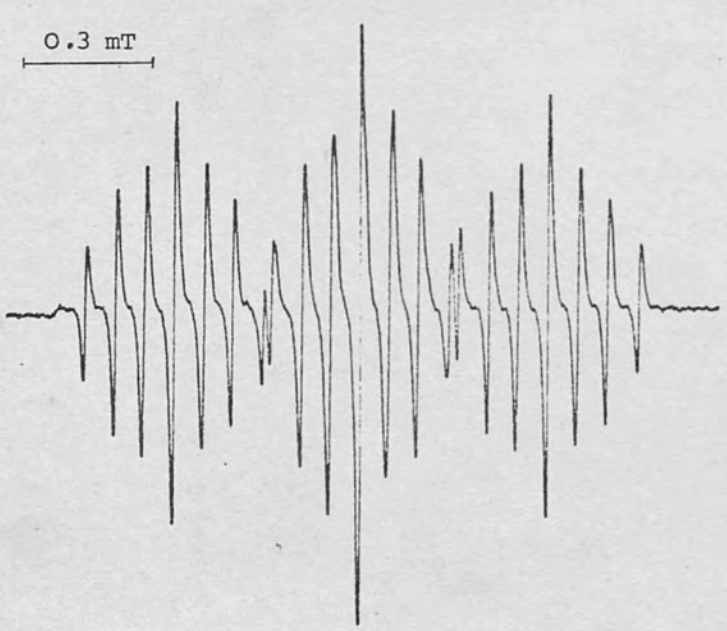

Fig. 7. 2,6-Naphthosemiquinone from 2,6-naphthalenediol.

2,6-Naphthalenediol

On autoxidation, 2,6-naphthalenediol spontaneously formed a radical whose well defined esr spectrum is shown in Fig. 7. The spectrum exhibted three pairs of equivalent protons, a_H = 0.07(×2), 0.13(×2), and 0.425 mT(×2) due to the primary radical 2,6-naphthosemiquinone ('amphi'-naphthosemiquinone)

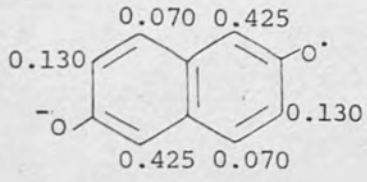

After about 15 minutes, it was replaced by another spectrum (Fig. 8), consisting of a large doublet (a_H = 0.525 mT) which is further resolved into eight broad lines of equal intensity indicating a further hyperfine coupling with three non-equivalent protons. This is attributed to the 6-hydroxy-1,2-naphthosemiquinone formed by the oxidation at the 1-position as in β-naphthol.

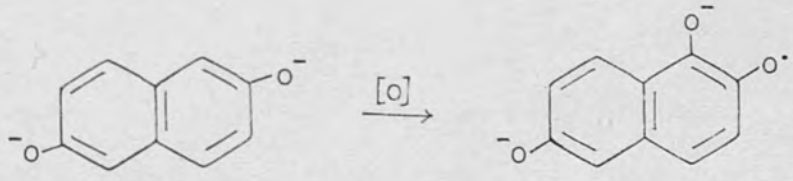

The proton coupling constants are assigned as follows:

a_3	a_4	a_5	a_7	a_8
0.035	0.525	0.110	0.010*	0.190

* a_7 = 0.010 mT inferred from the broad lines.

1,3-Naphthalenediol

Red fluorescence was observed after an induction period of about an hour and an esr signal, shown in Fig. 9 was detected. The hyperfine

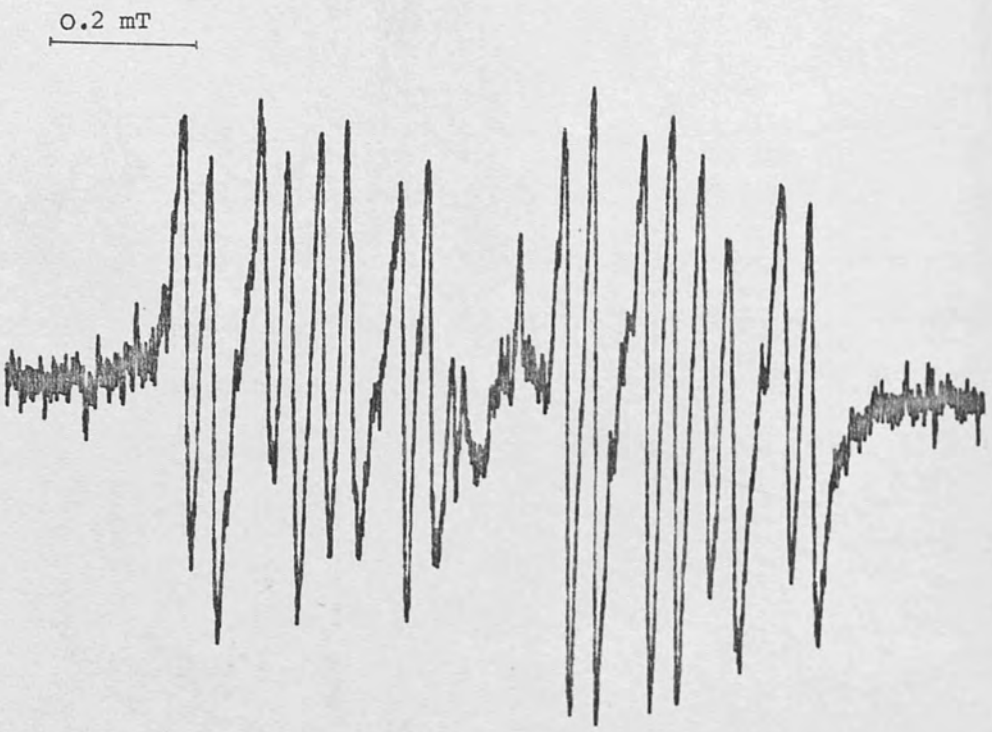

Fig. 8. 6-Hydroxy-1,2-naphthosemiquinone from 2,6-naphthalenediol

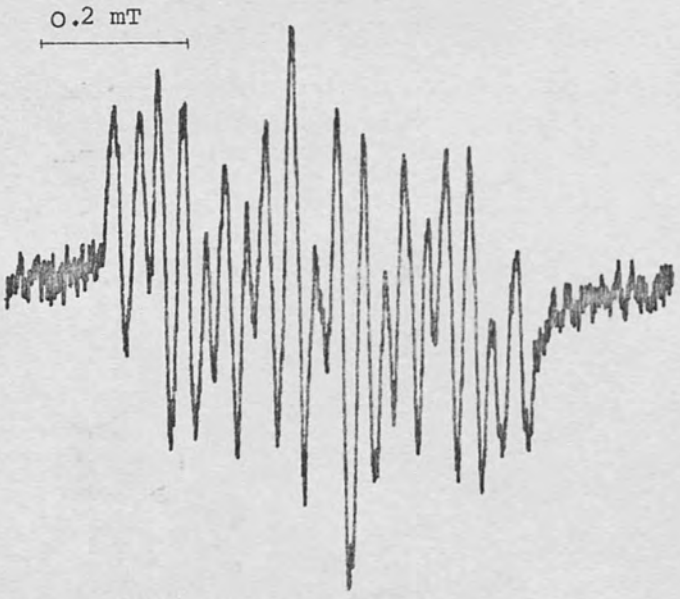

Fig. 9. 2-Hydroxy-1,4-naphthosemiquinone from 1,3-naphthalenediol.

splitting constants are 0.035, 0.060 (×2), 0.045, 0.155 mT. The absence of a large coupling constant in the radical indicated that the hydrogen at position-4 could possibly be replaced by an oxygen. This was confirmed when an identical spectrum was obtained from the 1,2,4-trihydroxynaphthalene. Thus the radical observed was due to the 2-hydroxy-1,4-naphthosemiquinone.

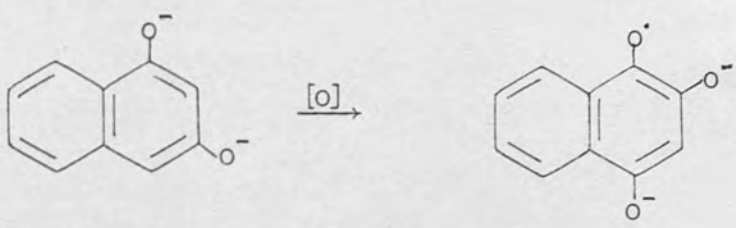

Solvent	a_3	a_5	a_6	a_7	a_8
HMPA	0.035	0.060	0.245	0.060	0.155
Water[61a]	0.025	0.013	0.197	0.011	0.154

From the above results, it is obvious that the coupling constants are quite different in the two solvent system.

The spectrum was then replaced by a simpler one consisting of a triplet of triplets, indicating there are two pairs of equivalent protons. This suggested that further oxidation had been taking place at the 3-position forming 2,3-dihydroxy-1,4-naphthosemiquinone.

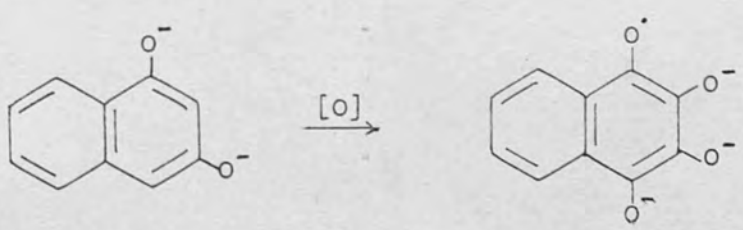

Solvent	a_5	a_6	a_7	a_8
HMPA	0.095	0.122	0.122	0.095
Water[61a]	0.103	0.073	0.073	0.103

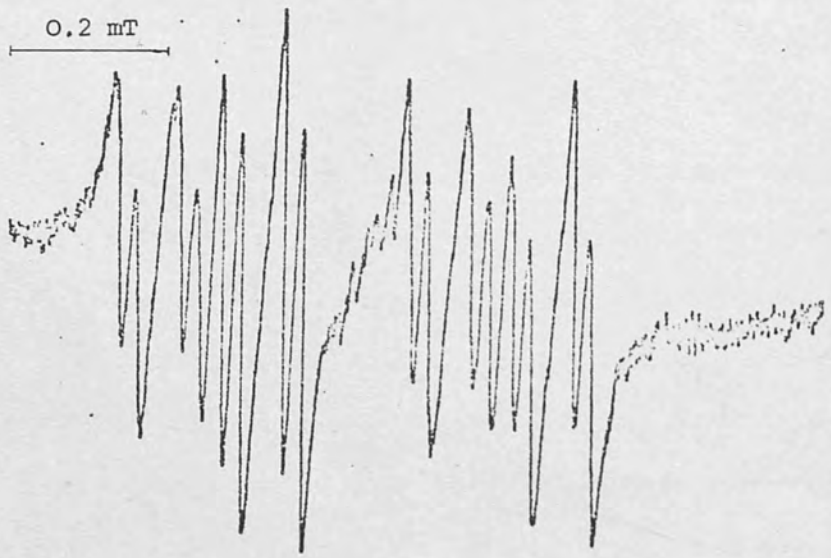

Fig. 10. 6-Hydroxy-1,2-naphthosemiquinone from 1,6-naphthalenediol

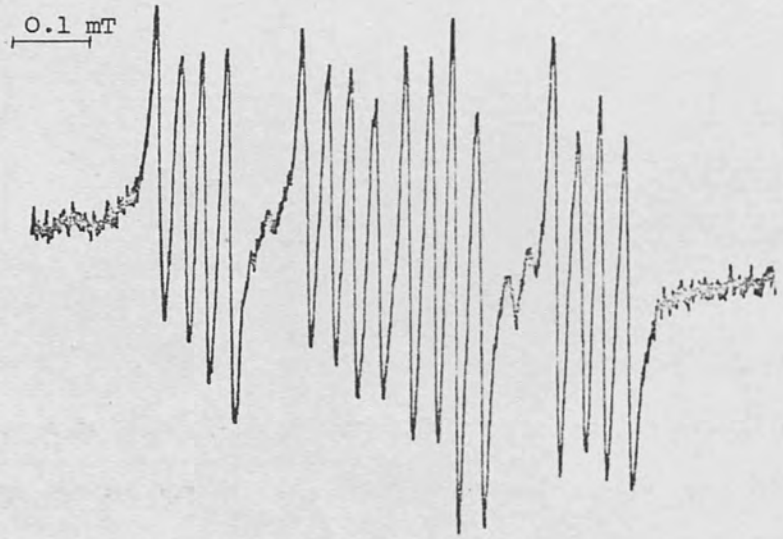

Fig. 11. 7-Hydroxy-1,2-naphthosemiquinone from 2,7-naphthalenediol

Fig. 13. Radical from 1,8-naphthalenediol

1,6-Naphthalenediol

After an induction period of about 30 minutes, the 1,6-naphthalenediol showed a greenish fluorescence and gave a spectrum (Fig. 10) identical to the second spectrum (i.e. Fig. 8) obtained from the 2,6-naphthalenediol. Therefore the 1,6-naphthalenediol had been oxidised at the 2-position to give 6-hydroxy-1,2-naphthosemiquinone. This signal then decayed to afford another spectrum which was identical to that of 7-hydroxy-1,4-naphthosemiquinone obtained previously. This showed that oxidation had also taken place at the 4-position at the later stage of the autoxidation.

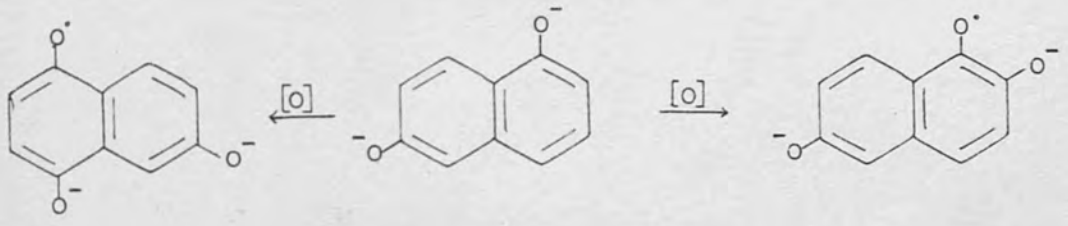

2,7-Naphthalenediol gave an esr spectrum (Fig. 11) which was accompanied by a green fluorescence, and was identical to the second spectrum obtained from the 1,7-naphthalenediol (see Fig. 6). Therefore the radical observed was the 7-hydroxy-1,2-naphthosemiquinone.

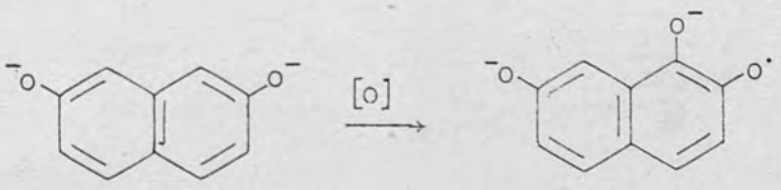

The autoxidation of 1,8- and 2,3-naphthalenediol in HMPA containing NaOMe or KOBu^{t} salt gave only weak esr spectra (Fig. 13) which could not be analysed.

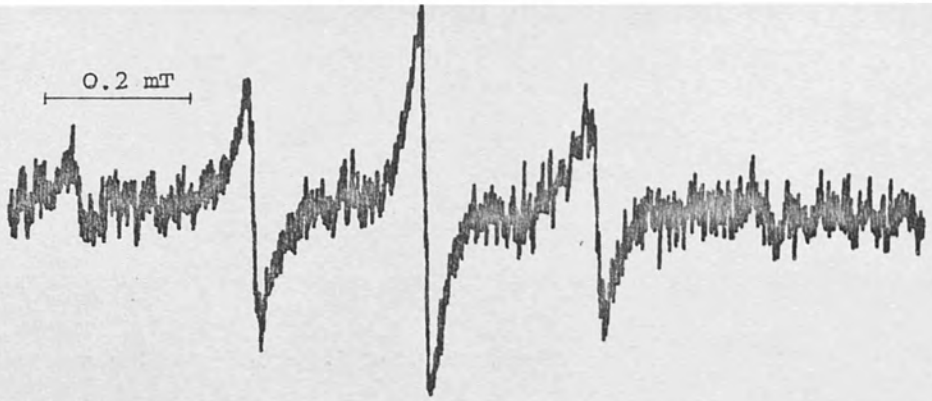

Fig. 12(a). 1,4-Benzosemiquinone from phenol

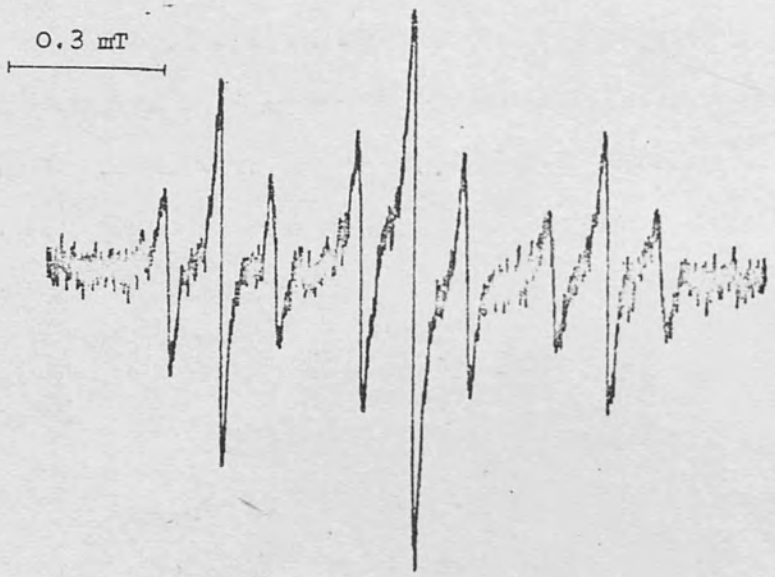

Fig. 12(b). 1,2-Benzosemiquinone from phenol

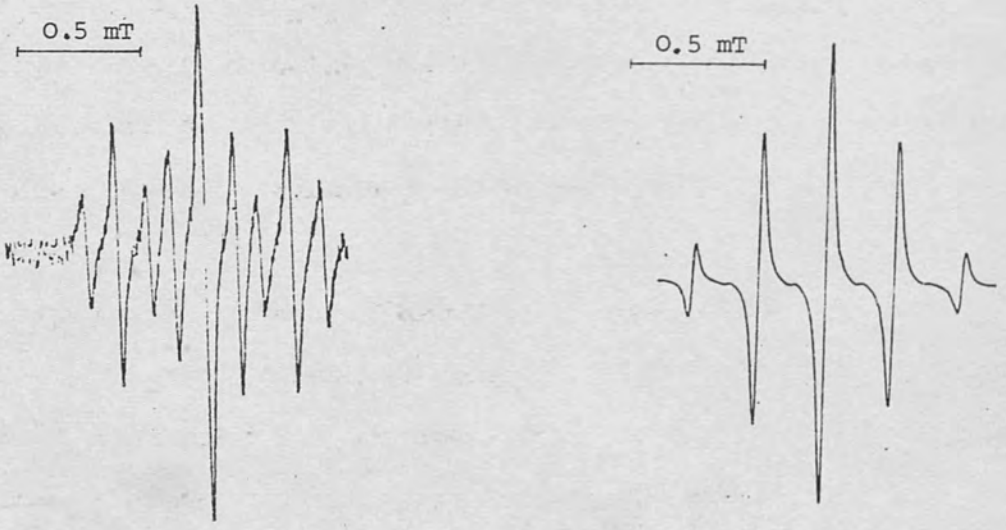

Fig. 14(a). 1,2-Benzosemiquinone from catechol

(b). 1,4-Benzosemiquinone from hydroquinone

B. Autoxidation of Phenols

Phenol

Phenol, on autoxidation in HMPA containing sodium methoxide or potassium tert-butoxide gave a broad esr singlet, which was later resolved into sharp lined spectra, due to first the 1,2- and then the 1,4-benzosemiquinones (Fig. 12). Identical spectra were observed from the corresponding quinones and dihydroxybenzenes when they were treated under the same conditions (Fig. 14(a), 14(b)). This suggested that phenol, which was difficult to autoxidise in aqueous media[107], has been successfully oxidised by molecular oxygen in this solvent-base system to form 1,2- and 1,4-benzosemiquinones.

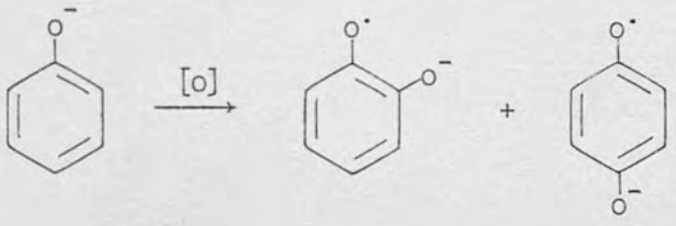

	a_2	a_3	a_4	a_5	a_6
1,2-benzosemiquinone		0.110	0.350	0.350	0.110
1,4-benzosemiquinone	o.240	0.240		0.240	0.240

Once again, the 1,4-semiquinone was only observed after the decay of the signal due to the 1,2-isomer.

The reaction was carefully followed by scanning the esr spectra at appropriate intervals over a period of several hours. It was found that the clear five lined spectrum persisted for a few hours and after its decay, no trace of other radical species was detected. Similarly, for the cases of 1,2- and 1,4-benzosemiquinones and dihydroxybenzenes, there were no other species observed.

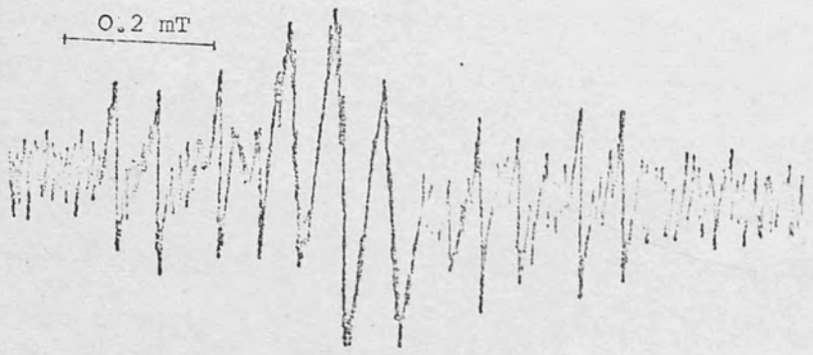

Fig. 15. Esr spectrum from resorcinol

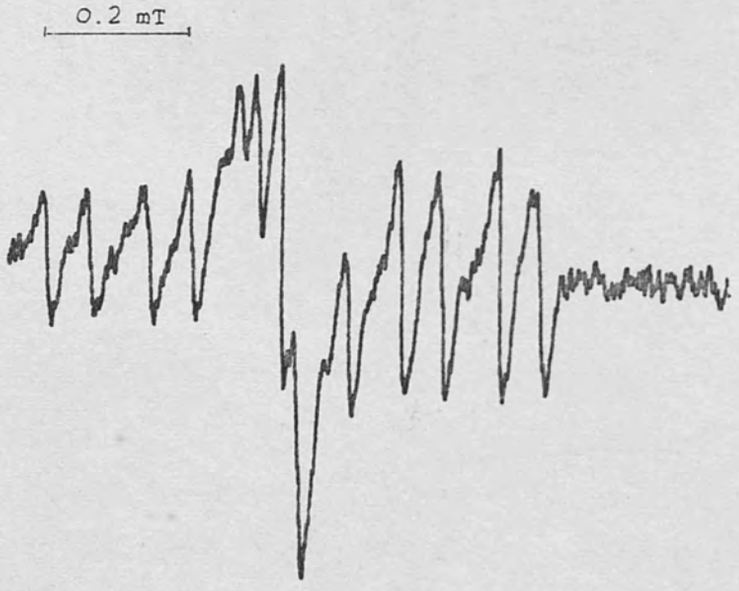

Fig. 16. 2-Hydroxy-1,4-benzosemiquinone from 1,2,4-trihydroxy-benzene

The formation of 1,2- and 1,4-benzosemiquinones from phenol, dihydric phenols and quinones is summarised in the following diagram.

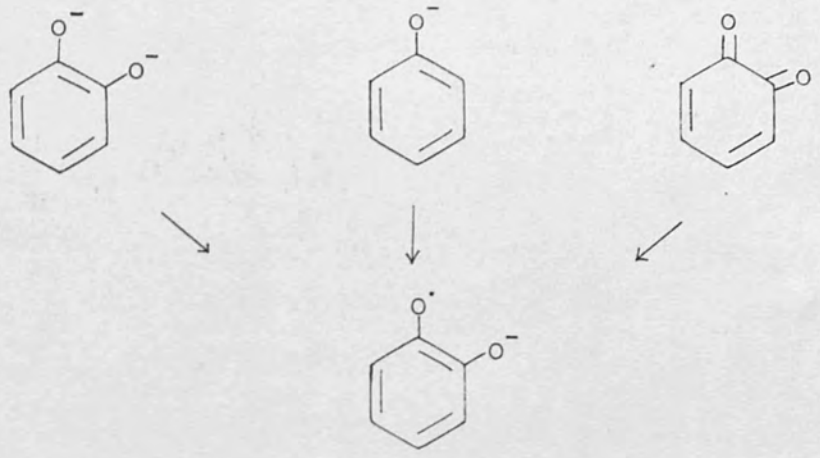

1,2-Benzosemiquinone

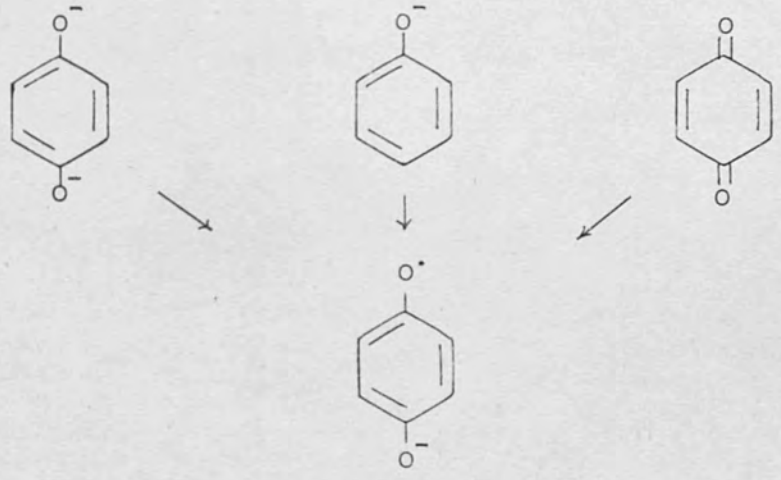

1,4-Benzosemiquinone

Resorcinol

A broad esr signal was initially obtained, however, on addition of a little water, a mixture of radicals was observed as revealed by the spectrum shown in Fig. 15. Using the results from resorcinol in aqueous solution[67], a spectrum could be picked out and ascribed to the 2-hydroxy-1,4-benzosemiquinone.

$$a_3 = 0.055,\ a_5 = 0.490,\ a_6 = 0.140$$

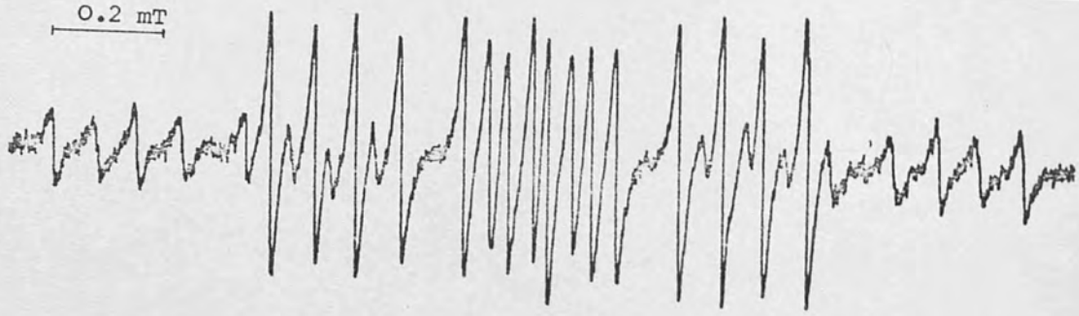

Fig. 17(a). 4-Methyl-1,2-benzosemiquinone from 4-methylphenol

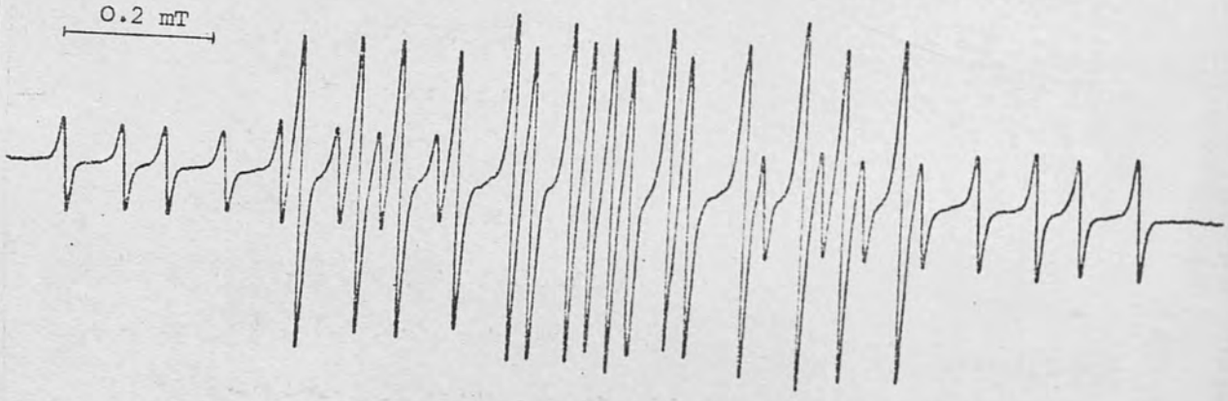

Fig. 17(b). 4-Methyl-1,2-benzosemiquinone from 4-methylcatechol

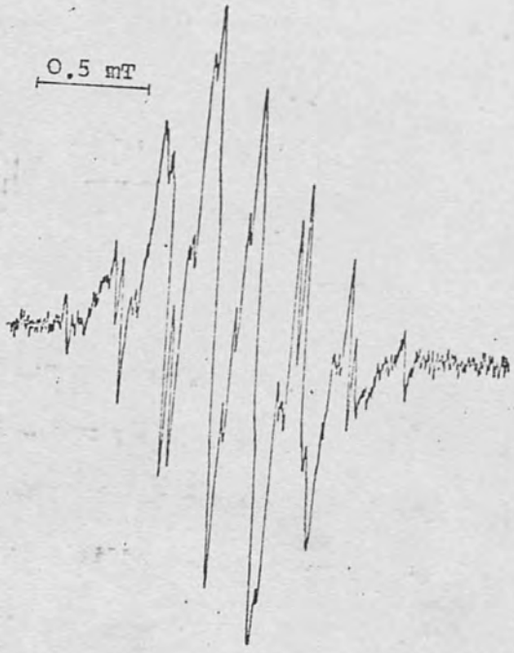

Fig. 18(a). Esr spectrum obtained instantaneously from o-cresol.

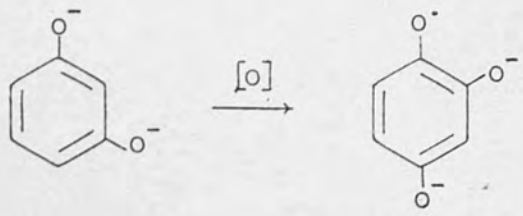

This was confirmed when 1,2,4-trihydroxybenzene gave an identical esr spectrum shown in Fig. 16. The additional lines in the spectra could possibly be due to other radical species formed by coupling.

4-methylphenol

After an induction period of about 30 minutes, a red fluorescence and an esr spectrum (Fig. 17(a)) was observed. Analysis of the spectrum gave the following coupling constants: 0.075 (doublet), 0.155 (doublet), 0.410 (triplet), 0.360 mT (doublet). The oxidation of 4-methylcatechol, under the same conditions gave a well resolved esr spectrum (Fig. 17(b)) identical to that obtained from 4-methylphenol. Therefore the radical observed from the oxidation of 4-methylphenol was ascribed to the 4-methyl-1,2-benzosemiquinone.

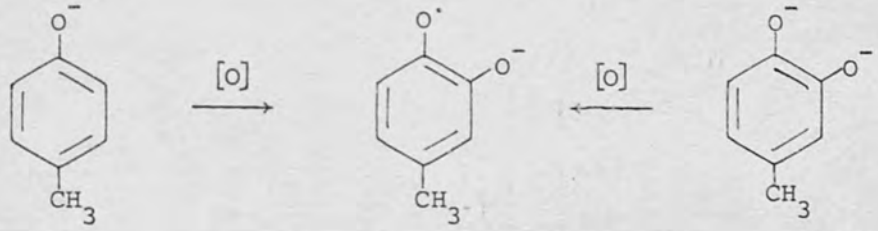

In both experiments, esr spectra were scanned at appropriate intervals over several hours, no secondary radicals were detected. o-Cresol (2-methylphenol) gave a poor resolved spectrum (Fig. 18a) which persisted for five hours. After addition of a little water, a well resolved spectrum as shown in Fig. 18(b) was obtained. To deduce

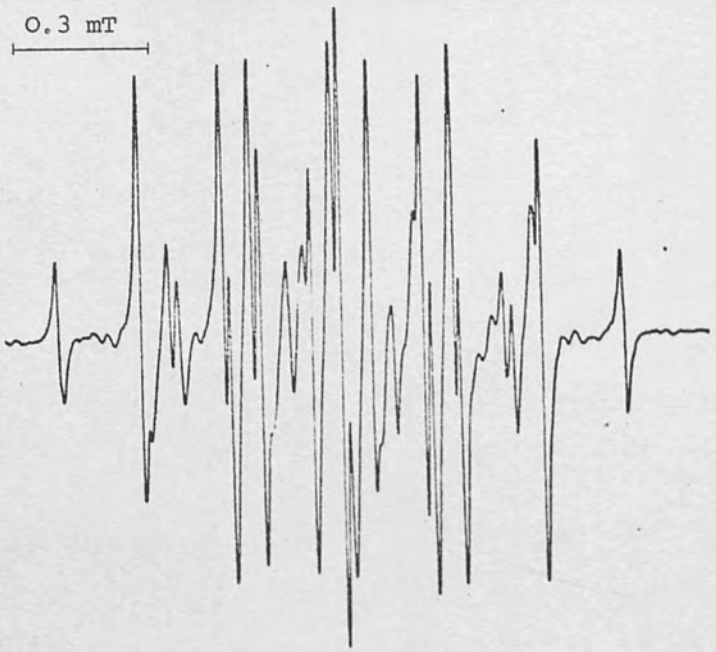

Fig. 18(b). 2-Methyl-1,4-benzosemiquinone from o-cresol after addition of water.

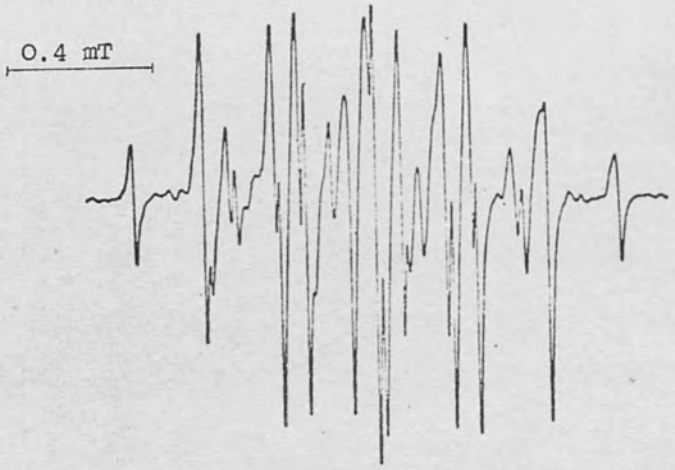

Fig. 18(c). 2-Methyl-1,4-benzosemiquinone from 2-methylhydroquinone

Fig. 19. 2-Hydroxy-5-methyl-1,4-benzosemiquinone from 4-methyl-resorcinol

the structure of the radical, methylhydroquinone was treated under the same conditions. It gave an esr spectrum (see Fig. 18(c)) identical to that from o-cresol. Therefore the radical observed from o-cresol was ascribed to the 2-methyl-1,4-benzosemiquinone.

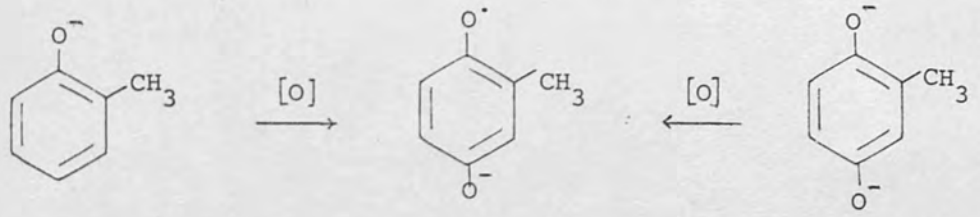

a_{Me}	a_3	a_5	a_6
0.183	0.200	0.270	0.245

4-Methylresorcinol

Upon standing the solution for about 30 hours, a well resolved spectrum consisting of a quartet, a_H = 0.500 mT, which is further resolved into two sets of doublets, coupling constants a_H = 0.050 and 0.085 mT was observed (Fig. 19). They are quite similar to those previously observed for the 2-hydroxy-5-methyl-1,4-benzosemiquinone in strong alkali solution (0.080 (1 proton)), 0.512 (methyl protons), 0.069 (1 proton))[61a]. Thus the radical observed was assumed to be the 2-hydroxy-5-methyl-1,4-benzosemiquinone corresponding to the attack of oxygen at carbon-6.

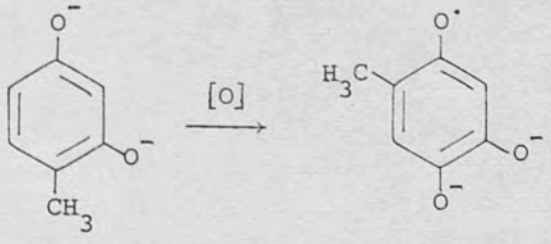

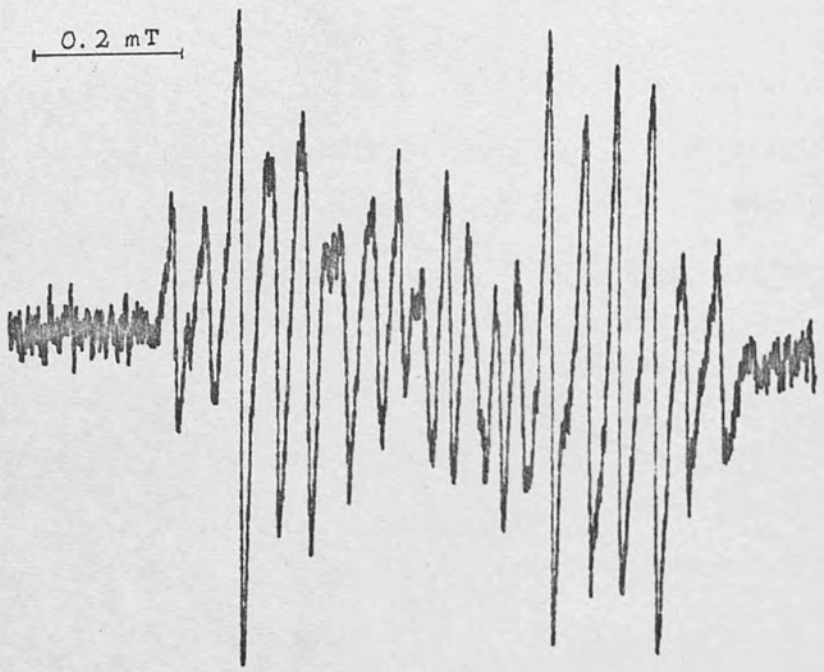

Fig. 20. 2-Hydroxy-6-methyl-1,4-benzosemiquinone from 5-methyl-resorcinol

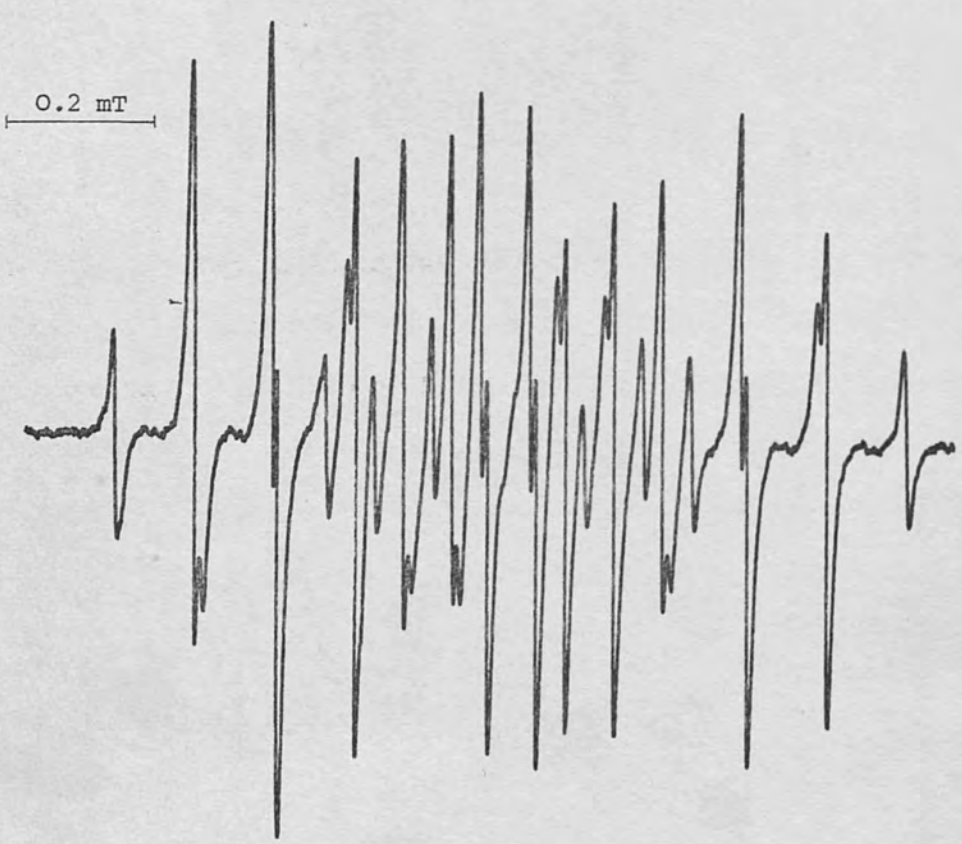

Fig. 21. 3-Methyl-1,2-benzosemiquinone from 3-methylcatechol

5-Methylresorcinol gave a broad singlet initially and after addition of a little water, a resolved spectrum was obtained (Fig. 20). The hyperfine splitting constants are 0.050 (1 proton), 0.430 (1 proton), 0.090 (3 equivalent protons), which are quite similar to those from 2-hydroxy-6-methyl-1,4-benzosemiquinone (a_3 = 0.055, a_5 = 0.415, a_{Me} = 0.095 mT)[61a], obtained by oxidation of 2-methylhydroquinone or the substituted quinone in aqueous solution.[61a] Therefore the observed spectrum was ascribed to the radical 2-hydroxy-6-methyl-1,4-benzosemiquinone.

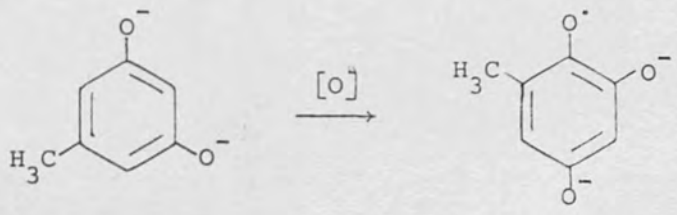

a_3	a_5	a_{Me}
0.050	0.430	0.090

3-Methylcatechol

A resolved esr spectrum (Fig. 21) was obtained from the solution after 20 hours. This spectrum was identical to that obtained in aqueous alkali[61a] and was attributed to the radical 3-methyl-1,2-benzosemiquinone, with assigned coupling constants as follows:

a_{Me}	a_4	a_5	a_6
0.105	0.360	0.290	0.110

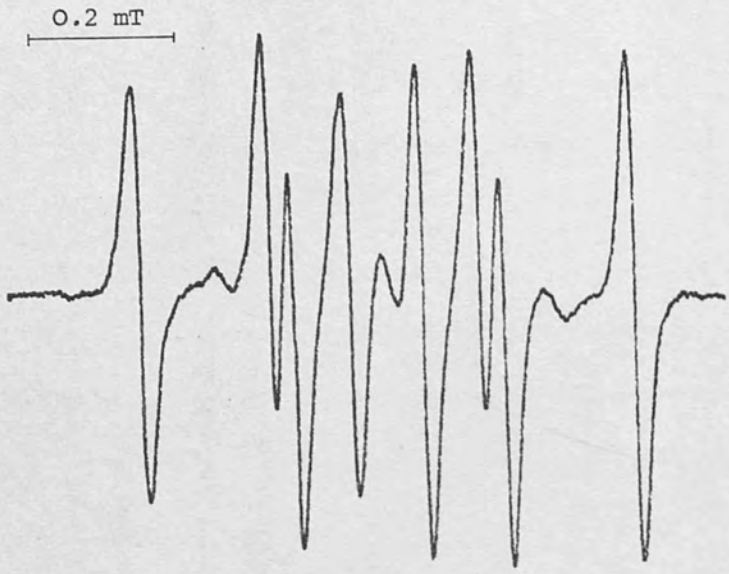

Fig. 22. 2-tert-Butyl-1,4-benzosemqiuinone from 2-tert-butyl-hydroquinone

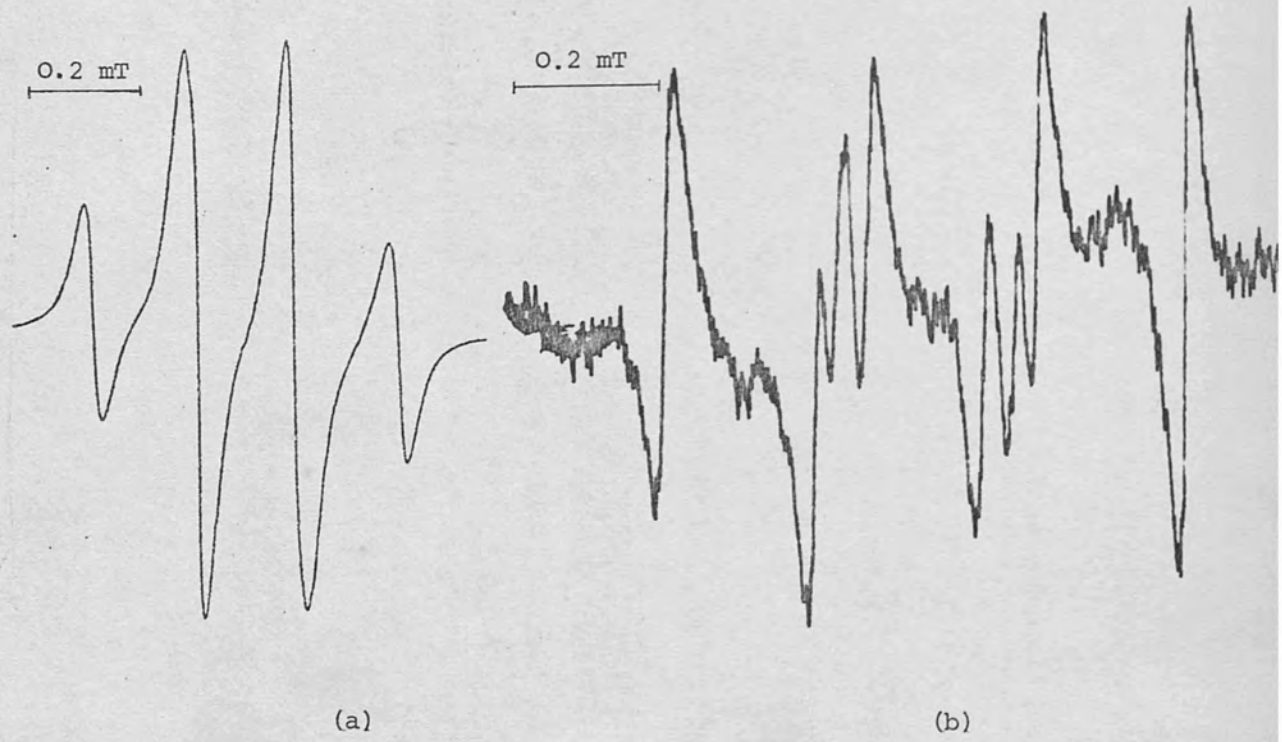

Fig.23 Esr spectra from 2-tert-butylphenol, (a) instantaneously (b) after a long period

2-tert-butylhydroquinone

When 2-tert-butylhydroquinone was added to the solvent-base system, four broad lines of intensity ratios approximately 1:3:3:1 were immediately obtained. After five days, it gave a well resolved esr spectrum consisting of eight lines with equal intensity (Fig. 22). This was assigned to the radical 2-tert-butyl-1,4-benzosemiquinone.

The coupling constants are:

a_3	a_5	a_6
0.180	0.210	0.290

o-tert-Butylphenol

An eight lined-spectrum (Fig. 23a) was obtained from o-tert-butylphenol in HMPA containing potassium tert-butoxide after exposure to air for several days. The spectrum shown in Fig. 23b was identical to that obtained from o-tert-butylhydroquinone. Thus the radical observed was 2-tert-butyl-1,4-benzosemiquinone.

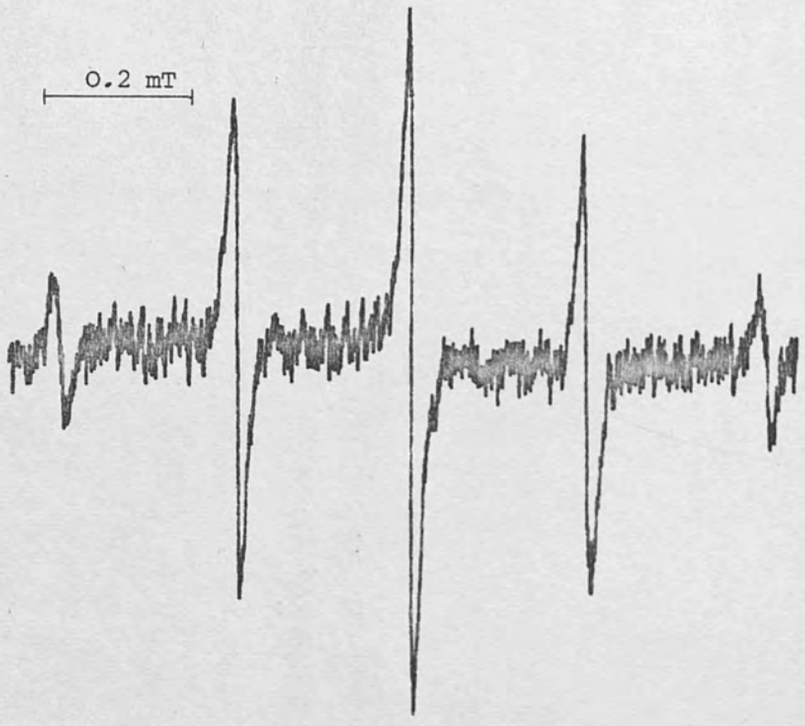

Fig. 24. 1,4-Benzosemiquinone from 1,4-dihydrobenzene

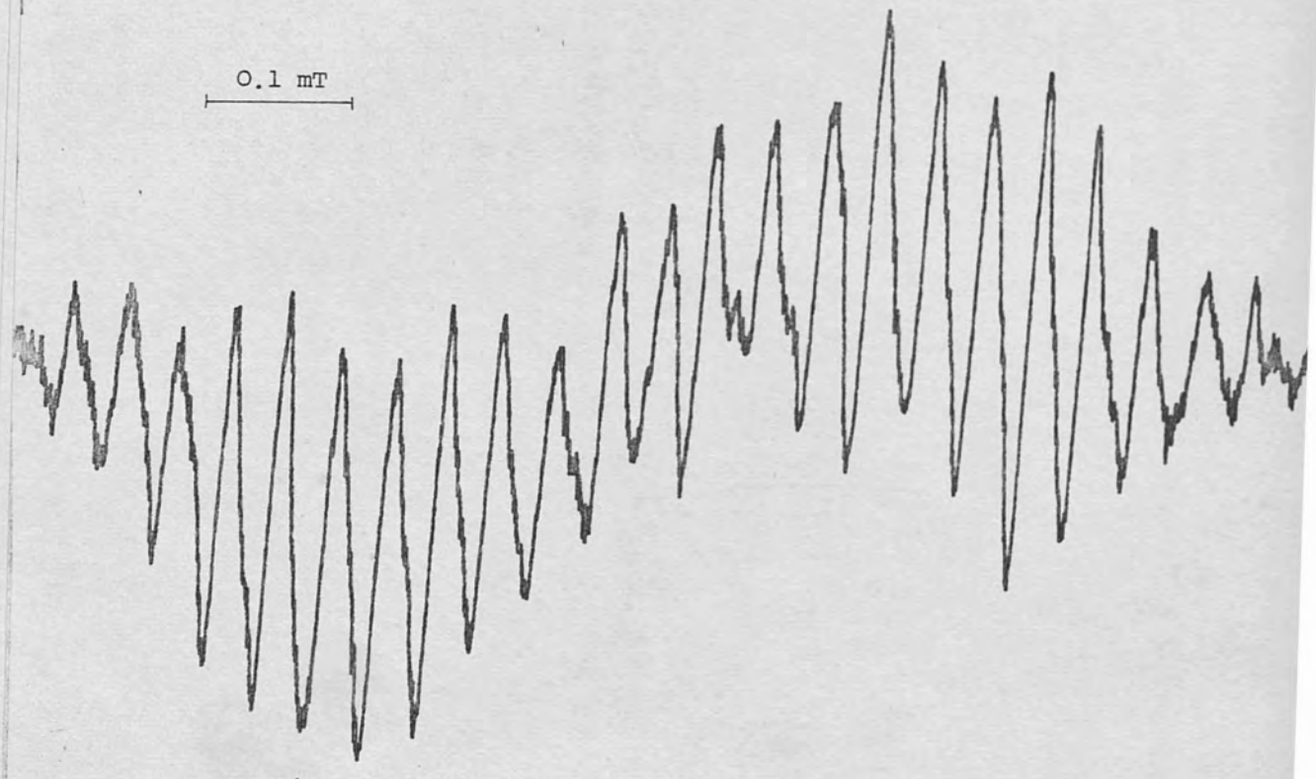

Fig. 25. 1,2-Naphthosemiquinone from 1,2-dihydronaphthalene

C. Autoxidation of dihydroaromatics

1,4-Dihydrobenzene

A sharp lined quintet was obtained immediately upon oxidation of 1,4-dihydrobenzene (see Fig. 24). It was obvious that oxidation had taken place by the replacement of the acidic hydrogens by two oxygens giving rise to the 1,4-benzosemiquinone as intermediate.

1,2-Dihydronaphthalene

After an induction period of a few hours, a green fluorescence was observed and a well resolved spectrum (Fig. 25) identical to those obtained from α-naphthol, 1,2-naphthoquinone, β-naphthol, 1,2-dihydroxy-naphthalene (i.e. Fig. 1(a) and 1(b) and 2(a)) was obtained. Therefore it was evident that this compound had been oxidised producing the 1,2-naphthosemiquinone observed by esr.

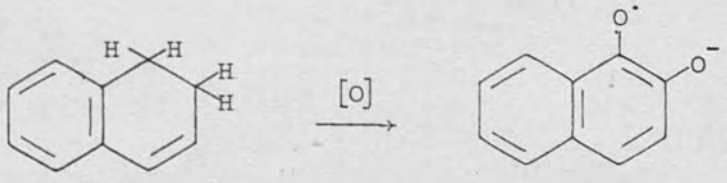

9,10-Dihydroanthracene gave a well resolved spectrum (Fig. 26) identical to those obtained from 9,10-dihydroxyanthracene, 9,10-anthraquinone or anthrone treated under the same conditions. Therefore the radical observed from the dihydroanthracene was attributed to the 9,10-anthra-semiquinone.

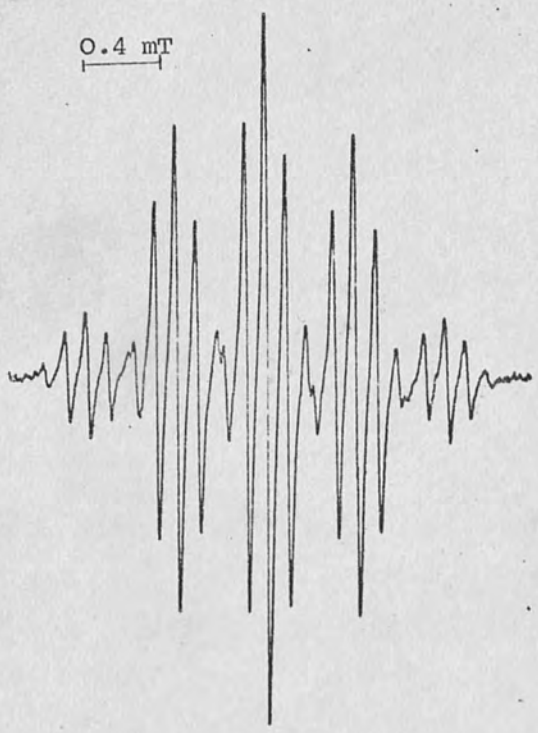

Fig.26. 9,10-anthrasemiquinone from 9,10-dihydroanthracene

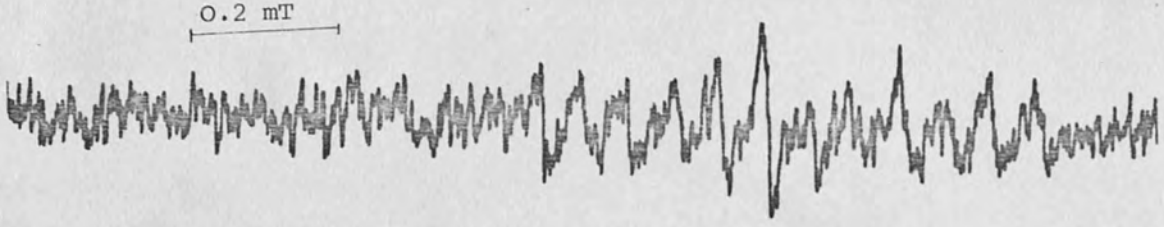

Fig. 27. Radical from 9,10-dihydrophenanthrene

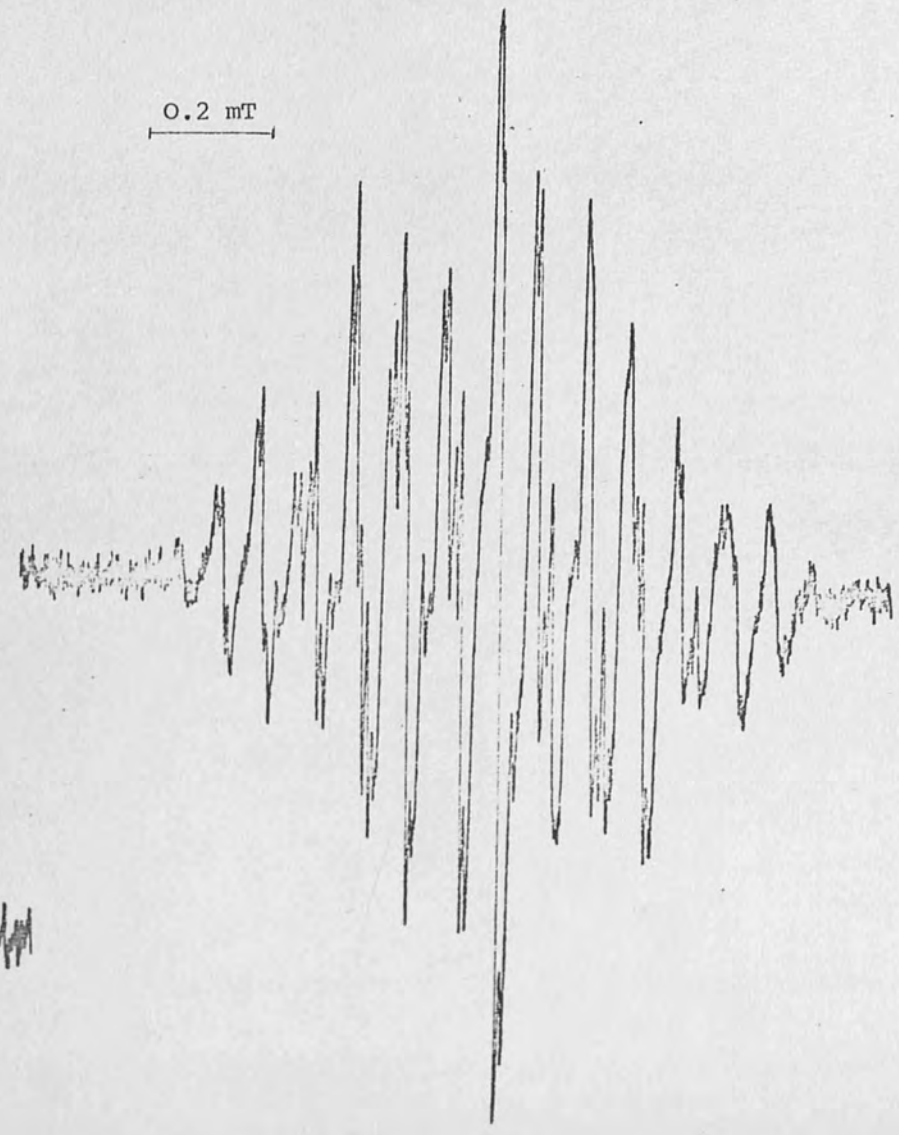

Fig.28. Pyrene-4,5-semiquinone from 4,5-dihydropyrene

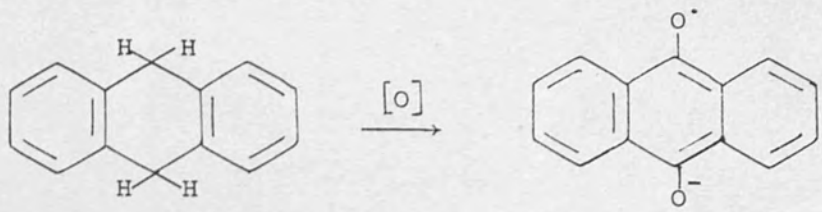

$$a_2 = a_3 = a_7 = a_6 = 0.10 \text{ mT (quintet)}$$

$$a_1 = a_4 = a_5 = a_8 = 0.024 \text{ mT (quintet)}$$

9,10-Dihydrophenanthrene gave a weak esr spectrum which could not be analysed (Fig. 27)

4,5-Dihydropyrene

The oxidation of 4,5-dihydropyrene in HMPA containing sodium methoxide gave a well resolved spectrum (Fig. 28) exhibiting four sets of two equivalent protons ascribed to the radical pyrene-4,5-semiquinone a_H = 0.015 (triplet), 0.086 (triplet), 0.270 (triplet), 0.330 mT (triplet).

It was reported by Russell[104] that the autoxidation of this compound in dimethylsulphoxide was unsuccessful.

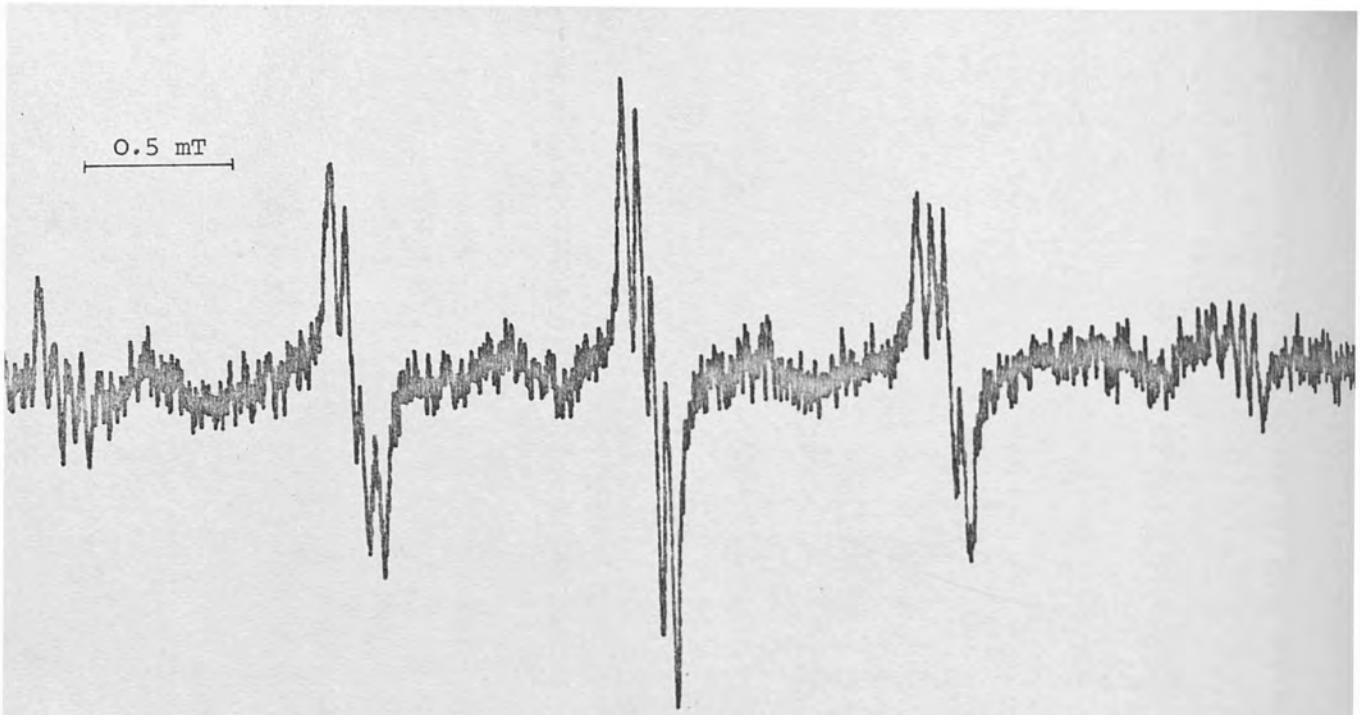

Fig. 29(a). Cyclohexane-1,2-semidione from cyclohexane with NaOMe used as a base.

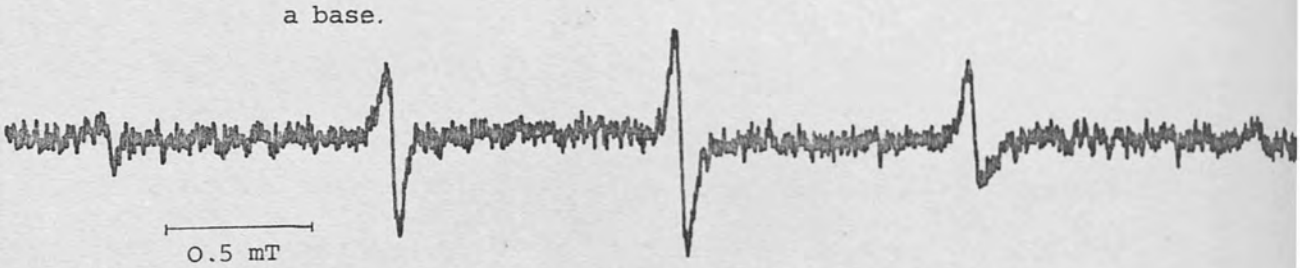

Fig. 29(b). Cyclohexane-1,2-semidione from cyclohexanone with $KOBu^t$ used as a base.

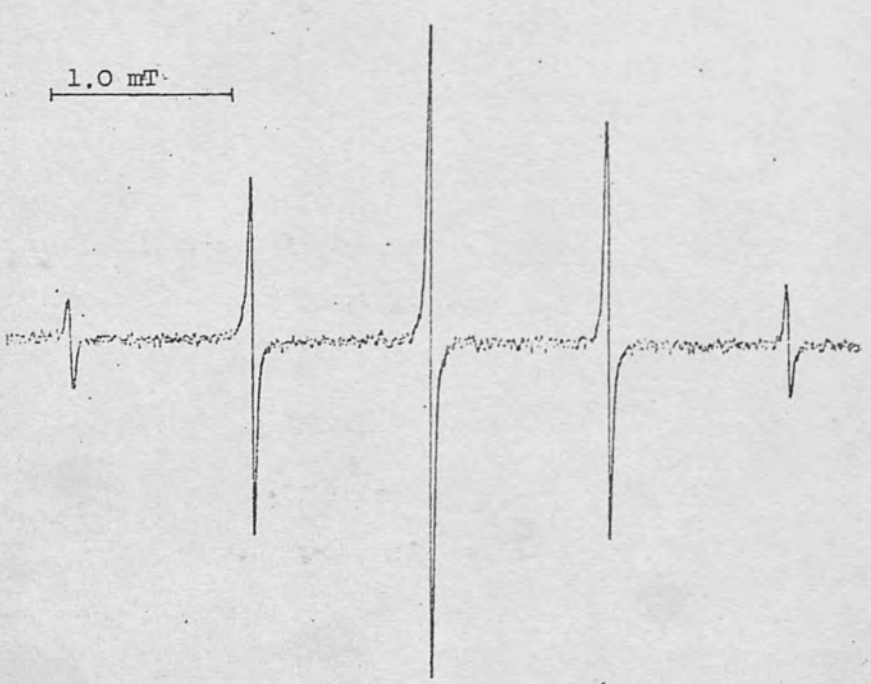

Fig. 30. Cyclohexane-1,2-semidione from 2-hydroxycyclohexanone

D. Autoxidation of alicyclic compounds

Cyclohexanone

This compound was readily oxidised to give a quintet (Fig. 29a) each component is further split into four lines of equal intensity due to the coupling of the odd electron with the sodium metal (a_{Na} = 0.050 mT) when sodium methoxide was used as a base. However, when potassium tert-butoxide was used as a base, no metallic hyperfine splittings were observed (see Fig. 29b), indicating that the sodium ion formed a more intimate ion pair, or that the potassium splittings were too small to be observed. The radical was probably the cyclohexane-1,2-semidione, coupling constants a_H = 0.996 mT (×4). Russell[108] obtained a_H = 0.982 mT (×4). The semidione has the half-chair conformations (B) and (C). The equivalence of the four α-protons indicates that the rate of interconversion between the two half-chair conformers is very rapid.

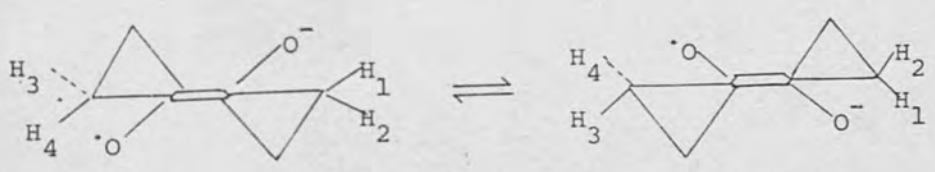

(B) (C)

2-Hydroxy-cyclohexanone gave an intense five line quintet identical to that obtained from cyclohexanone (Fig. 30), corresponding to the cyclohexane-1,2-semidione.

Cyclopentanone gave an esr signal consisting of a quintet, each line of which is further split into a triplet (Fig. 31). This indicated that the spin coupled with four equivalent α-protons, (a_H = 0.963 mT) and two equivalent β-protons (a_H = 0.663 mT). This radical could either

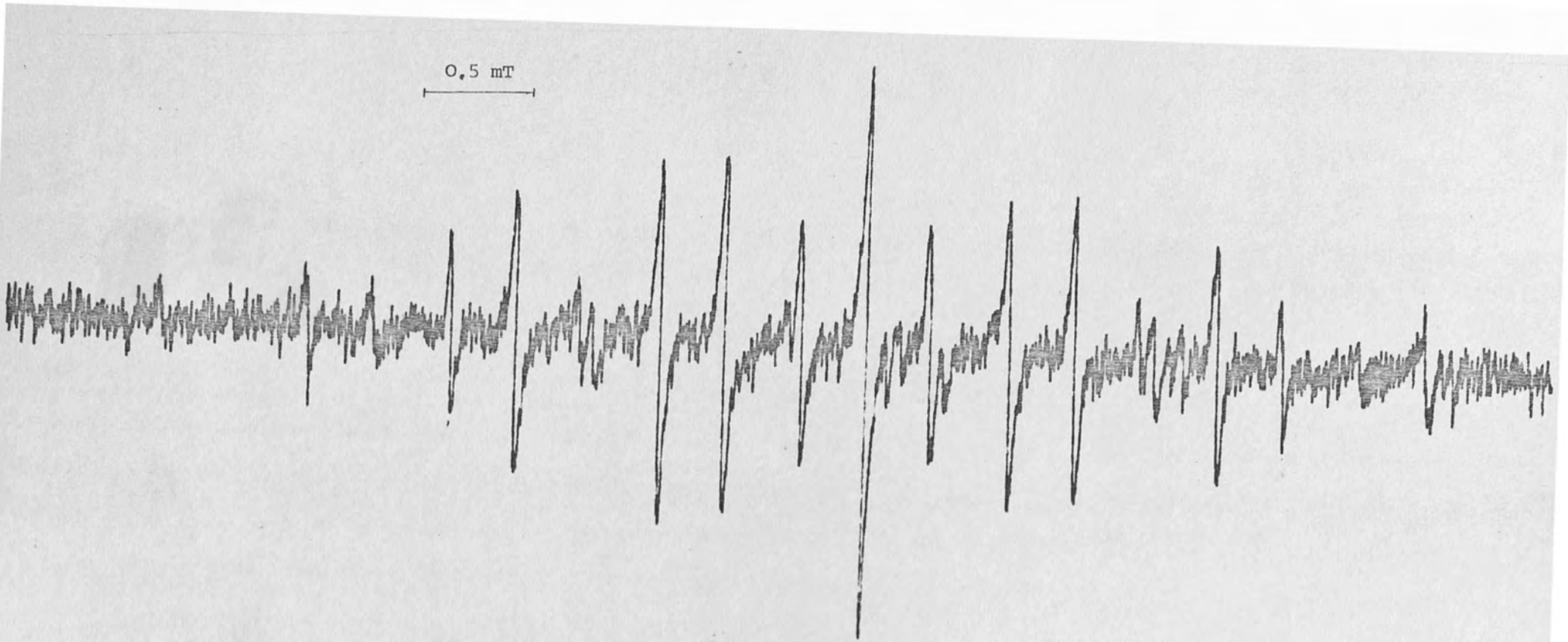

Fig. 31. Radical from cyclopentanone

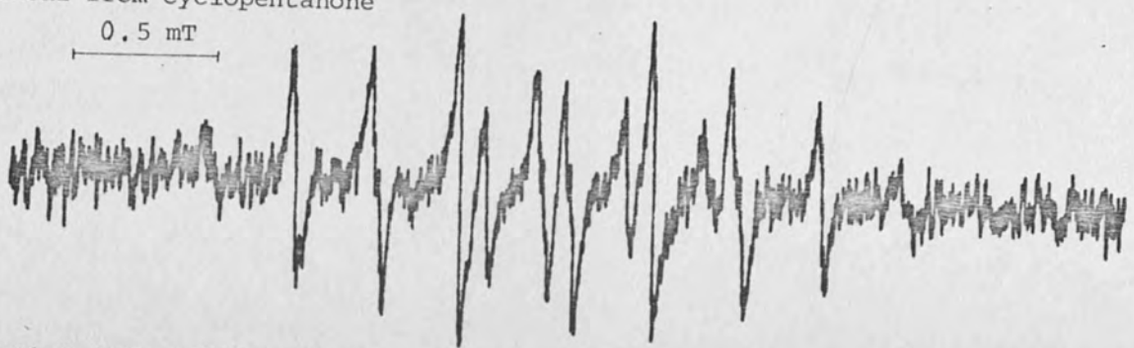

Fig. 32. 3-Methyl-1,2-semidione from 3-methyl-1,2-cyclopentanone

have planar structure (D) or have half-chair conformations (E) and (F) interconverting rapidly with each other as represented by the collowing diagram:

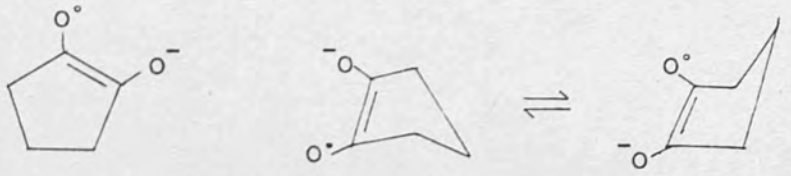

(D) (E) (F)

The equivalence of the four α-protons and the large β-proton hyperfine splittings observed seem to suggest that the radical has a planar structure. It was also suggested by Russell et al[108] that this radical is planar, because the hyperfine splittings are temperature independent. However, the coupling constants obtained[108] were different (a_H = 1.416 (×4)) from those obtained in HMPA.

3-Methyl-1,2-cyclopentanedione

The spectrum of 3-methylcyclopentane-1,2-dione is shown in Fig. 32. The hyperfine splittings are 0.275 (1 proton), 0.563 (3 equivalent protons), 0.675 (1 proton) and is assumed to be the radical 3-methylcyclopentane-1,2-semidione. (Compare a_H = 1.460, 1.40, and the methyl splittings are not resolved.[111b])

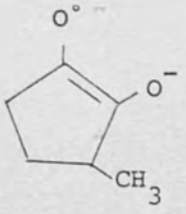

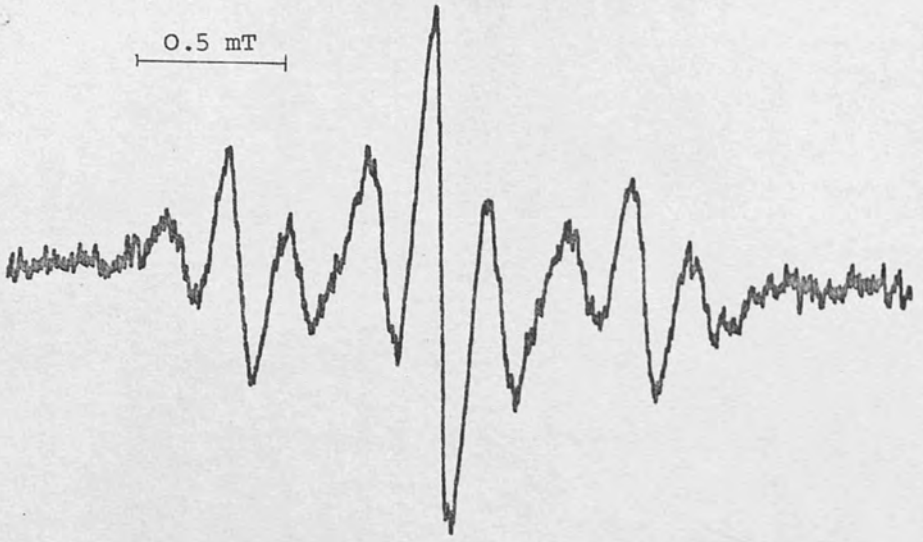

Fig. 33. Radical from cycloheptanone

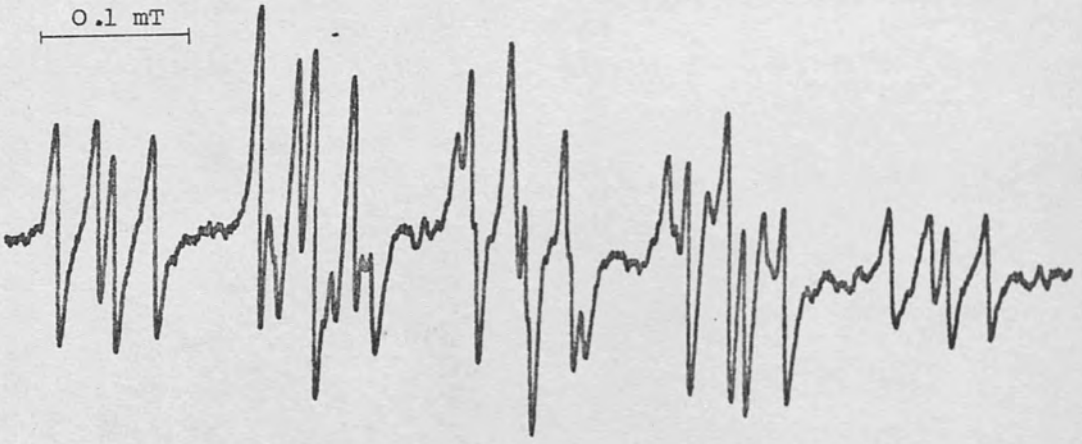

Fig. 34a. Indane-1,2-semidione from 1-indanone

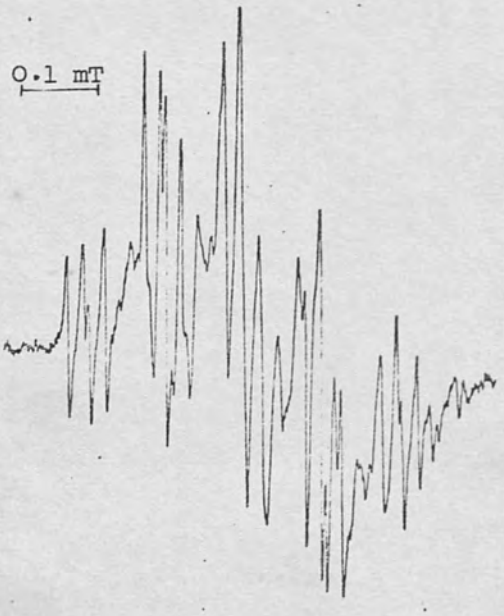

Fig. 34b. Indane-1,2-semidione from 2-indanone

Cycloheptanone gave three sets of triplets (see Fig. 33) attributed to the radical cycloheptane-1,2-semidione, with coupling constants $a_{\alpha H}$ = 0.700 mT (triplet), $a_{\beta H}$ = 0.200 mT (triplet) (compare $a_{\alpha H}$ = 0.670 mT and $a_{\beta H}$ = 0.197 mT.[108])

1-Indanone

The oxidation of 1-indanone gave a spectrum (Fig. 34a) which decayed after two minutes and transformed into a complex spectrum which is difficult to analyse. The esr spectrum obtained instantaneously was consistent with hyperfine splittings of

a_{CH_2} = 0.275 mT, a_H = 0.295, 0.290, 0.050, 0.075 mT.

These values are quite close to those obtained in dimethylsulphoxide, (a_{CH_2} =0·262, a_H =0.295, 0.283, 0.073, 0.056 mT)[108].

An identical spectrum (Fig. 34b) was obtained from 2-indanone when it was treated under the same conditions, indicating that the 2-indanone has been oxidised to give indane-1,2-semidione as an intermediate.

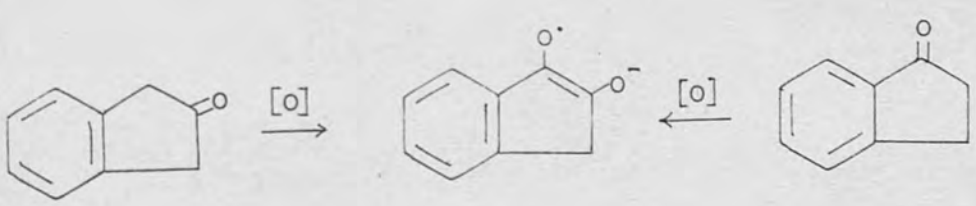

Cyclopentadiene gave a spectrum (Fig. 35) consisting of a triplet of triplets with coupling constants 0.360 and 0.155 mT, which evidently arose from the coupling with two pairs of equivalent protons. The radical was unlikely to have been derived from the dicyclopentadiene (G) although this is easily formed at room temperature, because the

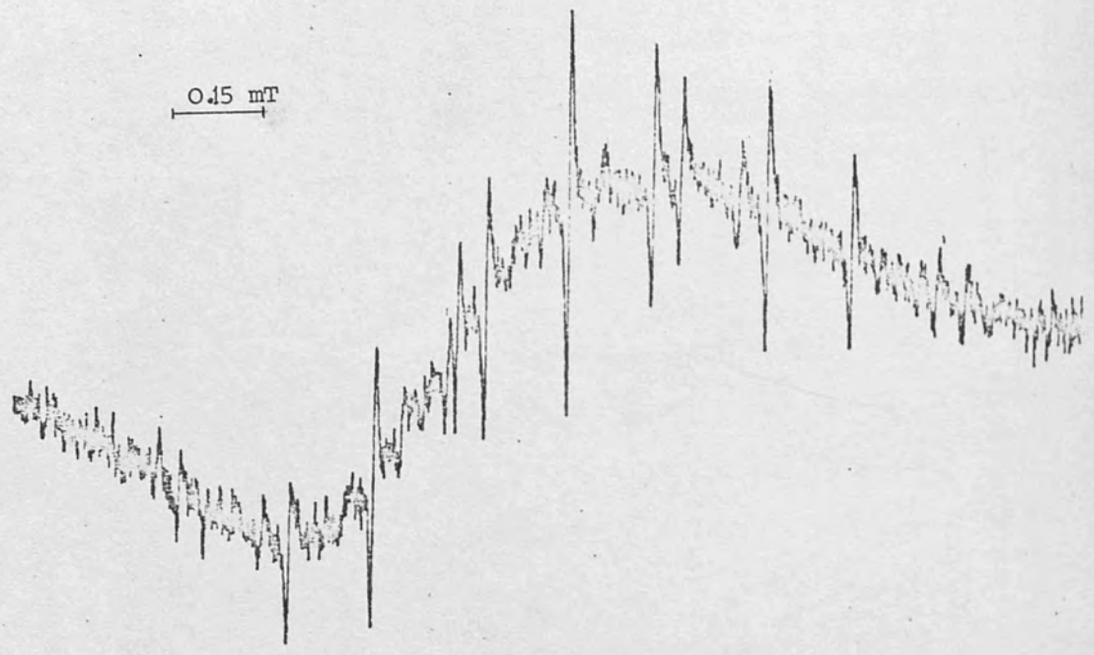

Fig. 35. Radical from cyclopentadiene

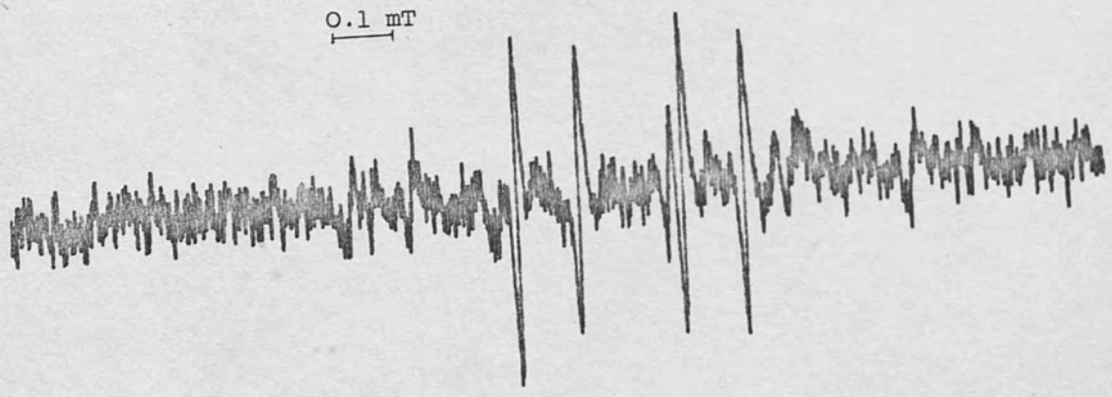

Fig. 38. Radical from phenyl allyl ether

dicyclopentadiene itself gave a different spectrum. The spectrum was assumed to be that from the ketyl radical from the cyclopentadienone (H) but the coupling constants differed from those predicted by theory [111] probably due to the solvent effect.

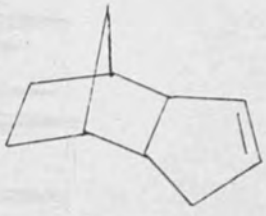

(G)

(H)

Cycloheptatriene

The spectrum of the radical produced in the autoxidation of the cycloheptatriene is shown in Fig. 36. The hyperfine splittings are: 0.135 (triplet). 0.230 (triplet), 0.650 (triplet), A possible intermediate of the sutoxidation of cycloheptatriene is the detyl radical of tropone, however, it was found that the spectrum obtained was different from that obtained by reduction of tropone with the sodium metal in HMPA (Fig. 37). (This spectrum is identical to that reported (0.858 (×2), 0.505 (×2), 0.010 (×2) [112]). Thus the radical observed could not be the ketyl radical of tropone and the identity of this radical is not known.

Phenyl allyl ether

Treatment of the phenyl allyl ether with sodium methoxide in HMPA gave a spectrum with intensity ratios approximately 1:1:3:3:3:3:1:1 Fig. 38). The structures of this radical is not established.

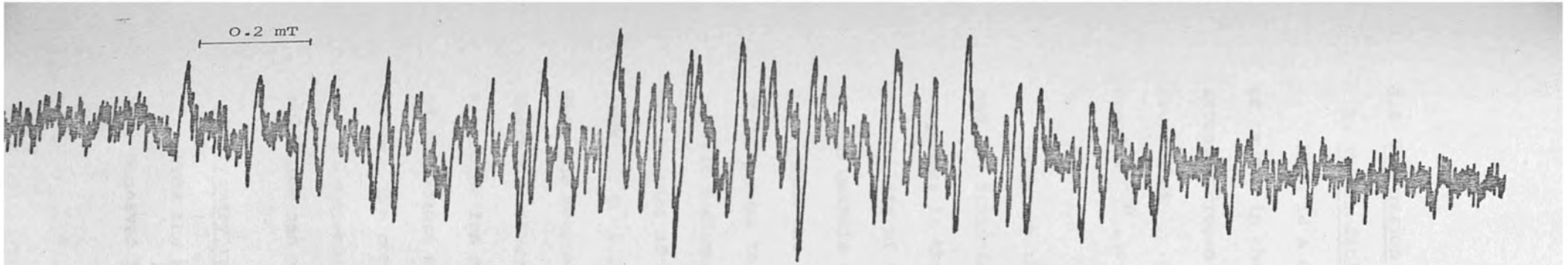

Fig. 36. Radical from cycloheptatriene

Fig. 37. Ketyl radical formed by sodium metal reduction of tropone

3.4 Discussion

A. The conditions of the solvent-base system

HMPA is a dipolar aprotic solvent.[103] The lone paired electrons of oxygen in the $\rangle P{=}O$ groups of an HMPA molecule tend to form extremely strong hydrogen bonds with any acidic proton present.[103] It has been found that phenol and the HMPA molecule form a hydrogen bonded complex[103b] as:

$$ArOH \ldots O^- \ldots P^+ \ldots [N(CH_3)_2]_3$$

The fact that there are no radicals other than the observed 1,2- and 1,4-semiquinones being observed in the autoxidation of these compounds in this solvent-base system seems to indicate that the possibility of the reaction involving the addition of the alkoxide ion on the quinols or quinones is not great. Such reactions were generally found when the autoxidation was carried out in alcoholic media.[59] This appears to suggest that on dissolution of the sparingly soluble sodium methoxide, the methoxide displaces the phenoxide ion because of its higher basicity.

$$ArOH \ldots O^- \ldots P^+ \ldots [N(CH_3)_2]_3 + {}^-OMe \longrightarrow MeOH \ldots OP[N(CH_3)_2]_3 + ArO^- \quad (3.1)$$

Thus the methoxide ion is complexed by the solvent molecules and therefore there is little chance for the nucleophilic addition of the methoxide ion on the quinone or hydroquinones. Hence the situation of the solute molecules in HMPA is apparently different from that in water. The concentration of free methoxide ion or of free protons in the solvent-base system is relatively low. Therefore dissolved oxygen molecules can approach the solvent-free phenoxide ion relatively easily.

B. Primary radicals

From the results of Table I, it can be seen that primary radicals were observed from 1,2-; 1,4-; 1,5-; 2,6-; and 1,7-naphthalenediols in

which the oxygen atoms are conjugated with respect to each other. The 1,4-naphthosemiquinone is more stable than the 1,2-naphthosemiquinone as reflected by their life times, while the other isomeric semiquinones are of transient existence only and are easily oxidised further to form secondary radicals. The primary radical species are presumably produced in the normal way as with hydroquinone and quinone[61] i.e. by simple electron transfer from naphthoxide anion to oxygen.

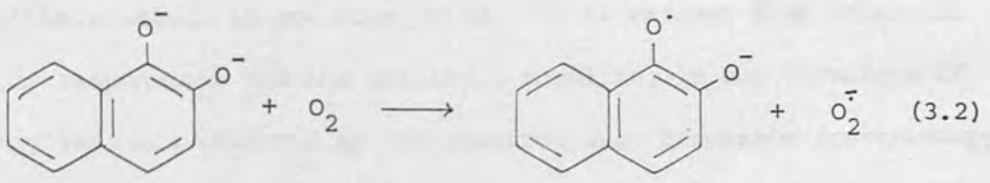

(3.2)

C. Secondary radicals

As mentioned in the results section, 1,2- and 1,4-naphthosemiquinones were observed at later stages of the autoxidation of α-naphthols with the exception of 1,5-naphthalenediol.

Generally, the 1,2-naphthosemiquinones were observed initially but the species decayed were replaced by those of the 1,4-naphthosemiquinones. This seems to indicate that 1,2-naphthosemiquinones are kinetically controlled intermediates while 1,4-naphthosemiquinones are thermodynamically controlled, in the autoxidation reaction. Thus the 1,2-naphthosemiquinones were formed at a faster rate than the 1,4-semiquinones, but then decayed by dimerization or by further oxidation by molecular oxygen at the site (position-4) of high spin density in the ring. On the other hand, the 1,4-naphthosemiquinone was formed at a slower rate, but once formed, persisted for a relatively longer time. However, 1,5-naphthalenediol was a special case in that oxidation took place only at position-4 giving rise to the 5-hydroxy-1,4-naphthosemiquinone. This is possibly due to the extra stability provided by the

peri-hydrogen (page 69).

The possible formation of secondary radicals of both 1,2- and 1,4-naphthosemiquinones from the same parent compound appears to indicate the non-fixation of the C_1-C_2 and C_3-C_4 double bonds, and the existence of mesomeric effects.

D. Formation of secondary radicals

The mechanism of the formation of secondary radicals from phenols and naphthalenediols is now considered. It is evident that molecular oxygen is responsible for the oxidation resulting in the formation of secondary radicals observed by the electron spin resonance spectroscopy.

It is now necessary to consider the mechanism involving the addition of molecular oxygen to phenoxide ion, resulting in the formation of secondary radicals. There are two possible pathways by which the molecular oxygen can undergo interaction with phenoxide ion. One is through a free radical chain process (Equations 3.3 - 3.6) and the other is a one step reaction mechanism (Equation 3.7).

$R^- + O_2 \longrightarrow R^\cdot + O_2^{\cdot-}$ Initiation (3.3)

$R^\cdot + O_2 \longrightarrow ROO^\cdot$ (3.4)

Propagation

$ROO^\cdot + R^- \longrightarrow ROO^- + R\cdot$ (3.5)

Radical combination $\longrightarrow$ products Termination (3.6)

$R^- + O_2 \longrightarrow ROO^-$ (3.7)

These two reaction paths are discussed as follows: If the free radical chain process operates, the initial step of the reaction would involve the transfer of an electron from the phenoxide ion to the molecular oxygen, forming the phenoxyl radical and the superoxide ion.

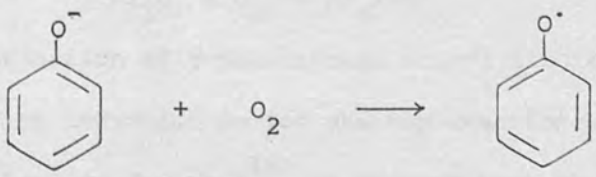

(3.8)

As it is known that the phenoxyl radicals, (especially the unsubstituted and monosubstituted ones studied in this work), are relatively short-lived, they may undergo dimerization via C-C or C-O coupling,[24,26] or attack another phenol molecule in the reaction mixture forming a cyclohexadienyl radical.[24] For example. in the autoxidation of p-cresol, the C-C or C-O coupled products and Pummerer's ketone (I) were always isolated.[24,26,19a] However, in our reaction, no such species were detected.

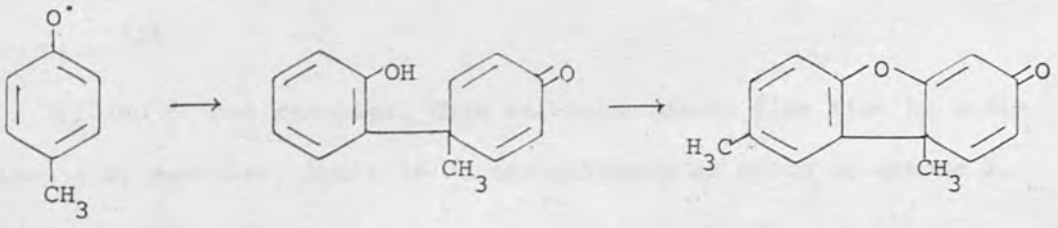

(I)

Consequently it seems more likely that the reaction between the molecular oxygen and the phenoxide ion is via a one step reaction mechanism.

There is evidence against the chain mechanism and in favour of the one step reaction mechanism. The autoxidation of di- and of triphenylmethane was shown to follow a one step reaction mechanism by Russell et al[109] who carried out kinetic studies of these reactions. They found that the rate determining step of the reaction is the ionisation of these hydrocarbons, which was found to be equal to the rate of oxygen absorption, hence the carbanion once formed is immediately trapped by oxygen. Thus

$$Ar_3CH \longrightarrow Ar_3C^- \qquad (3.9)$$

$$Ar_3C^- + O_2 \longrightarrow Ar_3COO^- \qquad (3.10)$$

The autoxidation of 9-substituted benzyl fluorene[114] was found to begin without an induction period and the reaction was insensitive to light, This lead to Sprinzak[114] to suggest that the reaction was not

a radical chain process. The autoxidation of sterically hindered phenols in tert-butyl-alcohol containing potassium tert-butoxide was followed by kinetic studies.[107] It was found that the reaction was a first order reaction directly dependent on the oxygen pressure, thus it was suggested that the reaction involves a bimolecular reaction of phenoxide ion and oxygen $R^- + O_2 \longrightarrow ROO^-$. Recently, kinetic studies of the autoxidation of 2,6-di-tert-butyl-4-alkyl-phenols in HMPA, dimethylsulphoxide or dimethylformamide, containing potassium tert-butoxide also indicated that the reaction follows a one step reaction mechanism.[115]

Applied to our reaction, this mechanism could give rise to semiquinones or secondary radicals of semiquinones as shown in scheme 1.

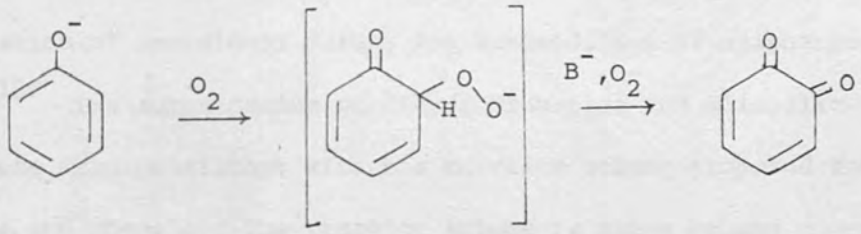

(J)

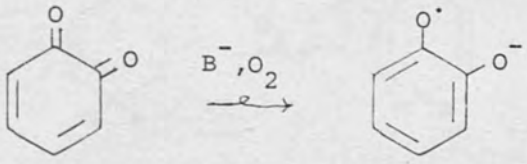

Scheme 1

In the above scheme, the combination of oxygen and the phenoxide (or naphthoxide) ion affords quinone, via the intermediate (J), which is then reduced possibly via the following paths (Scheme 2).

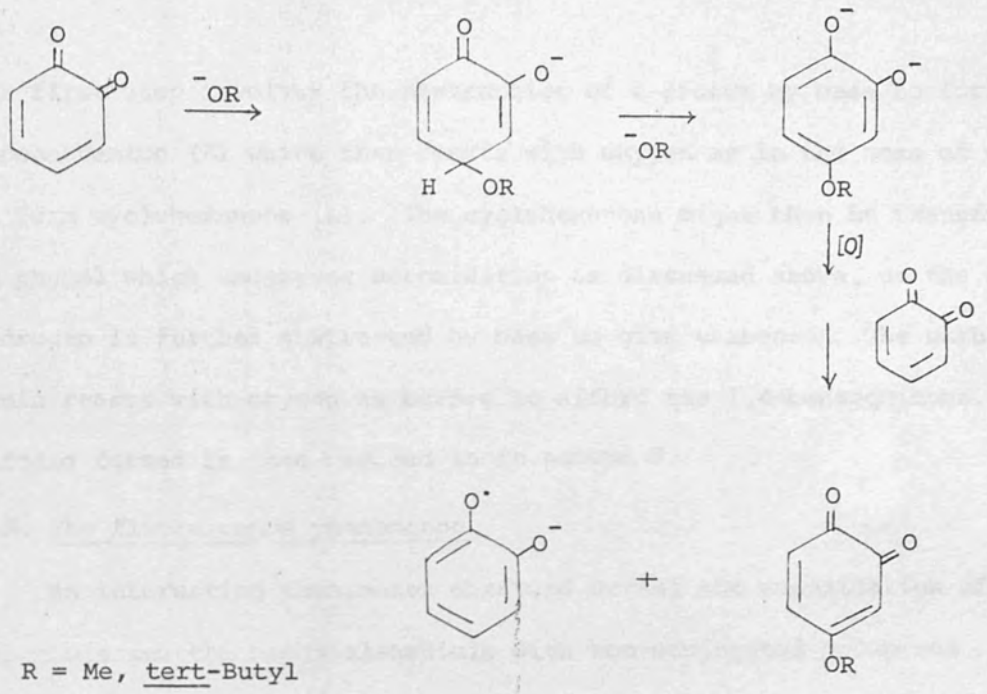

R = Me, tert-Butyl

Scheme 2

Intermediates analogous to (J) have been postulated to account for the formation of semidiones during the autoxidation of aliphatic ketones.[109] The autoxidation of dihydroaromatics and alicyclic ketones are also consistent with the reaction scheme proposed for naphthols and phenols. The reaction scheme is shown below:

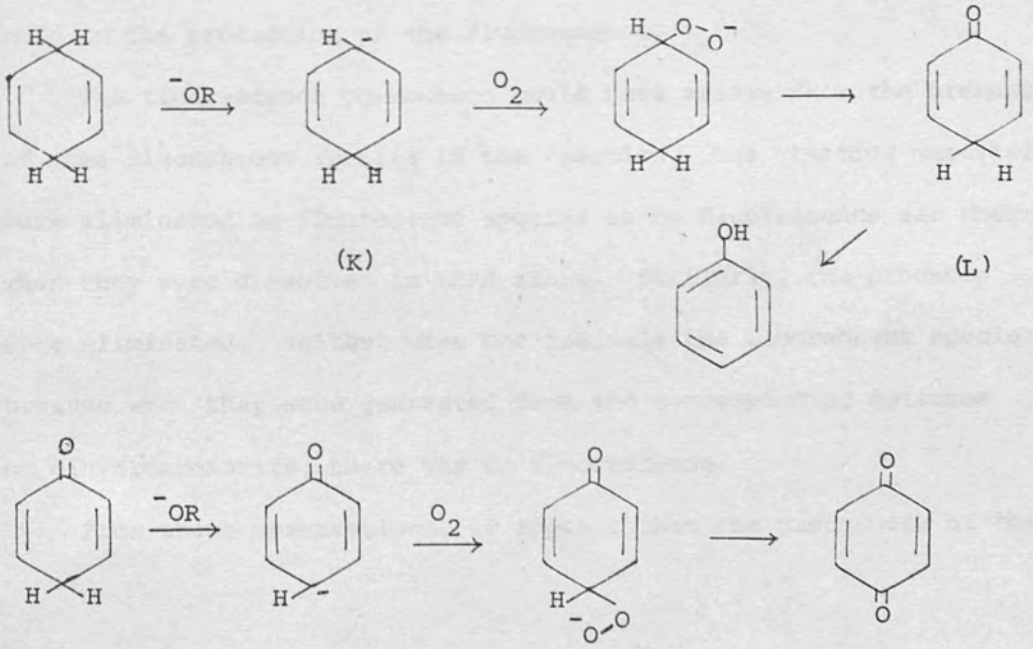

The first step involves the abstraction of a proton by base to form the monocarbanion (K) which then reacts with oxygen as in the case of phenols to form cyclohexenone (L). The cyclohexenone might then be transformed to phenol which undergoes autoxidation as discussed above, or the acidic hydrogen is further abstracted by base to give carbanion. The carbanion again reacts with oxygen as before to afford the 1,4-benzoquinone. The quinone formed is then reduced as in scheme 2.

E. The fluorescence phenomenon

An interesting phenomenon observed during the autoxidation of naphthols and the naphthalenediols with non-conjugated groups was the sudden rise of radical concentration accompanied by fluorescence after an induction period. As the concentration of the radical grew (as can be seen from the increasing intensity of the esr signal), the colour of fluorescence was more pronounced. After a period of a few hours, the fluorescence gradually decayed, accompanied by the decay of the esr signal. However, when the solution was stirred to allow more oxygen to dissolve, then both the fluorescence and the esr signal were regenerated. This seems to indicate that oxygen was playing a role in the production of the fluorescence.

The fluorescence phenomenon could have arisen from the presence of some fluorescent species in the reaction. The starting materials were eliminated as fluorescent species as no fluorescence was observed when they were dissolved in HMPA alone. Similarly, the products were eliminated. Neither were the radicals the fluorescent species, because when they were generated from the corresponding quinones or dihydroaromatics, there was no fluorescence.

From these observations, it appears that the precursors of the

radicals are responsible for the fluorescence observed since the colour of fluorescence is characteristic of the starting material, e.g. blue for the α- or β-naphthols and red for the 1,3-dihydroxy-naphthalene.

The most likely intermediate, in our reaction scheme (page 91) which might produce fluorescence is the complex formed between the oxygen and the naphthoxide ion (M). This is not unreasonable because the coumarins of type (N) are well known to be fluorescent and the substitution of electron donor leads to a shift to lower frequency[120].

The complex or adduct (M) appears to be relatively long lived (as indicated by the fluorescence observed) in HMPA and this could be due to the low concentration of free base and of free protons in the solvent under our conditions. In the presence of proton donors, the adduct (E) would isomerise to hydroperoxide which is easily decomposed in the presence of a base. This would explain why the fluorescence decayed after the addition of water.

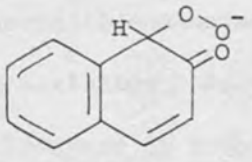

(M)

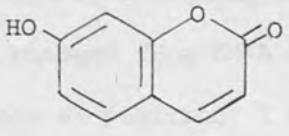

(N)

F. The solvent effect

Abundant esr evidence shows that the hyperfine splittings of organic free radicals containing polar substituents of heteroatoms are subjected to solvent effects due to the possible formation of localised complexes between the solvent molecules and the heteroatom of substituents. Thus the spin density in the radicals is redistributed

in such a way that the positions of low spin densities would have large fractional change.

We would like to see if there are any solvent effects on the naphthosemiquinones by comparing the coupling constants of these radicals in HMPA and ethanolic-water system. In HMPA, dipole-dipole interaction would be between the solvent and the semiquinones, while in the ethanolic-water system, the complex formation is via hydrogen bonding. Hence it is expected that solvent effects would be observed in these radicals and the spin distribution in these radicals in the two solvent systems would be different.

Table V shows the coupling constants in these two solvent systems It is noted that in the case of 1,2-naphthosemiquinones, the protons at C-5 and C-7 (which have small hyperfine splittings) shows large fractional changes in hyperfine splittings when the solvent changes from water to HMPA, while the changes in other positions are small. In the case of 1,4-naphthosemiquinones, the change in the coupling constants at C-7 is most marked when the solvent changes from ethanol-water to HMPA.

For monocyclic semiquinones, the coupling constants also change with solvent variation. As the solvent changes from HMPA to water, there is an increase in coupling constants at position 5 and a decrease in those at positions 6 and 3.

To further investigate the solvent effects on hyperfine splittings of semiquinones, molecular orbital calculations can be performed by chossing appropriate parameters for the coulomb integral for the oxygen atom, and by using C^{13} splittings for the -COR carbon atom[69]. This is because the C^{13} splittings for carbonyl groups are strongly solvent dependent[69].

However, it was not thought worth pursuing these calculations at the present time.

Table V

The coupling constants of naphthosemiquinones in water[67] and in HMPA.

Radical	Solvent	a_2	a_3	a_4	a_5	a_6	a_7	a_8 (a/mT)
1,2-naphthosemiquinone	Water		0.042	0.446	0.028	0.142	0.014	0.130
	HMPA		0.038	0.405	0.075	0.152	0.038	0.125
2-hydroxy-1,4-naphtho-semiquinone	Water		0.025		0.013	0.197	0.011	0.154
	HMPA		0.035		0.060	0.245	0.060	0.155
6-hydroxy-1,2-naphtho-semiquinone	Water		0.058	0.502	0.140		0.036	0.140
	HMPA		0.035	0.525	0.110		0.010	0.190
7-hydroxy-1,2-naphthosemiquinone	Water		0.048	0.497	0.048	0.243		0.102
	HMPA		0.048	0.460	0.0	0.268		0.085
2,3-dihydroxy-1,4 naphthosemiquinone	Water				0.103	0.073	0.073	0.103
	HMPA				0.095	0.122	0.122	0.095

Table V contd.

Radical	Solvent	a_2	a_3	a_4	a_5	a_6	a_7	a_8	a_H
1,4-naphthosemiquinone	Water	0.324	0.324		0.065	0.058	0.058	0.065	
	HMPA	0.330	0.330		0.025	0.065	0.065	0.025	
5-hydroxy-1,4-naphtho-	Water	0.390	0.270			0.080	0.030	0.112	0.080
semiquinone	HMPA	0.420	0.245			0.085	0.065	0.110	0.035
6-hydroxy-1,4-naphtho-	Water	0.442	0.278		0.060		0.164	0.0	
semiquinone	HMPA	0.330	0.220		0.048		0.096	0.048	

Table VI

Coupling constants (a/mT) of benzosemiquinones in water[34] and in HMPA.

Radical	Solvent	a_2	a_3	a_4	a_5	a_6
1,4-benzosemiquinone	HMPA	0.240	0.240		0.240	0.240
	Water	0.237	0.237		0.237	0.237
1,2-benzosemiquinone	HMPA		0.110	0.350	0.350	0.110
	Water		0.075	0.375	0.375	0.075
2-hydroxy-1,4-benzo-	HMPA		-0.055		0.490	0.140
semiquinone	Water		-0.060		0.498	0.135
2-methyl-1,4-benzo-	Water	a_{Me} = 0.210	0.170		0.255	0.237
semiquinone	HMPA	a_{Me} = 0.183	0.200		0.270	0.245
4-methyl-1,2-benzo	Water		0.015	a_{Me} = 0.485	0.380	0.095
semiquinone	HMPA		0.075	a_{Me} = 0.410	0.360	0.155
3-methyl-1,2-benzo-	Water		a_{Me} = 0.065	0.290	0.415	0.030
semiquinone	HMPA		a_{Me} = 0.105	0.290	0.360	0.110

Table VI contd.

Radical	Solvent	a_2	a_3	a_4	a_5	a_6
2-hydroxy-5-methyl-	Water		0.058		a_{Me} = 0.512	0.069
1,4-benzosemiquinone	HMPA		0.050		a_{Me} = 0.508	0.085
2-hydroxy-6-methyl-	Water		0.055		0.415	a_{Me} = 0.095
1,4-benzosemiquinone	HMPA		0.050		0.430	a_{Me} = 0.090

Conclusion

HMPA is evidently a good solvent in which to study base catalysed autoxidation of organic compounds, especially those which are inert towards oxygen in aqueous solution. The other advantage is that the autoxidation is very clean. A number of primary radicals of naphthosemiquinones which were not detected in aqueous solution were observed in this system. Phenols (unsubstituted and monosubstituted) resorcinols and dihydroaromatics were found to be successfully autoxidised in this system while they were found to be inert to autoxidation in aqueous media. Fluorescence phenomena were observed from those naphthalenediols which do not give rise to primary radicals. The complex between the oxygen molecule and the naphthoxide was suggested to be the fluorescent species.

CHAPTER 4

CALCULATION OF SUBSTITUENT EFFECTS ON THE SPIN DISTRIBUTION IN RADICALS FORMED BY ELECTRON-LOSS FROM PHENOLS AND FROM ALKYL ARYL ETHERS

4.1 Introduction

The McLachlan SCF method has been used extensively in the calculation of electron spin distributions of organic π radicals[15] and in particular, has been used successfully to account for substituent effects on the spin distribution in phenoxyl radicals[34]. It has also been used successfully to describe the spin distributions of alkoxybenzene radical cations[94,98].

In previous studies, when this method was applied to phenoxyl radicals, it was found to be better than more sophisticated methods, such as INDO (intermediate neglect of differential overlap). The McLachlan approach leads to good predictions for the magnitude and the sign of ring proton hyperfine splittings in certain substituted phenoxyl radicals when the substituents are treated as heteroatoms contributing a pair of electrons to the conjugated π system. However, the method fails for substituents which are strongly electron-withdrawing, for example, carbonyl-, carboxyl- and nitro-. In addition, the hyperfine splittings of the proton in substituents such as methyl and methoxy in phenoxyl radicals[34] and alkoxybenzene radical cations[102] were not directly calculable. To overcome these gaps in the theory, the McLachlan SCF method was used to calculate the electron spin distributions in phenoxyl radicals previously studied[34], and in the recently investigated[76b,102] phenol radical cations and alkyl aryl ether radical cations, using the correct number of the basis π-orbitals. Though the number of parameters involved is thereby increased, this disadvantage is more than offset by the scope of application.

4.2 The molecular orbitals of phenoxyl radicals

The assignment of an unpaired electron to a radical requires the knowledge of the number and ordering of the set of orbital energies of the system. The knowledge of the odd electron orbital enables one to obtain the spin distribution in the radical. Therefore it is necessary to consider the molecular orbitals of the phenoxyl radical in order to have an understanding of the electron spin distribution in this radical. Asaphenoxyl radical can be regarded as a substituted benzene anion or cation, the molecular orbitals of benzene are first considered.

The energy levels and the molecular wave functions of benzene are indicated diagramatically as follows:

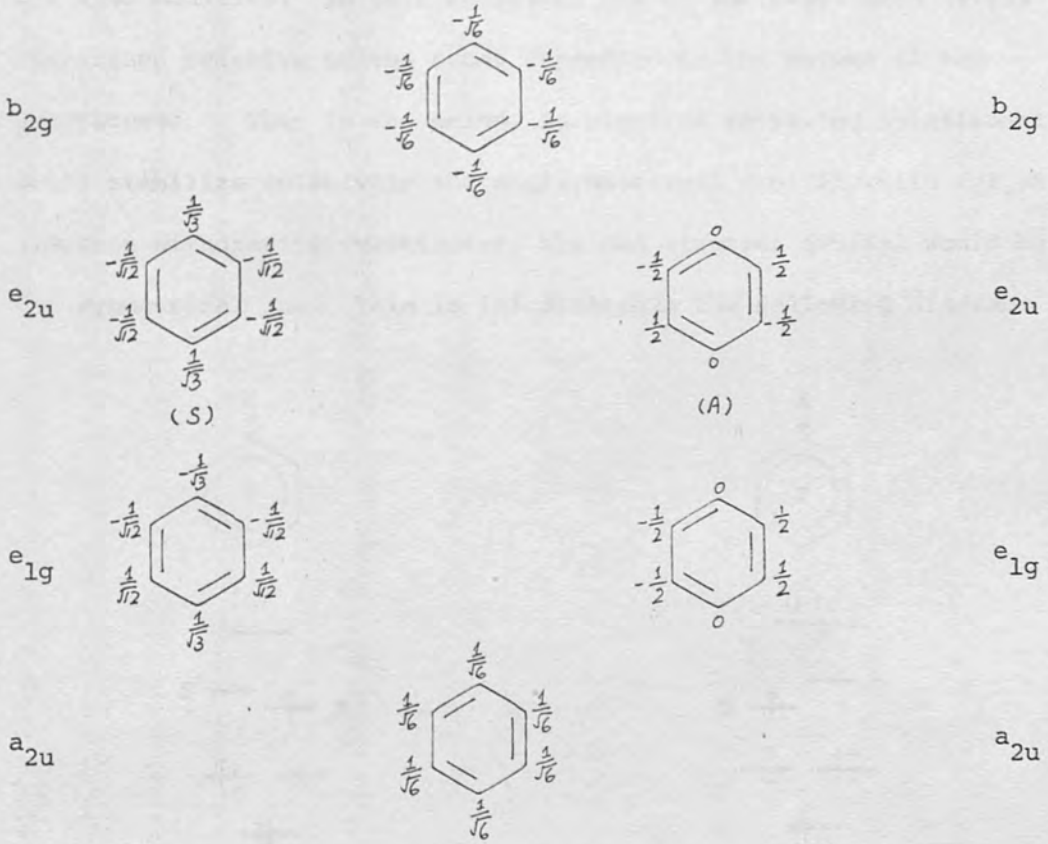

Fig. 1. The π molecular orbitals of benzene. The numbers are the coefficients of the atomic p orbitals.

The benzene π system has six electrons distributed among the a_{2u} and the doubly degenerate e_{1g} orbitals in the ground state. Removal of an electron from one of the degenerate e_{1g} orbitals produces the benzene radical cation while the addition of an electron to the degenerate e_{2u} orbitals produces the benzene radical anion. The odd electron can occupy either a symmetrical (S) or an antisymmetrical (A) orbital with respect to a plane passing through the carbon-1 and carbon-4 of e_{2u} orbitals, as they are degenerate in the case of an unsubstituted benzene radical anion. For the substituted benzene radical anions,[7] the substituent can be considered as a perturbation acting on the benzene ring so that the degeneracy of the e_{2u} orbitals is removed, or, all of the other orbitals are also modified. In this approach, one of the degenerate levels is stabilized relative to the other depending on the nature of the substituent. Thus in the anion, an electron releasing substituent would stabilize relatively the antisymmetrical orbital, while for an electron withdrawing substituent, the odd electron orbital would be the symmetrical one. This is illustrated in the following diagram.

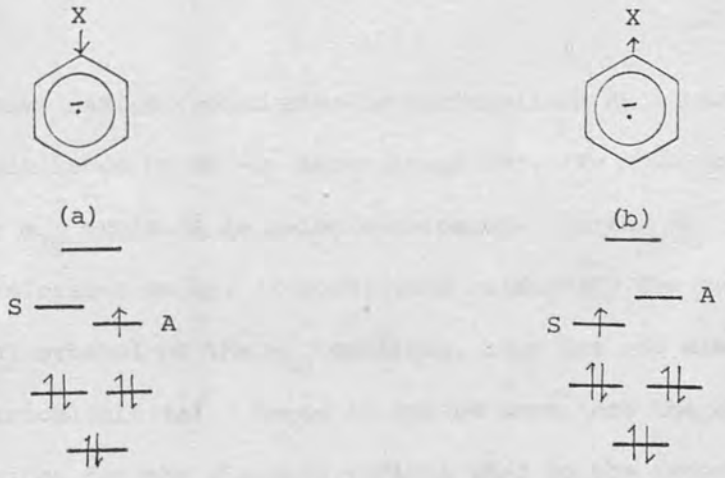

Fig. 2. The effect of substituent on the molecular orbitals of benzene radical anion, (a) with an electron releasing substituent, (b) with an electron withdrawing substituent.

The phenoxyl radical could be considered as a $-O^+$ substituted benzene radical anion[7] (A) as depicted below:

(A)

The electron withdrawing effect of the $-O^+$ stabilizes relatively the antibonding symmetrical orbital, so the odd electron goes to the symmetrical orbital.

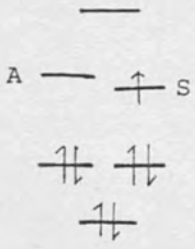

Fig. 3. Molecular orbital diagram of the phenoxyl radical by considering it to be $-O^+$ substituted benzene radical anion

A phenoxyl radical could also be rationalised as a benzene radical cation substituted by an $-O^-$ substituent (B). In this case, the set of degenerate e_{1g} orbitals is being considered. As the $-O^-$ is a strong electron releasing group, it stabilizes relatively the anti-symmetrical orbital of the e_{1g} orbitals, thus the odd electron occupies the symmetrical orbital. Hence it can be seen that the above two considerations for the phenoxyl radical lead to the same predictions for the symmetry of the odd electron orbital.

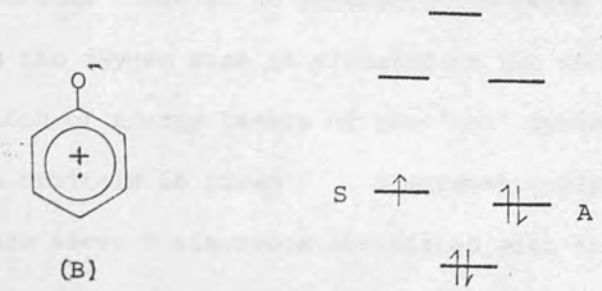

(B)

Fig. 4. Molecular orbital diagram of the phenoxyl radical when it is considered as a $-O^-$ substituted benzene radical cation.

Similarly, in the case of the phenol radical cation (C) and the anisole radical cation (D), the odd electron occupies the symmetrical orbital.

(C)

(D)

Recently, a new and useful theorem concerning the building up of energy levels of a molecular system has been advanced by Dixon[121a]. This can be applied to substituted benzene and it involves the modification of all of the orbitals of benzene. The theorem states that when an orbital system is increased by one orbital, the 'new' molecular orbital energy levels alternate with those of the 'old' system. The energy levels remain unchanged if there is no interaction between the added atomic orbital and the 'old' system. The phenoxyl radical could be depicted as the addition of an oxygen atomic orbital to the 'old' system, that is the benzene π system[121a]. The energy levels of the phenoxyl radical so built up lie alternately between those of benzene. The antisymmetrical orbitals of benzene

are not affected because there is no interaction between them and the oxygen orbital, as the oxygen atom is situated on the nodal plane (Fig. 1). Thus the distribution of energy levels of the 'new' system after the interaction of the orbitals is given diagramatically in Fig. 5 on page 108. There are seven π electrons associated with the phenoxyl radical, consequently the odd electron occupies the symmetrical orbital. This is in accord with the approach mentioned before.

However, it is difficult to ascertain the value of the energy level of the odd electron orbital of a substituted benzene by the two approaches mentioned above, (at least to a reasonable approximation), because the energy gap between the bonding and the antibonding orbitals of the benzene system is large. However, with the help of a new approach (i.e the bracketting method) of building up of molecular orbital system developed recently by Dixon[121b], the problem is to some extent solved. This method involves the building up of a molecular orbital system by different routes so that in each route, atomic orbitals are added successively, one at a time until the number of orbitals required by the molecule of interest is reached. In the case of the phenoxyl radical, the energy levels can be considered at least to be built up from two routes[121b] arising from (I) and from (II) (see Fig. 6). The molecular orbital energy levels of the phenoxyl radical are then obtained by taking these two routes into consideration in such a way that the 'new' orbitals lie above or below the dashed lines joining the orbitals of the same symmetry for the two systems. This is illustrated in Fig. 6 on page 109. From Fig. 6, it can be seen that this new approach predicts that the odd electron orbital lies in between the non-bonding orbital (i.e. $E = \alpha$) and the bonding orbitals of benzene without the need to specify the values for the parameters involved.

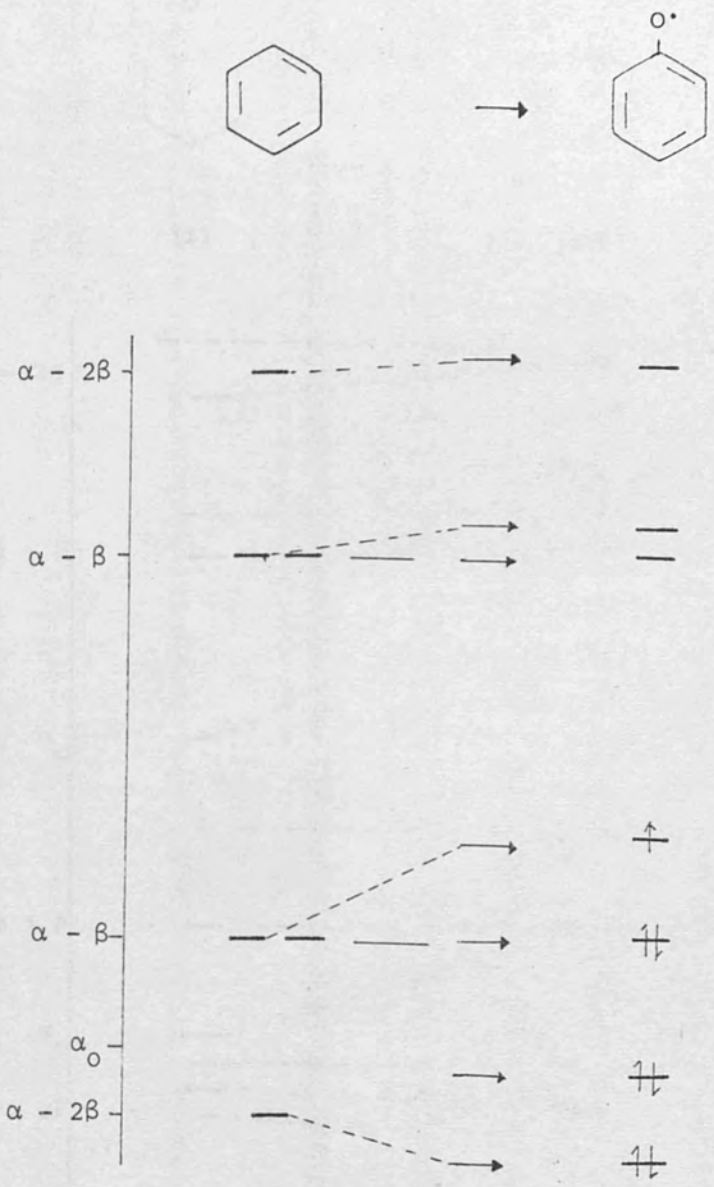

Fig. 5. The π molecular orbitals of the phenoxyl radical built up by Dixon's theorem[121a].

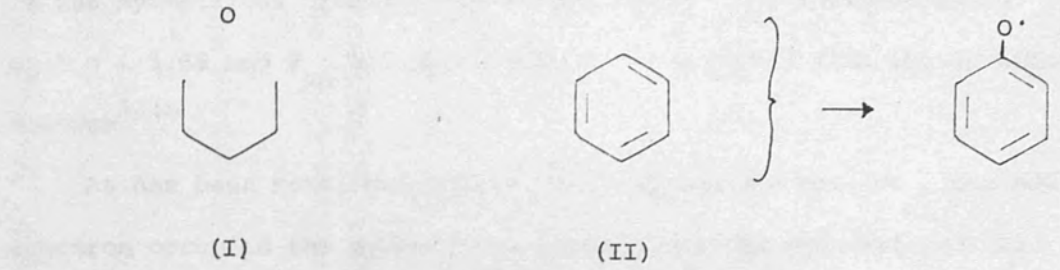

(I) (II)

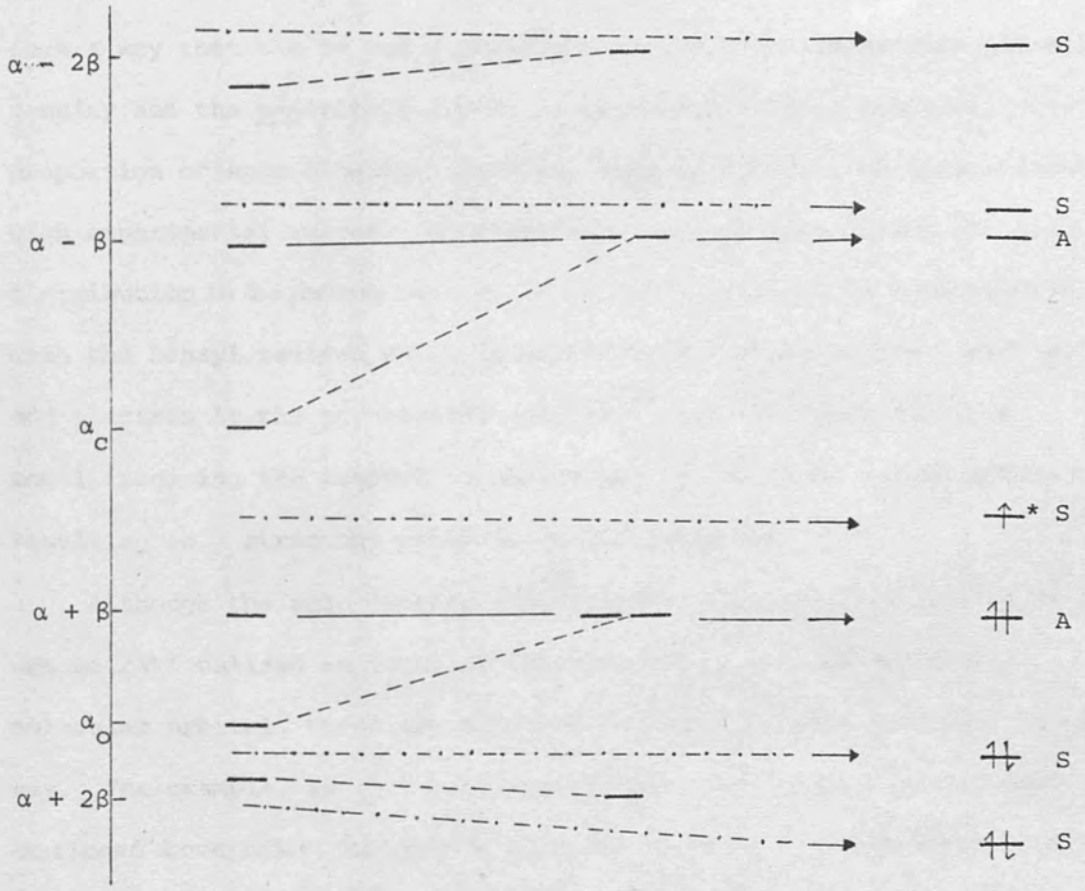

Fig. 6. Build up of energy levels diagram by the bracketting method for the phenoxyl radical.

* The odd electron orbital

It has been computed by the McLachlan method that the odd electron is in the symmetrical orbital with energy level $E = \alpha + 0.568\beta$ using $\alpha_o = \alpha + 1.6\beta$ and $\beta_{co} = 1.3\beta$. This is as expected from the interleaving theorem[121b].

As has been mentioned before, both approaches predict the odd electron occupied the symmetrical orbital for the phenoxyl radical, therefore the electron spin density is expected to be distributed in such a way that the o- and m-positions should have almost the same spin density and the p-position should be associated with a greater proportion of spin density. However, this is found to be inconsistent with experimental values. An alternative way of visualising the spin distribution in the phenoxyl radical is to consider it to be isoconjugate with the benzyl radical, which is an odd alternant hydrocarbon with an odd electron in the non-bonding orbital[124]; or alternatively by a model involving the removal of oxygen and the adjacent carbon atoms, resulting in a structure which is an odd alternant[124].

Although the spin density distribution of the phenoxyl radical could not be rationalised in terms of the symmetry of the odd electron molecular orbital, there are many radicals that can be predicted well in this way. For example, in 1,3-benzosemiquinone, the two approaches that have been mentioned above predict that the odd electron occupies the antisymmetrical orbital containing a node (Hückel approximation) through 2- and 5-positions, thereby predicting zero splittings for these two ring protons, while the positions 4 and 6 are predicted to have larger splittings. This is consistent with the experimental results. Fig. 7 shows the energy levels of 1,3-benzosemiquinone set up by Dixon's theorem.

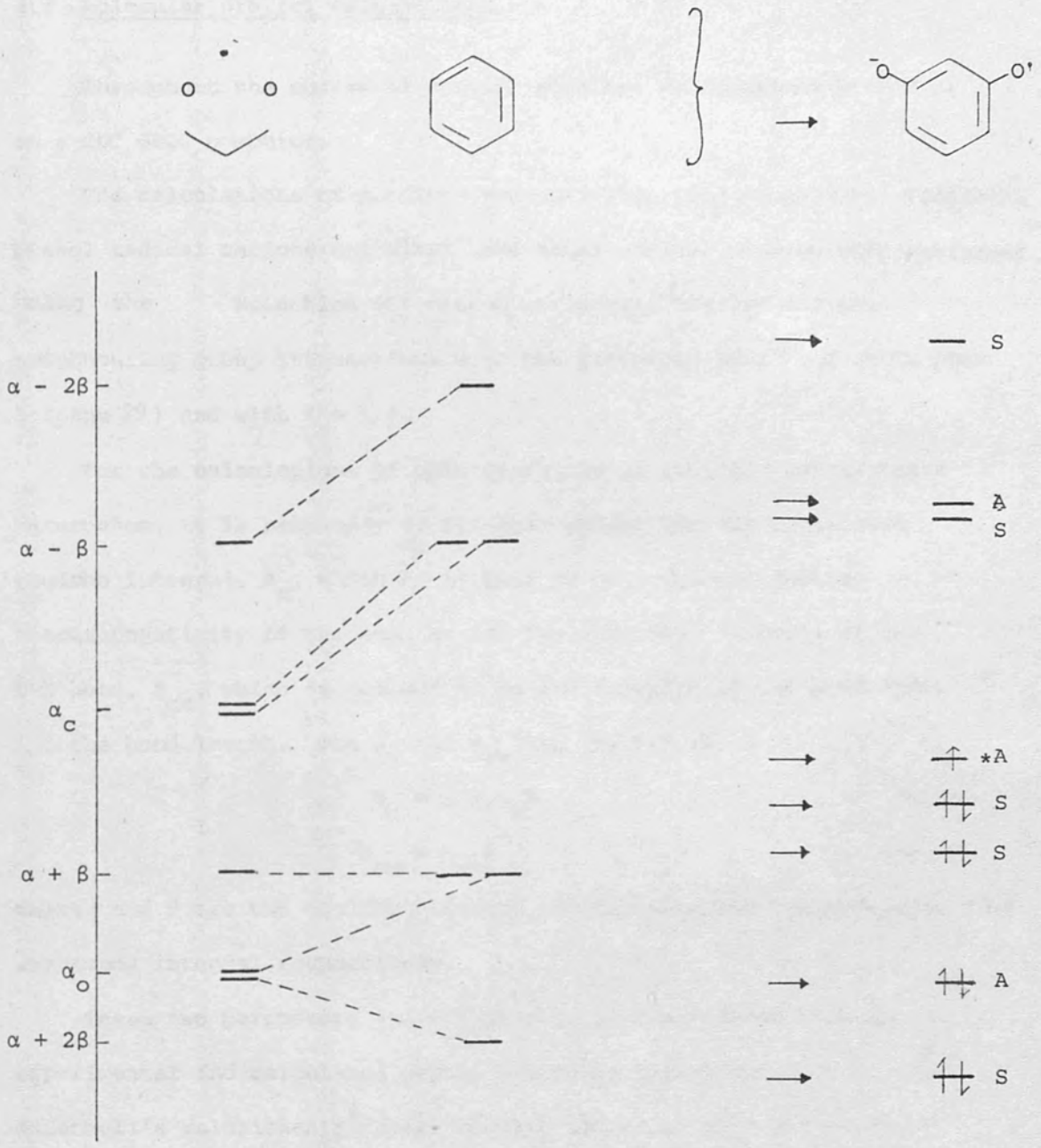

Fig. 7. Build up of energy level diagram by the bracketting method for the resorcinol

* The odd electron energy level

4.3 Molecular orbital calculations

Throughout the course of present studies, calculations were done on a CDC 6600 computer.

The calculations of electron spin distributions of phenoxyl radicals, phenol radical cations and alkyl aryl ether radical cations were performed using the McLachlan SCF method, neglecting overlap and non-neighbouring group interactions with the procedure described in Chapter 1 (page 29) and with $\lambda = 1.2$.

For the calculations of spin densities of radicals containing a heteroatom, it is necessary to fix some values for the heteroatom coulomb integral, α_x, which is assumed to be a function of the electronegativity of the atom X, and the resonance integral of the C-X bond, β_{cx}, which is assumed to be the function of the bond order and the bond length. The α_x and β_{cx} are defined by

$$\alpha_x = \alpha + h_x\beta \qquad (4.1a)$$

$$\beta_{cx} = k_{cx}\beta \qquad (4.1b)$$

where α and β are the coulomb integral and the standard carbon-carbon bond resonance integral respectively.

These two parameters are adjusted to give agreement between experimental and calculated proton hyperfine splittings using McConnell's relationship[8] (page 19) with the value of $Q = -3.0$ mT.

The set of parameters $\alpha_o = \alpha + 1.6\beta$ and $\beta_{co} = 1.3\beta$[34], which gave good agreement with experimental values for phenoxyl radicals, was used also in the work described in this chapter for the oxygen atom bonded to only one carbon atom.

A. The hydroxy group

(i) Choice of parameters for the hydroxy group.

It may be expected that the addition of a proton to the phenoxyl radical must decrease the overall electron spin density in the oxygen orbitals, and hence the electronegativity of the σ-orbitals of the oxygen should thereby be increased. In molecular orbital terms, this corresponds to a more negative value for the coulomb integral of the oxygen.

In the calculations, h_{OH} ($\alpha_{OH} = \alpha + h_{OH}\beta$) was varied in the range of 1.0 to 4.0 with increments of 0.1 (there is no reason not to use rounded off figures), and k_{C-OH} ($\beta_{C-OH} = k_{C-OH}\beta$) over the range $0.3 < k_{C-OH} < 2.0$. These two parameters were adjusted to fit the proton hyperfine splittings at the o- and the p-positions with $Q^H_{CH} = -3.0$ mT. (This value of Q^H_{CH} is used for all the radicals studied.) Satisfactory parameters were found to be

$$h_{OH} = 2.0 \text{ and } k_{C-OH} = 1.1$$

which is the only pair of a whole family of parameters which gave reasonable agreement with experimental values. (see Table I on page 116).

(a) h_{OH} and k_{C-OH} variation

The variation of h_{OH} and k_{C-OH} with ring proton splittings is summarised in graphs 1, 2 , and 3 . It can be seen that when h_{OH} is increased, the calculated coupling constants at positions 3 and 4 increase whereas that at position 2 decreases. The change of coupling costants with respect to the change in h_{OH} is more sensitive at position 4 and at position 2, than at position 3. When k_{C-OH} increases, the coupling constants at positions 3 and 4 decrease, the decrease being more rapid at position 3; while an increase in the calculated coupling constants is observed for position 2.

Graph 1 The variation of coupling constant (a_4) with molecular orbital parameters h_{OH} and k_{C-OH} for the phenol radical cation.

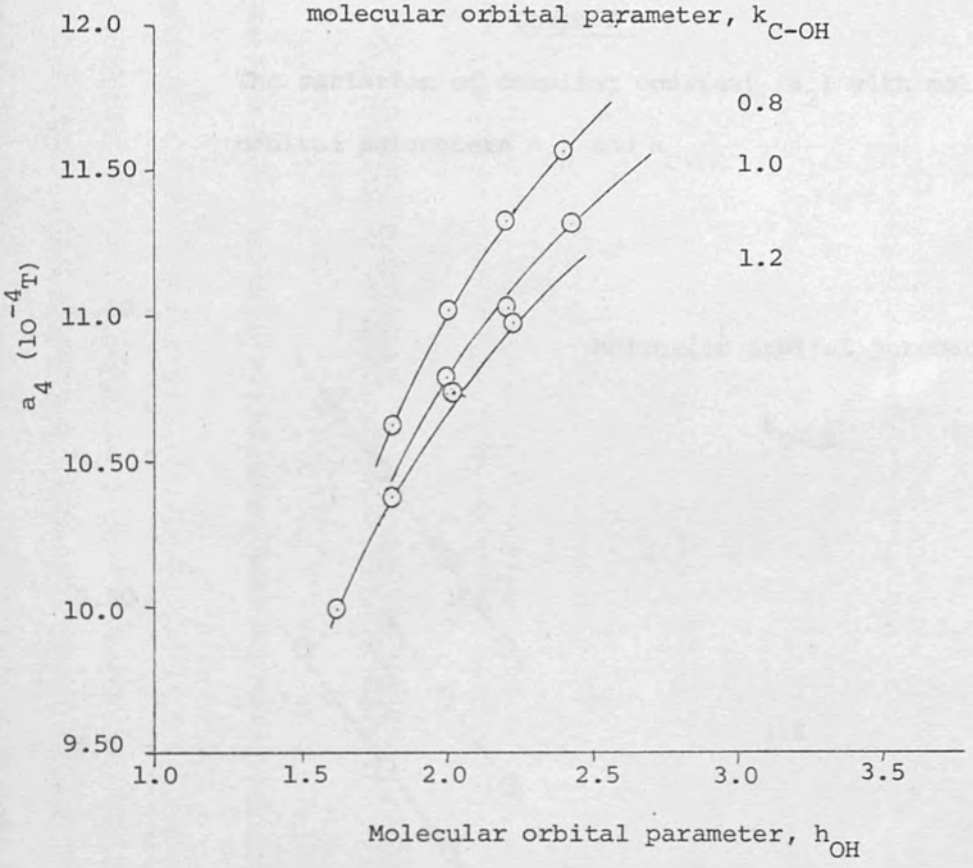

Graph 2 The variation of coupling constant (a_3) with molecular orbital parameters h_{OH} and k_{C-OH} for the phenol radical cation.

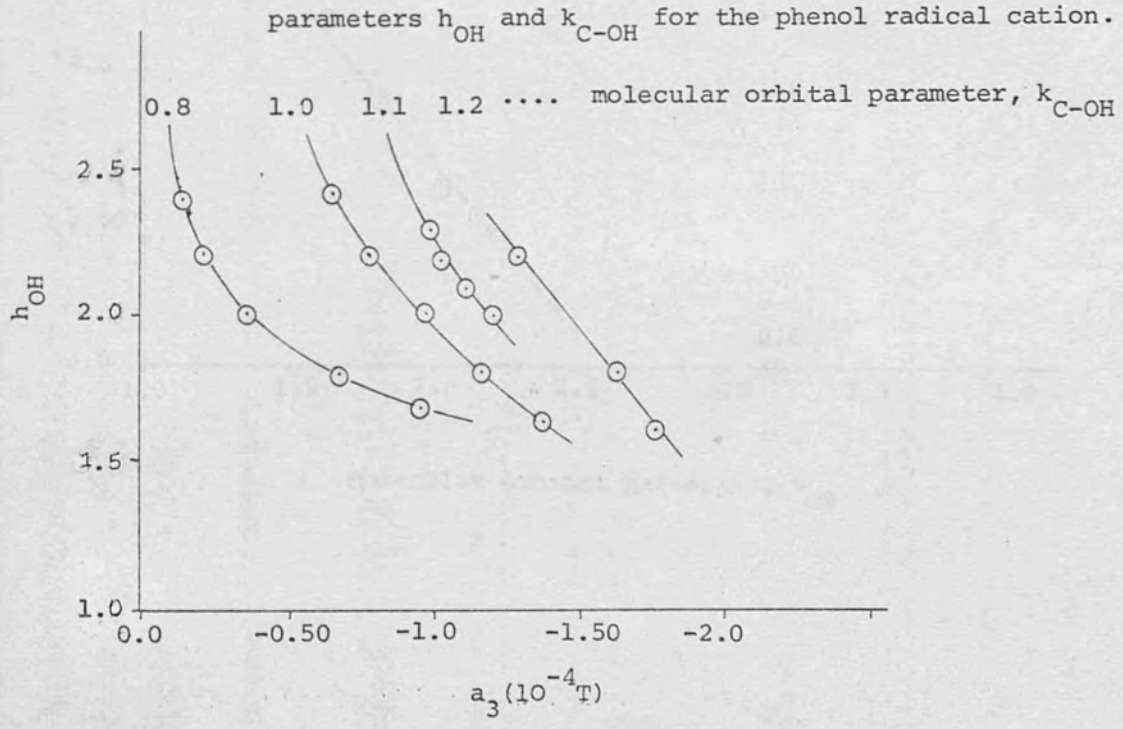

Graph 3

The variation of coupling constant (a_2) with molecular orbital parameters h_{OH} and k_{C-OH}

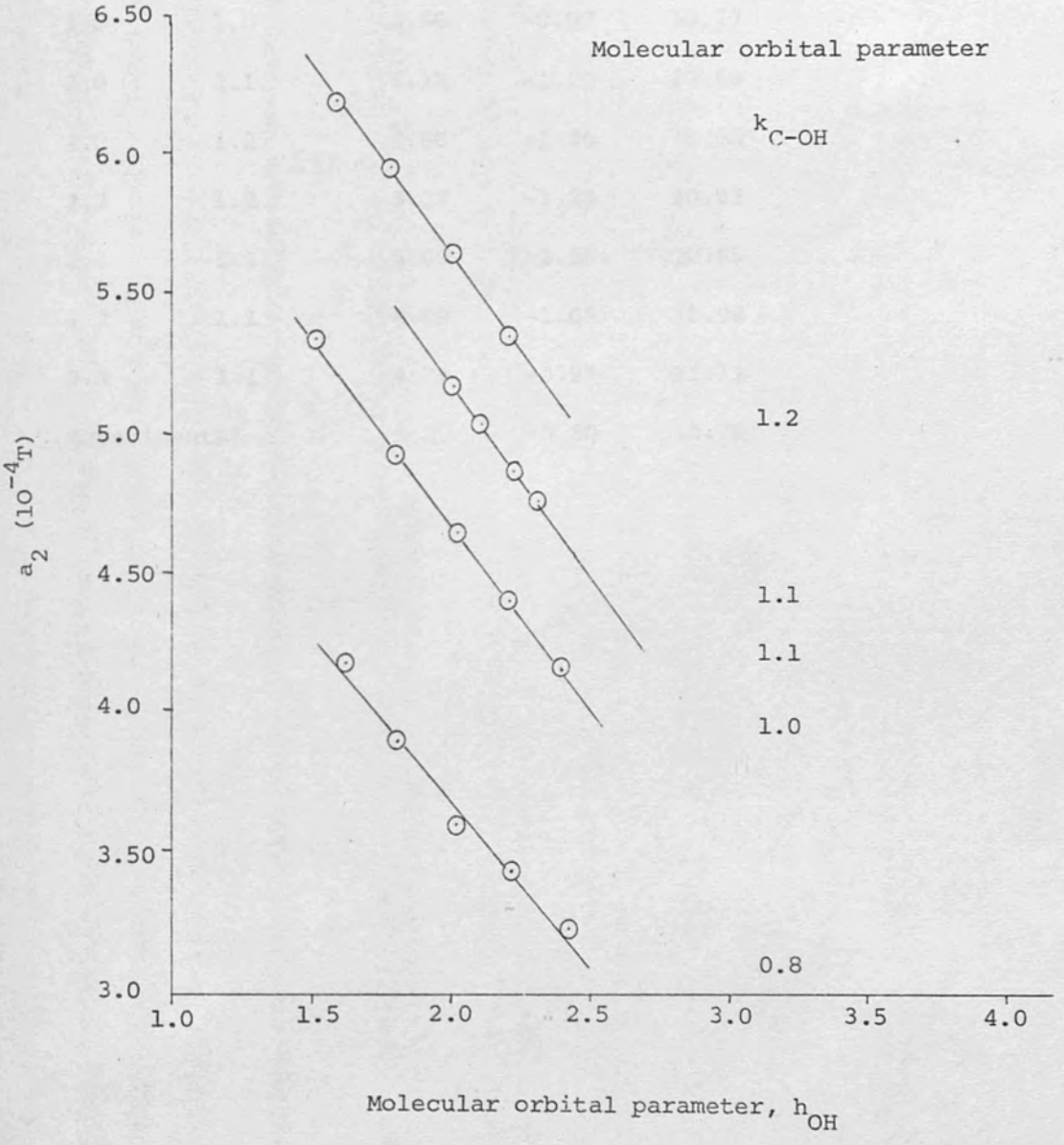

Table I

Satisfactory results of molecular orbital calculations on the phenol radical cation

h_{OH}	k_{C-OH}	a_2	a_3	a_4	$(a/10^{-4}T)$
1.8	1.0	4.94	-1.16	10.38	
2.0	1.0	4.56	-0.97	10.77	
2.0	1.1	5.16	-1.20	10.69	
2.0	1.2	5.66	-1.45	10.66	
2.2	1.2	5.38	-1.28	10.93	
2.1	1.1	5.03	-1.13	10.85	
2.2	1.1	4.89	-1.05	10.98	
2.3	1.1	4.76	-0.97	11.11	
Experimental		5.20	-0.80	10.70	

(ii) The hydroxy-substituted phenoxyl radicals and phenol radical cations.

The set of parameters chosen for the phenol radical cation was then used to calculate the coupling constants for monoprotonated phenoxyl radicals and hydroxy-substituted phenol radical cations. The results are summarised in Table II.

Table II

Calculated coupling constants for radicals from phenols and dihydroxybenzenes with $\alpha_{OH} = \alpha + 2.0\beta$ and $\beta_{C-OH} = 1.1\beta$

Substituents in 	Coupling constants (10^{-4}T)				
	a_2	a_3	a_4	a_5	a_6
1 - OH, 2 - OH		-0.78	4.46	4.46	-0.78
		(-0.25)	(4.85)	(4.85)	(-0.25)
1 - O^-, 2 - OH		-1.68	5.99	1.66	2.02
		(-1.2)	(7.0)	(1.20)	(3.0)
1 - OH, 3 - OH	-1.26		11.88	-3.19	11.88
	(0.40)		(10.90)	(-2.10)	(10.90)
1 - O^-, 3 - OH	1.81		12.14	-2.94	10.14
	(3.90)		(11.30)	(-2.30)	(8.70)
1 - OH, 4 - OH	2.15	2.15		2.15	2.15
	(2.25)	(2.25)		(2.25)	(2.25)
1 - O^-, 4 - OH	3.99	0.76		0.76	3.99
	(5.10)	(-0.30)		(-0.30)	(5.10)

Signs given are those of the spin density on the adjacent carbon atom and the values in brackets are experimental data.

From the results in Table II, it can be seen that the parameters chosen for the hydroxy group gave results in good agreement for the dihydroxylated benzene radical cations. However, for the monoprotonated phenoxyl radicals the agreement between the experimental coupling constants and theoretical values are not good. This discrepancy might be due to a relative decrease in the bond order of the C-OH bond in these radicals. This is further supported by the experimental observations that the energy barrier to rotation of the C-OH bond in the monoprotonated p-benzosemiquinone is very small[98]. Taking consideration of the above facts, attempts have been made to reduce the resonance integral of the C-OH bond. It was found that the value of $k_{C-OH} = 0.8$ provides a better agreement than those of $k_{C-OH} = 1.1$. The results in Table III show that this parameter also gave values which agreed better with experimental values when applied to the o- and the m- monoprotonated phenoxyl radicals; presumably a similar effect exists.

Table III

Calculated coupling constants ($a/10^{-4}T$) for phenol radical cations with $\alpha_{OH} = \alpha + 2.0\beta$ and $\beta_{C-OH} = 0.8\beta$.

Radicals	a_2	a_3	a_4	a_5	a_6
2-hydroxyphenoxyl		-2.82	7.91	0.02	3.69
		(-1.20)	(7.0)	(1.20)	(3.0)
3-hydroxyphenoxyl	4.32		11.10	-2.46	8.31
	(3.90)		(11.30)	(-2.30)	(8.70)
4-hydroxyphenoxyl	5.08	-0.52		-0.52	5.08
	(5.10)	(-0.30)		(-0.30)	(5.10)

Experimental data are in brackets.

This set of parameters happens to be identical to that chosen by Zweig et al[87] for the methoxy group in the molecular orbital calculations of methoxybenzene radical cations. This is not suprising as it has been shown that the methoxyprotonated phenoxyl radicals have esr spectra almost identical to those of the corresponding methoxy substituted phenoxyl radicals.[75,79]

From the results in Table II, it is apparent that the molecular orbital theory predicted that the coupling constants at the o- and the p- positions to the hydroxy-group would be smaller than those o- and p- to the $-O^-$ group. This indicates that the McLachlan method, with the set of parameters chosen, predicts that the hydroxy group has a smaller electron releasing effect than the $-O^-$ group, in accord with the experimental observations. Thus one would expect to observe a smaller value of the coupling constants at positions o- and p- to the hydroxy group in those radicals containing hydroxy and $-O^-$ groups when we use these sets of molecular orbital parameters to perform molecular orbital calculations on the radicals concerned.

B. The carbonyl group

The heteroatom model for the carbonyl group was found to be unsuccessful in the prediction of spin distributions in phenoxyl radicals.[34] A reason for the failure has been given by Dixon,[121b] who showed that for the odd electron orbital to have the correct symmetry in the nitrobenzene radical anion, to be consistent with experimental observations, the nitro- (or carbonyl-) group must be treated as a two orbital substituent. This is shown in Fig. 8. Therefore we attempted to calculate the spin distributions of these radicals by considering the carbonyl group as a two orbital substituent.

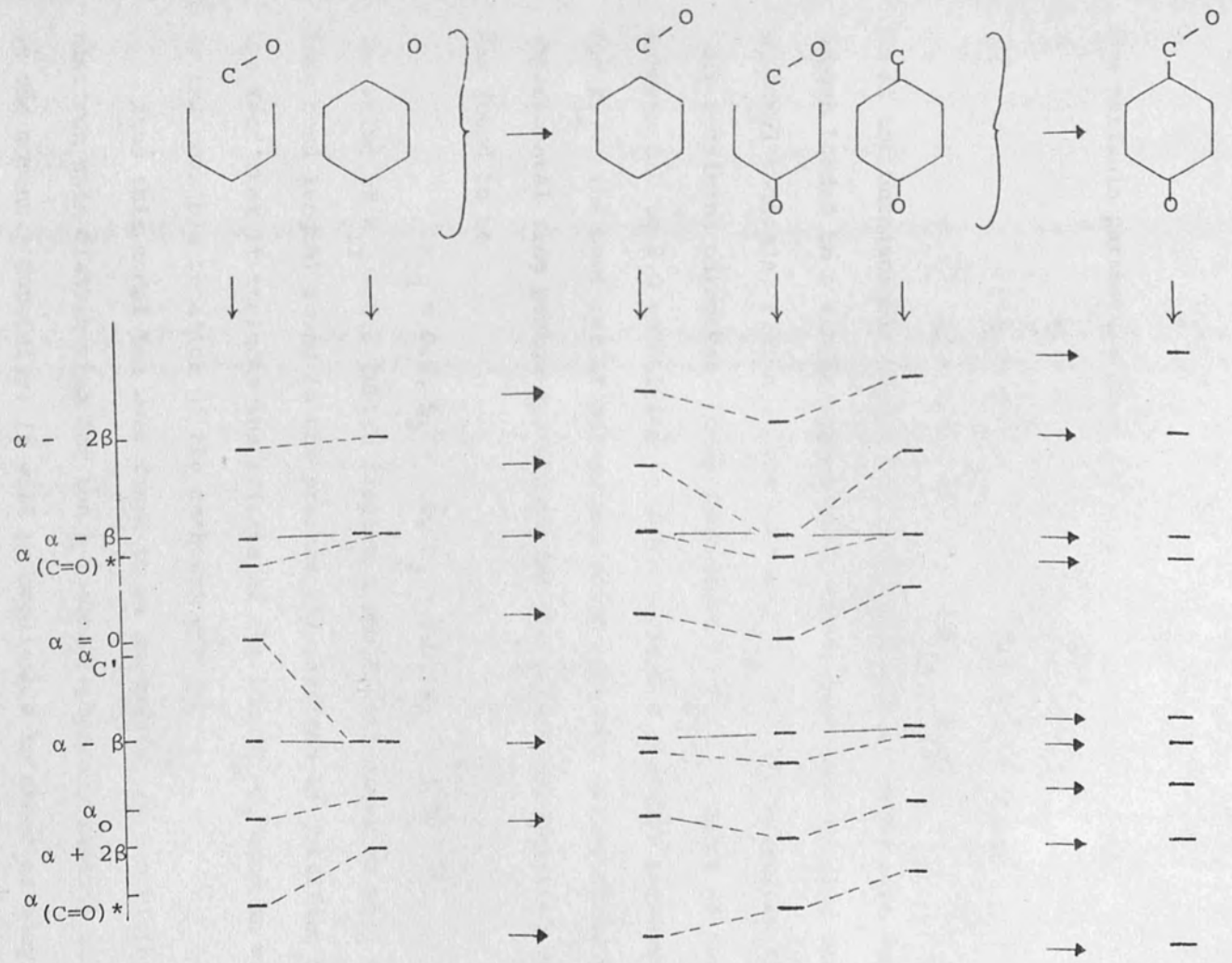

Fig. 8. Build up of energy levels diagram by the bracketting method for the p-carbonyl phenoxyl radical

(i) Choice of parameters for the carbonyl group

The notation for the carbonyl group in terms of two basis π-orbital system is as follows:

$C_1\text{-}C_2\text{=}O_3$ ≡ 

The variable parameters are:

$$\alpha_1 = \alpha$$

$$\alpha_2 = \alpha \qquad \beta_{12} = k_{12}\beta$$

$$\alpha_3 = \alpha + 1.6\beta \qquad \beta_{23} = k_{23}\beta$$

It is not unreasonable to use the previously chosen parameters for the oxygen bonded to a single carbon atom, which gave good results for phenoxyl radicals, i.e. $\alpha_o = \alpha + 1.6\beta$ and $\beta_{co} = 1.3\beta$, therefore the only remaining parameter to be considered is k_{12}. A range of values between 0.0 to 2.0 were tried in order to find a suitable parameter for k_{12}. The best set of parameters which provides values close to the experimental ring proton splittings for the p-carbonyl-phenoxyl radical was found to be

$$k_{12} = 0.5,\ h_2 = 0.0,\ h_3 = 1.6,\ k_{23} = 1.3$$

The value of $k_{12} = 0.5$ (which implies a small bond order as well as a long bond length) found in the present calculations is justified from the fact that it includes the effects of the long $C_1\text{-}C_2$ bond as well as the possible rotation of the carbonyl group.

Thus this model has been found to be successful in describing the electron spin distribution for the p-carbonyl-phenoxyl radical at least, at the moment. Hopefully, it will be applicable to other carbonyl-substituted radicals.

Table IV

The calculated coupling constants ($a/10^{-4}T$) of the p-carbonylphenoxyl radical with some of the parameters tested.

k_{12}	a_2	a_3
0.3	6.74	-2.03
0.5	6.82	-2.14
0.7	6.91	-2.24
1.0	7.10	-2.35
1.2	7.18	-2.46
Expt.	6.80	-2.20

(ii) The carbonyl-substituted phenoxyl radicals

The set of parameters chosen for the carbonyl group was tested on the carbonyl-substituted phenoxyl radicals. The results are summarised in Table V.

Table V

Calculated coupling constants ($a/10^{-4}T$) of radicals from carbonyl-substituted phenols with $\alpha_1 = \alpha$, $\alpha_2 = \alpha$ $\beta_{12} = 0.5\beta$, $\alpha_3 = \alpha + 1.6\beta$ and $\beta_{23} = 1.3\beta$.

	a_2	a_3	a_4	a_5	a_6
2 - COR		-1.37	10.05	-2.22	7.31
		(-1.35)	(10.0)	(-1.20)	(7.20)
3 - COR	7.20		9.85	-1.87	6.42
	(7.20)		(9.90)	(-1.95)	(6.75)
4 - COR	6.82	-2.21		-2.21	6.82
	(6.80)	(-2.20)		(-2.20)	(6.80)

R = H, CH_3. Experimental data are in brackets.

From Table V, it can be seen that an excellent agreement between the theoretical and the experimental coupling constants was obtained. This implies that the electron withdrawing property of the carbonyl group is very well predicted by considering it as a two orbital substituent and the success of this calculation lends support to Dixon's statement.[121b]

Since the McLachlan method with the carbonyl group treated as a two orbital substituent has successfully predicted the electron withdrawing effect of this group, one would expect to observe a small spin density associated with the positions o- and p- to the carbonyl group when the molecular orbital calculation using this method and with these parameters is performed on a new carbonyl-substituted phenoxyl-type radical.

C. The methyl group

(i) Molecular orbital calculation of the methyl proton hyperfine splittings

Molecular orbital theory[48] and valence bond theory[122] have been used to describe the methyl proton hyperfine splittings arising from the interaction between methyl protons and those organic π-radicals containing a methyl group. The methyl proton hyperfine interaction has been explained in terms of spin polarization[122] (ref. page 20) and in terms of hyperconjugation[48] (ref. page 20). It is believed that the spin polarization gives a relatively small contribution to the methyl proton splittings[7].

The aim of our calculation of methyl-substituted phenoxyl and related radicals was to obtain values of methyl proton hyperfine splittings directly, to this end we shall adopt the hyperconjugation model and neglect any contribution from spin polarization. The extent of the hyperconjugation interaction is dependent on the dihedral

angle θ, which is the angle between the projection of the C-H bond and the axis of the p_π orbital.

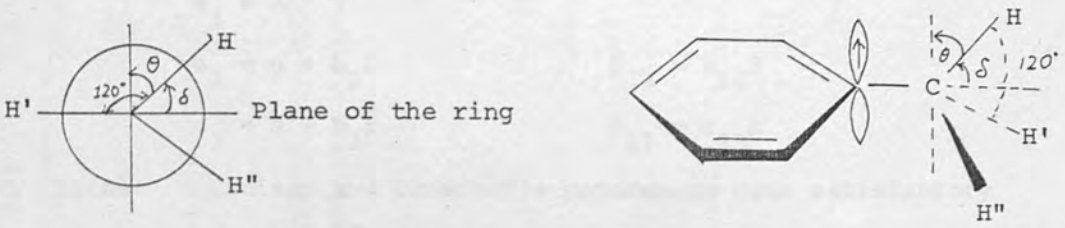

Fig. 9 (a). End-on-view of the methyl group.

(b). Side view of the methyl group.

The relationship between the hydrogen group orbital, ϕ_x, and the atomic orbitals, ϕ, ϕ' and ϕ'' of H, H' and H" respectively and the dihedral angle, θ, and δ, the angle between the hydrogen atomic orbitals and the planar benzene ring is given by the following expressions.

$$\sqrt{\frac{3}{2}}\,\phi_x = \phi \sin\delta + \phi' \sin(120^\circ + \delta) + \phi'' \sin(240^\circ + \delta)$$
$$= \phi \cos\theta - \phi' \cos(60^\circ + \theta) - \phi'' \cos(60^\circ - \theta) \qquad (4.2)$$

Since the methyl group is rotating rapidly, the three methyl protons are equivalent and the averaged dihedral angle is 45° and knowing that the coupling constant of the hydrogen atom is 50.8 mT[68] the Equation (4.3) is obtained.

$$a_{H_3} = \frac{1}{3} \times \rho_{H_3} \times 50.8 \text{ mT} \qquad (4.3)$$

where ρ_{H_3} is the total spin density on the hydrogen group orbital . Thus the methyl proton splittings can be directly calculated via the above equation.

(ii) Choice of parameters for the methyl group

In the hyperconjugation model, the methyl group is treated as a two orbital system with the notation written as follows:

$C_1\text{-}C_2\equiv H_3$ ≡ 

The variable parameters which apply to the methyl group are:

$$\alpha_1 = \alpha$$

$$\alpha_2 = \alpha + h_2\beta \qquad \beta_{12} = k_{12}\beta$$

$$\alpha_3 = \alpha + h_3\beta \qquad \beta_{23} = k_{23}\beta$$

Since Coulson and Crawford's parameters gave satisfactory results in their studies[99], and there are many reports on the molecular orbital calculations of methyl substituted radical ions using this set of parameters[94,48,49], it is logical to test this set of parameters as an initial step of our investigation. However, it was found that these parameters did not give satisfactory results for those radicals examined. (see Table VI(a)).

Table VI(a)

Calculated coupling constants for radicals from cresols with Coulson and Crawford's parameters i.e. $k_{12} = 0.7$, $h_2 = -0.1$, $k_{23} = 2.5$, $h_3 = -0.5$.

Substituents in 	Coupling constants ($a/10^{-4}$ T)					
	a_2	a_3	a_4	a_5	a_6	a_{Me}
1 - O^-, 2 - CH_3		-2.30	9.57	-1.57	5.93	3.68
		(-2.0)	(9.80)	(-1.50)	(6.0)	(7.50)
1 - O^-, 3 - CH_3	6.30		10.22	-2.06	6.95	-0.34
	(5.90)		(10.50)	(-1.90)	(7.10)	(-1.50)
1 - O^-, 4 - CH_3	6.24	-1.64		-1.64	6.24	4.94
	(6.10)	(-1.40)		(-1.40)	(6.10)	(12.70)

Experimental data are in brackets.

Therefore we have to find another set of parameters which could give satisfactory results for both the ring and the methyl proton hyperfine splittings for these radicals and hopefully for a large number of different classes of radicals as well. Guided by our previous experience[14], we varied the methyl group parameters within the following range i.e.

$0 > h_2 > -0.1$, $0 > h_3 > -0.5$, $0.5 < k_{12} < 1.0$, $1.0 < k_{23} < 3.0$

Permutation of these four parameters within these ranges still fails to give an optimum set of parameters for the methyl group, which should give results in good agreement with the experimental values. Some of the results are listed in Table VI(b) on page 128.

In addition to those poor results, the parameters within the range stated above gave a wrong prediction for the odd electron orbital in the case of toluene anion; i.e. it is symmetrical in character in contradiction to the experimental observations. In order to ensure that the odd electron goes to the antisymmetrical orbital in the toluene anion, the coulomb integral should be very large, i.e. the value of $h_3 \leqslant -1.0$ as suggested by Dixon[121b]. This is illustrated diagrametically in Fig. 10. Therefore the range of values for h_3 and h_2 was widened.

Perusual of the results listed in Table VI(c), it was found that a set of parameters

$$h_1 = -0.7,\ k_{12} = 0.7,\ h_2 = -1.0,\ k_{23} = 2.5$$

gave fairly good agreement for both the ring and the methyl proton hyperfine splittings for radicals from o- and m- cresols. However, for the radical from p-cresol, the methyl proton splittings predicted were too low. In the later case, the calculated methyl coupling constant had to be multiplied by a factor of 1.72 to give good agreement with the experimental value. It was not understood at this stage, as to why the p-methyl-proton coupling constant is underestimated.

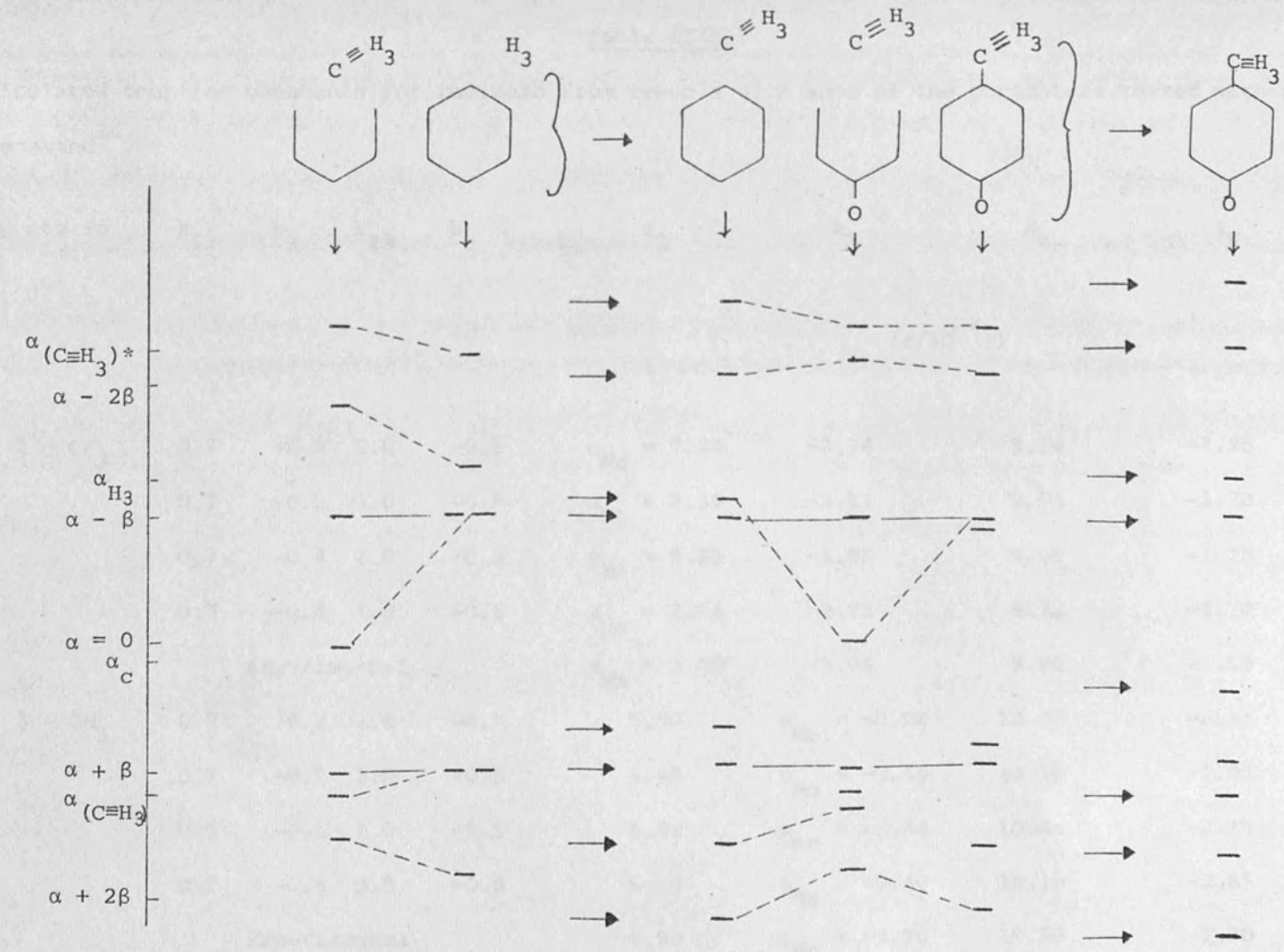

Fig. 10. Build up of energy levels diagram by the bracketting method for the toluene anion and the p-methylphenoxyl radical.

Table VI(b)

Calculated coupling constants for radicals from cresols with some of the parameters tested within the range suggested[14].

Substituents in 	k_{12}	h_2	k_{23}	h_3	a_2	a_3	a_4	a_5	a_6
						$(a/10^{-4}T)$			
1 - O^-, 2 - CH_3	0.7	-0.2	2.0	-0.5	a_{Me} = 7.24	-2.24	9.14	-1.25	5.38
	0.7	-0.2	3.0	-0.5	a_{Me} = 2.38	-2.21	9.73	-1.70	6.18
	0.7	-0.4	2.0	-0.5	a_{Me} = 8.29	-2.45	9.05	-1.20	5.28
	0.7	-0.4	3.0	-0.5	a_{Me} = 2.54	-2.22	9.72	-1.70	6.16
	Experimental				a_{Me} = 3.68	-2.08	9.80	-1.50	6.0
1 - O^-, 3 - CH_3	0.7	-0.2	2.0	-0.5	5.90	a_{Me} = -0.54	10.42	-2.14	7.24
	0.7	-0.2	3.0	-0.5	6.40	a_{Me} = -0.46	10.18	-2.05	6.90
	0.7	-0.4	2.0	-0.5	5.83	a_{Me} = -0.44	10.44	-2.15	7.27
	0.7	-0.4	3.0	-0.5	6.39	a_{Me} = -0.46	10.19	-2.05	6.90
	Experimental				5.90	a_{Me} = -1.50	10.50	-1.90	6.40

Table VI(b) contd.

Substituents in 	k_{12}	h_2	k_{23}	h_3	a_2	a_3	a_4	a_5	a_6
							$(a/10^{-4}T)$		
1 - O^-, 4 - CH_3	0.7	-0.2	2.0	-0.5	5.88	-1.20	a_{Me} = 8.03	-1.20	5.88
	0.7	-0.2	3.0	-0.5	6.39	-1.75	a_{Me} = 3.30	-1.75	6.39
	0.7	-0.4	2.0	-0.5	5.82	-0.44	a_{Me} = 10.44	-2.15	7.27
	0.7	-0.4	3.0	-0.5	6.38	-1.74	a_{Me} = 3.47	-1.74	6.38
	Experimental				6.10	-1.40	a_{Me} = 12.70	-1.40	6.10

Table VI (c)

(i) Calculated coupling constants for the p-cresol radical with the parameters tested and with $h_3 \leq -1.0$

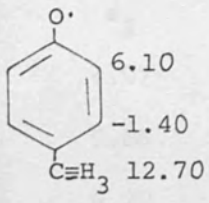

k_{12}	h_2	k_{23}	h_3	a_2	a_3	a_{Me} ($a/10^{-4}T$)
0.7	-0.1	2.0	-1.1	5.44	-1.04	9.10
0.7	-0.1	2.5	-1.1	6.00	-1.44	5.24
0.7	-0.1	3.0	-1.1	6.25	-1.63	3.38
0.7	-0.2	2.0	-1.1	5.36	-0.99	10.02
0.7	-0.2	2.5	-1.1	5.80	-1.33	5.60
0.7	-0.2	3.0	-1.1	6.24	-1.62	3.52
0.7	-0.4	2.0	-1.1	5.17	-0.87	12.12
0.7	-0.4	2.5	-1.1	5.91	-1.38	6.30
0.7	-0.4	3.0	-1.1	6.21	-1.60	3.83
0.7	-0.7	2.0	-1.1	4.79	-0.66	16.90
0.7	-0.7	2.5	-1.1	5.79	-1.31	7.68
0.7	-0.7	3.0	-1.1	6.17	-1.57	4.35
0.7	-0.2	2.0	-1.0	5.46	-1 06	9.90
0.7	-0.2	2.5	-1.0	6.02	-1.46	5.49
0.7	-0.2	3.0	-1.0	6.26	-1.64	3.49
0.7	-0.4	2.0	-1.0	5.29	-0.97	11.96
0.7	-0.4	2.5	-1.0	5.96	-1.42	6.17
0.7	-0.4	3.0	-1.0	6.24	-1.63	3.77

Table VI (c) contd.

Calculated coupling constants for the p-cresol radical with the parameters tested and with $h_3 \leqslant -1.0$

k_{12}	h_2	k_{23}	h_3	a_2	a_3	a_{Me}	$(a/10^{-4}T)$
0.7	-0.7	2.0	-1.0	4.97	-0.78	16.23	
0.7	-0.7	2.5	-1.0	5.86	-1.36	7.42	
0.7	-0.7	3.0	-1.0	6.20	-1.60	4.25	
0.7	0.0	2.0	-1.0	5.60	-1.15	8.30	
0.7	0.0	2.5	-1.0	6.06	-1.49	4.92	
0.7	0.0	3.0	-1.0	6.29	-1.66	3.24	
0.7	0.0	2.0	-1.1	5.52	-1.08	8.30	
0.7	0.0	2.5	-1.1	6.03	-1.46	4.84	
0.7	0.0	3.0	-1.1	6.26	-1.64	3.25	

Table VI (c) contd.

(ii) Calculated coupling constants for the o-cresol radical with parameters tested and with $h_3 \leq -1.0$

k_{12}	h_2	k_{23}	h_3	a_3	a_4	a_5	a_6	a_{Me} ($a/10^{-4}T$)
0.7	-0.2	2.0	-1.1	-2.56	8.39	-0.67	4.46	8.80
0.7	-0.2	2.5	-1.1	-2.47	9.24	-1.26	5.43	4.42
0.7	-0.2	3.0	-1.1	-2.40	9.90	-1.89	6.60	1.11
0.7	-0.4	2.0	-1.1	-2.53	8.09	-0.51	4.18	11.05
0.7	-0.4	2.5	-1.1	-2.48	9.16	-1.21	5.33	5.07
0.7	-0.4	3.0	-1.1	-2.41	10.24	-1 79	6.35	2.38
0.7	-0.7	2.0	-1.1	-2.44	7.47	-2.06	3.66	16.02
0.7	-0.7	2.5	-1.1	-2.51	9.0	-1.11	5.16	6.32
0.7	-0.7	3.0	-1.1	-2.61	8.80	-1.02	5.21	3.95
0.7	-0.2	2.0	-1.0	-2.55	8.54	-0.77	4.62	8.56
0.7	-0.2	2.5	-1.0	-2.45	9.30	-1.32	5.51	7.44
0.7	-0.2	3.0	-1.0	-2.33	9.60	-1.56	5.93	2.61
0.7	-0.4	2.0	-1.0	-2.54	8.28	-0.64	4.38	10.59
0.7	-0.4	2.5	-1.0	-2.46	9.23	-1.26	5.43	5.0
0.7	-0.4	3.0	-1.0	-2.33	9.57	-1.54	5.90	2.83
0.7	-0.7	2.0	-1.0	-2.48	7.77	-0.38	3.93	14.96
0.7	-0.7	2.5	-1.0	-2.48	9.11	-1.19	5.29	6.01
0.7	-0.7	3.0	-1.0	-2.35	9.53	-1.51	5.84	3.21
0.7	0.0	2.0	-1.1	-2.55	8.73	-0.80	4.82	7.01
0.7	0.0	2.5	-1.1	-2.51	9.0	-1.11	5.16	6.32
0.7	0.0	3.0	-1.1	-2.34	9.59	-1.55	5.91	2.43
0.7	0.0	2.0	-1.0	-2.55	8.63	-0.80	4.69	7.13
0.7	0.0	2.5	-1.0	-2.43	9.36	-1.36	5.59	3.83
0.7	0.0	3.0	-1.0	-2.32	9.62	-1.58	5.96	2.41
	(Experimental)			-2.0	9.80	-1.50	6.0	7.50

Table VI (c) contd.

(iii) Calculated coupling constants for the m-cresol radical with parameters tested and with $h_3 \leq -1.0$

k_{12}	h_2	k_{23}	h_3	a_2	a_4	a_5	a_6	a_{Me}	$(a/10^{-4}T)$
0.7	-0.2	2.0	-1.1	5.16	10.71	-2.28	7.70	-0.14	
0.7	-0.2	2.5	-1.1	5.90	10.41	-2.14	7.24	-0.46	
0.7	-0.2	3.0	-1.1	6.78	10.12	-2.06	6.69	-0.82	
0.7	-0.4	2.0	-1.1	4.91	10.79	-2.32	7.84	0.20	
0.7	-0.4	2.5	-1.1	5.84	10.44	-2.16	7.27	-0.42	
0.7	-0.4	3.0	-1.1	6.49	10.21	-2.10	6.72	-0.80	
0.7	-0.7	2.0	-1.1	4.36	10.93	-2.40	8.13	1.32	
0.7	-0.7	2.5	-1.1	5.72	10.48	-2.18	10.35	-0.36	
0.7	-0.7	3.0	-1.1	6.35	10.25	-2.12	11.50	-0.72	
0.7	-0.2	2.0	-1.0	5.30	10.66	-2.25	7.61	-0.22	
0.7	-0.2	2.5	-1.0	5.96	10.39	-2.13	7.19	-0.47	
0.7	-0.2	3.0	-1.0	6.23	10.26	-2.08	7.01	-0.42	
0.7	-0.4	2.0	-1.0	5.10	10.72	-2.2	7.73	-0.55	
0.7	-0.4	2.5	-1.0	5.92	10.41	-2.14	7.23	-0.45	
0.7	-0.4	3.0	-1.0	4.21	10.27	-2.08	7.03	-0.43	
0.7	-0.7	2.0	-1.0	4.67	10.84	-2.72	9.96	-0.89	
0.7	-0.7	2.5	-1.0	5.81	10.45	-2.16	7.29	-0.37	
0.7	-0.7	3.0	-1.0	6.80	10.29	-2.09	7.05	-0.42	
0.7	0.0	2.0	-1.1	5.35	10.65	-2.25	7.59	-0.33	
0.7	0.0	2.5	-1.1	5.96	10.39	-2.13	7.20	-0.47	
0.7	0.0	3.0	-1.1	6.22	10.27	-2.08	7.02	-0.41	
0.7	0.0	2.0	-1.0	5.46	10.60	-2.23	7.53	-0.39	
0.7	0.0	2.5	-1.0	6.0	10.37	-2.12	7.16	-0.86	
0.7	0.0	3.0	-1.0	6.25	10.25	-2.08	7.02	-0.41	
	(Experimental)			5.90	10.50	-1.90	7.10	-1.50	

The low value of k_{12} is justified to some extent in that it takes into consideration of the long C_1-C_2 bond.

The success of our calculation using the unusual parameter for the coulomb integral for the hydrogen i.e. h_3 = -1.0 supports the statement made by Dixon[121b].

(iii) Methyl-substituted phenol radical cations

The results of the molecular orbital calculations on the methyl-substituted phenol radical cations using the set of parameters chosen for the radicals from cresols were listed in Table VII.

Table VII

Calculated coupling constants for the methyl-substituted phenol radical cations ($a/10^{-4}T$) (experimental values in brackets)

Position of methyl-substituent	a_2	a_3	a_4	a_5	a_6	a_{Me}
2 - CH_3		-2.29	9.23	-0.1	2.89	6.89
		(-1.60)	(9.80)	(0.35)	(4.0)	(7.50)
3 - CH_3	3.29		11.30	-1.80	6.57	0.91
	(4.0)		(11.0)	(-1.20)	(6.40)	(-0.2)
4 - CH_3	4.12	-0.43		-0.43	4.12	9.23
	(4.50)	(-0.05)		(-0.05)	(4.50)	(15.10)

It can be seen that satisfactory agreement between theory and experiment was obtained for the ring and the methyl proton coupling constants in these radicals. However, the methyl hyperfine splittings of the p-methylphenol radical cation was again predicted too small.

The results in Table VII clearly indicated that the positions o- and p- to the methyl group have smaller coupling constants than those

o- and p- to the hydroxyl group. This suggests that the set of molecular orbital parameters chosen for the methyl group predicts a smaller electron releasing effect than that for the hydroxy group. This is consistent with experimental observations. By comparing the calculated coupling constants for the methylphenoxyl radical and the p-carbonylphenoxyl radical, it is found that the coupling constant o- to the methyl group is larger than that o- to the carbonyl group. Thus the molecular orbital calculation predicts the carbonyl group to have a stronger electron withdrawing effect than the methyl group, in accord with experimental observations.

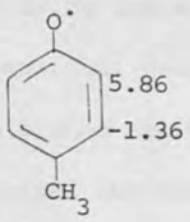

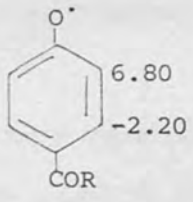

Thus it is expected that the positions o- and p- to the carbonyl group would have smaller coupling constants than those o- and p- to the methyl group in a new phenoxyl-type radical with these two substituents. For the hydroxy-methyl-substituted radical, the electron spin density would be expected to distribute in such a way that the positions o- and p- to the hydroxyl group have a greater proportion of spin density than those o- and p to the methyl group.

D. The methoxy group

There are four possible ways of treating the methoxy group in the molecular orbital calculations of electron spin distributions in methoxy-substituted aromatic radical ions; (1) by treating the methoxy group as a single heteroatom, (2) by using the inductive model, (3) by regarding the methoxy group as two heteroatoms, namely, the oxygen and the methyl group, each contributing two electrons to the

conjugated π-system, or (4) by treating the methoxy group in terms of a hyperconjugation model. In the last method, the methoxy proton hyperfine splittings are believed to occur via a hyperconjugative coupling between the unpaired electron located on the oxygen atom and the aliphatic protons. The spin densities on the hydrogen atoms arise from the overlapping between the $2p_z$ orbital of the oxygen and the p_π orbitals of the aromatic ring and this interaction could be a maximum when the methoxy group is co-planar with the aromatic plane. The methoxy proton coupling constants could be directly calculated by using Equation (4.3) while the former three methods can only be calculated by using the McConnell-type relationship (page 19) which involves an empirical parameter Q_{OMe}.

The ring proton splittings of methoxy substituted phenoxyl radicals are well accounted for when the methoxy group is treated as a heteroatom[34] (i.e. the first method). Zweig et al[87] have already used a heteroatom model for the methoxy group in the Hückel molecular orbital calculations of methoxy-substituted benzene radical cations for the purpose of assigning the ring proton coupling constants of the radicals examined. Poor results were obtained when only the inductive effect of the methoxy group is considered[34]. (i.e. the second method). Satisfactory results were obtained by Sullivan et al[88] who have used the last two methods to calculate the spin distribution of the p-dimethoxybenzene radical cation.

(i) Choice of parameters for the methoxy group

Since the first two methods have been used to calculate the spin density distribution of phenoxyl radicals, we intended to find a set of parameters for the methoxy group for the radicals examined by (1) treating the methoxy group as two heteroatoms, and (2) by the

complete hyperconjugation model. First we considered the method of treating the methoxy group as two heteroatoms. We followed Sullivan's procedure[88] by using the parameters chosen for the oxygen and the methyl group, in terms of a heteroatom model. The previously chosen[34] parameters for the $-O^-$ and for the methyl group for phenoxyl radicals, i.e. $h_1 = 1.6$, $h_2 = 1.5$, $k_{1'1} = 1.3$, $k_{12} = 0.4$ (instead of $k_{12} = 0.3$,[34] for the bond order is likely to increase by bonding to a more electronegative atom, i.e. the oxygen) were adopted and tested on the radicals examined. The results are summarised in Table VIII(a) on page 139.

The results show that the model does not satisfactorilly account for the electron spin distribution in these radicals except for the p-dimethoxybenzene radical cation. Therefore this method is discarded and we proceed to treat the methoxy group using a full hyperconjugation treatment.

The use of a hyperconjugation model in this investigation is justified because it has been found that the methoxy-group is 'co-planar' with the plane of the aromatic ring[88] in these radicals. The methoxy group is regarded as a three orbital system and can be written as

$$C_{1'} - O_1 - C_2 \equiv H_3$$

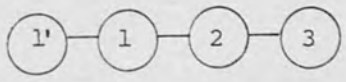

The variable parameters are as follows:

$$\alpha' = \alpha$$

$$\alpha_1 = \alpha + h_1 \qquad \beta_{1'1} = k_{1'1}\beta$$

$$\alpha_2 = \alpha + h_2 \qquad \beta_{12} = k_{12}\beta$$

$$\alpha_3 = \alpha + h_3 \qquad \beta_{23} = k_{23}\beta$$

The methoxy proton coupling constants can be calculated directly using Equation(4.3). The anisole radical cation was chosen as a reference compound for getting the set of parameters to use for the methoxy

group in terms of a hyperconjugation model. The numbering of the π-atomic orbitals is as shown in (E)

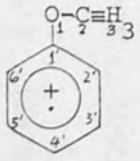

(E)

The methyl fragment in the methoxy group is treated in the same way as before (page 124) and the same parameters are employed; i.e.

$$k_1 = 0.7,\ k_{23} = 2.5,\ h_2 = -0.1,\ \text{and}\ h_3 = -1.0$$

Hence we need only to find suitable values of the coulomb integral for the oxygen atom and the resonance integral for the aromatic carbon-oxygen bond. By analogy with the phenol radical cation, the electronegativity of the oxygen is increased due to the presence of a positive charge on the oxygen as indicated by the resonance structures (F), so it is again necessary to increase the coulomb integral. Thus the parameter h_1 was varied in the range of $1.6 < h_1 < 4.0$

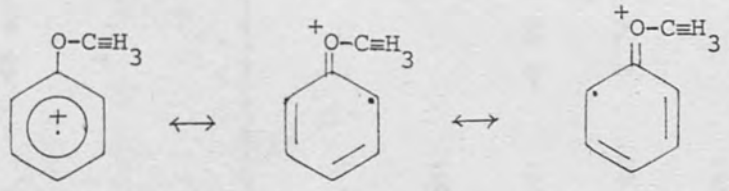

(F)

The parameter $k_{1'1}$ was varied in the range of 0.3 to 2.0. The results were tabulated in Table VIII(b). The combination of

$$h_1 = 2.3,\ k_{1'1} = 1.1,\ h_2 = -0.7,\ k_{12} = 0.7,\ k_{23} = 2.5,$$
$$h_3 = -1.0$$

was found to be one of the satisfactory sets of parameters for the anisole radical cation. The value of $k_{1'1} = 1.1$ is consistent with

Table VIII(a)

Calculated coupling constants for radical cations derived from substituted anisoles with $\alpha_1 = \alpha + 1.6\beta$, $\alpha_2 = \alpha + 1.5\beta$, $\beta_{12} = 0.4\beta$ and $\beta_{1'1} = 1.3\beta$.

Substituents in 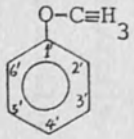	a_{OMe}	$a_{2'}$	$a_{3'}$	$a_{4'}$	$a_{5'}$	$a_{6'}$
			($a/10^{-4}$T)			
	a_{OMe} = 7.50 (5.0)	6.62 (4.90)	-0.83 (-0.65)	9.33 (10.60)	-0.83 (-0.65)	6.62 (4.90)
2' - O^-	a_{OMe} = 3.12 (1.80)		0.40 (4.30)	3.67 (0.0)	2.99 (8.50)	1.02 (-1.80)
3' - O	a_{OMe} = 3.80 (0.60)	-0.58 (3.50)		12.06 (9.0)	-3.36 (-2.30)	12.21 (11.40)
4' - O^-	a_{OMe} = 3.13 (2.10)	2.78 (-0.24)	2.24 (5.05)		2.24 (5.05)	2.78 (-0.24)
2' - OMe	a_{OMe} = 5.34 (3.25)		0.82 (0.0)	3.20 (4.90)	3.20 (4.90)	0.82 (0.0)
3' - OMe	a_{OMe} = 3.20 (3.0)	-0.77 (0.0)		12.45 (10.75)	-0.33 (2.10)	12.45 (10.75)
4' - OMe	a_{OMe} = 3.89 (3.40)	2.47 (2.25)	2.47 (2.25)		2.47 (2.25)	2.47 (2.25)

Experimental data are in brackets.

the fact that the C-OMe bond has a partial double bond character. As with the calculations of the phenoxyl radical and the phenol radical cation, there is a family of parameters for the methoxy group, which are in satisfactory agreement with the experimental values (See Table VIII(b)

(a) The variation of h_1 and $k_{1'1}$ with ring proton coupling constants and the methoxy proton coupling constant

From the graphs 4 , 5 and 6 , it can be seen that the coupling constant at position 2' is very sensitive to the variation of h_1 and $k_{1'1}$ while the methoxy proton splitting and that at position-4' is less sensitive to the variation of these two parameters. The methoxy proton splitting increases with an increase of h_1 and $k_{1'1}$. The coupling constants at positions 3' and 4' increase with an increase in h_1 and decrease with an increase of $k_{1'1}$. The coupling constant at position 2' decreases rapidly as h_1 increases, on the other hand, it increases rapidly when $k_{1'1}$ increases.

(ii) Methoxybenzene radical cation and its derivatives

The results of molecular orbital calculations on substituted methoxybenzene radical cations using the set of parameters chosen for the anisole radical cation are recorded in Table VIII(c) on page 145.The methoxy hyperfine splittings in all the radicals studied are well accounted for in terms of a hyperconjugation model for the methoxy group. It was also found that the ring proton splittings of the dimethoxybenzene radical cations agreed well with experiment. However, poor agreement between the calculated ring proton coupling constants and the experimental values was observed for the o- and the p-methoxyphenoxyl radicals. It was found that a reduction of the parameter $k_{1'1}$ to a value of $k_{1'1} = 0.8$ provide a better agreement for

Table VIII(b)

Satisfactory results of molecular orbital calculations on the anisole radical cation by treating the methoxy group in terms of a hyperconjugation model.

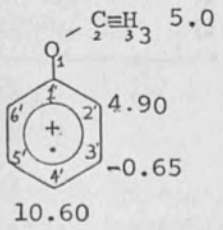

h_1	$k_{1'1}$	k_{12}	h_2	k_{23}	h_3	$a_{2'}$	$a_{3'}$	$a_{4'}$	$a_{5'}$	$a_{6'}$	a_{OMe} $(a/10^{-4}T)$
2.0	1.0	0.7	-0.7	2.5	-1.0	4.71	-1.10	9.82	-1.10	4.71	6.72
2.0	1.1	0.7	-0.7	2.5	-1.0	5.19	-1.34	9.81	-1.34	5.19	6.59
2.3	1.0	0.7	-0.7	2.5	-1.0	4.38	-0.88	10.42	-0.88	4.38	5.46
2.3	1.1	0.7	-0.7	2.5	-1.0	4.84	-1.11	10.34	-1.11	4.84	5.52
2.3	1.3	0.7	-0.7	2.5	-1.0	5.77	-1.52	10.34	-1.52	5.77	5.35
2.5	0.9	0.7	-0.7	2.5	-1.0	3.71	-0.50	10.82	-0.50	3.71	4.62
2.5	1.0	0.7	-0.7	2.5	-1.0	4.16	-0.73	10.73	-0.73	4.16	4.76
2.5	1.1	0.7	-0.7	2.5	-1.0	4.61	-0.96	10.64	-0.96	4.61	4.89
2.5	1.3	0.7	-0.7	2.5	-1.0	5.53	-1.38	10.59	-1.38	5.53	4.86
2.7	1.1	0.7	-0.7	2.5	-1.0	4.39	-1.25	10.88	-1.25	10.88	4.33

Graph 4

The variation of coupling constant at position 2' ($a_{2'}$) with molecular orbital parameters h_1 and $k_{1'1}$ for the anisole radical cation.

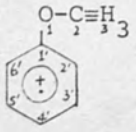

Graph 5

The variation of coupling constant ($a_{3'}$) with molecular orbital parameters h_1 and $k_{1'1}$ for the anisole radical cation.

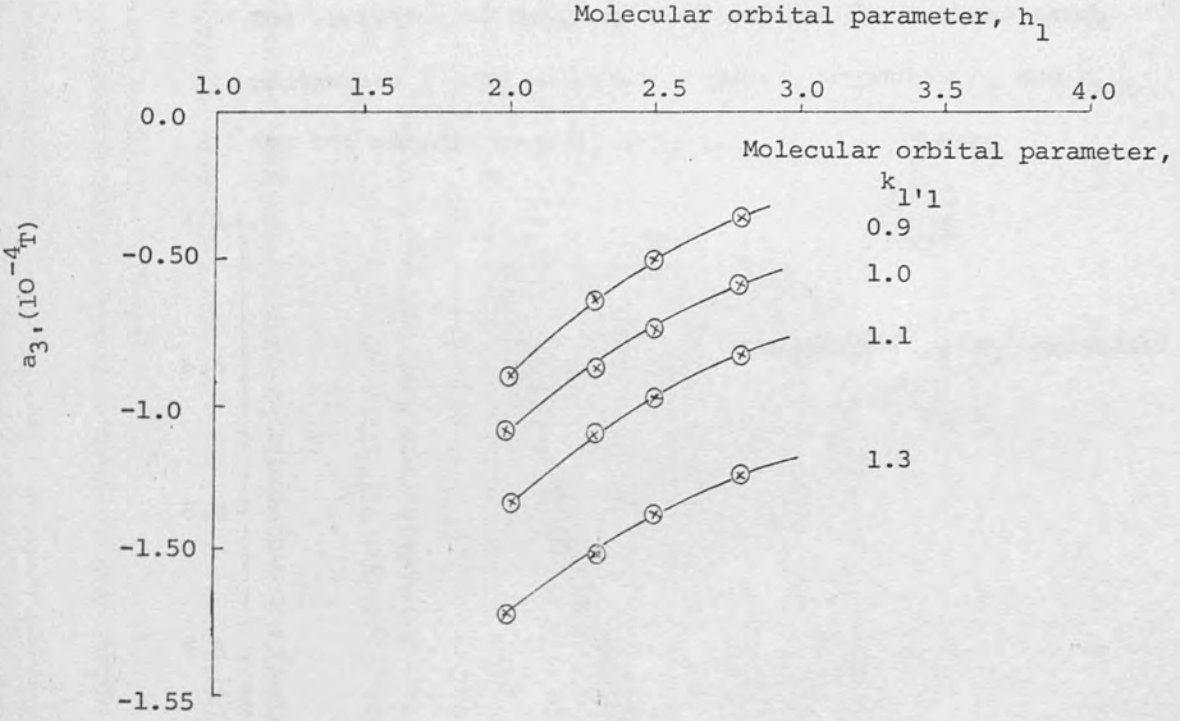

Graph 6 (a)

The variation of coupling constant ($a_{4'}$) with molecular orbital parameters h_1 and $k_{1'1}$ for the anisole radical cation.

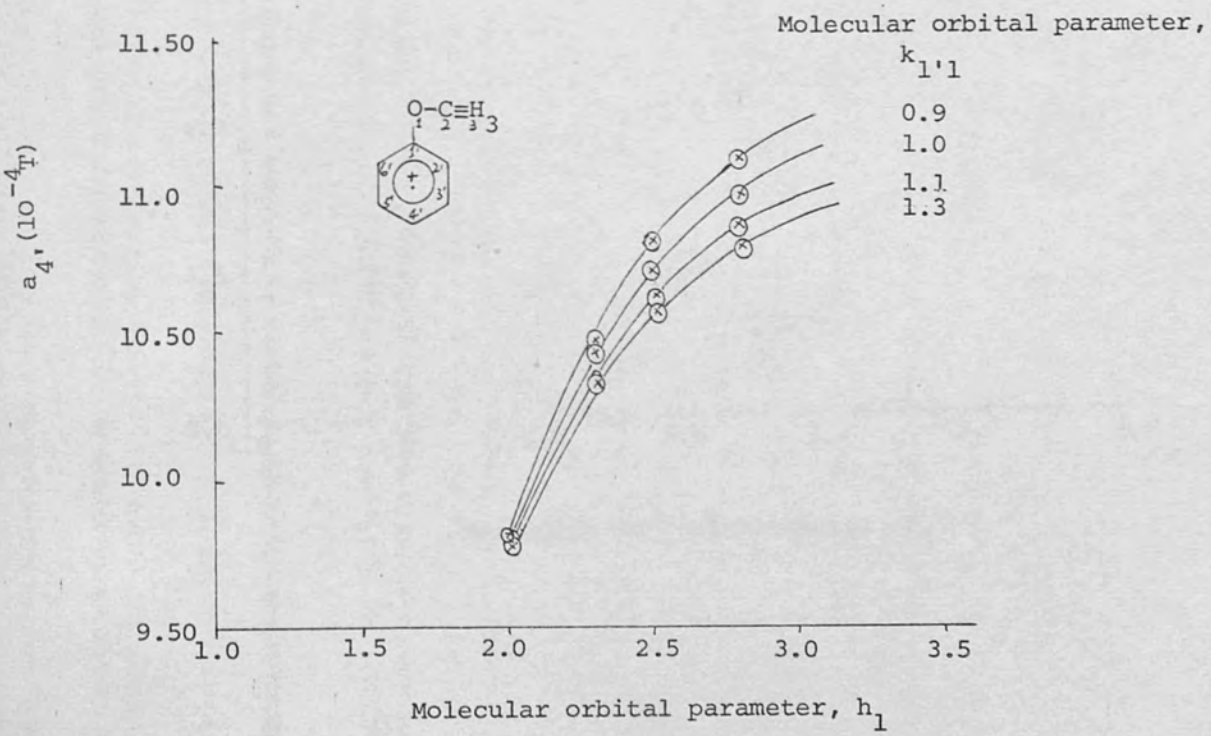

Graph 6 (b)

The variation of coupling constant for the methoxy group protons (a_3) with molecular orbital parameters h_1 and $k_{1'1}$ for the anisole radical cation.

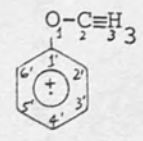

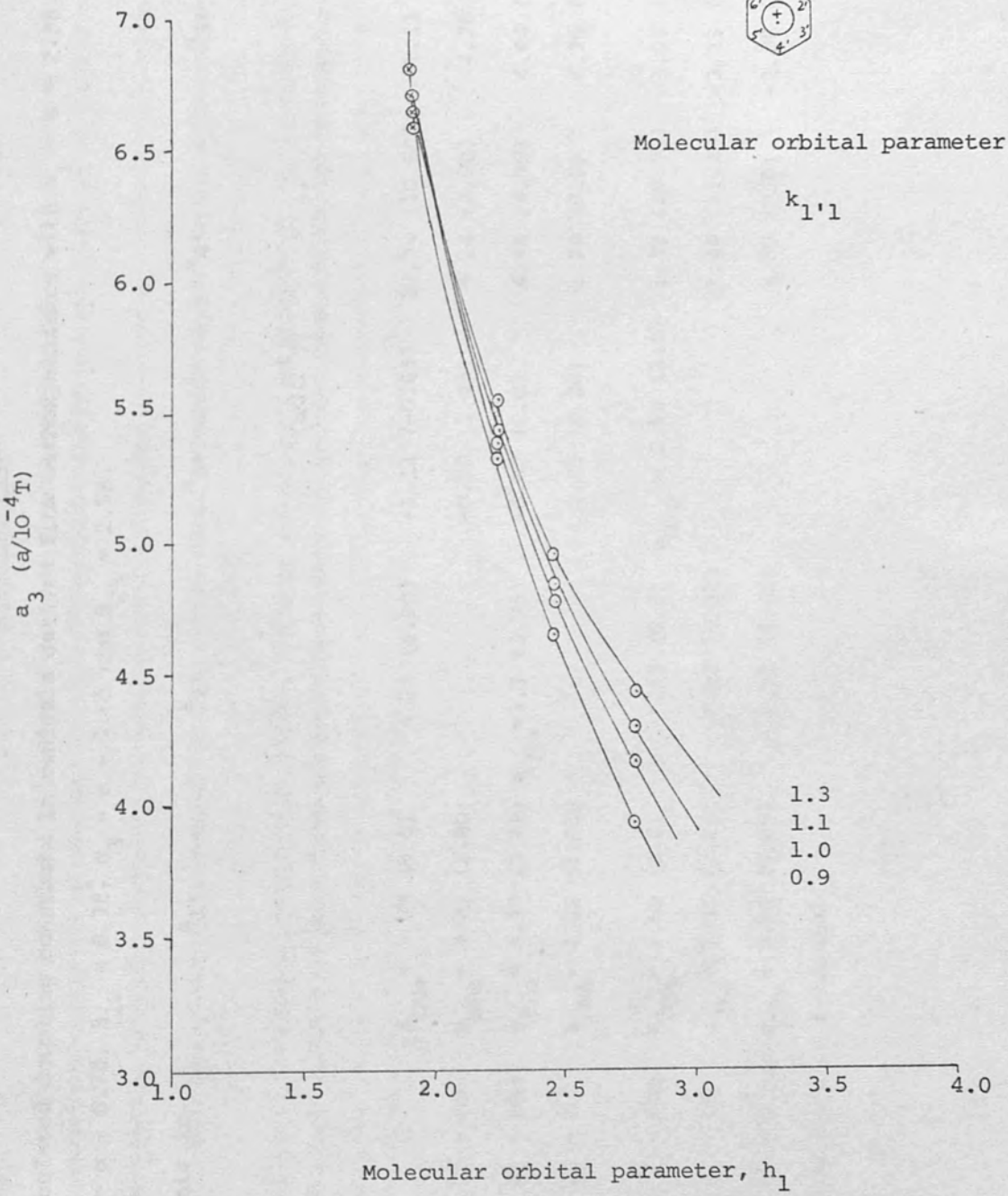

Table VIII(c)

Calculated coupling constants in radicals derived from methoxybenzenes with $\alpha_1 = \alpha + 2.3\beta$, $\beta_{1'1} = 1.1\beta$, $\alpha_2 = \alpha - 0.7\beta$, $\beta_{12} = 0.7\beta$, $\alpha_3 = \alpha - 1.0\beta$ and $\beta_{23} = 2.5\beta$.

Substituents in 	$a_{1'}$	$a_{2'}$	$a_{3'}$	$a_{4'}$	$a_{5'}$	$a_{6'}$
			($a/10^{-4}$ T)			
1' - OMe	a_{OMe} = 5.50 (5.0)	4.84 (4.90)	-1.11 (-0.65)	10.34 (10.60)	-1.11 (-0.65)	4.84 (4.90)
1' - OMe, 2' - OH	a_{OMe} = 3.22 (2.90)		-0.59 (1.45)	4.14 (2.90)	-4.76 (6.80)	-1.50 (-1.1)
1' - OMe, 2' - OMe	a_{OMe} = 3.30 (3.25)	a_{OMe} = 3.3 (3.25)	-0.87 (0.0)	4.44 (4.90)	4.44 (4.90)	-0.87 (0.0)
1' - OMe, 2' - O^-	a_{OMe} = 2.22 (1.80)		2.25 (4.30)	1.38 (0.0)	6.26 (8.50)	-1.88 (-1.9)
1' - OMe, 3' - OMe	a_{OMe} = 2.52 (3.0)	-1.25 (0.0)	a_{OMe} = 2.52 (3.0)	11.39 (10.75)	-3.07 (-2.10)	11.39 (10.75)
1' - OMe, 3' - OH	a_{OMe} = 2.31 (2.60)	-1.22 (0.30)		11.44 (11.25)	-3.13 (-2.15)	11.83 (10.85)
1' - OMe, 3' - O^-	a_{OMe} = 0.50 (0.60)	2.22 (3.50)		9.80 (9.0)	-2.85 (-2.30)	11.94 (11.40)

(Experimental data in brackets)

Table VIII(c) contd.

Substituents in 	$a_{1'}$	$a_{2'}$	$a_{3'}$	$a_{4'}$	$a_{5'}$	$a_{6'}$
			$(a/10^{-4}T)$			
1' - OMe, 4'- OMe	a_{OMe} = 2.97 (3.40)*	2.03 (2.25)*	2.03 (2.25)*	a_{OMe} = 2.97 (3.40)	2.03 (2.25)*	2.03(2.25)*
1' - OMe, 4'- OH	a_{OMe} = 2.90 (3.20)*	1.90 (2.60)*	2.29 (1.90)*		2.29 (1.90)*	1.90(2.60)*
1' - OMe, 4'- O^-	a_{OMe} = 2.10 (2.10)	0.53 (-0.20)	4.15 (5.05)		4.15 (5.05)	0.53(-0.2)
1' - OMe, 4' - CH_3	a_{OMe} = 4.42 (4.30)*	3.84 (3.80)*	-0.23(-0.30)*	a_{CH_3} = 9.13 (15.25)	-0.23(-0.30)*	3.84(3.80)*
1'-, 2'-, 3'-$(OMe)_3$	a_{OMe} = 1.57 (2.05)	a_{OMe}=4.40 (5.25)	a_{OMe}=1.57 (2.05)	-1.37(-0.43)	5.86 (6.25)	-1.37(-0.43)

* average values

both the ring and the methoxy proton splittings in these radicals as indicated below:

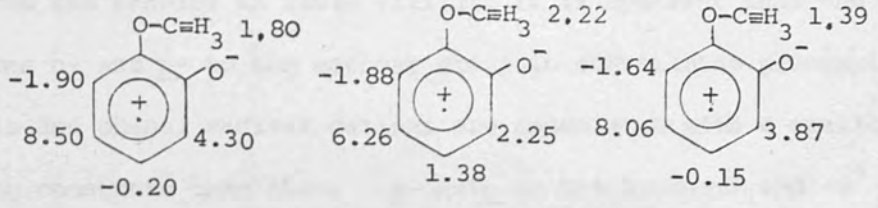

Experimental $\beta_{1'1} = 1.1\beta$ $\beta_{1'1} = 0.8\beta$

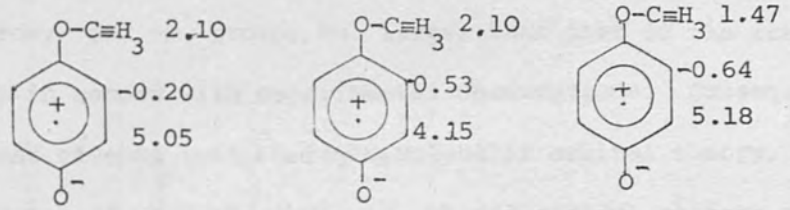

Experimental $\beta_{1'1} = 1.1\beta$ $\beta_{1'1} = 0.8\beta$

For the p-hydroxymethoxybenzene radical cation, the calculated coupling constants are in the reverse order of the assignment made by graphical methods[34] which suggested that the set of larger coupling constants is o- to the hydroxy group while the smaller ones are o- to the methoxy group. This obvious disagreement could arise from the missassignment of the observed coupling constants. Recent results support this possibility.

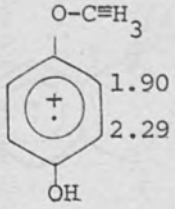

Calculated

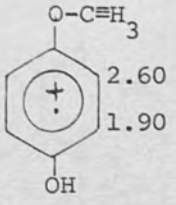

Experimental averaged values[34]

Once again, the predicted p-methyl- coupling constant in the p-methylanisole radical cation is rather low.

From the results in Table VIII(c), it is apparent that the positions o- and p- to the methoxy group in substituted phenoxyl radicals and phenol radical cations are associated with a smaller coupling constants than those o- and p- to the hydroxyl and $-O^-$ group. On the other hand, larger values are found in the p-methyl-methoxybenzene radical cation. This indicates that the set of parameters chosen for the methoxy group predicts that it has a smaller electron releasing effect than the hydroxy- and $-O^-$ groups, but larger than that of the methoxy group. This trend is in accord with experimental observations. Consequently the substituent effects, predicted by the molecular orbital theory, on the spin distribution of phenoxyl radicals, phenol radical cations and methoxybenzene radical cations can be arranged in the following series, in the order of their electron donating ability.

$$-O^- > OH > OMe > CH_3 > COR$$

This series is in accord with that previously suggested[34] and with experimental observations.

E. The methylenedioxy group

From molecular orbital point of view, 1,3-benzodioxole (G) can be regarded as a modified 1,2-dimethoxybenzene (H).

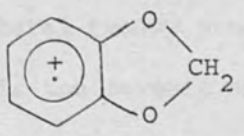

(G)

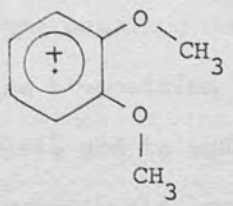

(H)

Therefore it seems reasonable to use those parameters that give satisfactory results for the spin distribution in 1,2-dimethoxybenzene radical cation, i.e.

$h_{1'} = 0.0$, $h_1 = 2.3$, $h_2 = -0.7$, $h_3 = 1.0$, $k_{1'1} = 1.1$, $k_{23} = 2.5$,

(where h_x and k_{xy} have the usual meaning as before) to perform the molecular orbital calculation on this radical cation. Since the methylene proton splittings in the 1,3-benzodioxole radical cation showed that the two protons were equivalent, their averaged dihedral angle must be 30°. Thus the methylene proton splittings can be calculated directly from the following formula:

$$a_{H_2} = \tfrac{1}{2} \times \rho_{H_2} \times 50.8 \text{ mT} \qquad (4.4)$$

It was found that the calculated coupling constants were in satisfactory agreement with experimental values, (in brackets, $a/10^{-4}$T) as shown below

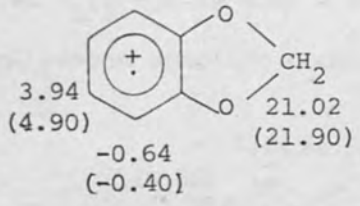

(ii) 1,3-Benzodioxole radical cation and its derivatives

The results listed in Table IX on page 151 were obtained by adopting the set of parameters chosen for the 1,3-benzodioxole radical cation.

In the case of the 3'-substituted 1,3-benzodioxole radical cation, the molecular orbital theory predicted that the coupling constant at the 5'-position is the largest and that at the 6'-position is the smallest (except the radical 3'-O^{-}-1,3-benzodioxole), and in addition, the coupling constants vary smoothly with substitution as in the case of phenoxyl radicals. These results are consistent with the assignment

made previously.

For the case of the 4'-substituted-1,3-benzodioxole radical cations, the coupling constant at position-5' is predicted to have the largest value while the position-3' is to have the smallest value, except for the radical from sesamol (I) which is an anomalous case in that the coupling constant at the 3'-position is larger than that at the position-6'. This trend is also observed from the assignment made previously, except for the radical (J) where the position-6' was assigned to have smaller coupling constant than the position-3'. Thus the molecular orbital theory on the whole, confirms the assignments made previously.

Attempts were made to obtain better correlation between theory and experiment by reducing the resonance integral between the ring and the methylene oxygen for the radicals (I) and (K). It was found that the resonance integral $\beta_{1'1} = 0.8\beta$ gave a better agreement with the ring and the methylene proton coupling constants.

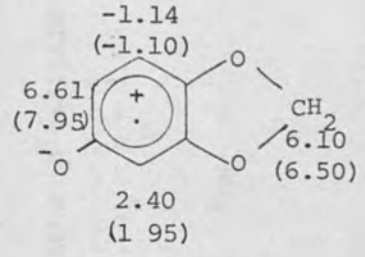

(I)

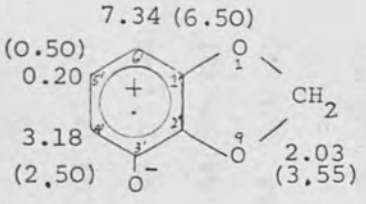

(K)

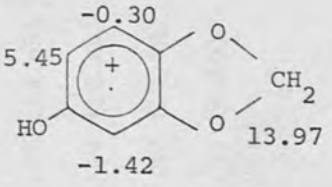

(J)

A graph of calculated methylene proton splittings versus experimental values give a good straight line with gradient equals to unity. (see graph 7). A deviation from the linear plot was observed for the methylene proton splittings of sesamol (I) and the radical (K) if $\beta_{1'1} = \beta_{2'9} = 1.1\beta$ were used in the calculation, but they were found to lie close to the straight line when $\beta_{1'1} = \beta_{2'9} = 0.8\beta$

Table IX

Calculated coupling constants in radicals derived from 1,3 benzodioxoles with $\alpha_1 = \alpha + 2.3\beta$, $\beta_{1'1} = 1.1\beta$, $\alpha_2 = \alpha - 0.7\beta$, $\beta_{12} = 0.7\beta$, $\alpha_3 = \alpha - 1.0\beta$, $\beta_{23} = 2.5\beta$.

Substituents in 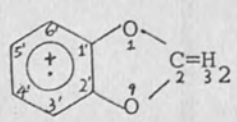	Positions in graph	a_{CH_2}	$a_{3'}$	$a_{4'}$	$a_{5'}$	$a_{6'}$
				$(a/10^{-4}T)$		
———	1	21.02 (21.90)	-0.64 (-0.40)	3.94 (4.90)	3.94 (4.90)	-0.64 (-0.40)
3' - CH_3	2	20.98 (21.40)	a_{CH_3} = 0.46 (0.40)	3.08 (4.20)	4.28 (5.30)	-1.03 (-0.60)
3' - OCH_3	3	18.54 (19.25)	a_{OMe} = 1.15 (1.50)	-0.78 (0.85)	5.22 (6.05)	-1.67 (-0.85)
3' - O^-	4	6.64 (3.55)		-0.63 (2.50)	3.0 (0.50)	-1.95 (6.50)
4' - CHO	5	21.46 (22.80)	-0.99 (-0.25)		3.80 (4.05)	-0.75 (0.0)
4' - CH_3	6	19.28 (19.45)	-1.20 (-0.75)	a_{CH_3} = 3.58 (7.95)	4.19 (5.15)	-0.45 (-0.25)
4' - OCH_3	7	14.48 (14.45)	-1.49 (-0.45)	a_{OMe} = 1.49 (2.65)	5.28 (6.25)	-0.18 (-0.45)
4' - OH	8	13.97 (13.50)	-1.42 (0.0)		5.45 (6.25)	-0.30 (-0.40)
4' - O^-	9	9.73 (6.50)	0.03 (1.95)		6.49 (7.95)	-0.41 (-1.0)

Graph 7

The correlation between the calculated and observed methylene proton splitting constants of 1,3-benzodioxole radical cations.

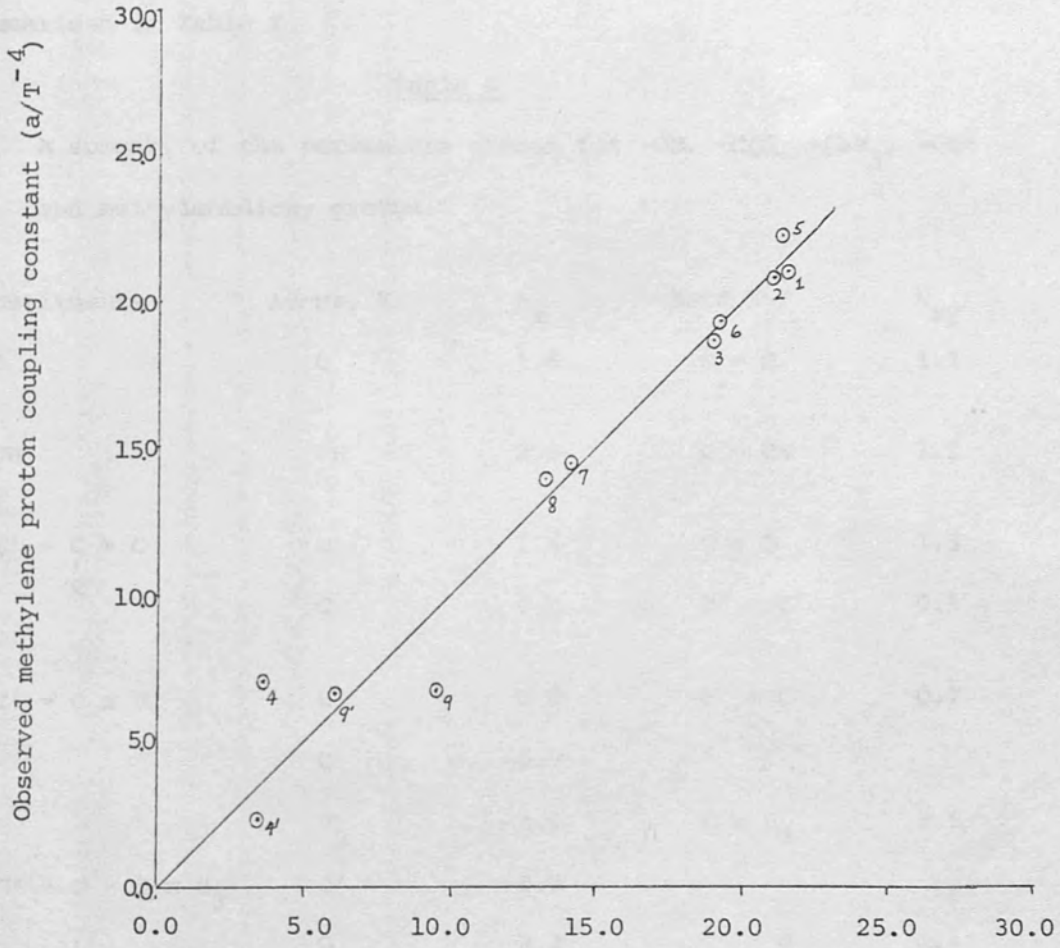

Calculated methylene proton coupling constant ($a/10^{-4}T$)

The numbers on the graph are radicals listed in Table IX. 9' and 4' are the calculated methylene proton coupling constants for 9 and 4 with $\beta_{1'1} = 0.8\beta$

was used.

The linear plot indicates that a good correlation between the molecular orbital theory of hyperconjugation for the methylene protons and experiment exists in this case.

The parameters chosen for the various functional groups are summarised in Table X.

Table X

A summary of the parameters chosen for -OH, -COR, -C≡H_3, -OMe and methylenedioxy groups.

Substituents	Atoms, X	h_x	Bond X-Y	k_{xy}
$-O^-$	O	1.6	C = O	1.3
- OH	OH	2.0	C - OH	1.1
- C' - C(R) = O	O	1.6	C = O	1.3
	C	0.0	C' - C	0.5
- C' - C ≡ H_3	C'	0.0	C' - C	0.7
	C	-0.7		
	H_3	-1.0	C ≡ H_3	2.5
- C' - O - C ≡ H_3	C'	0.0		
	O	2.3	C' - O	1.1
	C	-0.7	O - C	0.7
	H_3	-1.0	C ≡ H_3	2.5
C' - O, C' - O, C = H_2	O	2.3	O - C	0.7
	C	-0.7		
	H_2	-1.0	C = H_2	2.5
	C'	0.0	C' - O	1.1

R = H, CH_3

To support our parameters chosen for the methyl group, they were tested on some heterocyclic radicals such as those from kojic acid and maltol. The results, shown in Table XI, were in satisfactory agreement with experiment and were better than those calculated previously[126] by treating the methyl group in terms of a heteroatom model.

Table XI

Calculated coupling constants ($a/10^{-4}$ T) of radicals from kojic acid (L) and maltol (M)

Radical skeleton	a_3	a_2	a_5
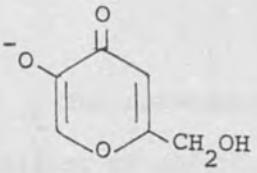	-1.18	a_{CH_2} = 1.03	12.23
	0.35*	a_{CH_2} = 1.38*	13.20*
	0.63†	a_{CH_2} = -2.0†	-7.40†

(L)

	a_5	a_6	a_2
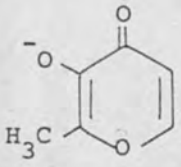	-1.16	1.16	a_{CH_3} = 7.10
	0.25*	1.38*	a_{CH_3} = 11.75*
	0.63†	-2.0†	a_{CH_3} = -7.40†

(M)

* and † are the experimental and calculated coupling constants respectively, taken from ref. 126.

The success of the molecular orbital calculations with the sets of parameters chosen for the various substituents (-OH, $-CH_3$, -COR, -OMe, and methylenedioxy) on a great number of radicals gave us confidence in using the sets of parameters to test on other radicals in future.

We can sometimes use the chosen parameters (Table X) to calculate the spin distribution of radical whose nature is not known and then the coupling constants. With the values of the theoretical coupling constants, we may be able to analyse the complicated esr spectrum and deduce the structure of the unknown radical.

F. Asymmetric ring proton coupling constants in methoxybenzene radical cation and its derivatives.

The esr spectrum of the p-dimethoxybenzene radical cation shows the presence of both cis and trans- isomers.[88] This is due to the fact that the rate of isomerism is slow. This is attributed to the partial double bond character of the C-O bond.

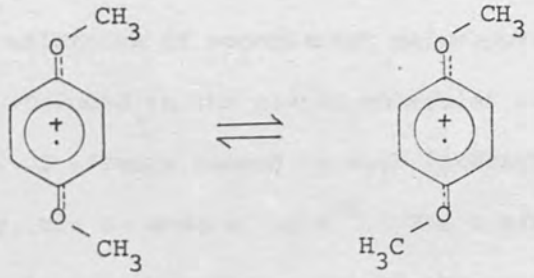

The non-equivalence of ring proton coupling constants in radical cations of anisole, p-methylmethoxybenzene are also resulted from the fixation of the methoxy group conformation.

Similarly, in the radicals from the p-hydroxymethoxybenzene, where the proton exchange averages out the effects of the two conformations of the hydroxyl group, the two ring proton coupling constants o- to the hydroxyl group are equivalent, while those o- to the methoxy group are not.

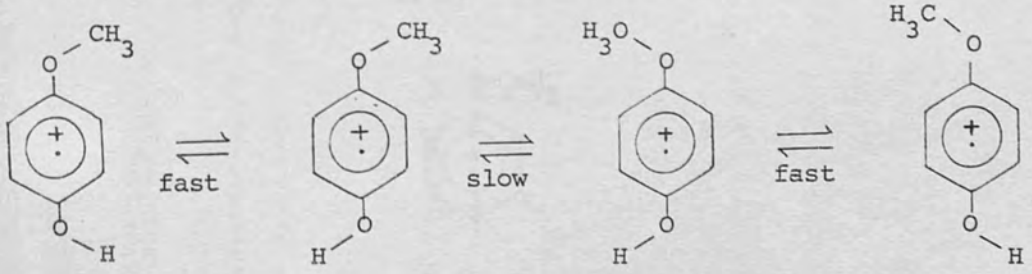

In summary, asymmetrical ring proton splittings are observed experimentally in radical cations of anisole, p-methylmethoxybenzene, p-dimethoxybenzene and phydroxymethoxybenzene.

However, only symmetrical spin densities can be calculated with simple molecular orbital calculation and with McLachlan's method. The discrepancy between experimental results and theoretical predictions suggests the existence of non-nearest neighbouring group interactions, which can be included in the simple molecular orbital theory. There are two types of effects caused by such interactions on the ring carbon atoms; namely, the α- and β-effects[88]. The α-effect can be considered as an electrostatic effect across space to the nearby carbon atoms of the ring. The β-effect is assumed to reflect the overlap between the nearby ring carbon atom and the methoxy group. Presumably, for these radicals the interaction of the lone pair electrons on the oxygen atom with the ring carbon could be small and therefore could be neglected.

In considering the α-effect, the coulomb integral of the carbon atom nearest to the methoxy proton is modified from $\alpha_A = \alpha$ to $\alpha_A = \alpha + \delta\beta$ where α_A is the coulomb integral of the nearest ring carbon atom.

In the anisole radical cation (N), the methoxy proton has a residual positive charge, therefore δ is positive. The carbon atom which is most susceptible to be affected by the electrostatic effect of the methoxy proton is carbon-2'. As a result, the coulomb integral of carbon-2' is changed to $\alpha_{(2'2)} = \alpha + \delta\beta$.

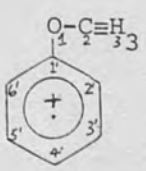

(N)

In considering the β-effect, the resonance integral between the methoxy proton group orbital and the nearest ring carbon atom is modified from zero to $\beta_{AB} = k_{AB}\beta$ (where A denotes the position of the ring carbon atom and B is the methoxy proton group orbital). For the anisole radical cation, the overlap would be between the p-orbital of carbon-2' and that of methoxy proton group orbital-3. Consequently the resonance integral $\beta_{2'3}$ is modified from the zero value to $\beta_{2'3} = k_{2'3}\beta$ where $k_{2'3}$ is a small numerical constant slightly greater than zero.

In considering the α-effect of the cis-p-dimethoxybenzene (O) radical cation, the carbon atoms that are susceptible to be affected by the methoxy protons are carbon-2' and carbon-3', therefore the coulomb integrals at these carbons are changed; (i.e. $\alpha_{(2'2)} = \alpha + \delta\beta$ and $\alpha_{(3'3)} = \alpha + \delta\beta$) while the resonance integral between the methoxy protons and carbon-2' and carbon-3' are modified (i.e. $\beta_{(2'3)} = k_{2'3}\beta$ and $\beta_{(3'9)} = k_{3'9}\beta$) when the β-effect is being considered. On the other hand, for the trans- isomer (P), the interactions are between the methoxy group protons and carbon-2' and carbon-5', therefore the coulomb integrals at these carbon atoms are modified. When the β-effect is considered, the resonance integrals between carbon-2' and the methoxy protons-3 and that between carbon-5' and methoxy group protons-9 are affected.

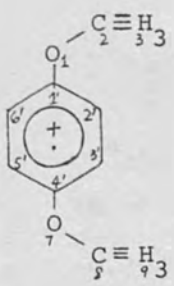

(O)

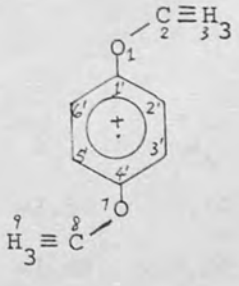

(P)

In order to find out the appropriate value for the coulomb integral for the interacting ring carbon atom(s) when α-effect is included in the molecular orbital calculations, the anisole radical cation was chosen as a reference compound for the test. Thus the value of δ in $\alpha_{(2'2)} = \alpha + \delta\beta$ was scanned between the range of 0.01 to 0.1 (some of the results are summarised in Table XII(a)). It was found that the value of $\alpha_{(2'2)} = \alpha + 0.5\beta$ reproduced the experimental results for the radical reasonably well.

The interaction arising from the β-effect was also considered in the molecular orbital calculations. It was found that the values of $k_{2'3} = 0.1$ and $k_{2'3} = 0.2$ both gave satisfactory predictions for the asymmetrical proton splittings in the anisole radical cation but that $k_{2'3} = 0.1$ gave better agreement with experiment. The results were tabulated in Table XII(b).

It can be seen that both effects led to the same prediction that the ring proton coupling constants are in the order $a_{4'} > a_{6'} > a_{2'} > a_{3'} > a_{5'}$, which is consistent with experimental observations.

Table XII(a)

Molecular orbital calculations on the anisole radical cation with the inclusion of α-effect.

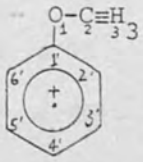

$h_{2'2}$	$a_{2'}$	$a_{3'}$	$a_{4'}$	$a_{5'}$	$a_{6'}$	$a_{OMe}/10^{-4}$T
0.03	4.54	-0.90	10.42	-1.30	5.10	5.58
0.05	4.33	-0.71	10.45	-1.40	5.33	5.54
0.07	4.14	-0.54	10.48	-1.51	5.52	5.55

Table XII(b)

Molecular orbital calculations on the anisole radical cation with the inclusion of β-effect.

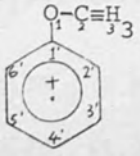

$h_{2'3}$	$a_{2'}$	$a_{3'}$	$a_{4'}$	$a_{5'}$	$a_{6'}$	a_{OMe} $(a/10^{-4}T)$
0.10	4.28	-0.73	10.61	-1.35	5.39	4.65
0.20	3.95	-0.35	10.82	-1.55	5.69	3.82

The inclusion of α-effect and β-effect in the molecular orbital calculations of p-substituted methoxybenzene radical cations with asymmetrical ring proton splittings are recorded in Tables XIII(a) and (b) respectively; using the set of parameters chosen for the anisole radical cation.

Table XIII(a)

The results of the molecular orbital calculations on p-substituted methoxybenzene radical cations with the inclusion of α-effect.

Substituents	$a_{1'}$	$a_{2'}$	$a_{3'}$	$a_{4'}$	$a_{5'}$	$a_{6'}/10^{-4}T$
4' - H	a_{OMe}=5.54	4.33	-0.71	10.45	-1.40	5.33
	(a_{OMe}=5.0)	(4.40)	(-0.20)	(10.60)	(-1.10)	(5.50)
4' - OMe (cis)	a_{OMe}= 3.0	2.19	2.19	a_{OMe}=3.0	1.96	1.96
	(a_{OMe}= 3.3)	(2.70)	(1.80)	(a_{OMe}=3.50)	(2.70)	(1.80)
4' - OMe (trans-)	a_{OMe}= 3.0	1.65	2.50	a_{OMe}=3.0	1.65	2.50
	(a_{OMe}= 3.5)	(3.00)	(1.20)	(a_{OMe}=3.50)	(1.50)	(3.0)

Table XIII(a) contd.

Substituents		$a_{1'}$	$a_{2'}$	$a_{3'}$	$a_{4'}$	$a_{5'}$	$a_{6'}$	$(a/10^{-4}T)$
4' - CH_3	a_{OMe} =	3.77	3.37	0.28	a_{CH_3} = 9.44	-0.55	4.26	
	(a_{OMe} =	4.30]	(3.50]	(0.20)	(a_{CH_3} = 15.2)	(-0.80)	(4.30)	
4' - OH	a_{OMe} =	2.88	1.73	2.63		2.08	2.03	
	(a_{OMe} =	3.20)	(2.20)	(1.90)		(1.90)	(3.0)	

Experimental data are in brackets.

Table XIII(b)

The results of the molecular orbital calculations on p-substituted methoxybenzene radical cations with the inclusion of β-effect.

$(a/10^{-4}T)$

Substituents		$a_{1'}$	$a_{2'}$	$a_{3'}$	$a_{4'}$	$a_{5'}$	$a_{6'}$	$k_{2'3}$
4' - H	a_{OMe} =	4.65	4.38	-0.73	10.61	-1.35	5.39	0.1
	a_{OMe} =	3.82	3.94	-0.35	10.82	-1.55	5.69	0.2
4' - OMe (cis-)	a_{OMe} =	2.59	2.18	2.18	a_{OMe} = 2.59	2.00	2.00	0.1
	a_{OMe} =	2.10	2.30	2.30	a_{OMe} = 2.19	1.97	1.97	0.2
4' - OMe (trans-)	a_{OMe} =	2.62	1.73	2.46	a_{OMe} = 2.62	1.73	2.46	0.1
	a_{OMe} =	2.27	1.44	2.85	a_{OMe} = 2.27	1.44	1.85	0.2
4' - CH_3	a_{OMe} =	3.71	3.50	0.13	a_{CH_3} = 9.48	-0.41	4.10	0.1
	a_{OMe} =	3.04	3.18	0.47	a_{CH_3} = 9.76	-0.55	4.31	0.2
4' - OH	a_{OMe} =	2.48	1.96	2.18		2.62	1.72	0.1
	a_{OMe} =	2.07	2.09	2.09		2.72	1.56	0.2

The results given in the above two tables show that the inclusion of either α or β- effects in the molecular orbital calculations can lead to asymmetrical ring proton splittings in these radicals as well. The calculated coupling constants are in good agreement with experiment. Apparently, the results obtained with the inclusion of β-effect for the radicals examined provide better agreement than those obtained by considering the α-effect except that the calculated methoxy splittings are as usual smaller than the experimental values. The better agreement obtained with the β-effect seems to suggest that α-effect is less important than the β-effect in these radicals.

It was found that the calculated ring proton coupling constants with $\beta_{2,3} = 0{\cdot}1\beta$ for radical cations of anisole, p-methyl-, p-hydroxy methoxybenzeneswere in better agreement with experiment than those with $\beta_{2,3} = 0{\cdot}2\beta$. However, it was observed that for the cis- and for the trans- p-dimethoxybenzene radical cations the use of $\beta_{AB} = 0{\cdot}2\beta$, (where A denotes the nearest ring carbon atom to the methoxy protons, B), yielded better results. The inclusion of β-effect has also successfully explained the experimental observations that the trans isomer has slightly larger methoxy proton splittings than those of the cis-isomer.

G. The inclusion of β-effect in the molecular orbital calculations of other methoxybenzene radical cations with symmetrical ring proton splittings

The inclusion of the β-effect in the calculations could also be useful in the case of the o-dimethoxybenzene and the o-hydroxymethoxy-benzene radical cations, and of the o-methoxyphenoxyl radical. It is expected that the favourable conformation for these radicals is that in which the methoxy group is flipping away from the substituent due to steric effects (Q)

Thus the methoxy protons would interact with the nearest ring carbon atom, atom-6', by a similar mechanism as suggested for the p-substituted methoxybenzene radical cations.

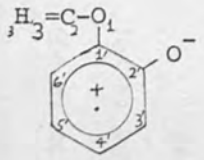

(Q)

The results of the calculations were summarised in Table XIV on page 163. For convenience of comparison, the coupling constants calculated without the consideration of β effect were also listed in Table XIV on page 163. It was found that the results with an additional parameter β_{AB} = 0.2β were in excellent agreement with experiment; except for the o-hydroxymethoxybenzene radical cation, when only fair agreement was obtained. The fact taht the inclusion of β-effect in the calculations provided a better description of the electron spin distribution of these radicals than that without, suggested that the conformation (Q) is indeed the more favourable one.

For m-substituted methoxybenzene radical cations, the results in Table XV (page 165) show that there is no great improvement in the results obtained when β-effect was considered. This could possibly be because there is no prefered conformation for these radicals, and the spectrum observed was the average of the possible conformations

Molecular orbital calculations with the inclusion of β-effect were also performed on the p-methoxyphenoxyl radical. It was found that the results were not better than those without taking into consideration of non-nearest neighbouring group interactions (see Table XVI on page 166).

Table XIV

The calculated coupling constants of o-substituted methoxybenzene radical cations with the inclusion of β-effect.

Substituents in 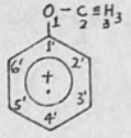	$k_{6'3}$	$k_{3'9}$		a_{OMe}	$a_{3'}$	$a_{4'}$	$a_{5'}$	$a_{6'}$
						$(a/10^{-4}T)$		
2' - O-C≡H (7 8 9 3)	0.1	0.1	a_{OMe} =	3.65 (3.25)	-0.88 (0.0)	4.70 (4.90)	4.70 (4.90)	-0.88 (0.0)
	0.2	0.2	a_{OMe} =	2.77 (3.25)	-0.89 (0.0)	4.94 (4.90)	4.94 (4.90)	-0.89 (0.0)
	0.0	0.0	a_{OMe} =	3.30	-0.87	4.40	4.40	-0.87
2' - OH	0.1	0.0	a_{OMe} =	2.91 (2.90)	-0.34 (1.45)	3.92 (2.90)	5.22 (6.80)	-1.25 (-1.50)
	0.2	0.0	a_{OMe} =	2.65	-0.10	3.71	5.65	-1.42
	0.0	0.0	a_{OMe} =	3.22	-0.59	4.14	4.76	-1.50
2' - O^-	0.1	0.0	a_{OMe} =	1.35(1.80)	4.07(4.30)	-0.24(0.0)	8.26(8.50)	-2.62(-1.90)
	0.2	0.0	a_{OMe} =	1.31	4.27	-0.33	8.45	-2.60
	0.0	0.0	a_{OMe} =	2.22	2.25	1.38	6.26	-1.88

(Experimental values in brackets)

Table XV contd.

Calculated coupling constants for m-substituted methoxybenzene radical cations with the inclusion of β-effects.

Substituents in 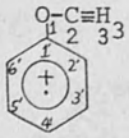	$k_{6'3}$	$k_{4'9}$	$a_{1'}$	$a_{2'}$	$a_{3'}$	$a_{4'}$	$a_{5'}$	$a_{6'}$
						$(a/10^{-4}T)$		
3' - OMe	0.1	0.1	$a_{OMe} = 1.75$	-1.29	$a_{OMe} = 1.75$	11.64	-3.12	11.64
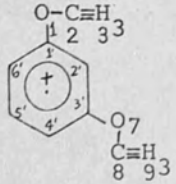	0.2	0.2	$a_{OMe} = 0.95$	-1.33	$a_{OMe} = 0.95$	11.77	-3.15	11.77
	$k_{2'3}$	$k_{4'9}$						
	0.1	0.1	$a_{OMe} = 2.52$	-1.25	$a_{OMe} = 1.78$	11.16	-3.o8	11.83
	0.2	0.2	$a_{OMe} = 2.56$	-1.24	$a_{OMe} = 1.06$	10.88	-3.04	12.17
	0.0	0.0	$a_{OMe} = 2.52$	-1.25	$a_{OMe} = 2.52$	11.39	-3.07	11.39
	Experimental		$a_{OMe} = 3.0$	0.0	$a_{OMe} = 3.0$	10.75	-2.10	10.75

Table XV

Calculated coupling constants for m-substituted methoxybenzene radical cations with the inclusion of β-effect

($a/10^{-4}T$)

Substituents	$k_{2'3}$	$k_{6'3}$	$a_{2'}$	$a_{4'}$	$a_{5'}$	$a_{6'}$	a_{OMe}
3' - O^-	0.0	0.0	2.22	9.80	-2.85	11.94	0.50
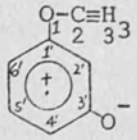	0.1	0.0	2.24	9.71	-2.83	11.93	0.67
	0.2	0.0	2.30	9.57	-2.77	11.90	0.84
	0.0	0.1	2.74	9.48	-2.79	11.77	0.81
	0.0	0.2	3.26	9.09	-2.68	11.55	0.24
	Experimental		3.50	9.0	-2.30	11.40	0.60
3' - OH	0.1	0.0	1.09	8.36	-2.41	11.87	1.04
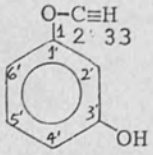	0.2	0.0	1.0	8.15	-2.21	11.90	0.86
	0.0	0.1	-1.16	11.45	-3.15	11.99	1.35
	0.0	0.2	-1.0	11.23	-3.12	12.11	0.47
	0.0	0.0	-1.22	11.44	-3.13	11.44	2.31
	Experimental		0.30	11.25	-2.15	10.85	2.60

Table XVI

Calculated coupling constants ($a/10^{-4}T$) of the p-methoxyphenoxyl radical with the inclusion of β-effect.

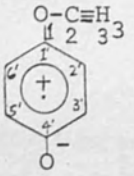

$k_{2'3}$	a_{OMe}	$a_{2'}$	$a_{3'}$	$a_{5'}$	$a_{6'}$
0.1	1.25	-0.71	5.44	5.08	-0.62
0.2	1.04	-0.77	5.68	5.01	-0.60
0.0	2.10	-0.64	5.18	5.18	-0.64
Expt.	2.10	-0.20	5.05	5.05	-0.20

Thus it was found that the inclusion of β-effect in the simple molecular orbital calculations can predict asymmetric ring proton hyperfine splittings satisfactorily as well as predicting better agreement with experimental values in some cases.

4.4 Conclusion

It has been shown that the carbonyl-group treated in terms of two basis π atomic orbitals can provide an excellent description of the spin distribution of carbonyl-substituted radicals. The set of parameters chosen for the methyl-, methoxy- and methylenedioxy substituents, when they are treated in terms of the hyperconjugation model, gave reliable and satisfactory results. The asymmetric ring proton splittings were found to be satisfactorily accounted by the inclusion of the β-effect.

CHAPTER 5

CORRELATION OF g-FACTORS OF PHENOXYL RADICALS AND ALKYL ARYL ETHER RADICAL CATIONS WITH THE ENERGY-LEVEL COEFFICIENTS OF ODD ELECTRON HÜCKEL MOLECULAR ORBITAL AND WITH THE TOTAL SPIN DENSITY ON THE OXYGEN ATOMS

5.1 Introduction

As has been seen in Chapter 1, the general form of the time-averaged $\underline{g}$-tensor is:

$$\underline{g}_{zz} = \underline{g}_e + \Delta \underline{g}_{zz} \tag{5.1}$$

where $\underline{g}_e$ is the free electron $\underline{g}$-factor, 2.0023, and $\underline{g}_{zz}$ is given by

$$\Delta \underline{g}_{zz} = 2 \sum_{n} \sum_{k,j} \frac{\langle \psi_o | \zeta_k L_{zk} | \psi_n \rangle \langle \psi_n | L_{zj} | \psi_o \rangle}{E_n - E_o} \tag{5.2}$$

From this Stone[78] has developed an equation to give the $\underline{g}$-factor of an axially asymmetric planar radical viz:

$$\underline{g}_{av} = 2.0023 + \Delta \underline{g}_{av} \tag{5.3}$$

$$\Delta \underline{g}_{av} = \Sigma \Delta \underline{g}_i$$

$$\Delta \underline{g}_i = \frac{2}{3} \sum_{m}^{a,b} \frac{\zeta_r (c^m_{rx})^2 (c^p_r)^2 + \zeta_s (c^m_{sx})^2 (c^p_s)^2 + (\zeta_r + \zeta_s) c^m_{rx} c^m_{sx} c^p_r c^p_s}{E^p - E^m_i}$$
$$+ \frac{2}{3} \sum_{m}^{a,b} \frac{\zeta_r (c^m_{ry})^2 (c^p_r)^2 + \zeta_s (c^m_{sy})^2 (c^p_s)^2 + (\zeta_r + \zeta_s) c^m_{ry} c^m_{sy} c^p_r c^p_s}{E^p - E^m_i} \tag{5.4}$$

$\underline{g}_{av}$ and $\Delta \underline{g}_{av}$ are the average of the three spatial axes (x,y,z) where $\underline{g}_i$ are the contributions to $\Delta \underline{g}_{av}$ from the i^{th} σ-bond, a and b indicating the bonding and the antibonding orbitals of the i^{th} σ-bond between atom r and s. When the nodal plane of the orbital is the xy-plane, c^p_r is the coefficient of the p_z atomic orbital of the atom r in the odd electron orbital; c^m_{rx} and c^m_{rx} and c^m_{ry} are the coefficients of the p_x and p_y atomic orbitals of the atom r in the m^{th} σ-bond and so on. ζ_r and ζ_s are spin-orbit coupling constants for the r^{th} and s^{th} atoms. Thus $\underline{g}$-shift contribution is directly proportional to the spin density on, and the spin-orbit coupling constant of, the atom concerned and

inversely proportional to the excitation energy. The excitation energies are of two main types: first, those corresponding to an excitation of an electron from the odd electron orbital to an antibonding orbital ($\Delta E_a = E^p - E^{\sigma_a}$, effectively negative) and accompanied by a negative g-shift contributions; and second, those corresponding to a pairing of electron in the highest occupied orbital leaving an unpaired electron in a lower orbital ($\Delta E_b = E^p - E^{\sigma_b}$, effectively positive) and associated with a positive g-shift contribution. This is illustrated in the following diagram:

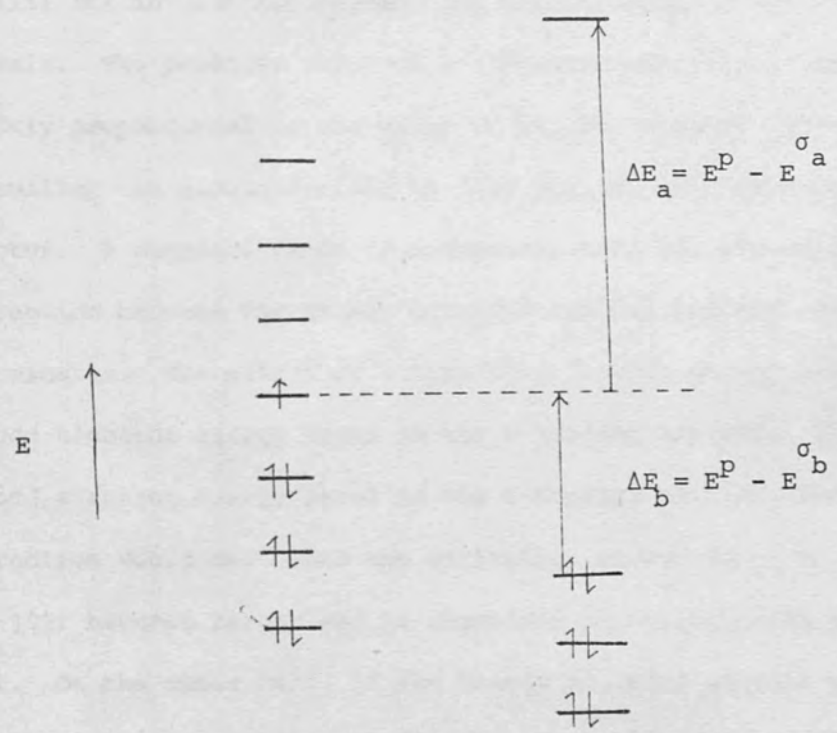

Fig. 1. The correlation diagram of g-factors with excitation energies

Stone[78] also arrived at a simple semi-empirical equation for the g-shift of the aromatic molecule by using Hückel molecular orbital approximations.

$$\Delta g_{av} = g_x - g_e = (a + \lambda b)\Sigma c_{io}^2 \qquad (5.5)$$

where g_x is the g-factor of an aromatic hydrocarbon molecule, x, c_{io} are the coefficients of the atomic orbitals in singly occupied Hückel molecular orbital, ϕ_o, λ is the energy level coefficient of ϕ_o with energy $E = \alpha + \lambda\beta$, and a and b are empirical constants to be determined from the experimental results. The sign of b is an indication of the balance between the two effects, namely, (i) the excitation energy and (ii) the interaction between the singly occupied and the bonding orbitals. The positive value of b indicates that the g-factor is directly proportional to the value of λ. The greater the value of λ, the smaller the excitation energy (see Fig. 1) and hence the larger the g-factor. A negative value of b suggests that the effect due to the interaction between the singly occupied orbital and the σ-bonding orbital predominates. The extent of interaction depends on the proximity of the odd electron energy level to the σ-bonding orbital. The closer the odd electron energy level to the σ-bonding orbital, the greater the interaction would be. Thus the excitation energy (ΔE_A, in Fig. 2 on page 172) becomes larger and is therefore associated with a smaller g-shift. On the other hand, if the singly occupied orbital and the doubly occupied σ-bonding orbital is far from each other, the interaction is small and therefore the excitation energy (i.e. ΔE_B, in Fig. 2) is smaller and hence is associated with a larger g-shift. This is illustrated in Fig. 2

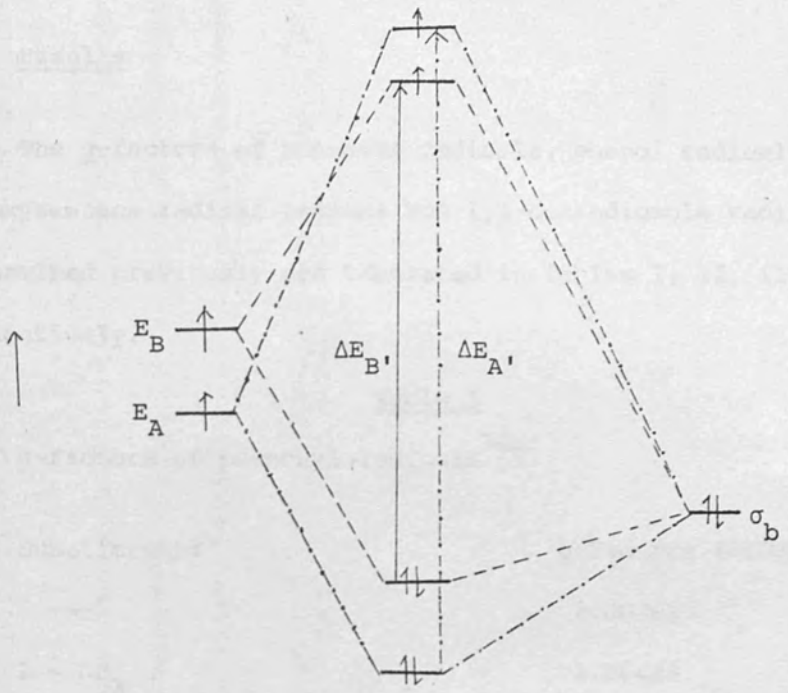

Fig. 2. Correlation diagram of g-factors with the excitation energies when the interaction between the odd electron orbital and the σ-bonding orbital predominates.

The experimental values of g-factors of phenoxyl radicals[76b], phenol radical cations[76b] and alkoxybenzene radical cations[102] have been reported but so far no theoretical interpretations have been made. This chapter is an attempt to account for the isotropic g-factors observed for these various radicals with the hope that they might be predicted quantitatively.

5.2 Results

The g-factors of phenoxyl radicals, phenol radical cations, and alkoxybenzene radical cations and 1,3-benzodioxole radical cations determined previously are tabulated in Tables I, II, III, and IV respectively.

Table I

g-Factors of phenoxyl radicals[76b]

Substituents	g-Factors (±0.00015)
—	2.00461
2 - CH_3	2.00429
2 - OCH_3	2.00435
2 - O^-	2.00447
2 - OH	2.00428
2 - COR	2.00520
3 - CH_3	2.00447
3 - OCH_3	2.00429
3 - O^-	2.00392
3 - OH	2.00435
3 - COR	2.00480
4 - CH_3	2.00432
4 - OCH_3	2.00445
4 - O^-	2.00455
4 - OH	2.00427
4 - COR	2.00540

R = H, CH_3

Table II

g-Factors of the phenol radical cation and its derivatives[76b]

Substituents	g-Factors (±0.00015)
——	2.00291
2 - CH_3	2.00331
2 - OMe	2.00362
2 - O^-	2.00438
3 - CH_3	2.00312
3 - OCH_3	2.00315
3 - O^-	2.00435
3 - OH	2.00312
4 - CH_3	2.00317
4 - OCH_3	2.00358
4 - O^-	2.00352
4 - OH	2.00427

Table III

g-Factors of the methoxybenzene radical cation and its derivatives[102]

Substituents	g-Factors (±0.00015)
—	2.00322
2 - OCH_3	2.00340
3 - OCH_3	2.00327
4- CH_3	2.00321
4 - OH	2.00358
4 -OCH_3	2.00368
4 - O^-	2.00445
2,3 - $(OCH_3)_3$	2.00376

Table IV

g-Factors of the 1,3-benzodioxole radical cation and its derivatives[102]

Substituents	g-Factors (±0.00015)
—	2.00390
3' - CH_3	2.00390
3' - OH	2.00391
3' - OCH_3	2.00400
3' - O^-	2.00460
4' - CH_3	2.00380
4' - OH	2.00395
4' - OCH_3	2.00400
4' - O^-	2.00430
4' - COR	2.00435

R = H, CH_3

5.3 Discussion

A. Qualitative account of g-factors of phenoxyl radicals, phenol radical cations and alkyl aryl ether radical cations

First of all, it is of interest to look at the trends of g-factors of the radicals examined from qualitative point of view.

From the results in Table I on page 173, it is apparent that the g-factors of phenoxyl radicals are larger than those of aromatic hydrocarbon radical anions and cations[125]. This is because of the larger spin-orbit coupling constants of the oxygen atom (ζ_o = 152 cm^{-1}) than carbon (ζ_c = 28 cm^{-1}) and the small excitation energy due to the excistence of loosely bonded or non-bonded oxygen orbitals which are naturally of higher energy than σ-bonding orbitals. The phenoxyl radicals with $-O^-$ and -COR as o- and as p-substituents, have g-factors larger than those with -OH and -OMe attached to these positions. This is attributed to the fact that the -OH and -OMe substituents each have effectively only one lone pair of electrons while the former have two. Hence there are two possible positive contributions to the g-shifts for the former two radicals,

It is interesting to observe that the g-factor of the phenoxyl radical itself is larger than those of semiquinones which have an additional oxygen atom. This could possibly be due to the total spin density on oxygen atoms is more than offset by the larger excitation energy for the latter.

For the m-isomers, the g-factors change in the reverse sense to those of o- and p-isomers and more or less parallel to the electron donating effects of the substituents, i.e. in the order

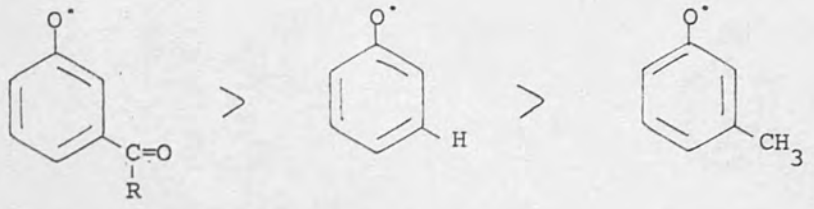

g = 2.00480 > 2.00461 > 2.00447

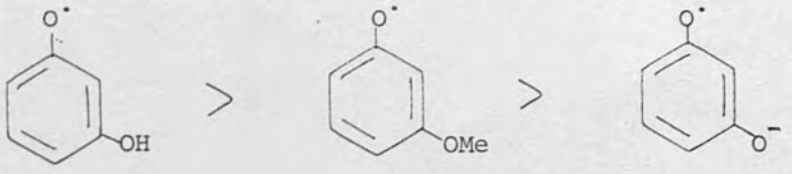

2.00435 > 2.00429 > 2.00392

The results in Table II on page 174 reveal that the g-factors of phenol radical cations are smaller than those of the corresponding phenoxyl radicals. This is because the number of lone paired-electrons on the $-O^-$ is four whereas on -OH, it is only two. There is another way of looking at this situation. Applying Dixon's theorem[121] to our σ-molecular framework, the protonation of oxygen in the phenoxyl radicals could be regarded as the addition of a 'new' σ-orbital to the original (old) σ-molecular orbital system and therefore a new set of molecular orbitals would be generated in such a way that each 'new' σ-orbital lies in between those 'old' ones as shown in Fig. 3, with phenoxyl radical and phenol radical cation as examples. Thus the 'old' σ-bonding orbitals and the σ-antibonding orbitals have been lowered. As illustrated in the diagram, the excitation energy from the 'new' σ-highest occupied bonding molecular orbital (i.e.ΔE_2) is greater than that from the 'old' σ-bonding orbital to the same odd electron orbital (i.e. ΔE_1). This leads to a smaller positive g-shift. The

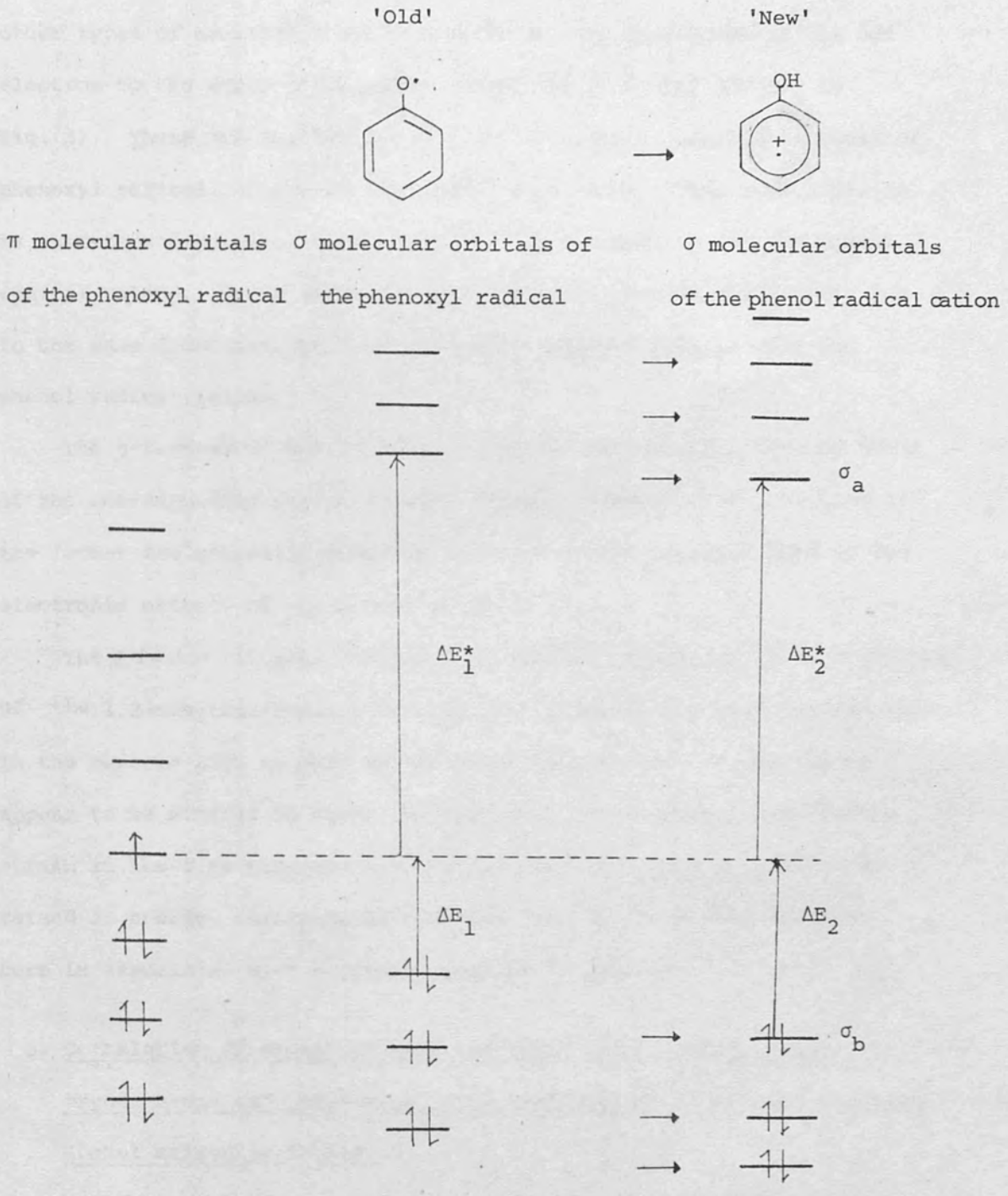

Fig. 3. The energy interaction diagram of σ-orbitals and the correlation of g-factors with excitation energies of the phenoxyl and the protonated phenoxyl radicals.

other types of excitation energies involve the excitation of the odd electron to the empty antibonding σ-orbitals (i.e. ΔE_1^* and ΔE_2^* in Fig. 3). These are smaller for the phenol radical cation than those of phenoxyl radical, as can be seen from the diagram. (See page 178). It is therefore associated with a larger negative g-shift for the phenol radical cation. Hence these two contributions towards the g-shift are in the same direction, that is, towards a smaller g-factor for the phenol radical cation.

The g-factors of methoxybenzene radical cations lie close to those of the corresponding phenol radical cation. However, the g-factors of the former are generally somewhat larger and this is attributed to the electronic effects of the methyl group[88].

The g-factor of the 1,3-benzodioxole radical cation is larger than that of the 1,2-dimethoxybenzene radical cation though the spin distribution in the benzene ring as well as the total spin density on the oxygen appear to be similar in these two radicals. This might be due to the strain in the five-membered ring causing the lone-pair orbital to be raised in energy, resulting in a smaller excitation energy which in turn is associated with a greater positive g-shift.

B. Correlation of g-factors with the total spin density on the oxygen atoms and the energy level coefficients of the odd electron Hückel molecular orbitals

A good correlation of g-factors of hydrocarbon radical cations and anions with the energy coefficients of the Hückel molecular orbitals occupied by the odd electron has been obtained by Segal, Karplan and Fraenkel[125] using Stone's semi-empirical equation (Equation 5.4). They obtained a straight line graph in the plot of g-factors against λ.

The negative slope of the line has been explained to be due to the fact that the interaction between filled orbitals and the odd electron orbital predominates[78].

The g-factors of o- and p-benzosemiquinones have also been correlated by Stone[78] by employing Equation (5.5) and assuming $\gamma_o = a + \lambda b$. He plotted γ_o against λ and obtained two different straight lines for the o- and p-benzosemiquinones. The former has a negative slope while the latter has a positive slope. The explanation for the negative value of b is as above.

We attempt to correlate the g-factors of phenoxyl radicals, phenol radical cations and alkyl aryl ether radical cations with λ and with the total spin densities on the oxygen atoms. (Since the spin-orbit coupling constant of oxygen is much greater than that of carbon, we consider that the major contribution to the g-factors will be due to the oxygen atoms.) Graphs of g-factors against λ and g-factors against the total spin densities on the oxygen atoms were plotted. The two unknown parameters were determined by Hückel molecular orbital calculations on these radicals using the chosen parameters for various functional groups listed in Table X in Chapter 4. The results are summarised in Tables V, VI, VII, VIII and IX (pages 181 - 185).

The correlation of g-factors of all the radicals examined with λ is shown in Graph A. It was obvious from Graph A that a single straight line could not be drawn for all the radicals concerned but rather a number of lines, suggesting that the radicals should be divided into groups. As the resonance effect of substituents situated at the m-positions is believed to be a minimum, the perturbation on the energy levels of the parent molecule by the m-substituents must not be great. Therefore the odd electron energy levels are not

Table V

g-Factor correlation of m-substituted phenoxyl radicals and o- and p-substituted (-COR and CH_3) phenoxyl radicals.

Substituents in 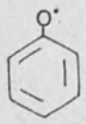	Positions in graphs 1 and 2	g-Factors observed	Energy level coefficients of Hückel molecular orbital containing odd electron (λ)	Total spin density on the oxygen atoms ($\Sigma\rho_o$)
2 - COR	1	2.00520	0.5863	0.2310
2 - CH_3	2	2.00429	0.5360	0.2181
3 - COR	3	2.00480	0.5702	0.2288
——	4	2.00461	0.5681	0.2258
3 - CH_3	5	2.00447	0.5642	0.2205
3 - OH	6	2.00435	0.5417	0.2126
3 - OMe	7	2.00429	0.5447	0.2117
3 - O^-	8	2.00428	0.4944	0.2136
4 - COR	9	2.00540	0.5950	0.2430
4 - CH_3	10	2.00432	0.5260	0.2068

R = H, CH_3

Table VI

g-Factor correlation of o- and p-substituted ($-O^-$ and -OH) phenoxyl radicals and phenol radical cations

Substituents	Positions in Graphs 3 and 4	g-Factors observed	Energy level coefficients of Hückel molecular orbital containing odd electron (λ)	Total spin density on the oxygen atoms ($\Sigma \rho_o$)
1 - O^-, 2 - O^-	11	2.00447	0.2929	0.3276
1 - O^-, 2 - OH	12	2.00428	0.4075	0.2915
1 - O^-, 4 - O^-	13	2.00455	0.2807	0.3044
1 - O^-, 4 - OH	14	2.00427	0.3888	0.2705
1 - OH, 2 - OH	15	2.00355	0.5399	0.2420
1 - OH, 4 - OH	16	2.00352	0.5110	0.2254
1 - OH, 4 - H	17	2.00352	0.5110	0.2254

Table VII

g-Factor correlation of o- and p-substituted methoxybenzene radical cations.

Substituents	Positions in Graphs 3 and 4	g-Factors observed	Energy level coefficients of Hückel molecular orbital containing odd electron (λ)	Total spin density on the oxygen atoms ($\Sigma\rho_o$)
2 - O^-	21	2.00435	0.4211	0.2785
2 - OCH_3	22	2.00340	0.5676	0.2106
2 - OH	23	2.00362	0.5539	0.2113
2,3, - $(OCH_3)_3$	24	2.00376	0.5203	0.2793
4 - O^-	18	2.00445	0.4023	0.2588
4 - OCH_3	19	2.00368	0.5383	0.1972
4 - OH	20	2.00358	0.5248	0.2113

Table VIII

g-Factor correlation of (i) m-substituted phenol radical cations , and (ii) m-substituted methoxybenzene radical cations and the 4-methylmethoxybenzene radical cation.

	Substituents in	Positions in Graphs 5 and 6	g-Factors observed	Energy level coefficients of Hückel molecular orbital containing odd electron (λ)	Total spin density on the oxygen atoms ($\Sigma\rho_o$)
(ii)	—	25	2.00322	0.730	0.1401
	3 - OCH_3	26	2.00327	0.6631	0.1464
	3 - OH	27	2.00315	0.6554	0.1557
	4 - CH_3	28	2.00321	0.6760	0.1220
(i)	2 - CH_3	29	2.00331	0.6827	0.1494
	3 - CH_3	30	2.00312	0.7094	0.1454
	4 - CH_3	31	2.00317	0.6639	0.1375
	3 - OH	32	2.00312	0.6481	0.1636

Table IX

g-Factor correlation of 1,3-benzodioxole radical cations.

Substituents	Positions in Graphs 7 and 8	g-Factors observed	Energy level coefficients of Hückel molecular orbital containing odd electron (λ)	Total spin density on the oxygen atoms ($\Sigma \rho_o$)
3' - O^-	33	2.00460	0.4897	0.2659
3' - OCH_3	34	2.00400	0.4889	0.2550
3' - OH	35	2.00391	0.4823	0.2634
3' - CH_3	36	2.00390	0.5240	0.2260
4' - COR	37	2.00435	0.5430	0.2352
—	38	2.00390	0.5291	0.2250
4' - CH_3	39	2.00380	0.5081	0.2115
4' - O^-	40	2.00430	0.4466	0.2485
4' - OCH_3	41	2.00400	0.4308	0.2324
4' - OH	42	2.00395	0.4214	0.2397

R = H, CH_3

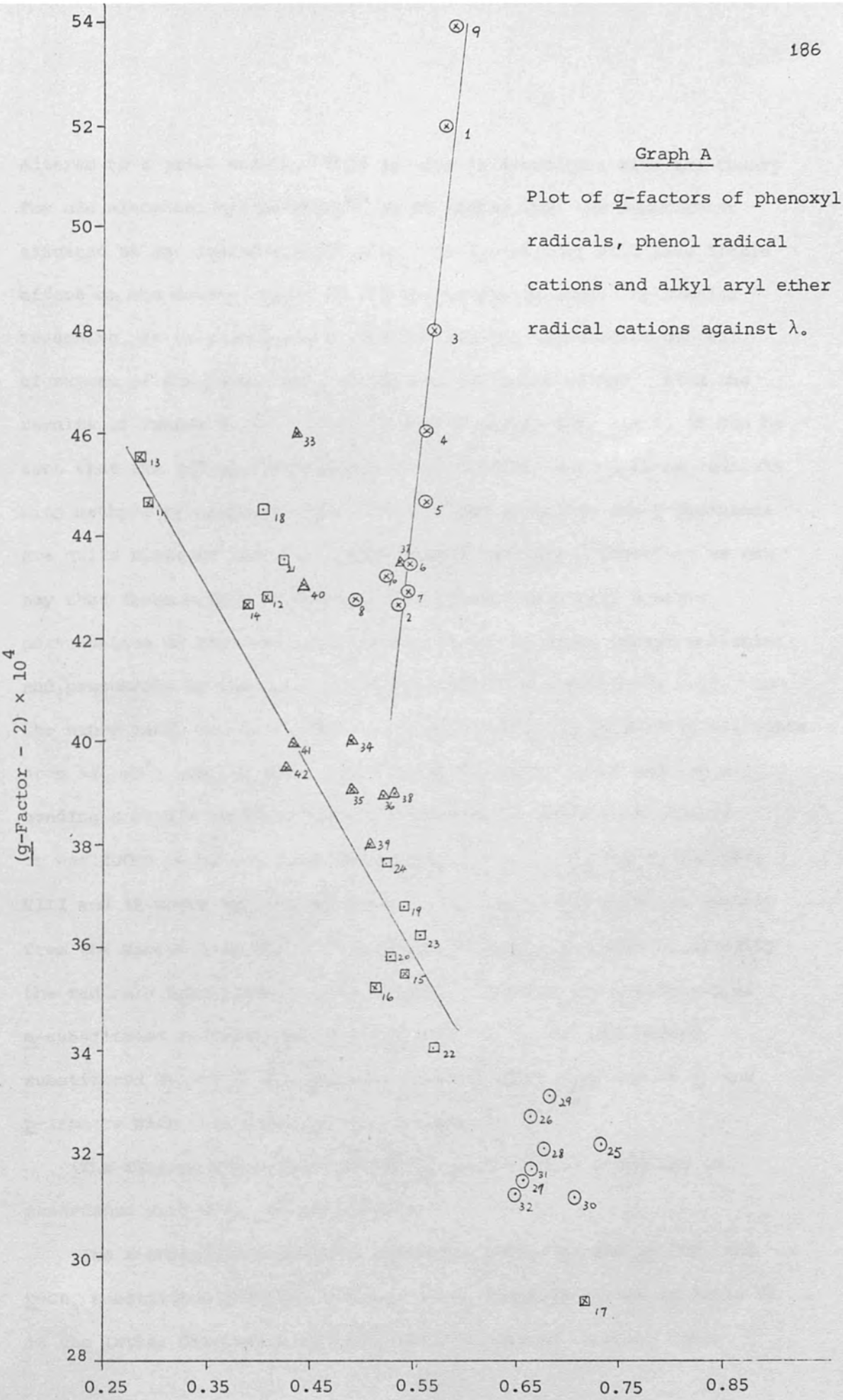

Graph A

Plot of g-factors of phenoxyl radicals, phenol radical cations and alkyl aryl ether radical cations against λ.

altered to a great extent. This is also in accordance with the theory for odd alternant hydrocarbons[124] which stated that any substituent situated at an 'inactive site' (i.e. the m-position) will have little effect on the energy levels of the unsubstituted ones. By similar reasoning, it is reasonable to assume that the non-bonding orbital of oxygen of the parent molecule is not perturbed either. From the results of Tables V, VI, VII, VIII and IX (pages 181- 185), it can be seen that the odd electron energy level coefficients of those radicals with methyl- or carbonyl- group substituted at the o- and p-positions are quite close to those of unsubstituted radicals. Therefore we can say that these weakly conjugated substituents have only a minor perturbation on the π-electron energy levels of these parent molecules and presumably on the non-bonding and σ-bonding orbitals as well. On the other hand, the o- and p-isomers with highly conjugated substituents such as $-O^-$, -OH and -OMe, the π electron energy level and the σ-bonding orbitals would be greatly perturbed by these substituents. It was found to be so, from the results listed in Tables V, VI, VII, VIII and IX where the odd electron energy levels are differed greatly from the parent molecules. Therefore it seems reasonable to classify the radicals into groups on this basis. Thus one group consists of m-substituted radicals and radicals with $-CH_3$ and -COR groups substituted at the o- and p-positions; the other consists of o- and p-isomers with strong interacting groups.

(The results summarised in the Tables mentioned above are in accordance with this classification.)

The m-substituted phenoxyl radicals, o-CH_3, o- and p- COR, and p-CH_3 substituted phenoxyl radicals (i.e. radicals listed in Table V; in the latter discussion we refer the radicals as to which Table

they belong for the sake of simplicity) are first considered. The plots of g-factors of these radicals against λ and the g-factors against $\Sigma\rho_o$ are shown in Graphs 1 and 2 respectively. These graphs show that the correlation of g-factors with these two parameters are excellent. The positive slope in Graph 1 indicates that the g-factors are directly proportional to the energy level coefficients of the Hückel molecular orbital containing the odd electron. As has been mentioned before, the σ-bonding orbitals are not greatly different from each other, we can therefore use the same reference basis for the excitation energies. From Fig. 4 on page 191, it can be seen that the larger the value of λ, the closer the odd electron orbital to the highest occupied σ-bonding orbital, and therefore the smaller the excitation energy. This is accompanied by a greater positive contribution to the g-shifts. Consequently not only the g-factors show a correlation with the substituent effects on the phenoxyl radicals (m-substituted; see page 191) but also the value of λ.

However, a negative slope was obtained from the plot of g-factors against λ for radicals listed in Table VI (see Graph 3, line A - A'). This indicates that the g-factors are not directly proportional to the value of λ and the effect arising from the interaction between the odd electron orbital and the bonding orbital predominates.

It can be seen from graph 3 (line B - B') that there is a satisfactory correlation between the g-factors of radicals listed in Table VII and λ. The slope of this plot is also negative, presumably a similar effect operates. However, the correlation of g-factors and the total spin densities on oxygen atoms for these two groups of radicals are rather poor (see Graph 4 line C - C' and line D - D').

The linear correlation between the g-factors and λ and with the total spin densities on oxygen atoms exist in those radicals listed

Graph 1

Plot of g-factors of m-substituted phenoxyl radicals and o- and p-substituted (-COR and $-CH_3$) phenoxyl radicals against λ

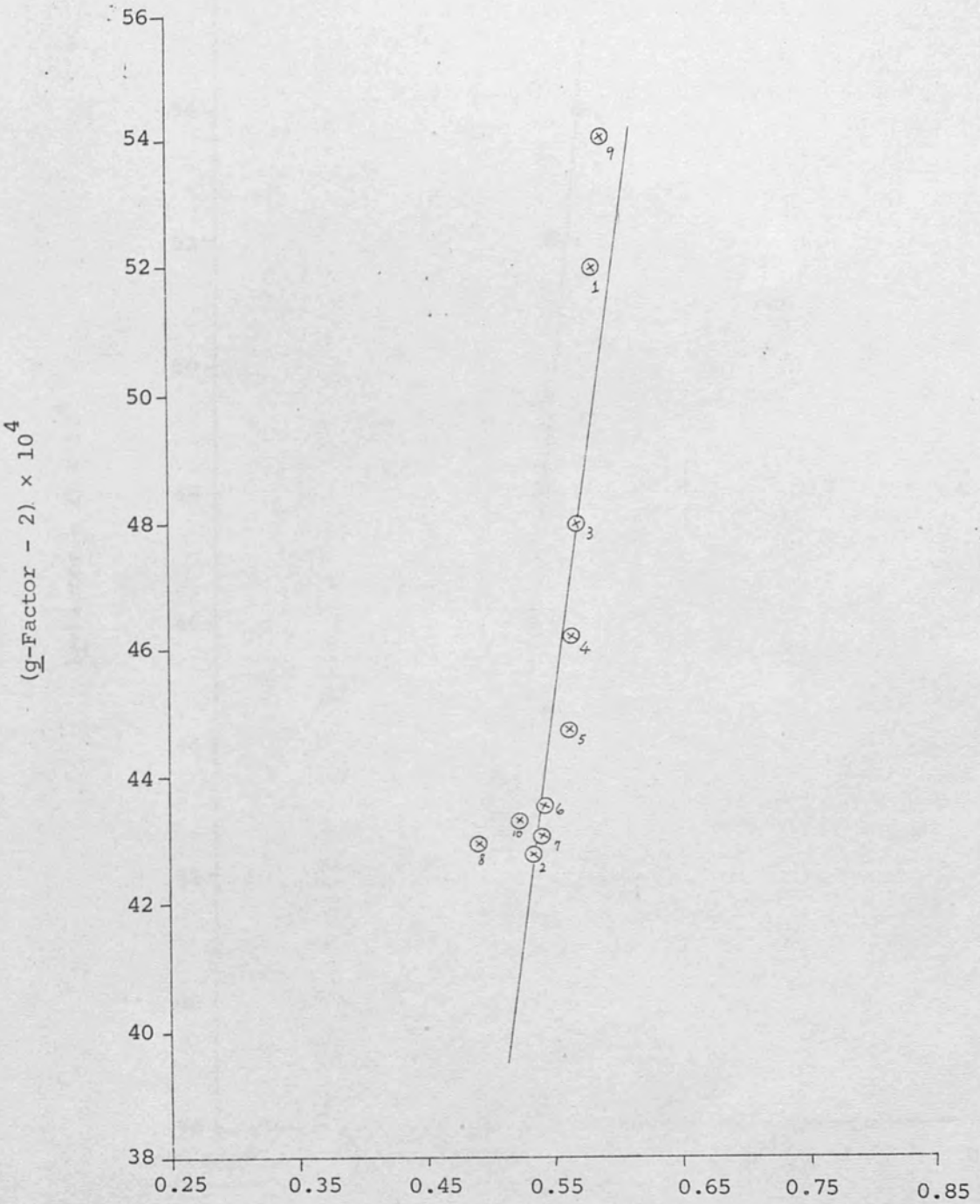

Energy level coefficients of odd electron Hückel molecular orbital, λ.

Pages 208 and 209 fold out to give a key to the numbering of the points.

Graph 2

Plot of g-factors of m-substituted phenoxyl radicals and o- and p-substituted (-COR, and $-CH_3$) phenoxyl radicals against $\Sigma\rho_o$

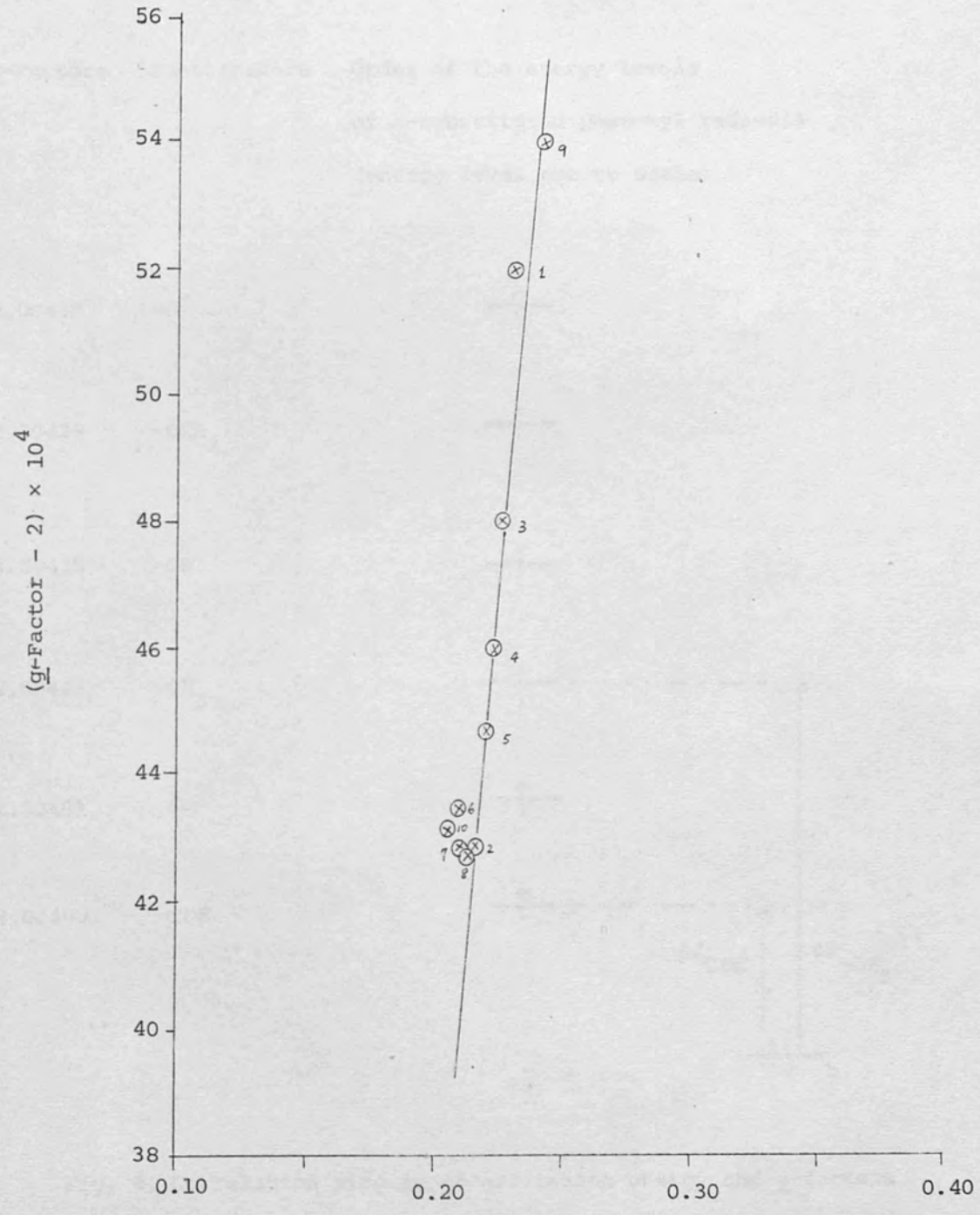

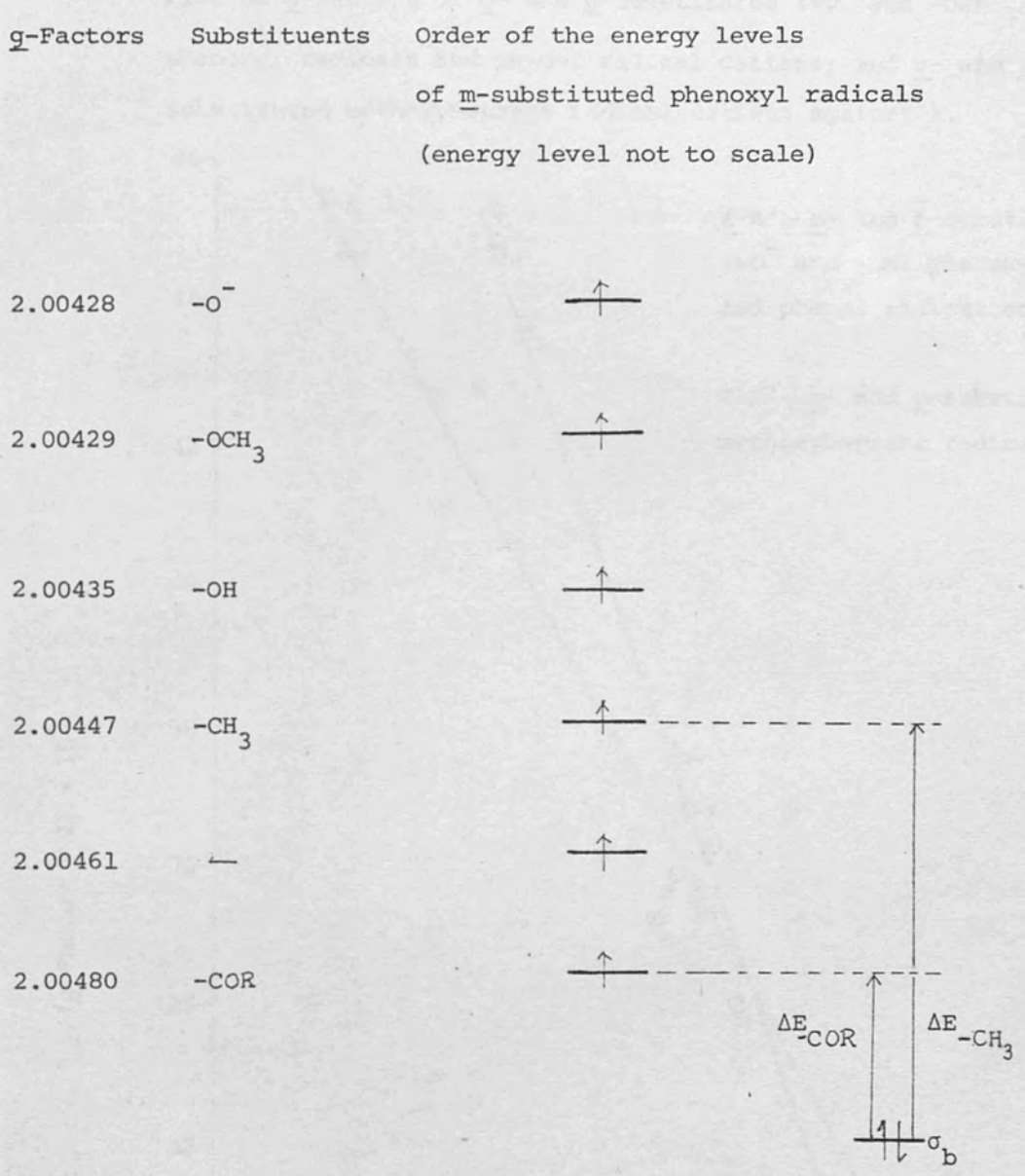

Fig. 4. Correlation diagram of excitation energy and g-factors of m-substituted phenoxyl radicals.

Graph 3

Plot of g-factors of o- and p-substituted ($-O^-$ and -OH) phenoxyl radicals and phenol radical cations; and o- and p-substituted methoxybenzene radical cations against λ.

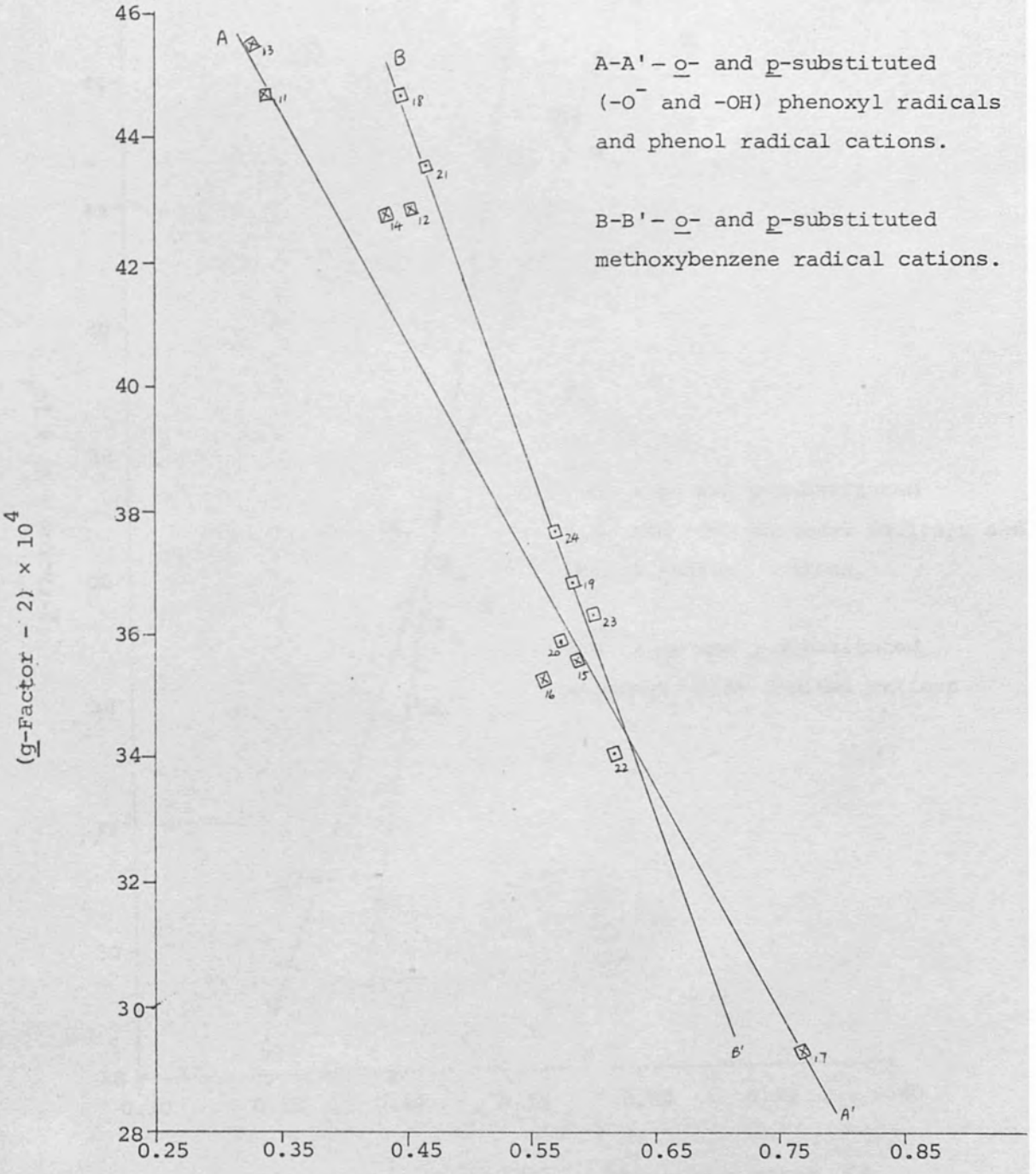

Graph 4

Plot of g-factors of o- and p substituted ($-O^-$ and -OH) phenoxyl radicals and phenol radical cations; and o- and p-substituted methoxybenzene radical cations against $\sum \rho_o$.

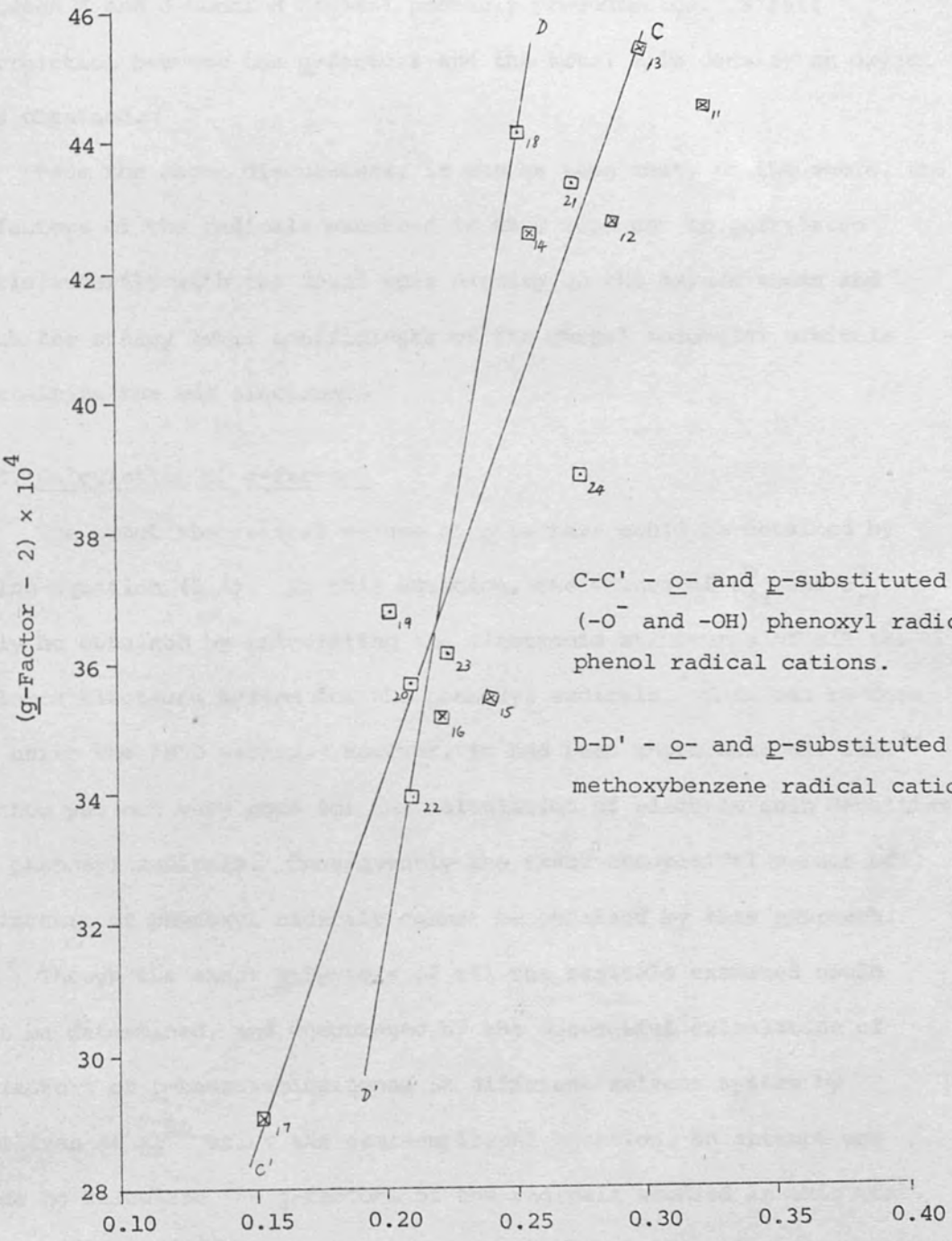

in Table VIII as revealed by Graphs 5 and 6.

The g-factors of 1,3-benzodioxole radical cations vary in an approximately linear fashion and negatively with λ and the interaction between π and σ-bonding orbital probably predominates. A fair correlation between the g-factors and the total spin density on oxygen was obtained.

From the above discussions, it can be seen that, on the whole, the g-factors of the radicals examined in this work can be correlated satisfactorily with the total spin density on the oxygen atoms and with the energy level coefficients of the Hückel molecular orbitals containing the odd electron.

C. Calculation of g-factors

The exact theoretical values of g-factors could be obtained by using Equation (5.3). In this equation, the values of c^m_{jx} and c^m_{ry} can only be obtained by calculating the electronic structures of all the valence electrons system for the phenoxyl radicals. This can be done by using the INDO method. However, it had been shown that the INDO[34] method was not very good for the calculation of electron spin densities of phenoxyl radicals. Consequently the exact theoretical values of g-factors of phenoxyl radicals cannot be obtained by this approach.

Though the exact g-factors of all the radicals examined could not be determined, and encouraged by the successful calculation of g-factors of p-benzosemiquinones in different solvent systems by Sullivan et al[80] using the semi-empirical equation, an attempt was made to calculate the g-factors of the radicals studied in this work, in an analogous manner. The values of a and b in Equation 5.5 can be determined from the plot of $\Delta g_{obs}/\Sigma\rho_o$ versus λ. The slope of the graph equals to b and the intercept is equal to a. The results of

Graph 5

Plot of g-factors of m-substituted phenol radical cations; and m-substituted methoxybenzene radical cations and 4-methylmethoxybenzene radical cation against λ.

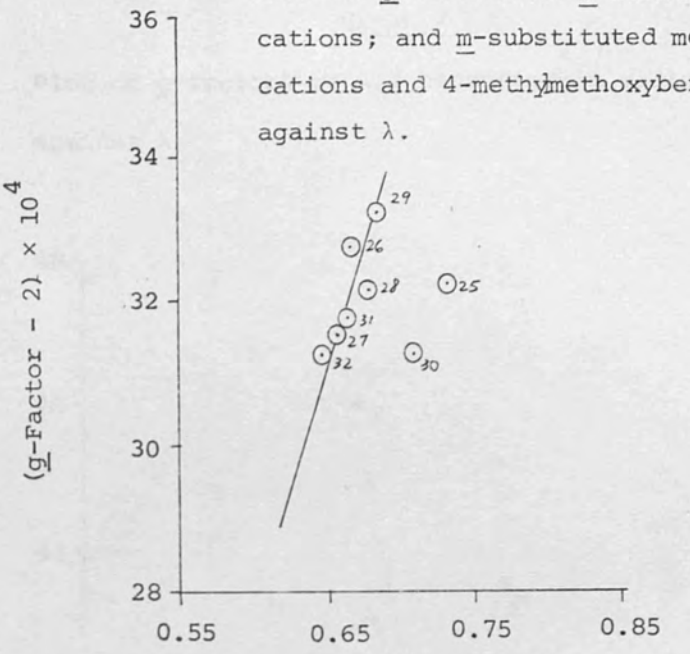

Energy level coefficient of odd electron Hückel molecular orbital, λ

Graph 6

Plot of g-factors of m-substituted phenol radical cations; and m-substituted methoxybenzene radical cations and 4-methylmethoxybenzene radical cation against $\sum \rho_o$.

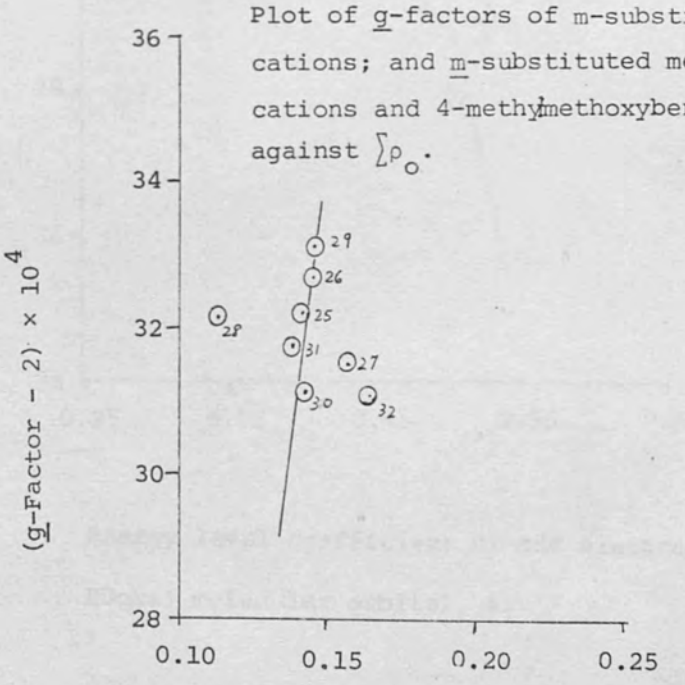

Total spin density on oxygen, $\Sigma \rho_o$

Graph 7

Plot of g-factors of 1,3-benzodioxole radical cations against λ.

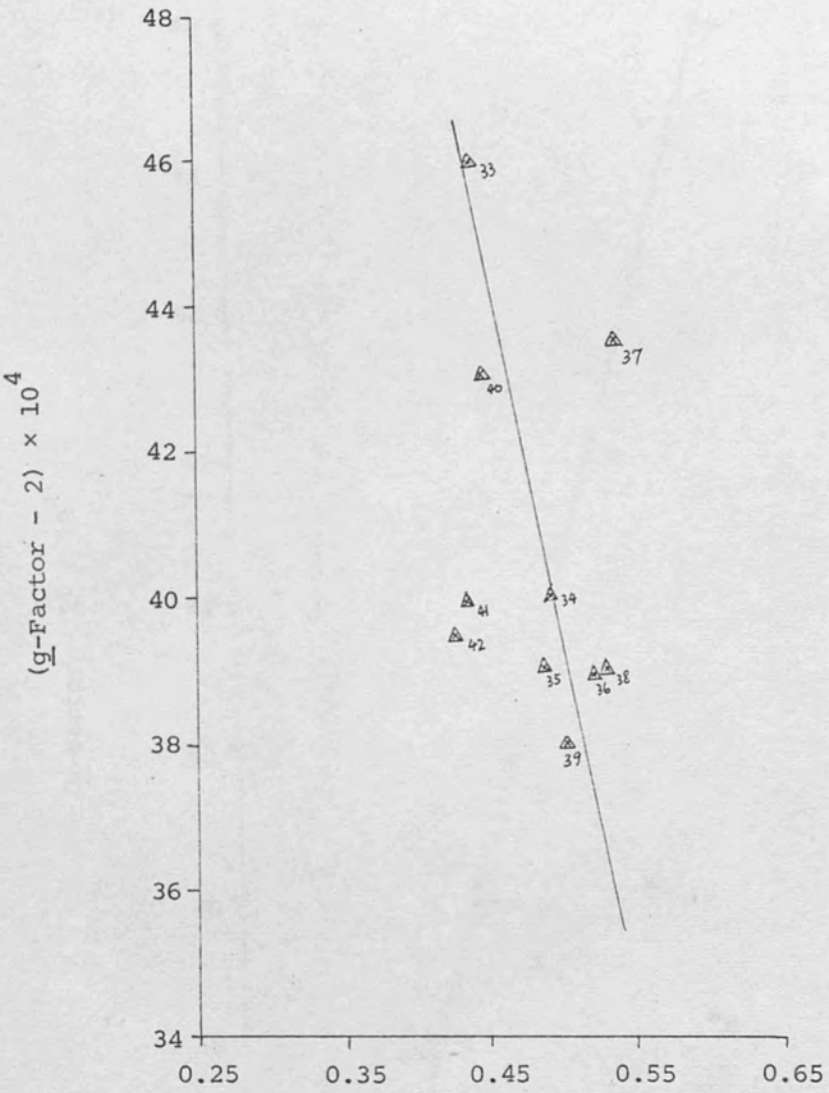

Energy level coefficient of odd electron Hückel molecular orbital, λ.

Graph 8

Plot of g-factors of 1,3-benzodioxole radical cations against $\sum\rho_o$.

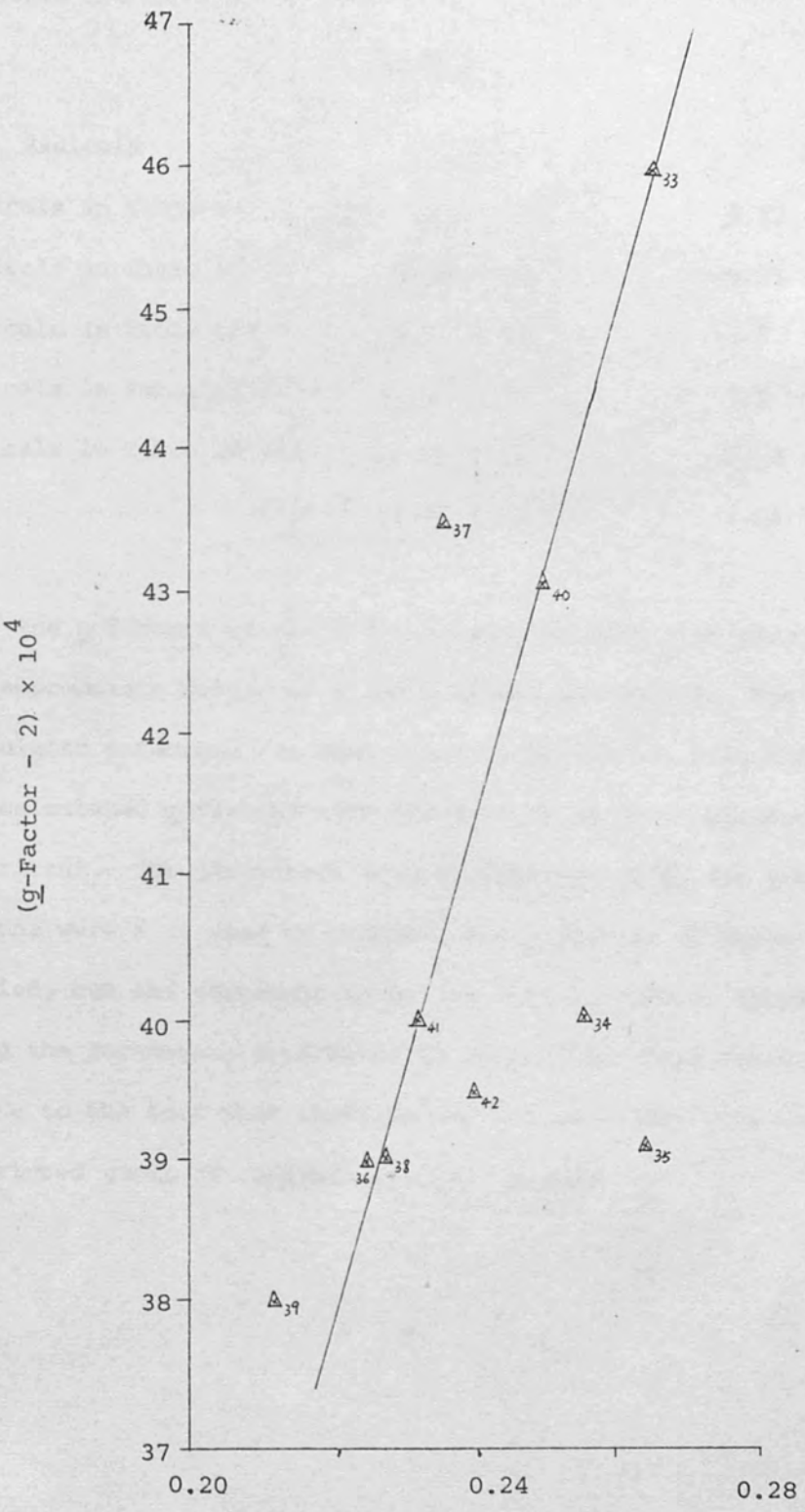

these plots (from Graphs 9 - 11 On pages 199 -201) of the various radicals are summarised in Table X.

Table X

Radicals	a	b
Radicals in Table V	-1.58×10^{-2}	4.62×10^{-2}
Radicals in Table VI	9.86×10^{-3}	-9.03×10^{-3}
Radicals in Table VII	1.6×10^{-2}	-1.88×10^{-2}
Radicals in Table VIII	-6.47×10^{-2}	1.0×10^{-1}
Radicals in Table IX (i)	-1.80×10^{-2}	5.08×10^{-2}
(ii)	-1.47×10^{-2}	5.08×10^{-2}

The g-factors of the radicals studied were then calculated using the appropriate values of a and b listed in Table X. The results of calculated g-factors are summarised in Tables XI, XII, XIII and XIV. The calculated g-factors were found to be in good agreement with experiment. The parameters used by Sullivan et al for p-benzosemiquinone were also used to estimate the g-factors of these radicals studied, but the agreement is not as satisfactory as those calculated using the parameters determined in this work. This could possibly be due to the fact that their parameters were only true for the relatively restricted group of radicals studied by them.

Graph 9

Plot of $\Delta g/\Sigma\rho_o$ against λ

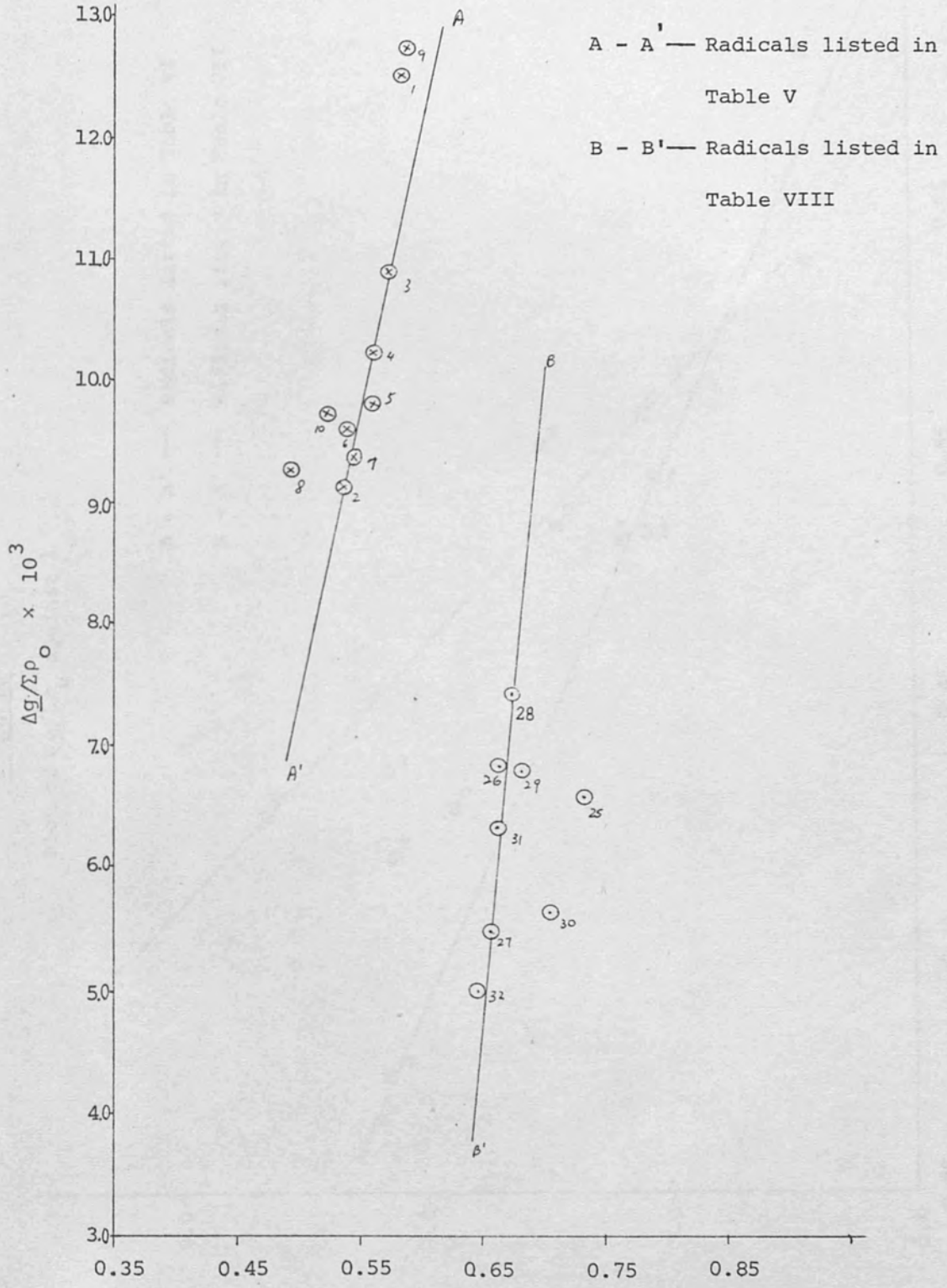

Energy level coefficient of odd electron Hückel molecular orbital, λ

Graph 10

Plot of $\Delta g/\Sigma\rho_o$ against λ

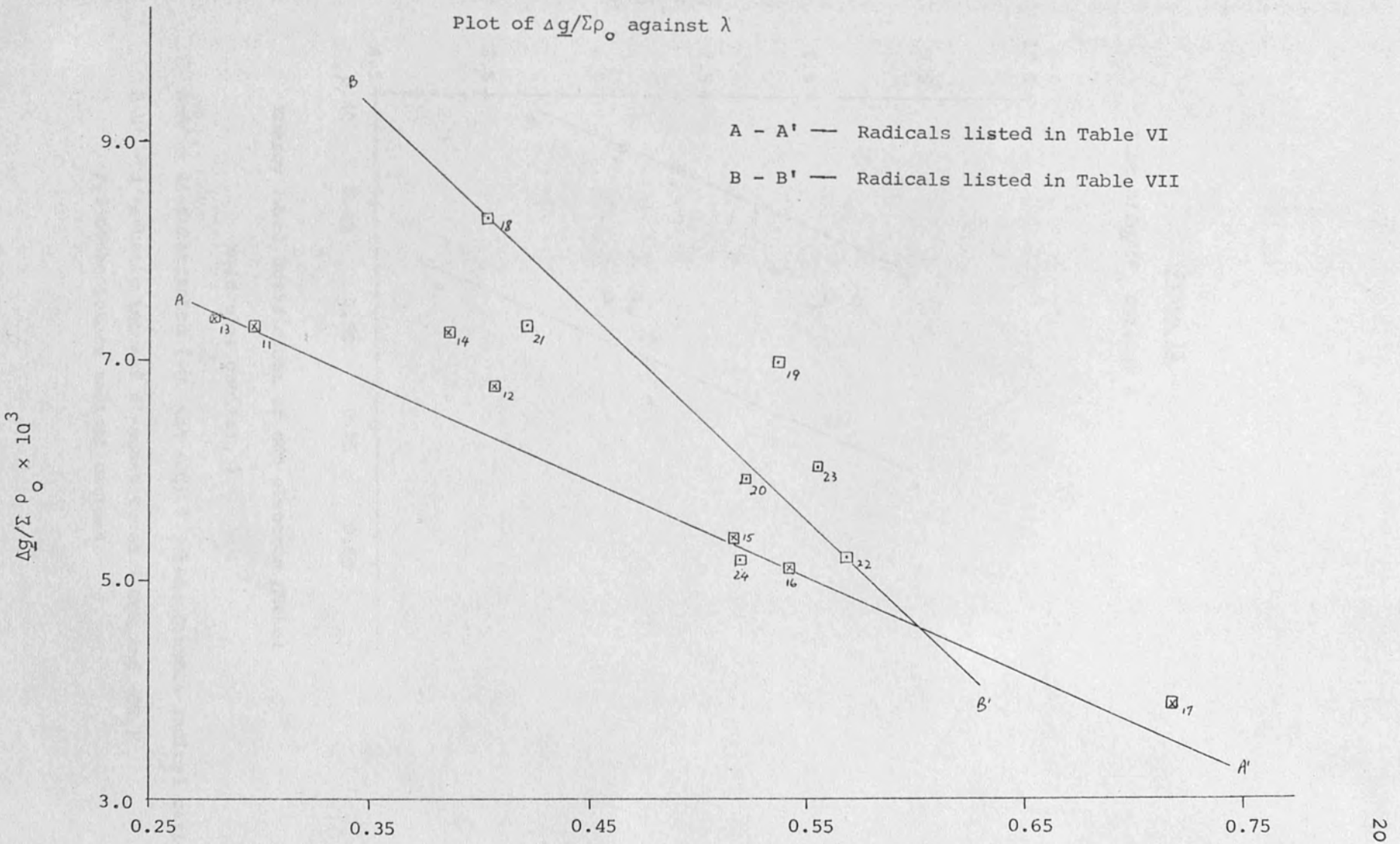

Graph 11

Plot of $\Delta g/\Sigma\rho_o$ against λ

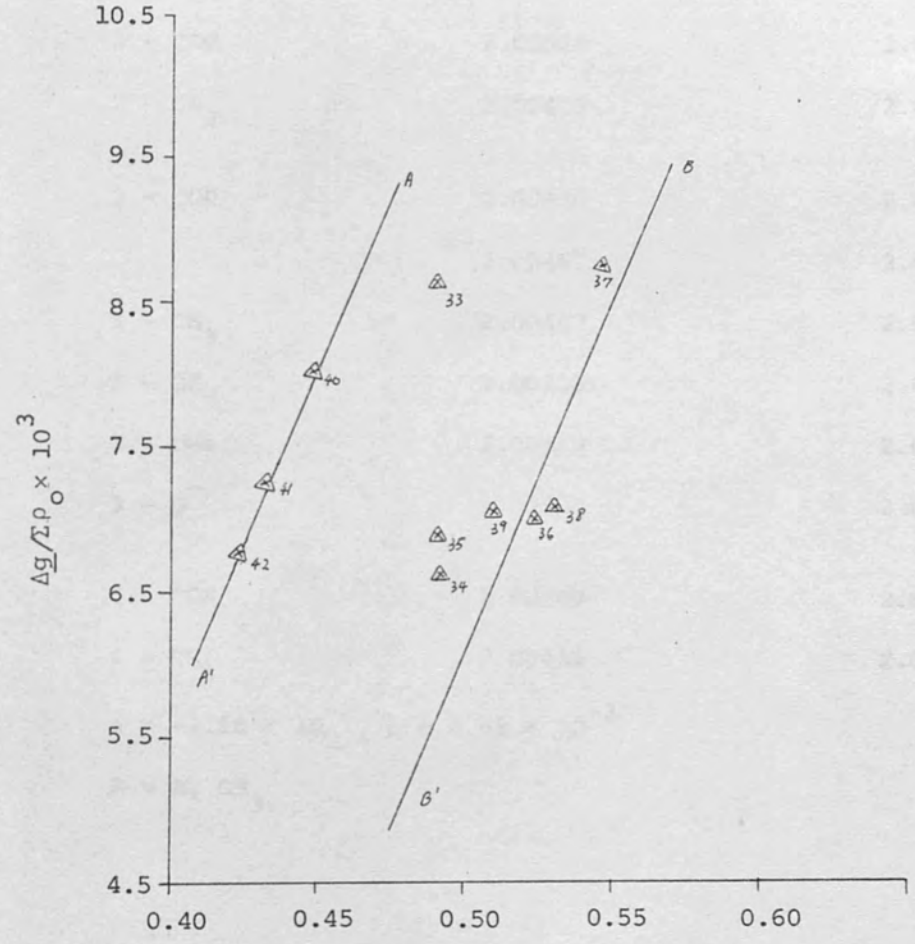

Energy level coefficient of odd electron Hückel molecular orbital, λ

A-A' - 4'-substituted ($-O^-$ and -OH) 1,3-benzodioxole radical cations.

B-B' - 3'-substituted and 4'-substituted (-COR and $-CH_3$) 1,3-benzodioxole radical cations.

Table XI

Calculated and experimental g-factors of m-substituted phenoxyl radicals and o- and p- methyl- and carbonyl- substituted phenoxyl radicals.

Substituents	g-factors observed	g-factors calculated
2 - COR	2.00520	2.00492
2 - CH_3	2.00429	2.00427
3 - COR	2.00480	2.00472
	2.00461	2.00467
3 - CH_3	2.00447	2.00457
3 - OH	2.00435	2.00427
3 - OMe	2.00429	2.00429
3 - O^-	2.00428	2.00382
4 - COR	2.00540	2.00515
4 - CH_3	2.00432	2.00407

$a = -1.58 \times 10^{-2}$, $b = 4.62 \times 10^{-2}$

R = H, CH_3

Table XII

Calculated and experimental g-factors of o- and p- substituted phenoxyl radicals ($-O^-$, -OH) and o- and p-dihydroxybenzene radical cations and phenol radical cations.

Substituents in 	g-factors observed	g-factors calculated
1 - O^-, 2 - O^-	2.00447	2.00466
1 - O^-, 2 - OH	2.00428	2.00410
1 - O^-, 4 - O^-	2.00455	2.00453
1 - O^-, 4 - OH	2.00427	2.00402
1 - OH, 2 - OH	2.00355	2.00359
1 - OH, 4 - OH	2.00352	2.00348
1 - OH,	2.00291	2.00283

$a = 9.86 \times 10^{-3}$, $b = -9.03 \times 10^{-3}$

Table XIII

Calculated and experimental g-factors of o- and p-substituted methoxybenzene radical cations

Substituents	g-factors observed	g-factors calculated
4 - O^-	2.00445	2.00448
4 - OMe	2.00368	2.00346
4 - OH	2.00358	2.00359
2 - O^-	2.00435	2.00455
2 - OMe	2.00340	2.00342
2 - OH	2.00362	2.00348
1,2,3 - $(OMe)_3$	2.00376	2.00404

$a = 1.6 \times 10^{-2}$, $b = -1.88 \times 10^{-2}$

Table XIV

Calculated and experimental g-factors of (i) m-substituted phenol radical cations, (ii) m-substituted methoxybenzene radical cations and 4-methylmethoxybenzene radical cation.

	Substituents	g-factors (observed)	g-factors (calculated)
(ii)	——	2.00322	2.00412
	3 - OMe	2.00327	2.00322
	3 - OH	2.00315	2.00316
	4 - CH_3	2.00321	2.00322
(i)	2 - CH_3	2.00331	2.00353
	3 - CH_3	2.00312	2.00389
	4 - CH_3	2.00317	2.00318
	3 - OH	2.00312	2.00309

$a = -6.47 \times 10^{-2}$, $b = 1.0 \times 10^{-1}$

Table XV

Calculated g-factors of 1,3-benzodioxole radical cationsand its derivatives

	Substituents	g-factors (observed)	g-factors (calculated)
(i)	3'- O^-	2.00460	2.00397
	3'- OMe	2.0040	2.00389
	3'- OH	2.00391	2.00386
	3'- CH_3	2.00390	2.00411
	4'- COR	2.00435	2.00441
	—	2.00390	2.00417
	4'- CH_3	2.00380	2.00383
	$a = -1.80 \times 10^{-2}$, $b = 5.08 \times 10^{-2}$		
(ii)	4'- O^-	2.00430	2.00428
	4'- OMe	2.00400	2.00396
	4'- OH	2.00395	2.00392
	$a = -1.47 \times 10^{-2}$, $b = 5.08 \times 10^{-2}$		
	R = H, CH_3		

D. Conclusion

The g-factors of m-substituted phenoxyl radicals and o- and p-substituted (CH_3 and -COR) phenoxyl radicals are well correlated with the values of λ and with the total spin density on oxygen atoms; while a fair correlation was obtained for the ether radicals examined.

Supplement to the graphs of Chapter 5

Substituents in 	Positions in the graphs	Symbols in the graphs
1 - O^-, 2 - COR	1	⊗
1 - O^-, 2 - CH_3	2	⊗
1 - O^-, 3 - COR	3	⊗
1 - O^-, 3 - H	4	⊗
1 - O^-, 3 - CH_3	5	⊗
1 - O^-, 3 - OH	6	⊗
1 - O^-, 3 - OMe	7	⊗
1 - O^-, 3 - O^-	8	⊗
1 - O^- 4 - COR	9	⊗
1 - O^-, 4 - CH_3	10	⊗
1 - O^-, 2 - O^-	11	⊠
1 - O^-, 2 - OH	12	⊠
1 - O^-, 4 - O^-	13	⊠
1 - O^-, 4 - OH	14	⊠
1 - OH, 2 - OH	15	⊠
1 - OH, 3 - OH	16	⊠
1 - OH, 4 - OH	17	⊠
1 - O^-, 4 - OMe	18	⊡
1 - OMe,4 - OMe	19	⊡
1 - OMe,4 - OH	20	⊡
1 - O^-, 2 - OMe	21	⊡
1 - OMe,2 - OMe	22	⊡
1 - OMe,2 - OH	23	⊡
1, 2, 3, - OMe	24	⊡

Supplement to the graphs contd.

Substituents in 	Positions in the graphs	Symbols in the graphs
1 - OMe, 3 - H	25	⊙
1 - OMe, 3 - OMe	26	⊙
1 - OMe, 3 - OH	27	⊙
1 - OMe, 4 - CH_3	28	⊙
1 - OH, 2 - CH_3	29	⊙
1 - OH, 3 - CH_3	30	⊙
1 - OH, 4 - CH_3	31	⊙
1 - OH, 3 - OH	32	⊙
Substituents in 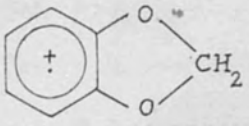		
3' - O^-	33	◬
3' - OMe	34	◬
3' - OH	35	◬
3' - CH_3	36	◬
4' - COR	37	◬
4' - H	38	◬
4' - CH_3	39	◬
4' - O^-,	40	◬
4' - OMe	41	◬
4'' - OH	42	◬

References

1. E. Zavoiskii, J. Phys. (U.S.S.R.) 1945, 9, 245, 447.
2. B.M. Kozyrov and S.G. Salikov, Dokl. Akad. Nauk. SSSR, 1947, 58, 1023.
3. A. Carrington, D.H. Levy and T.A. Miller, J. Chem. Phys. 1966, 45, 3450.
4. A. Carrington and A.D. McLachlan 'Introduction to Magnetic Resonance' Harper and Row, International, 1967.
5. J.E. Wertz and J.R. Bolton, 'Electron Spin Resonance' Plenum Press, 1972.
6. W.T. Dixon, 'Theory and Interpretation of Magnetic Resonance' Plenum Press, 1972.
7. M.C.R. Symons, Adv. in Phys. Org. Chem., Vol. 1, 283, 1963.
8. (a) H.M. McConnell, J. Chem. Phys., 1966, 24, 764.
   (b) H.M. McConnell and D.B. Chesnut, J. Chem. Phys., 1958, 28, 107.
9. H.S. Jarrett, J. Chem. Phys., 1956, 25, 1289 .
10. S.I. Weissman, J. Chem. Phys., 1956, 25, 890.
11. A. Carrington, Quart. Rev. 1963, 17, 67.
12. A.J. Stone, Proc. Roy. Soc. 1963, A 271, 424.
13. R.O.C. Norman, Adv. in Phys. Org. Chem., 1967, 5, 53.
14. A. Streitweiser, 'Molecular Orbital Theory for Organic Chemists', Wiley, 1961.
15. A.D. McLachlan, Mol. Phys. 1963, 3, 233.
16. J.A. Pople and R.K. Nesbet J. Chem. Phys. 1954, 22, 571.
17. K.U. Ingold, Chem. Rev., 1961, 61, 563.
18. W.I. Taylor and A.R. Battersby, 'Oxidative Coupling of Phenolic Compounds', Marcel Dekker, N.Y. 1967.

19. T.J. Stone and W.A. Waters, Proc. Chem. Soc., 1962, 253; J. Chem. Soc., 1964, 213.

20. G.E. Penketh, J. Appld. Chem., 1957, 512.

21. L.R. Mahoney and S. A. Weiner, J. Am. Chem. Soc., 1972, 94, 585.

22.(a) E.J. Land and G. Porter, Trans. Faraday Soc., 1963, 59, 2016

(b) E.J. Land and G. Porter and E. Strand, Trans Faraday Soc., 1961, 54, 1886.

23. L.F. Fieser and M. Fieser, 'Reagents for Org. Synthesis' Wiely, N.Y. 1966, 147-151.

24. D.H.R. Barton, Chem. in Britain, 1967, 3, 330.

25. E. Müller, K. Ley, K. Scheffler and R. Mayer, Chem. Ber., 1958, 91, 2682.

26.(a) E.R. Atwick, Chem. Rev. 1967, 67, 475.

(b) H. Musso, Angew. Chem. Int. Ed. 1963, 2, 273.

(c) A.I. Scott, Quart. Rev. (Lond), 1965, 1, 19.

27. W.T. Dixon and R.O.C. Norman, J. Chem. Soc., 1964, 4857

28. W.T. Dixon and R.O.C. Norman, J. Chem. Soc., 1963, 3119.

29. H.M. Swartz, J.R. Bolton, D.C. Borg, 'Biological Application of Electron Spin Resonance' Wiley, N.Y.

30. G.E. Adams, B,E. Michael and E.J. Land, Nature, 1966, 211, 293.

31. C.R.E. Jefcoate and R.O.C. Norman, J. Chem. Soc., 1968, (B), 48.

32. M. Tomkiewicz, A. Green and M. Coccivera. J. Am. Chem. Soc., 1971, 93, 7102 and J. Am. Chem. Soc., 1972, 94, 6598.

33. P. Neta and R.W. Fessenden, J. Phys. Chem., 1974, 78, 523.

34. W.T. Dixon, M.Moghimi and D. Murphy, J. Chem. Soc. Trans. Faraday II, 1974, 70, 1713.

35. W.T. Dixon, E.J. Foster, and D. Murphy, J. Chem. Soc., Perkin II, 1973, 2124.

36. M. Blois, Jr., J. Maling and R.N. Adams, Biochem Biophys. Res. Comm., 1960, 3, 132.

37. J. Fritsch, S.V. Tatwawadi and R.N. Adams, J. Phys. Chem., 1967, 71, 338.

38.(a) I. Yamazaki, T. Ohnishi, Biochim. Biophys. Acta, 1966, 469, 112.

(b) D. Backstrom, B. Norling, A. Ehrenberg and L. Ernster, Biochim. Biophys. Acta, 1970, 197, 108.

39. L. Michaelis, Chem. Rev., 1935, 16, 243.

40. B. Venkataraman, G.K. Fraenkel, J. Am. Chem. Soc., 1955, 77, 2707.

41. M. Adams, M.S. Blois and R.H. Sands, J. Chem. Phys., 1958, 28, 774.

42. S. Blois, J. Chem. Phys., 1955, 23, 1351.

43. R.H. Hoskins and B.R. Loy, J.Chem. Phys., 1955, 23, 2461.

44. R.H. Hoskins, J. Chem. Phys., 1955, 23, 1975.

45. E. Müller, R. Mayer and K. Ley, Angew. Chem., 1958, 70, 73.

46. K. Ley and E. Müller, Angew. Chem., 1958, 70, 469.

47. B. Venkataraman, G.K. Fraenkel, B.G. Segal J.Chem. Phys., 1959, 30, 1006.

48. R. Bersohn, J. Chem. Phys., 1956, 24, 1006.

49. G. Vincow and G.K. Fraenkel J. Chem. Phys., 1961, 34, 1333.

50. R.W. Brandon and E.A.C. Lucken, J. Chem. Soc., 1961, 4273.

51. A. Fairborn and E. Lucken, J. Chem. Soc., 1963, 258.

52. G. Vincow, J. Chem. Phys. 1963, 38, 917.

53. T.J. Stone and W.A. Waters, J. Chem. Soc., 1964, 4302.

54. T.J. Stone and W.A. Waters, J. Chem. Soc., 1965, 1488.

55. C. Trapp, C.A. Tyson and G. Giacometti, J. Chem. Am. Soc., 1968, 90, 1394.

56. T.K. Lott and E.G. Short and D.N. Waters, J.Chem. Soc.(B), 1969, 1232.

57. D.H. Anderson, P.J. Frank and H.S. Gutowsky, J. Chem. Phys., 1960, 32, 196.

58. D.C. Reitz, J.P. Hollahan, F. Dravnieks and J.E. Wertz, J. Chem. Phys., 1960, 34 , 1457.

59.(a) J. Pillar, I. Buben, and J. Popisil, Tet. Lett., 1968, 4203.

60.(b) N.M. Atherton, A.J. Blackhurst, J. Chem. Soc. Faraday Trans. II 1972, 68, 470.

60. F.R. Hewgill, T.J. Stone and W.A. Waters, J. Chem. Soc., 1964, 408.

61.(a) P. Ashworth and W.T. Dixon, J. Chem. Soc. Perkin II, 1972, 1130.

.(b) J.A. Pedderson, J. Chem. Soc., Perkin II, 1973, 424.

62. P. Ashworth and W.T. Dixon, J. Chem. Soc., Perkin II, 1973, 2128.

63. J.E. Wertz and J.C. Vivo, J. Chem. Phys., 1956, 24, 479.

64. J.H. Freed and G.K. Fraenkel J.Chem. Phys. 1963, 38, 2020.

65. M.R. Das, H.D. Connor, D.G. Leniart and J.H. Freed, J. Am. Chem. Soc., 1970, 92, 2258.

66.(a) L.H. Piette , M. Okamura, G. Robold, R. Ogota, R. Moore and P. Scheller, J. Chem. Phys., 1967, 71, 29.

(b) G.P. Robold, R.T. Ogota, M. Otamura and L.H. Piette, J. Chem. Phys. 1967, 46, 1161.

67. P. Ashworth and W. T. Dixon, J. Chem. Soc., Perkin II, 1974, 739.

68. E.W. Stone and A.H. Maki, J. Chem. Phys., 1962, 36, 1944.

69. J.G. Gendell, J.H. Freed and G.K. Fraenkel, J. Chem. Phys. 1962, 37, 2831.

70. W.M. Gullick and D.H. Geske, J. Am. Chem. Soc., 1966, 88, 4119.

71. E.W. Stone and A.H. Maki, J. Am. Chem. Soc., 1965, 87, 454.

72. M. Broze, Z. Luz and B.C. Silver, J. Chem. Phys., 1967, 46, 4891.

73.(a) W.G.B. Huysmans and W.A. Waters, J. Chem. Soc., (B), 1966, 1047.

(b) W.G.B. Huysmans and W.A. Waters, J. Chem. Soc., (B), 1967, 1163.

74. I. Yamazaki and L.H. Piette, J. Am. Chem. Soc., 1965, 87, 986.

75. A. Carrington, I.C.P. Smith, Mol. Phys., 1967, 12, 439.

76.(a) W.T. Dixon and D. Murphy, J. Chem. Soc., Faraday Trans. II, 1976, 72, 135.

(b) W.T. Dixon and D. Murphy, Trans. Faraday II, 1976, 72, 1221.

77. H.B. Stegmann, K. Scheffler, Angew. Chem. Int. Ed. 1964, 3, 656.

78. A.J. Stone, Mol. Phys., 1963, 6, 509.

79. A. Carrington and I.C.P. Smith, Mol. Phys., 1964, 8, 101.

80. P.D. Sullivan, J.R. Bolton and G.E. Geiger,Jr., J. Am. Chem. Soc., 1970, 92, 4176.

81. G,N. Lewis, and J. Bigeleisen, J. Am. Chem. Soc. 1943, 65, 424.

82. I.J. Chkheidze, V.I. Trofeninov, N.V. Buben, Zh. Strukt. Khim. 1964, 5, 624.

83.(a) W.M. Schubert and R.H. Quacchia. J. Am. Chem.Soc., 1962, 84, 3728.

(b) E.M. Arnott, C.Y. Wu, J.N. Anderson, R.D. Bushwick , J. Am. Chem. Soc., 1964, 84, 1674.

84. (a) A.J. Kresge and Y Chiang, Proc. Chem. Soc. 1961, 81.

(b) E.M. Arnott and C.Y. Wu, J. Am. Chem . Soc. 1960, 82, 5660.

(c) A.J. Kresge, G.W. Barry, K.R. Charles and Y. Chiang, J. Am. Chem. Soc., 1962, 84, 4343.

85. J.R. Bolton and A. Carrington, Proc. Chem. Soc., 1961, 385.

86. D.L. Allara, B.C. Gilbert and R.O.C. Norman, Chem. Comm.1965, 319.

87. A. Zweig, W.G. Hodgson, and W.H. Jura, J. Am. Chem. Soc., 1964, 44, 1501.

88. W.F. Forbes and P.D. Sullivan, Can. J. Chem. Soc., 1966, 44, 1501.

89. W.F. Forbes, P.D. Sullivan, J. Am. Chem. Soc., 1966, 88, 2862.

90. A. Nishinaga, H. Hayashi, and T. Matsuura, Bull, Chem.Soc. Jap. 1974, 47, 1813.

91. D. Barrer, A. Foucourt, J. Electrochemistry, 1972, 39, 377.

92. P.D. Sullivan, J. Am.Chem.Soc., 1967, 89, 4294.

93. P.D. Sullivan J. Chem.Phys., 1968, 48 , 1411.

94. P. D. Sullivan, J. Phys. Chem., 1970, 74, 2563.

95. W.F. Forbes, P.D. Sullivan and H.M. Wang, J. Am.Chem. Soc. 1967, 89, 2705.

96. P.D. Sullivan, J. Phys. Chem.,1971, 75, 2195.

97. P.D. Sullivan, J. Phys. Chem., 1969, 73, 2791.

98. W.F. Forbes and P.D. Sullivan, Can.J. Chem. Soc., 1968, 46, 317.

99. C.A. Coulson and V.A. Crawford, J. Chem. Soc., 1953, 2052.

100. D. Lazdins and M.Karplus, J. Am. Chem. Soc.,1965, 87, 920.

101.(a) P.O'Neill,S. Steenken, D. Schulte-Frohlinde, J. Phys. Chem., 1975, 79, 2773.

(b) P. O'Neill, S. Steenken, D. Schulte-Frohlinde, Angew. Chem. Int. Ed. 1975, 15, 430.

102. W.T. Dixon and D. Murphy, J. Chem.Soc., Perkin II, 1976, 1824.

103.(a) N. Normant, Angew. Chem. Int. Ed. 1967, 6, 1046.

(b) R. Kuopio, A. Kivinen and J. Mürto, Acta Chem. Scand., 1976, A(30), 1.

104. G.A. Russell, A.G. Berious, E.J. Goles, E.G. Janbon and A.J. Moye, Adv. Chem. Ser. No. 75, 1968, 174.

105. Jack-Emik Dubois and G Dodin, J. Am. Chem. Soc., 1972, 94, 7520.

106. G.A. Russell, C.L. Myers, Paolo Bruni, F.A. Nergebauer and R. Blankespoor, J. Am. Chem. Soc., 1970, 92, 2762.

107. H.R. Gersmann and A.F. Bickel, J. Chem. Soc.,1959, 2711.

108. G.A. Russell and E.T. Strom, J. Am. Chem. Soc., 1964, 86, 744.

109. G.A. Russell, E.G. Jantzan, A.G. Bemis, E.J. Gells, A.J. Moye S. Mark, E.T. Strom. Adv. Chem. Ser.,1965, 51, 173.

110. H.J. Teuber and N. Gvtz, Chem.Ber.,1954, 87, 1276.

111.(a) G.A. Russell, R.L. Blankspoor, Tet. Lett., 1971, 4573.

111(b) G.A. Russell, J.Org. Chem., 1966, 31, 3455.

112. Yusaku Ikegami, Schuichi Seto, Bull. Chem. Soc. Jap., 1968, 41, 2225.

113.(a) M.St.C. Fleet, J. Chem. Soc., 1948, 1441.

(b) I.S. Romodamov, N.V. Arshara, A.E. Dulskii, Teor. Eskp. Chem., 1973, 968.

114. Y. Speinzak, J. Am. Chem. Soc., 1958, 80, 6449.

115. F.R. Hewgill and S.L. Lee, J. Chem. Soc., 1969, (C), 2080.

116. F.C.S. Foote, Acc. of Chem. Res., 1968, 1, 104.

117. J. Griffiths, K.Y. Chu, C. Hawkins, Chem. Comm.,1976, 676.

118. G. Russell and A.G. Bemis, J.Am. Chem. Soc., 1966, 88, 5491.

119. S.F. Nelson, P.D. Bartlett, J. Am. Chem. Soc., 1966, 88, 143.

120. A. Bienes, C.V. Share, A.M. Trozzolo, 'Creation and Detection of the Excited States.' Ed. W.R. Ware, Dekker, N.Y. 1974, 149.

121.(a) W.T. Dixon, J. Chem.Soc., Faraday Trans., II 1976, 72, 282.

(b) W.T. Dixon, J. Chem. Soc., Faraday Trans., II,1977, 73, 67.

122. A.D. McLachlan, Mol. Phys. 1958, 1, 233.

123, E.W. Stone and A.H. Maki, J. Chem. Phys.,1963, 38, 1999.

124.(a) M.J.S. Dewar, 'The Molecular Orbital Theory of Organic Chemistry' McGraw-Hill, N.Y., 1969.

(b) M.J.S. Dewar and R.C. Dougherty, 'The PMO Theory of Organic Chemistry', Plenum Press, N.Y., 1975.

125. B.G. Segal, m. Kaplan and G.K. Fraenkel, J. Chem. Phys., 1965, 43, 4191.

126.(a) W.T. Dixon, M. Moghimi, D. Murphy, J. Chem. Soc., Perkin II, 1975, 101.

(b) W.T. Dixon, M. Moghimi, D. Murphy, J. Chem. Soc., Perkin II, 1975, 1189.

127. D. L. Beveridge and J. A. Pople, 'Approximate Molecular Orbital Theory', McGraw Hill, N. Y. 1970.

Appendix

```
      PROGRAM LKH(INPUT,OUTPUT)
C     THIS PROGRAM IS TO CALCULATE    PI ELECTRON SPIN DENSITIES BY
C     MCLACHLAN METHOD
      INTEGER PAIRED
      INTEGER ODD
      REAL LAMDA
      DIMENSION A (30,30), ENERGY(30,30), VEC(30,30),U1(30), CC(30,30)
      DIMENSION X(30), Y(30), SPIN(30), TOTAL(30,30), AA(30,30)
      DIMENSION SUM(30,30)
C     READ IN THE SIZE OF THE MATRIX AND THE ODD ELECTRON ENERGY LEVEL
      READ 2, N, M, ODD
    2 FORMAT(3I4)
      PRINT 100, N, M, ODD
  100 FORMAT (1X, * N= *,I4, * M= *, I4, * ODD   *, I4)
      IFAIL=1
C     READ IN THE MATRIX A
      READ 1, ((A(I,J), J=1, M), I=1,N)
C     TO HOLD THE MATRIX
      DO 35 I=1,N
      DO 35 J=1,M
      AA(I,J)= A(I,J)
   35 CONTINUE
C     HMO CALCULATION IS PERFORMED BY THE CONTROL     PARAMETER L=1
C     WHEN L=2 THE SPIN DENSITIES IS COMPUTED BY MCLACHLAN METHOD
      L=1
      GO TO 12
C     TO READ IN THE TESTED MOLECULAR PARAMETERS
   34 READ 37, AA(1,1), AA(2,1), AA(1,2)
   37 FORMAT(3F10.5)
      IF (AA(1,1).EQ.8.8) GO TO 99
      L=1
      DO 36 I=1,N
      DO 36 J=1,M
   36 A(I,J)=AA(I,J)
   12 PRINT 200
  200 FORMAT(//,1X, *   INPUT MATRIX   *,//)
      PRINT 101, ((A(I,J), J=1,M), I=1,N)
      CALL F02ABF(A, 30, N, ENERGY,VEC, 30, U1, IFAIL)
      DO 30 I=1,N
   30 ENERGY(I)=-ENERGY(I)
      PRINT 300
  300 FORMAT(//,*   ENERGY LEVELS   *,//)
      PRINT 102, ( ENERGY(I), I=1,N)
      PRINT 500
  500 FORMAT(//,1X, *   COEFFICIENTS   *,//)
      DO 15 I=1,N
   15 PRINT 104, (VEC(I,J),J=1,M)
      DO 5 I=1,N
      DO 5 J=1,M
    5 CC(I,J)=VEC(I,J)**2
      PRINT 400
  400 FORMAT(//, 1X, *   SQUARES   *,//)
      PRINT 105, ((CC(I,J),J=1,M), I=1,N)
C     TO MODIFY THE DIAGONAL ELEMENTS OF THE MATRIX
      IF(L.EQ.2) GO TO 7
C     TO COMPUTE MCLACHLAN SPIN DENSITIES
      LAMDA=1.2
```

```
      DO 6 I=1,N
    6 A(I,I)=A(I,I)+2.0*LAMDA*VEC(I,ODD)**2
    7 DO 8 I=1,N
    8 X(I)=VEC(I,ODD)**2
      PAIRED =ODD+1
      DO 9 J=1,M
      TOTAL(L,J)=0.0
       DO 9 I=PAIRED,N
      TOTAL(L,J)=TOTAL(L,J)+VEC(J,I)**2
    9 CONTINUE
      IF (L.EQ.1) GO TO 10
      DO 11 I=1,N
      Y(I)=TOTAL(2,I)-TOTAL(1,I)
   11 SPIN(I)=X(I)+Y(I)
      PRINT 108, (SPIN(I),I=1,N)
      IF (L.GE.2) GO TO 34
   10 L=L+1
      GO TO 12
  800 FORMAT(/,1X, *   ODD=    *,I5,/)
    1 FORMAT(3F10.4)
  101 FORMAT(3F10.4)
  102 FORMAT(3F10.4)
  104 FORMAT(3F10.4)
  105 FORMAT(3F10.4)
  108 FORMAT(//, 1X, *   SPIN DENSITY=    *, 3 F10.4)
   99 STOP
      END
```

Tetrahedron Letters No. 8, pp 623 - 626, 1976. Pergamon Press. Printed in Great Britain.

THE ELECTRON SPIN RESONANCE SPECTRA OF RADICALS FORMED IN THE AUTOXIDATION OF PHENOLS

William T. Dixon*, Pat M. Kok and David Murphy
Department of Chemistry, Bedford College (University of London),
Regent's Park, London NW1 4NS

(Received in UK 3 December 1975; accepted for publication 15 January 1976)

Hexamethyl phosphoramide (HMPA) is much more stable towards base than other commonly available aprotic solvents which are also highly polar[1]. Its inert quality in this respect makes this solvent especially suitable for autoxidation studies which are generally catalysed by base, and a variety of intermediate radicals have been generated and observed by means of electron spin resonance spectroscopy[2,3].

These radicals often appear only after several steps, the first being the formation of a negative ion, the second, oxygenation by molecular oxygen[2], subsequent stages leading to products which can give radicals either by reduction or by direct interaction with O_2.

Hexamethyl phosphoramide is a particularly suitable solvent for studying semiquinones because the concentration of base can be kept low by using an alcohol salt, e.g. sodium methoxide, which is sparingly soluble, at the same time the concentration of acidic protons is also very low.

Direct autoxidation of α- and β-naphthol: In aqueous or in alcoholic solutions it is not generally possible to detect evidence of appreciable autoxidation of the naphthols or of their sodium salts over a period of an hour or so. In HMPA we obtain from both naphthols, strong e.s.r. signals due to 1,2-naphthosemiquinone, which, in the case of α-naphthol, decays after some minutes to leave weaker spectrum due to 1,4-naphthosemiquinone (see Table 1). The same spectra can be obtained directly from the corresponding naphthoquinones, or from the two corresponding dihydroxy naphthalenes. The coupling constants are rather different from those observed in aqueous solution[4,5].

Autoxidation of dihydroxy naphthalenes: In some cases the dihydroxynaphthalenes behave as simple extensions of the naphthols, for example 1,5-dihydroxynaphthalene gives rise to the same e.s.r. spectrum as juglone showing preferred oxidation in the 4-position, perhaps due to the extra stability provided by the peri-hydrogen[6] (see Table 1) or to extra stability of 1,4-semiquinones. Similarly

oxygenation of the 4-position takes place with the 1,6- and 1,7-isomers. In the latter case, in which the two oxygen atoms are conjugated with respect to each other, a transient signal can be observed which decays in about 5 minutes and which we attribute to a primary radical. The coupling constant of 0.93 mT is the largest we have observed for an aromatic proton in a static system. A transient signal, ascribed to a primary radical, is also observed in the case of the 1,5-isomer in which the two oxygen atoms are similarly conjugated.

Table 1

E.S.R. parameters (a/mT) of radicals from autoxidation of naphthols in HMPA in the presence of NaOMe or $KOBu^t$

Position of oxygens (i) in radical (ii) in precursor*		a_1	a_2	a_3	a_4	a_5	a_6	a_7	a_8
1,2-	1;2; 1,2-			0.038	0.405	0.075	0.152	0.038	0.115
1,2,4-	1,3-; 1,2,4-			0.035		0.060	0.245	0.060	0.155
1,2,3,4-	1,3-					0.095	0.122	0.122	0.095
1,2,6-†	1,6-; 2,6-			0.035	0.525	0.110		0.010	0.190
1,2,7-†	1,7-; 2,7-			0.048	0.460	0.0	0.268		0.085
1,4-	1; 1,4-		0.330	0.330		0.025	0.065	0.065	0.025
1,4,5-≠	1,5-; 1,4,5-		0.245	0.420			0.085	0.065	0.100
1,4,6-	1,6-; 1,7-		0.330	0.220		0.048		0.096	0.048
2,6-	2,6-	0.425		0.130	0.070	0.425		0.130	0.070
1,7-	1,7-		0.020	0.345	0.135	0.0	0.120		0.930
1,5-	1,5-		0.380	0.055	0.525		0.380	0.055	0.525

* Where a precursor is autoxidised to a mixture of 1,2- and 1,4-naphthosemiquinones the signal from the 1,4-semiquinone is seen after the decay of the spectrum of the 1,2-semiquinone.

† Obtained using $KOBu^t$/HMPA only: use of NaOMe gives sodium splittings, a_{Na}=0.040.

≠ a_H = 0.035 (peri-hydrogen)[4].

Weak, indistinct spectra are obtained from the 1,8- and 2,3-dihydroxynaphthalenes and the results from the other dihydroxynaphthalenes are given in Table 1.

A particularly interesting result is that obtained from 2,6-dihydroxynaphthalene which gives an intense spectrum to amphi-naphthosemiquinone. The corresponding quinone is destroyed in hydroxylic solvents.[7]

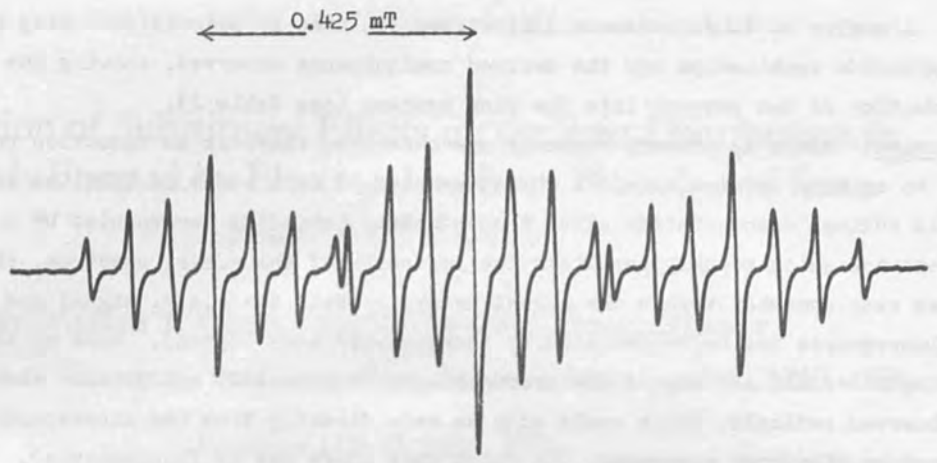

Figure: e.s.r. spectrum of 2,6-naphthosemiquinone

Direct autoxidation of phenol and resorcinol: The successful autoxidation of α- and of β-naphthols led us to investigate a corresponding possibility for phenol itself. As with the hydroxynaphthalene compounds a definite sequence of events occurs after shaking a mixture of phenol in HMPA with sodium methoxide or potassium t-butoxide in air, prior to transfer to the e.s.r. aqueous cell. First there is a broad e.s.r. absorption but later sharp-lined spectra of o- or of p-benzosemiquinone can be observed.

Table 2

E.s.r. parameters (a/mT) of semiquinones produced by autoxidation in HMPA in the presence of NaOMe or $KOBu^t$

Radical		Coupling constants
1,2-benzosemiquinone	phenol, catechol, 1,2-benzoquinone	0.35 (x2) 0.11 (x2)
1,4-benzosemiquinone	phenol, hydroquinone, 1,4-benzoquinone, 1,3- and 1,4-dihydrobenzene	0.24 (x4)
2-hydroxy-1,4-benzosemiquinone	resorcinol, 1,2,4-trihydroxybenzene	0.055, 0.14, 0.49 (after addition of H_2O)
1,2-naphthosemiquinone	1- and 2-naphthol, 1,2-dihydroxynaphthalene, 1,2-naphthoquinone	0.038 (x2), 0.075, 0.405, 0.152, 0.115
1,4-naphthosemiquinone	1-naphthol, 1,4-dihydroxynaphthalene, 1,4-naphthoquinone	0.025 (x2), 0.065 (x2), 0.33 (x2)
9,10-anthrasemiquinone	9,10-anthraquinone, 9,10-dihydroxyanthracene, anthrone, 9,10-dihydroanthracene	0.10 (x4), 0.024 (x4)
pyrene-4,5-semiquinone	4,5-dihydropyrene	0.015 (x2), 0.086 (x2), 0.207 (x2), 0.330 (x2)

In the case of resorcinol a sharp lined spectrum is observed only after the HMPA solution is diluted with water, when the semiquinone from 1,2,4-trihydroxybenzene can be identified.

A number of dihydrobenzene derivatives can also be autoxidised using the HMPA/alkoxide combination and the derived semiquinones observed, showing the introduction of two oxygens into the ring systems (see Table 2).

Discussion: Where no primary radicals are observed, there is an induction period of up to an hour or even more. A characteristic of such cases is that the sudden rise in radical concentration after the induction period is accompanied by a fluorescence which roughly parallels the intensity of the e.s.r. spectrum, though it dies away somewhat before the signal decays. [Both the e.s.r. signal and the fluorescence can be regenerated by shaking with more oxygen]. None of the starting material, nor any of the products were fluorescent, and neither were the observed radicals, which could also be made directly from the corresponding quinones or dihydroxy compounds, (on which case there was no fluorescence). From these observations it appears that the fluorescence was probably due to some precursor of the radicals, especially since its colour was characteristic of the starting material, e.g. blue for α- or β-naphthol, red for 1,3-dihydroxynaphthalene.

A likely intermediate is the complex I, between the negative ion of the starting material and oxygen. This is not unreasonable, because molecules of the coumarin type II, are well known to be fluorescent and substitution of electron donor substituents leads to a shift to lower frequency[8]. Intermediates analogous to I have been postulated to account for the formation of semidiones[2] during the autoxidation of aliphatic ketones.

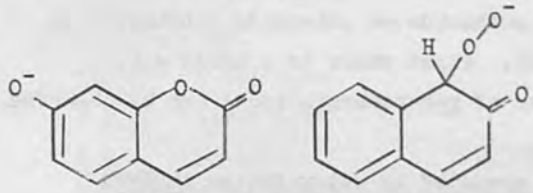

II I

REFERENCES

1. N. Normant, Angew. Chem. Internat. Edit., 1967, 6, 1046.
2. G.A. Russell, A.G. Berious, E.J. Goels, E.G. Jansen and A.J. Moye, Advan. Chem. Ser., No. 75, 1968, 174.
3. J.E. Dubois and G. Dodin, J. Amer. Chem. Soc., 1972, 94, 7520.
4. P. Ashworth and W.T. Dixon, J. Chem. Soc., Perkin II, 1974, 739.
5. P. Ashworth and W.T. Dixon, J. Chem. Soc., Perkin II, 1972, 1130.
6. (a) M. St. C. Flett, J. Chem. Soc., 1948, 1441.
   (b) I.S. Romodanov, N.V. Arshara, A.E. Dutskii, Teor. Eskp. Khim., 1973, 9, 68.
7. R. Willstätter and J. Parnas, Ber., 1907, 1406.
8. A. Dienes, C.V. Shank and A.M. Trozzolo, "Creation and Detection of the Excited State", Ed. W.R. Ware, Dekker, N.Y., 1974, 149.

Offprinted from the *Journal of The Chemical Society, Faraday Transactions II*, 1977, Vol. 73.

Calculation of Substituent Effects on the Spin Distribution in Radicals Formed by Electron-loss from Phenols and from Alkyl Aryl Ethers

By William T. Dixon,* Pat M. Kok and David Murphy

Department of Chemistry, Bedford College, Regent's Park, London, NW1 4NS

Received 11*th October*, 1976

Using the McLachlan S.C.F. method, the spin distributions in some phenoxyl radicals, phenol radical cations, and some alkyl aryl ether radical cations were calculated using a full set of basis π-electron orbitals. This made it possible to estimate the aliphatic proton splittings directly, also to explain trends in spin distribution caused by electron withdrawing groups, such as carbonyl.

Molecular orbital theory, with the McLachlan refinement,[1] can be used to explain the magnitudes, signs and trends in coupling constants observed in the e.s.r. spectra of aromatic radicals containing oxygen.[2, 3] The predictions made from this type of theory are even reliable enough for them to confirm the nature of new types of radical.[4] The utility of such semi-empirical theories rests on the fact that from comparatively few parameters a large number of successful predictions can be made in situations where more sophisticated theories fail.[3]

The device of treating all substituents in aryloxyl radicals as heteroatoms has been quite successful but has been found to suffer from two main disadvantages, *i.e.*, first, the spin densities within a substituent group cannot be ascertained; and secondly, no parameters can be found which account for the changes in spin density arising from the introduction of electron withdrawing groups such as nitro- or carboxyl, into the aromatic ring.[3]

In view of the recent observations of phenol radical cations [5] and of alkyl aryl ether radical cations,[6] it has become appropriate to extend previous work and include the structure of substituents in the theory. The necessary increase in the number of parameters is more than off-set by the increased scope of application.

THEORY AND CHOICE OF PARAMETERS

We have used McLachlan's simplified SCF procedure, neglecting overlap and non-nearest neighbour interactions.[3] The variable parameters for a heteroatom X are its coulomb integral $\alpha_x = \alpha + h_x\beta$ and the resonance integrals $\beta_{xy} = k_{xy}\beta$, where α and β are the coulomb and resonance integrals respectively pertaining to aromatic carbon p_π orbitals.

In previous work [3] on phenoxyl radicals the oxygen parameters used were $h_O = 1.6$, $k_{CO} = 1.3$ and we have not found it necessary to change these values for oxygen bound to one other atom (*i.e.*, carbon or nitrogen). However, when we consider oxygen in the phenol radical cation, it is clear that addition of the proton to phenoxyl must decrease the overall electron density in the oxygen σ-orbitals. To account for this we increase the electrogenativity of the oxygen π-orbital, *i.e.*, by increasing its coulomb integral. The values $h_{OH} = 2.0$, $k_{C-OH} = 1.1$ lead to results which approximately reproduce the spin densities in the phenol radical cation

and also give good predictions for a whole series of hydroxylated aromatic radicals (see table 1).

TABLE 1.—CALCULATED COUPLING CONSTANTS FOR RADICALS FROM PHENOL AND THE DIHYDROXYBENZENES

substituents in 	coupling constants/10^{-4} T				
	a_2	a_3	a_4	a_5	a_6
1-O^-	6.69 (6.65)	−1.98 (−1.85)	10.03 (10.20)	−1.98 (−1.85)	6.69 (6.65)
1-OH	5.16 (5.2)†	−1.2 (−0.8)	10.69 (10.7)	−1.2 (−0.8)	5.16 (5.2)
1-O^-, 2-O^-		0.59 (0.75)	3.48 (3.70)	3.48 (3.70)	0.59 (0.75)
1-O^-, 2-OH		−1.68 (−1.2)	5.99 (7.0)	1.66 (1.2)	2.02 (3.0)
1-OH, 2-OH		−0.78 (−0.25)	4.46 (4.85)	4.46 (4.85)	−0.78 (−0.25)
1-O^-, 3-O^-	−0.87 (−0.7)		12.82 (11.5)	−3.46 (−2.4)	12.82 (11.5)
1-O^-, 3-OH	1.81 (3.9)		12.14 (11.3)	−2.94 (−2.3)	10.14 (8.7)
1-OH, 3-OH	−1.26 (0.4)		11.88 (10.9)	−3.19 (−2.1)	11.88 (10.9)
1-O^-, 4-O^-	2.53 (2.37)	2.53 (2.37)		2.53 (2.37)	2.53 (2.37)
1-O^-, 4-OH	3.99 (5.1)	0.76 (−0.3)		0.76 (−0.3)	3.99 (5.1)
1-OH, 4-OH	2.15 (2.25)	2.15 (2.25)		2.15 (2.25)	2.15 (2.25)

† signs given are those of the spin density on the adjacent carbon atom and experimental data, (in brackets) are from ref. (3)-(6).

CARBONYL AND METHYL GROUPS

A marked improvement over previous work [3, 4] is obtained by considering both orbitals when a substituent has effectively two π orbitals. For example, from the hyperconjugative model of the methyl group we obtain directly the spin density, ρ_3, in the hydrogen group orbital, and thence can calculate the hyperfine splitting from the formula

$$a_{CH_3} = \tfrac{1}{3}\rho_3 \times 50.8 \text{ mT}. \qquad (1)$$

The parameters used were as follows:

$$\rangle C^1\text{—}C^2\text{=}O^3 \quad k_{12} = 0.5, \qquad h_2 = 0.0,\ h_3 = 1.6,\ k_{23} = 1.3$$

$$\rangle C^1\text{—}C^2\text{≡}H_3^3 \quad k_{12} = 0.7, \qquad h_2 = -0.7,\ h_3 = -1.0,\ k_{23} = 2.5.$$

The low values of k_{12} are justified to some extent in that they include the effect of (*a*) long C_1—C_2 bonds and (*b*) possible effects of rotation about the C_1—C_2 bond. The unusual parameters for the methyl group were chosen so that the odd electron in the toluene negative ion [7, 8] should go into an orbital which is symmetrical with respect to rotation about the C_2 axis of the radical, as indicated from experiment. If the parameter $h_3 > -1$ this condition will not be satisfied. The results given in table 2 are encouraging, though predicted *p*-methyl proton splitting are always too small.

THE METHOXY GROUP

The ring proton splittings in methoxy phenoxyls are well accounted for in terms of a heteroatom model;[3] calculations by Sullivan *et al.*[9, 10] for *p*-dimethoxybenzene radical cations have also yielded results in good agreement with experiment. However, by these methods the methoxy proton splittings were not directly calculable.

TABLE 2.—CALCULATED COUPLING CONSTANTS IN RADICALS FROM CARBONYL- AND FROM METHYL-SUBSTITUTED PHENOLS

substituents in 	coupling constants/10^{-4} T				
	a_2	a_3	a_4	a_5	a_6
1-O^-, 2-COR		−1.37 (−1.35)†	10.05 (10.0)	−2.23 (−2.2)	7.31 (7.2)
1-O^-, 2-CH_3	a_{CH_3} = 6.01 (7.5)	−2.48 (−2.0)	9.11 (9.8)	−1.19 (−1.5)	5.29 (6.0)
1-OH, 2-CH_3	a_{CH_3} = 6.89 (7.5)	−2.29 (−1.6)	9.23 (9.8)	0.35 (−0.1)	2.89 (4.0)
1-O^-, 3-COR	7.20 (7.2)		9.85 (9.9)	−1.87 (−1.95)	6.42 (6.75)
1-O^-, 3-CH_3	5.82 (5.9)	a_{CH_3} = −0.37 (−1.5)	10.45 (10.5)	−2.16 (−1.9)	7.29 (7.1)
1-OH, 3-CH_3	3.29 (4.0)	a_{CH_3} = 0.91 (−0.2)	11.30 (11.0)	−1.8 (−1.2)	6.57 (6.4)
1-O^-, 4-COR	6.82 (6.8)	−2.11 (−2.2)		−2.11 (−2.2)	6.82 (6.8)
1-O^-, 4-CH_3	5.86 (6.1)	−1.36 (−1.4)	a_{CH_3} = 7.42 (12.7)	−1.36 (−1.4)	5.86 (6.1)
1-OH, 4-CH_3	4.12 (4.5)	−0.43 (−0.05)	a_{CH_3} = 9.33 (15.1)	−0.43 (−0.05)	4.12 (4.5)

† as in table 1. R = H, CH_3

TABLE 3.—CALCULATED COUPLING CONSTANTS IN RADICALS DERIVED FROM THE ANISOLE RADICAL CATION

substituents in 	coupling constants/10^{-4} T					
	a_1	a_2	a_3	a_4	a_5	a_6
1-OCH_3	a_{OMe} = 5.5 (5.0)†	4.84 (4.9)*	−1.11 (−0.65)	10.34 (10.6)	−1.11 (−0.65)*	4.84 (4.9)*
1-OCH_3, 2-OCH_3	a_{OMe} = 3.3 (3.25)	a_{OMe} = 3.3 (3.25)	−0.87 (0.0)	4.44 (4.9)	4.44 (4.9)	−0.87 (0.0)
1-OCH_3, 2-OH	a_{OMe} = 3.22 (2.9)		−0.59 (1.45)	4.14 (2.9)	4.76 (6.8)	−1.5 (−1.1)
1-OCH_3, 2-O^-	a_{OMe} = 2.22 (1.8)		2.25 (4.3)	1.38 (0.0)	6.26 (8.5)	−1.88 (−1.9)
1-OCH_3, 3-OCH_3	a_{OMe} = 2.52 (3.0)	−1.25 (0.0)	a_{OMe} = 2.52 (3.0)	11.39 (10.75)	−3.07 (−2.1)	11.39 (10.75)
1-OCH_3, 3-OH	a_{OMe} = 2.31 (2.6)	−1.22 (0.3)		11.44 (11.25)	−3.13 (−2.15)	11.83 (10.85)
1-OCH_3, 3-O^-	a_{OMe} = 0.5 (0.6)	2.22 (3.5)		9.8 (9.0)	−2.85 (−2.3)	11.94 (11.4)
1-OCH_3, 4-OCH_3	a_{OMe} = 2.97 (3.4)*	2.03 (2.25)*	2.03 (2.25)	a_{OMe} = 2.97 (3.4)	2.03 (2.25)*	2.03 (2.25)*
1-OCH_3, 4-OH	a_{OMe} = 2.9 (3.2)	1.9 (2.6)*	2.29 (1.9)*		2.29 (1.9)*	1.9 (2.6)*
1-OCH_3, 4-O^-	a_{OMe} = 2.1 (2.1)	0.53 (−0.2)	4.15 (5.05)		4.15 (5.05)	0.53 (−0.2)
1-OCH_3, 4-CH_3	a_{OMe} = 4.42 (4.3)	3.84 (3.8)*	−0.23 (−0.3)*	a_{OMe} 9.13 (15.25)	−0.23 (−0.3)*	3.84 (3.8)*
1-, 2-, 3-$(OCH_3)_3$	a_{OMe} = 1.57 (2.05)	a_{OMe} = 4.4 (5.25)	a_{OMe} = 1.57 (2.05)	−1.37 (−0.43)	5.86 (6.25)	−1.37 (−0.43)

† as in table 1 * average values

Using Sullivan's approach [10] we obtained only poor agreement with experiment when it was applied to the less symmetrical methoxybenzene derivatives.

It seems probable that the O—Me group lies roughly symmetrically about the plane of the aromatic ring [10] in these radicals, so we can consider the group as a three orbital system. By analogy with the situation in the phenol radical cations, there will be a tendency for the oxygen to avoid positive charge, so it is again necessary to raise its coulomb integral.

The methyl group is treated in the same way as above, so the parameters used were as follows:

$$\rangle C^1—O^2—C^3 \equiv H_3^4$$

$$h_2 = 2.3,\ h_3 = -0.7,\ h_4 = -1.0$$

$$k_{12} = 1.1,\ k_{23} = 0.7,\ k_{34} = 2.5.$$

The results for radicals derived from the anisole radical cation (A) are given in table 3.

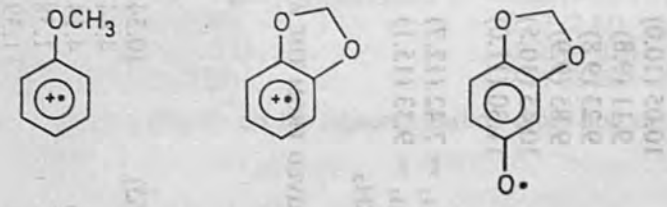

(A) (B) (C)

It is significant that the methoxy proton splittings calculated *via* eqn (1) are in excellent agreement with experiment. Once again the predicted *p*-methyl splitting is rather low, *i.e.*, in the *p*-methylanisole radical cation.

APPLICATION TO SOME HETEROCYCLIC RADICALS

(i) THE METHYLENE DIOXY GROUP $\left(\begin{matrix}O^2\\O^{2'}\end{matrix}\rangle C^3{=}H_2^4\right)$

1,3-Benzodioxole (B) can, from an m.o. viewpoint, be regarded as a modified *o*-dimethoxybenzene, so the same parameters are applied and the results of calculations are given in table 4.

TABLE 4.—CALCULATED COUPLING CONSTANTS IN RADICALS DERIVED FROM BENZODIOXOLE RADICAL CATION

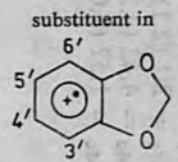

	a_{CH_2}	$a_{3'}$	$a_{4'}$	$a_{5'}$	$a_{6'}$
—	21.02 (21.9)†	−0.64 (−0.4)	3.94 (4.9)	3.94 (4.9)	−0.64 (−0.4)
3′-CH_3	20.98 (21.4)	a_{OMe} = 0.46 (0.4)	3.08 (4.2)	4.28 (5.3)	−1.03 (−0.6)
3′-OCH_3	18.54 (19.25)	a_{OMe} = 1.15 (1.5)	−0.78 (0.85)	5.22 (6.05)	−1.67 (−0.85)
4′-CHO	21.46 (22.8)	−0.99 (0.25)		3.8 (4.05)	−0.75 (0.0)
4′-CH_3	19.28 (19.45)	−1.2 (−0.75)	a_{CH_3} = 3.58 (7.95)	4.19 (5.15)	−0.45 (−0.25)
4′-OCH_3	14.48 (14.45)	−1.49 (−0.45)	a_{OMe} = 1.49 (2.65)	5.28 (6.25)	−0.18 (−0.45)
4′-OH	13.97 (13.5)	−1.42 (0.0)		5.45 (6.25)	−0.30 (−0.40)
4′-O^-	9.73 (6.5)	0.03 (1.95)		6.49 (7.95)	−0.41 (−1.1)

† as in table 1

The large triplet splittings are well accounted for by the theory. A particularly severe test was provided by the two radicals from sesamol (C) due to the comparatively violent change which has to occur on replacing —OH by —O^-. Better agreement with experiment can of course be obtained by juggling with the parameters in each case, but we prefer to keep to one set which seems reliable over the whole range of derivatives.

(ii) HYDROXYPYRONES

As a further test the splittings in the radicals from kojic acid (D) and from maltol (E) can be compared with those predicted using the same parameters as those used above.

The agreement is quite satisfactory.

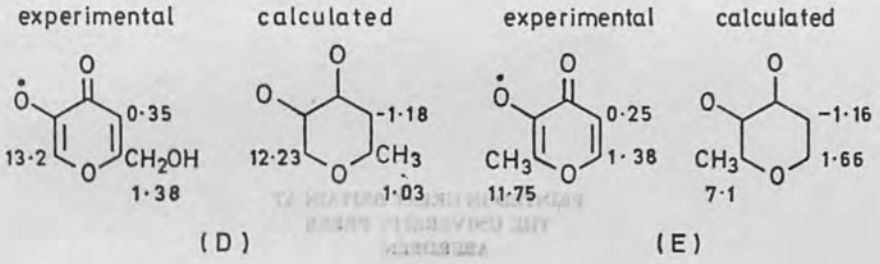

(D) (E)

g-FACTORS

For small variations on a given type of radical, such as those considered by Sullivan *et al.*[9, 10] there seems to be reasonable correlations between overall spin density on oxygen atoms and the *g*-factors of the radicals concerned. However, no sensible trend between theory and experiment was apparent when the *g*-values of radicals of widely different types were considered and compared. Perhaps this illustrates a deficiency in the type of approach outlined by Stone [11] for hydrocarbon radicals, in the present context.

CONCLUSION

From the above results it would appear that the system of parameters adopted gives quite reliable results over a range of different substitution patterns. Any further improvements would have to involve taking changes in the carbon skeletons into account.

[1] A. D. McLachlan, *Mol. Phys.*, 1960, **3**, 233.
[2] K. A. Lott, E. I. Short and D. N. Waters, *J. Chem. Soc.* (*B*), 1969, 1232.
[3] W. T. Dixon, M. Moghimi and D. Murphy, *J.C.S. Faraday II*, 1974, **70**, 1713.
[4] W. T. Dixon, M. Moghimi and D. Murphy, *J.C.S. Perkin II*, 1975, 101.
[5] W. T. Dixon and D. Murphy, *J.C.S. Faraday II*, 1976, **72**, 1221.
[6] W. T. Dixon and D. Murphy, *J.C.S. Perkin II*, 1976, 1824.
[7] A. Carrington, *Quart. Rev.*, 1963, **17**, 67.
[8] J. E. Wertz and J. R. Bolton, *Electron Spin Resonance* (McGraw-Hill, N.Y., 1972), chap. 5. pp. 103-105.
[9] P. D. Sullivan and J. R. Bolton, *J. Amer. Chem. Soc.*, 1968, **90**, 5366.
[10] P. D. Sullivan, *J. Phys. Chem.*, 1971, **75**, 2195.
[11] A. J. Stone, *Proc. Roy. Soc. A*, 1963, **271**, 424.

(PAPER 6/1906)